

**Comparative immunohistochemical and
molecular investigations of metabolic and
stromal events in HPV positive and HPV
negative oropharyngeal squamous cell
carcinoma**

Khaled Ben Salah BDS (Benghazi), MSc (Lyon)

Thesis submitted in accordance with the requirements of the University of Liverpool
for the degree of
Doctor of Philosophy

Department of Molecular and Clinical Cancer Medicine,
Institute of Translational Medicine
University of Liverpool
Cancer Research Centre

September 2018

Abstract

Background It has been shown that HPV positive (HPV+) oropharyngeal squamous cell carcinoma (OPSCC) are characterised by extensive nodal disease, but are associated with significantly better prognosis than HPV negative (HPV-) OPSCC. It has also been proposed that glycosaminoglycans (GAGs) and myofibroblasts are components of the desmoplastic stroma that characterizes many advanced carcinomas. They are considered to play an important role in the pathogenesis of head and neck squamous cell carcinomas (HNSCC) and their presence is of high prognostic value. A 'three compartment tumour metabolism' model has been proposed in head and neck cancer comprising a proliferative, monocarboxylate transporter1 (MCT1)-expressing carcinoma cell population at the tumour advancing front (front) with both a deeper population of monocarboxylate transporter 4 (MCT4)+ cancer cells and (MCT4)+ cancer associated fibroblasts (CAFs) providing a source of metabolic fuels via a lactate shuttle. This thesis investigates the presence and distribution of GAGs and myofibroblasts in HPV+ and HPV- OPSCC, and their correlation with clinicopathological features. We also investigate the metabolic activities of OPSCC in relation to HPV status.

Materials and methods The metabolic status of 45 HPV+ and 63 HPV- OPSCC was determined by immunohistochemical staining using antibodies to MCT1, MCT4, Cell proliferation (Ki-67), and mitochondria (TOMM20).

Results The presence of desmoplasia was determined by histological examination of H&E stained whole sections and by Alcian Blue staining at pH 2.5 (GAGs) and alpha smooth muscle actin (α SMA: myofibroblasts). Histopathological staining of tissue micro array (TMAs) from archival tissue blocks of 45 patients with HPV+ and 63 with HPV- OPSCC.

Only in HPV+ OPSCC, depth of invasion correlated with the presence of histologically defined desmoplasia at both the tumour core and front ($p < 0.0005$ and $p = 0.045$), but these associations were not observed for individual components of desmoplasia determined by histopathological methods. Data from HPV+ OPSCCs shows that GAGs are more often found at the tumour front and was generally less prevalent at the tumour core (65% in the front *vs* 48% in tumour core), whereas in HPV- OPSCC the converse was true. Myofibroblasts are found throughout these

tumours, which suggests that the invasion process in HPV+ OPSCCs is mainly driven by GAGs and myofibroblasts are more bystanders. The presence of myofibroblasts in the tumour core is distinctive for HPV+ OPSCC and may indicate that this cell type plays a different role in these tumours compared with HPV- OSCC. No correlation was observed between histological desmoplasia and survival outcome in OPSCC.

Using (TMAs) we assessed levels of MCT1, MCT4, Ki-67 and TOMM20 and their intracellular distribution. We were able to show that carcinoma cells in both HPV+ and HPV- OPSCC are highly proliferative, rich in mitochondria and consume mitochondrial fuels (Ki-67+ /TOMM20+ /MCT1+). These proliferating cells co-exist with non-proliferating stromal cells which express MCT4 and, presumably, excrete metabolic fuels. Although all CAFs in HPV+ tumours were strongly TOMM20 positive only 58% of CAFs in HPV- OPSCCs were (p = 0.005). While 85% of HPV+ OPSCC tumours co-express MCT1 and MCT4 in the same cells, only 50% of HPV- OPSCC do so, indicating that the three compartment model is more compatible with data from HPV- OPSCC. Strong MCT4 CAF immunoreactivity was less prevalent in HPV- than in HPV+ OPSCCs (p = 0.031).

By means of co-culturing between two epithelial cancer cells and two fibroblasts with different HPV, and probing for MCT1 and MCT4, up-regulation of MCT1 was achieved in the epithelial cancer cell lines when co-cultured with fibroblasts originating from HPV- tumours. Based on tissue data and preliminary functional data, there may be some differences in metabolism in HPV+ and HPV- tumours.

Conclusions Carcinoma cells in both HPV+ and HPV- OPSCC are highly proliferative, rich in mitochondria and consume mitochondrial fuels (Ki-67+/TOMM20+/MCT1+). These proliferating cells co-exist with non-proliferating stromal cells which express MCT4 and, presumably, excrete metabolic fuels. While 85% of HPV+ OPSCC tumours co-express MCT1 and MCT4 in the same cells, only 50% of HPV- OPSCC do so, indicating that the three compartment model is more compatible with data from HPV- OPSCC. Differences in the stromal compartment metabolism are also observed between HPV+ and HPV- tumours.

Statement of Originality

I, Khaled Ben Salah hereby confirm that the research work that makes up this thesis has been carried out by me during the course of studies in the Department of Molecular and Clinical Cancer Medicine, Institute of Translational Medicine, University of Liverpool, between October 2014 and September 2018, with due reference ascribed to originators in areas where collaboration has been required and reference sought. I hereby attest to having ensured the work presented is original, does not go against the laws of the land and does not break copyright laws. All work described was performed by me unless clearly indicated. The thesis was written wholly by me under the valued guidance of my supervisors.

The copyright of this thesis does rest with the author.

Khaled Ben Salah

Acknowledgements

Very many thanks to my supervisors, Dr Janet M Risk, Dr Asterios Triantafyllou, Prof Richard Shaw and Dr Andrew Schache for her unquantifiable role through my PhD. I appreciate all the members of the Janet Risk research team; Frances Greaney, Laura Cossar, Matthew Agwae, Okoturo Eyituoyo. Many thanks to all the members of the other head and neck groups at the Cancer research centre.

I gratefully acknowledge the financial support for my PhD study from the Ministry of Higher Education and Scientific Research in Libya.

A special thanks to my family, my parents and my wife for their unlimited support, encouragement and love, without which I would not have come this far. I would also like to thank my close friends for their help and support throughout these years.

Table of Contents

Chapter 1	20
1.1 The hallmarks of cancer	20
1.1.1 Sustained proliferative signalling.	23
1.1.2 Insensitivity to growth inhibition signals.	25
1.1.3 Evading apoptosis.	25
1.1.4 Limitless replicative potential.....	29
1.1.5 Sustained angiogenesis.	30
1.1.6 Tissue invasion and metastasis.	31
1.1.7 Reprogramming energy metabolism.....	33
1.1.8 Evading immune surveillance.....	34
1.1.9 Tumour-promoting inflammation	34
1.1.10 The p53 gene in relation to cell cycle and apoptosis.	36
1.1.11 Genome instability	37
1.2 The cancer microenvironment.....	43
1.2.1 Cancer-Associated Fibroblasts (CAFs)/ myofibroblasts	43
1.2.2 The desmoplastic reaction	50
1.3 The metabolism of cancer	53
1.3.1 Glycolysis and conversion of pyruvate to lactate	53
1.3.2 Citric acid cycle and oxidative phosphorylation.....	53
1.3.3 The Warburg effect.....	54
1.3.4 Symbiosis of aerobic and anaerobic tumour cells	55
1.3.5 Metabolic interactions between tumour and stroma (reverse Warburg effect).....	56
1.3.6 Causes of hypoxia in tumours.....	59
1.3.7 Gene control of tumour metabolism with particular emphasis on hypoxia-inducible factors (HIF) and their regulations	60
1.3.8 The clinical significance of hypoxia.....	63
1.3.8.1 Hypoxia and radioresistance	63
1.3.8.2 Hypoxia and chemoresistance.....	64
1.3.8.3 Hypoxia and the metastatic phenotype	64
1.3.8.4 Hypoxia and treatment outcome	65
1.4 Head and neck squamous cell carcinomas (HNSCC)	66
1.4.1 General features with emphasis on prognostic factors in HNSCC.....	66
1.5 Oropharyngeal squamous cell carcinoma (OPSCC)	69

1.5.1 Structural and functional aspects of oropharynx	69
1.5.2 Human papillomavirus in OPSCC.....	72
1.5.3 Epidemiology and clinical presentation of HPV+ and HPV- OPSCC	82
1.5.4 Histopathology of OPSCC.....	84
1.5.5 Prognostic features.....	87
1.6 Hypothesis, aims and objectives.....	87
Chapter 2	91
2.1 Introduction	91
2.2 Subjects	91
2.3 Histopathological assessment.....	92
2.4 Scoring matrices	92
2.5 TMA production.....	93
2.6 Histochemistry.....	93
2.7 Immunohistochemistry	94
2.8 Slide scanning.....	101
2.9 Scoring.....	101
2.10 Statistical analysis	102
Chapter 3	103
3.1 Introduction	103
3.2 Materials and methods.....	105
3.2.1 Reagents.....	105
3.2.2 Evaluation	106
3.3 Results	109
3.4 Discussion	129
Chapter 4	142
4.1 Introduction	142
4.2 Materials	148
4.2.1 Reagents.....	148
4.2.2 Evaluation	148
4.3 Results	149
4.4 Discussion	156
Chapter 5	163
5.1 Introduction	163
5.2 Materials and methods.....	166
5.2.1 Reagents.....	166

5.2.2 Cell lines.....	166
5.2.3 Expression of MCT1 & MCT4.....	167
5.2.3.1 Protein extraction.....	167
5.2.3.2 Western blotting.....	167
5.2.3.3 Data collection and Analysis.....	168
5.2.4 Proliferation assays.....	169
5.2.4.1 Crystal violet assay.....	169
5.2.4.2 MTT assay.....	169
5.2.5 Effect of availability of metabolic fuel on MCT1 expression.....	170
5.2.7 Statistical tests.....	170
5.3 Results.....	170
5.3.1 Baseline expression of MCT1 and MCT4 in cell lines.....	170
5.3.2 Effect of metabolic fuel availability on MCT1 expression.....	172
5.3.3 Effect of metabolic fuel availability on cell proliferation.....	178
5.4 Discussion.....	183
Chapter 6.....	187
6.1 Introduction.....	187
6.2 Overall aim and specific objectives of the chapter.....	190
6.3 Materials and methods.....	191
6.3.1 Cohort selection.....	191
6.3.2 Antibodies.....	191
6.3.3 Assessment of staining.....	192
6.3.4 Statistics.....	192
6.4 Results.....	193
6.4.1 HPV positive samples.....	193
Expression of HIF1 α	193
Expression of GLUT1.....	194
Expression of VEGF.....	194
Expression of VEGFR2.....	195
6.4.2 HPV negative samples.....	196
Expression of HIF1 α	196
Expression of GLUT1.....	197
Expression of VEGF.....	197
Expression of VEGFR2.....	198
6.3.3 Co-expression evaluation.....	199

6.3.3.1 HPV positive samples	199
MCT4 vs HIF-1 α	199
VEGF vs HIF-1 α	201
6.3.3.2 HPV negative samples	204
MCT4 vs HIF-1 α	204
VEGF vs HIF-1 α	206
6.4 Discussion	210
Chapter 7	215
7.1 Introduction	215
7.2 Summary of findings	215
7.3 MCT4 expression in head in neck SCC	216
7.4 Increased expression of MCT4 and its effect	217
7.5 Clinical implications.....	217
7.6 Limitations.....	219
7.7 Future experiments	219
7.7.1 Tissue experiments	220
7.7.2 Western blot experiments	221
7.7.3 Expanding experiment with cell lines.....	221
7.7.4 Migration and proliferation assays, and other functional studies.	222
References	223
Appendices	260

List of Figures and Tables

Figure 1.1. Hallmarks of cancer.	22
Figure 1.2. MAPK pathway.	23
Figure 1.3. Apoptosis.	26
Figure 1.4. Members of the Bcl-2 family.	27
Figure 1.5. Diagram represents the intrinsic and extrinsic pathways of apoptosis. ...	29
Figure 1.6. The tumour invasion–metastasis cascade.	32
Figure 1.7. Showing a collection of distinct cell types that make up the tumour microenvironment in solid tumours.	43
Figure 1.8. Typical histological desmoplasia (D) in OSCC.	52
Figure 1.9. Myofibroblasts in stroma of a conventional SCC (Left, arrows); the arrowhead points to an islet of malignant keratinocytes. GAGs (right) gives the stroma its pale/‘oedematous’ appearance in desmoplastic stroma (S) of cystic SCC metastasis of a cervical lymph node. Adapted from Woolgar et al [235].	52
Figure 1.10. The oxidative phosphorylation metabolism.	54
Figure 1.11. The reverse Warburg metabolic model.	58
Figure 1.12. Determinants of the metabolic phenotype.	61
Figure 1.13. Examples of HIF-1 target genes.	62
Figure 1.14. The oxygen fixation hypothesis.	64
Figure 1.15. Boundaries of oropharynx. Adapted from Junqueira et al. [346].	70
Figure 1.16. Genomic organisation of HPV16. From Faraji et al. [323].	73
Figure 1.17. Steps of HPV integration and promotion of tumorigenesis.	77
Figure 1.18. Events of cancer progression in infected keratinocyte with HPV.	78
Figure 1.19. Perturbation of cell cycle by HPV.	80
Figure 1.20. Tumour progression in HPV+ OPSCC. From Faraji et al [323].	85
Figure 2.1. An example for primary antibodies optimization.	98
Figure 2.2. Typical examples for positive (left) and negative (right) IHC staining. Panel of FFPE tissues were used for this purpose; Cervix (1&2), Colon (3, 4 & 7), Skin (5), Placenta (6) and Gall bladder (8). Original magnification 20x.	100
Figure 3.1. A typical example of scoring for expression of α SMA and serpin E1, and presence of GAGs in OPSCC performed on TMA sections.	107
Figure 3.2. Histological subtype of 43 cases of HPV+ OPSCC.	110
Figure 3.3. Correlation between desmoplasia and depth of invasion in OPSCCs. .	111
Figure 3.4. A typical example of staining for GAGs and myofibroblasts/CAFs in the stroma of HPV+ OPSCC performed on TMA sections.	114
Figure 3.5. A typical example of staining for GAGs and myofibroblasts/CAFs in the stroma of HPV- OPSCC performed on TMA sections.	116
Figure 3.6. A typical example of serpin E1 staining performed on TMA sections showing expression at tumour core (1 and 3) and front (2 and 4) in HPV+ and HPV- OPSCC done on TMA sections. Tumour (T); stromal cells (arrows). The rectangled areas in panels 1, 2, 3 and 4 are magnified in panels 5, 6, 7 and 8 respectively. Tumour (T); stroma (S).	119
Figure 3.7. Step sections done on TMAs allowing comparison of expression of α SMA, presence of GAGs and expression of serpin E1 in the core of OPSCCs (two cases). Tumour (T); stroma (S). Note that the immunoreactivity of serpin E1 in HPV+ is stronger than HPV- OPSCCs. Also, expression of serpin E1 by carcinoma	

cells was always stronger than the expression by stromal cells. For stromal expression of serpin E1, there was not a statistical difference between the two types of OPSCC at the tumour core.....	120
Figure 3.8. Step sections done on TMAs allowing comparison of expression of α SMA, presence of GAGs and expression of serpin E1 in the front of OPSCCs (two cases). Tumour (T); stroma (S).Note that the immunoreactivity of serpin E1 in HPV+ is stronger than HPV- OPSCCs. Also, expression of serpin E1 by carcinoma cells was always stronger than the expression by stromal cells. For stromal expression of serpin E1, there was not a statistical difference between the two types of OPSCC at the tumour front.....	121
Figure 3.9. Negative immunostaining for α SMA in stromal cells in HPV+ and HPV- OPSCC.....	122
Figure 3.10. The Alcian Blue staining at the tumour core showed a significant correlation with the survival status ($p = 0.009$) in HPV- OPSCC.	124
Figure 3.11. The α SMA expression at the front correlated significantly with the survival status ($p = 0.004$) in HPV- OPSCC.....	125
Figure 4.1. Lactate shuttle in tumour.	145
Figure 4.2. A typical example of immunohistochemical staining showing expression of Ki-67, TOMM20, MCT1 and MCT4 in HPV+ and HPV- OPSCC performed on tissue microarray sections.	152
Figure 4.3. Metabolic compartmentalisation in OPSCC.....	154
Figure 4.4. A typical example of metabolic compartmentalisation in HPV+ OPSCC.	155
Figure 4.5. Three (Multicompartment) Metabolism Model.....	156
Figure 5.1. Baseline expression of MCT4 in cell lines. Western blot showing MCT4 expression in carcinoma (left) and cancer-associated fibroblast (right) cell lines. HeLa cells and NOK cells are used as a positive controls and Beta Actin as a loading control.	171
Figure 5.2. Baseline expression of MCT1 in cell lines. Western blot showing MCT1 expression in carcinoma (left) and cancer-associated fibroblast (right) cell lines. HeLa cells and NOK cells are used as a positive control and Beta Actin as a loading control.	171
Figure 5.3. Line graph shows MCT1 expression in the four different media by the HPV+ cancer cells.....	172
Figure 5.4. Line graph showing MCT1 expression by UMSCC74A (HPV-) cancer cells in four different metabolic media.	173
Figure 5.5. Detailed raw data of densitometry analysis of western blotting for different media over four days with average value of three experiments.....	175
Figure 5.6. Bar graph generation from raw data of densitometry analysis of western blotting for different media over four days with average values of three experiments.	176
Figure 5.7. Average values of densitometry analysis of three experiments of western blotting for different media over four days. The line graphs used in this study are generated from these average values using charts function in Excel 2013.....	177
Figure 5.8. Effect of metabolic fuel availability on proliferation of (HPV-) cancer cells (UMSCC74A).....	180

Figure 5.9. Effect of metabolic fuel availability on proliferation of (HPV+) cancer cells (UPCISCC154).	181
Figure 6.1. A typical example of HIF-1 α expression in HPV+ OPSCC.....	193
Figure 6.2. A typical example of GLUT1 expression in HPV+ OPSCC.....	194
Figure 6.3. A typical example of VEGF expression in HPV+ OPSCC.	194
Figure 6.4. A typical example of VEGFR2 expression in HPV+ OPSCC.	195
Figure 6.5. A typical example of HIF-1 α expression in HPV- OPSCC.....	196
Figure 6.6. A typical example of GLUT1 expression in HPV- OPSCC.....	197
Figure 6.7. A typical example of expression VEGF in HPV- OPSCC.....	197
Figure 6.8. A typical example of VEGFR2 expression in HPV- OPSCC.	198
Figure 6.9. A typical example of co-expression of MCT4 and HIF-1 α in HPV+ OPSCCs.	199
Figure 6.10. A typical example of co-expression of GLUT1 and HIF-1 α in HPV+ OPSCCs.	200
Figure 6.11. A typical example of co-expression of VEGF and HIF-1 α in HPV+ OPSCCs.	201
Figure 6.12. A typical example of co-expression of VEGFR2 and HIF-1 α in HPV+ OPSCCs.	202
Figure 6.13. A typical example of co-expression of GLUT-1 and TOMM20 in HPV+ OPSCCs.	203
Figure 6.14. A typical example of co-expression of MCT4 and HIF-1 α in HPV- OPSCCs.	204
Figure 6.15. A typical example of co-expression of GLUT1 and HIF-1 α in HPV- OPSCCs.	205
Figure 6.16. A typical example of co-expression of VEGF and HIF-1 α in HPV- OPSCCs.	206
Figure 6.17. A typical example of co-expression of VEGFR2 and HIF-1 α in HPV- OPSCCs. Step sections from a HPV- OPSCCs tumour show diffuse expression of VEGFR2. VEGFR2 was often co-expressed with HIF-1 α . (A and C vs B and D). This was not, however, a feature when HIF-1 α was not expressed at the periphery of tumour cell aggregate (E vs F). Note, the localisation of HIF-1 α immunoreactivity is not uniform and varied between centre and periphery of tumour cell aggregates (B and F). Tumour (T). Objective magnification, x 20.....	207
Figure 6.18. A typical example of co-expression of GLUT-1 and TOMM20 in HPV- OPSCCs.	208

Table 1.1. Histological differences between tonsils.....	70
Table 1.2. Differences between tonsils with lymph nodes.....	71
Table 2.1. Desmoplasia composite score system.	93
Table 3.1. Details of antibodies.....	106
Table 3.2. Expression of Alcian Blue, α SMA and serpin E1 in HPV+ and HPV- OPSCC cases at the core and front.	113
Table 3.3. Strong correlation between Alcian Blue reaction and α SMA expression at the tumour front in HPV+ OPSCC.	113
Table 3.4. Details of different groups (High and Low) of desmoplasia and its two components; the Alcian Blue and α SMA in both HPV+ and HPV- OPSCC are shown in table (A).Summary of the statistically significant correlations between the three variables are shown in table (B).* Indicates statistically significant values. ...	117
Table 3.5. The GAGs reaction at the tumour core between the two types of OPSCC. *Presence of significant statistical difference, $p = 0.031$. p16/cISH indicates that positivity of HPV infection is based on positivity of both p16 and chromogenic in situ hybridization tests	118
Table 3.6. Correlations of α SMA and serpin E1 expressions with ECS in HPV+ and HPV- OPSCC.....	126
Table 3.7. Depth of invasion and α SMA and serpin E1 expression in HPV+ and HPV- OPSCC.....	127
Table 3.8. Survival data in both HPV+ and HPV- OPSCC.	127
Table 3.9. Survival and α SMA and serpin E1 expression.....	128
Table 4.1. Details of antibodies.....	148
Table 4.2. Frequency of strong immunoreactivity of each biomarker in HPV+ and HPV- OPSCC in the tumour core.	150
Table 4.3. Frequency of strong immunoreactivity in HPV + and HPV- OPSCC at the advancing front.....	150
Table 5.1. The used additives, their concentrations, and their general role.	167
Table 5.2. Summary of MCT1 upregulation profile in the four different types of media by the two epithelial cancer cells.	174
Table 6.1. Details of antibodies.....	192
Table 6.2. Summary table for expression of HIF-1 α , GLUT1, VEGFR and VEGFR2 in HPV+/HPV- OPSCC.	198
Table 6.3. Summary table for co-expression of HIF-1 α vs MCT4, GLUT1, VEGFR and VEGFR2 in HPV+/HPV- OPSCC. Absence of correlation between HIF-1 α expression and expression of MCT4, GLUT1, VEGF and VEGFR2 in the HPV+ OPSCC whereas in HPV- OPSCC this correlation is largely present.	209

List of Abbreviations

ADP	adenosine diphosphate
AGC	protein kinase A/protein kinase G/protein kinase C
AIF	apoptosis-inducing factor
AML	acute myeloid leukaemia
AMP	adenosine monophosphate
AMPK	AMP-activated protein kinase
Apaf1	apoptotic protease activating factor 1
APS	ammonium persulfate
ATM	ataxia telangiectasia mutated
ATP	adenosine triphosphate
AZD3965	MCT1 inhibitor
bFGF	basic fibroblast growth
BAK	Bcl-2 homologous antagonist killer
BAX	Bcl-2-associated X protein
BSA	albumin from bovine serum
BSO	buthionine sulfoximine
BRCA1	breast cancer 1
BRCA2	breast cancer 2
CAFs	cancer-associated fibroblasts
CAIX	carbonic anhydrase IX
CAM	cell adhesion molecules
CDKN1A	cyclin Dependent Kinase Inhibitor 1A
CGH	comparative genomic hybridization
CO ₂	carbon dioxide
CRC	colorectal cancer
CTCs	circulating tumor cells
CTLs	cytotoxic T lymphocytes
CTLA-4	cytotoxic T lymphocyte-associated protein 4

DCs	dendritic cells
2-DG	2-Deoxy-D-glucose
DISC	death-inducing signalling complex
DMEM	dulbecco's modified Eagle's medium
DMSO	dimethylsulfoxide
DNA	deoxyribonucleic acid
DPBS	dulbecco's PBS
PD-L1	death protein ligand 1
PD-L2	death protein ligand 2
DSBs	double-strand-breaks
ECM	extracellular matrix
EGF	epidermal growth factor
EGFR	epidermal growth factor receptor
EMT	epithelial-mesenchymal transition
EndMT	endothelial- mesenchymal transition
ER	endoplasmic reticulum
ERK	extracellular signal-regulated kinase
ETC	electron transport chain
FADD	Fas-associating protein with death domain
FADD/MORT1	Fas-associated death domain protein (FADD)/mediator of receptor-induced toxicity-1
Fas	first apoptosis signal receptor
FasL	Fas ligand
FAP α	fibroblast-activation protein α
Fas/APO-1	Fas also known as apoptosis antigen 1
FBS	fetal bovine serum
FDG	fluorodeoxyglucose
FDG-PET	fluoro-2-deoxy-glucose positron emission tomography
FDXR	ferredoxin reductase
FFPE	formalin fixed paraffin embedded
FGF	fibroblast growth factor

FSP-1	fibroblast-specific protein 1
FUCA1	alpha-L-fucosidase 1
GADD45	Growth Arrest and DNA Damage
GAGs	glycosaminoglycans
GLS2	Glutaminase 2
GLUT	glucose transporter
GLUT1	glucose transporter 1
H ⁺	hydrogen ion
HCO ₃ ⁻	bicarbonate
HNSCC	head and neck squamous cell carcinoma
HIF-1	hypoxia-inducible factor-1
HIF-1 α	hypoxia-inducible factor 1-alpha
HIF-1 β	hypoxia-inducible factor 1-beta
HIF2 α	hypoxia-inducible factor 2-alpha
HO \bullet	hydroxyl radicals
H ₂ O	water
H ₂ O ₂	hydrogen peroxide
HPH	prolyl hydroxylases
HPV	human papilloma virus
HPV-	human papilloma virus negative
HPV+	human papilloma virus positive
HREs	hypoxia-response elements
HRP	horseradish peroxidase
IARC	International Agency for Research on Cancer
IMC	immature monocyte
IF	immunofluorescence
IGF-2	insulin-like growth factor 2
IAP	Inhibitor of apoptosis proteins
IL-8	interleukin 8
IRL	intrinsic radiation of Lutetium-176

LDH	lactate dehydrogenase
LDH-A	lactate dehydrogenase A
LDH-B	lactate dehydrogenase B
LOX	lysyl oxidase
MAPK	mitogen-activated protein kinase
MAP4K3	mitogen-activated protein kinase kinase kinase kinase 3
MBP	myelin basic protein
MCT1	monocarboxylate transporter 1
MCT4	monocarboxylate transporter 4
MCTs	monocarboxylate transporters
β -ME	β -Mercaptoethanol
MEM	minimum essential medium
NEMA	national electrical manufacturers association
MMR	mismatch repair proteins
MP1	MAPK binding partner 1
MSI	microsatellite instability
MTV	metabolic tumour volume
NaCl	sodium chloride
NAD	nicotinamide adenine dinucleotide
NADPH	nicotinamide adenine dinucleotide phosphate hydrogen
NG2	neuronglial Antigen-2
NK	natural killer cells
NSCLC	non-small-cell lung carcinoma
O ₂	oxygen
O ₂ ^{•-}	superoxide anions
OSCC	oral squamous cell carcinoma
OPSCC	oropharyngeal squamous cell carcinoma
OXPHOS	oxidative phosphorylation
PAI-1	plasminogen activator inhibitor-1
PANK1	Pantothenate kinase 1

PBS	phosphate buffered saline
PCa	prostate cancer
PCD	programmed cell death
PCR	polymerase chain reaction
PDGF	Platelet-derived growth factor
PDGFR- β	platelet-derived growth factor receptor- β
PFK1	phosphofructokinase 1
PHD	prolyl hydroxylase domain protein
PKM2	Pyruvate kinase muscle isozyme M2
PO4	phosphate group
PRKAB1	Protein Kinase AMP-Activated Non-Catalytic Subunit Beta 1
PTMs	post-translational modifications
ROS	reactive oxygen species
RTK	receptor tyrosine kinases
PUMA	p53 upregulated modulator of apoptosis
SASP	senescence-associated secretory phenotype
SCC	squamous cell carcinoma
SD	standard deviation
SDS	sodium dodecyl sulfate
SDS-PAGE	SDS-polyacrylamide gel electrophoresis
siRNA	small interfering RNA
α SMA	alpha smooth muscle actin
SOD	superoxide dismutases
SUVmax	maximum Standard Uptake Value
TCA	tricarboxylic acid cycle or the Krebs cycle
TGF β	transforming growth factor beta
TH1	T helper cells
TH2	T helper
TKD	tyrosine kinase domain
TOMM20	translocase of outer mitochondrial membrane 20

TP53	Tumour protein p53
TRADD	tumour necrosis factor receptor type 1-associated DEATH domain protein
TREGs	regulatory T cells
TSP-1	thrombospondin-1
UICC	union for International Cancer Control
WB	western blotting
VEGF	vascular endothelial growth factor
VEGFR	vascular endothelial growth factor receptor
VEGFR1	vascular endothelial growth factor receptor 1
VEGFR2	vascular endothelial growth factor receptor 2
VHL	von Hippel Lindau
VN	vitronectin

Chapter 1

Introduction

1.1 The hallmarks of cancer

A large proportion of current research on cancer is focused on unravelling the molecular basis of cancer initiation and development. So much effort has gone into trying to identify specific biomarkers, targets for therapy and possible parameters of prognoses. This study intends to examine the potential role of the metabolic biomarkers, MCT1, MCT4, Ki-67 and TOMM20 in the pathogenesis of HNSCC, in particular HPV+ and HPV- oropharyngeal cancers, with a focus on proposed interactions between the tumour cells and associated fibroblasts.

A previous study examined samples from HNSCC to investigate the coexistence of diverse metabolic compartments; oxidative phosphorylation and glycolysis. A group of well-known biomarkers was used to study the metabolic events of tumour cells. Proliferation of cancer cells, as detected via Ki-67 immunohistochemistry, was strongly associated with oxidative phosphorylation metabolism and the use of metabolic fuels, as marked by expression of MCT1 [1]. More precisely, a metabolic model was proposed containing three compartments described as the following: (1) Proliferative cancer cells rich in mitochondria (Ki-67positive, TOMM20 positive and MCT1 positive); (2) less proliferative cancer cells poor in mitochondria (Ki-67negative, TOMM20negative and MCT1negative); and (3) less proliferative stromal cells poor in mitochondria (Ki-67negative, TOMM20negative and MCT1negative) [1].

For normal cells to become cancerous, several rather complex processes (many of which are not fully understood) take place. A number of mechanisms have been put forward in an attempt to fully describe a processes leading to these cellular changes in which normal healthy cells are converted into cancerous cells. In an attempt to explain carcinogenesis, most of the mechanisms are centred on changes in four crucial and intersecting cellular activities: growth, proliferation, differentiation and cell death. The process by which healthy cells become transformed to malignant cells does involve several-stages and is assumed to result in progressive and consecutive genetic changes

that eventually result in the achievement of a “growth advantage” for the transformed cancer cells [2]. Currently, several characteristics have been described, and these enable cancer cells to thrive in their acquired milieu. Eight characteristics have been named, known as the hallmarks of cancer and almost consistent with all types of cancer [3].

These survival capabilities empower cancerous cells and make them adopt a new mechanism which acts in contrast to the original anticancer defence mechanisms possessed by healthy non-cancerous cells. It is vital to have a profound comprehension of the basic hallmarks of cancer to be able to develop a range of effective anticancer therapeutic agents in addition to bringing to light possible prognostic biomarkers [4]. The initial six hallmark capabilities first proposed include; sustained proliferative signalling, evading growth suppressors, activating invasion and metastasis, enabling replicative immortality, resisting cell death and inducing angiogenesis. Latest additional two hallmarks are: evading immune surveillance and reprogramming of energy metabolism. In addition to two enabling characteristics; tumour promoting inflammation and genome instability and mutation [3] (Fig. 1.1).

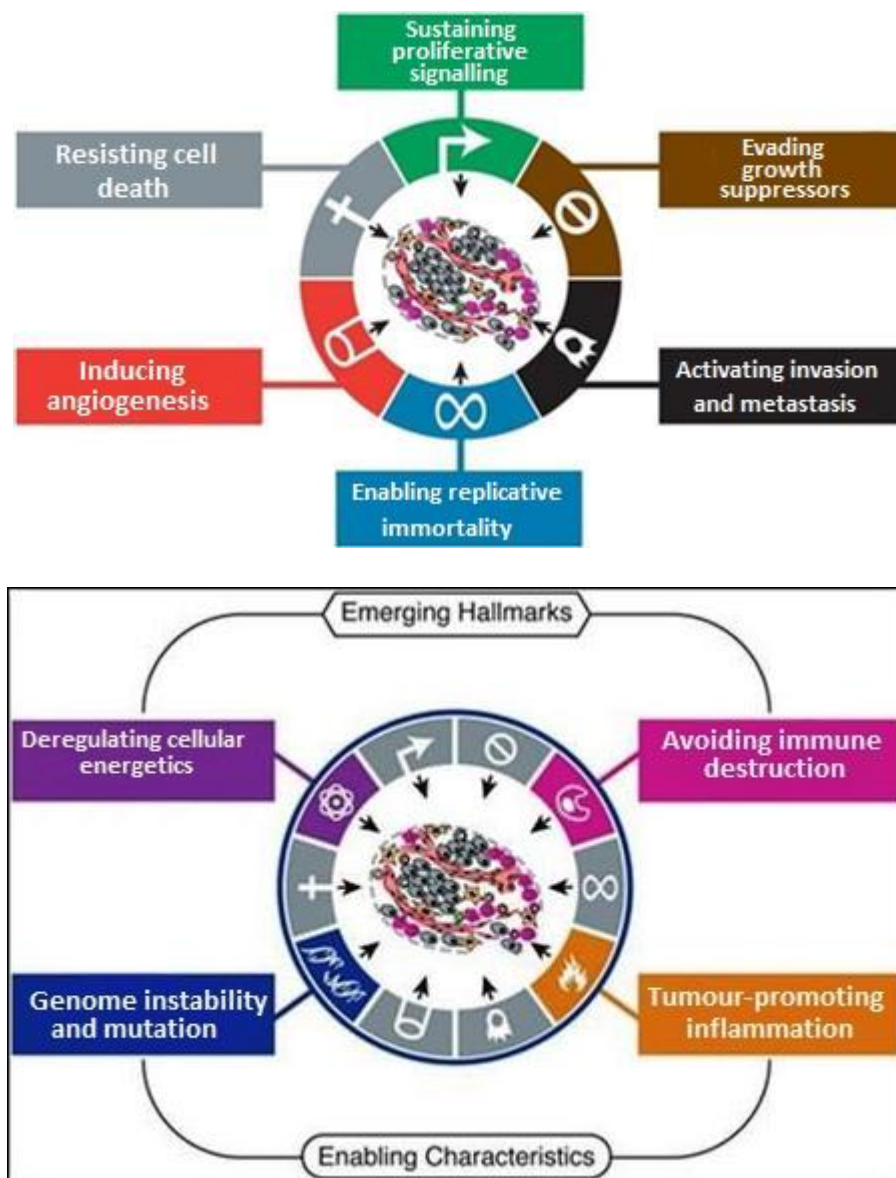


Figure 1.1. Hallmarks of cancer.

Top diagram represents the first six hallmark capabilities initially suggested. Bottom diagram shows two additional hallmarks and also two enabling characteristics identified. Adapted from Hanahan *et al* [3].

1.1.1 Sustained proliferative signalling.

Generation of signals is important in order to maintain the different cellular activities including proliferation, and this would require signalling molecules binding to membrane bound or transmembrane receptors to generate a response (Fig. 1.2) [5, 6]. The extracellular matrix (ECM) components are namely; collagen and glycoproteins [7] and soluble growth factors including, bFGF and VEGF which are examples of common signalling molecules [8-10]. These extracellular signalling molecules act as ligands, binding to specific membrane bound receptors for onward conduction of signals intracellularly. For example, the RAS- RAF-MEK1/2 pathway is stimulated by the binding of ligands such as soluble growth factors, hormones or other stimuli, resulting in the transmission of signals intracellularly, and terminating in a response that takes one form or another, for example proliferation or specific control on gene expression (Fig. 1.2) [11].

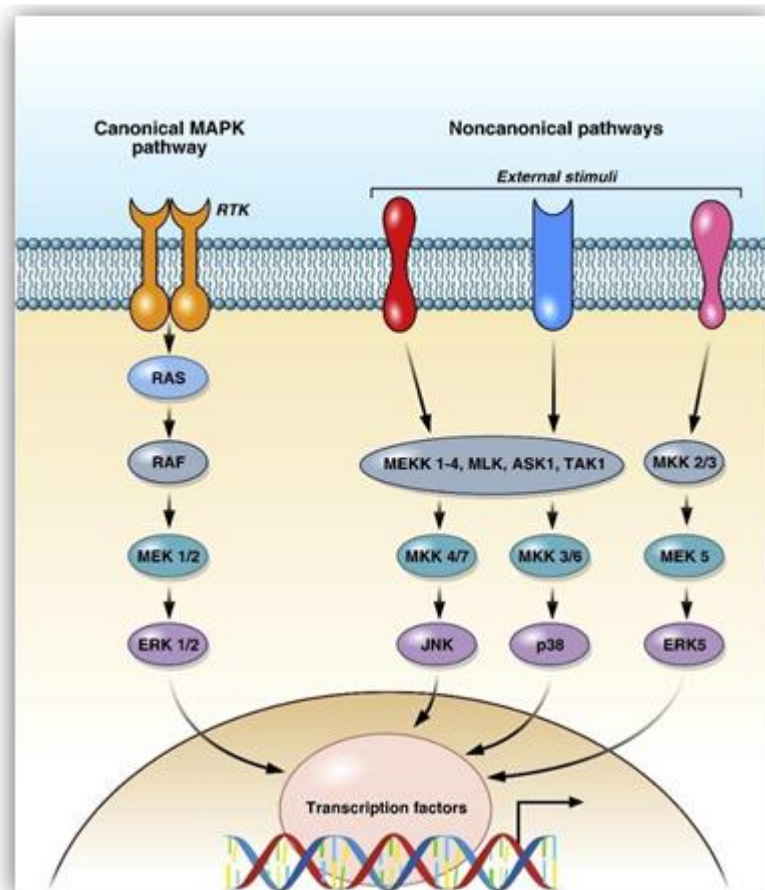


Figure 1.2. MAPK pathway.

An illustration of the MAPK pathway. The RAS- RAF-MEK1/2 pathway which is stimulated by the binding of ligands such as soluble growth factors. Adapted from Martineli *et al* [11].

Normal cells therefore rely on extracellular or exogenous molecules for the maintenance of growth or proliferation. This dependence on exogenous factors is less evident with tumour cells which are often able to mimic signal transduction by numerous means and thereby enhance / sustain cell proliferation [3], such as for instance, the hypoxia-inducible factor 1-alpha (HIF-1 α) dependent autocrine feedback which augments survival of prostate cancer cells deprived of serum [12]. Acquired growth signal autonomy is believed to be regulated by several oncogenes which act to the advantage of tumour proliferation. In the same way, the normal firmly controlled growth signal pathway may be decontrolled at any of the three different phases – the extracellular molecules, the transmembrane receptors, or the intracellular mechanism taking charge of translation of signals, for example the SOS-Ras-Raf-MAP cascade [13]. An example is the autocrine stimulation of glioblastomas by PDGF (platelet-derived growth factor) [14]. Deregulation of membrane bound receptors often presents in the form of overexpression of such receptors, that way, tumour cells become oversensitive to normal or subnormal levels of growth factors, for example up-regulated expression of EGFR has been shown to in brain and breast cancer is an example [15, 16]. The overexpressed receptors may even signal constitutively in the absence of the binding of ligands, further initiating the proliferation of tumour cells [17, 18]. Deregulation of intracellular mechanism / pathway may also occur, with that of Ras protein in the SOS-Ras-Raf-MAP cascade a notable example illustration. In this instance, Ras protein is shown to be structurally modified in approximately a quarter of all cancer patients, resulting in constitutive signalling, and this can continue even in the lack of stimulations by ligand-receptor complexing [19].

1.1.2 Insensitivity to growth inhibition signals.

For normal cell function and proliferation, growth inhibitory, as well as growth stimulatory signals are important. These signals function in a synchronized way for the homeostasis of cells, thereby ensuring controlled proliferation and growth [20]. Growth inhibitory signalling molecules, could be in the form of soluble molecules, immobilised constituents of the extracellular matrix (ECM), or in fact as cell membrane receptors [21]. TGF β , probably the best documented and of the most commonly identified negative controllers of growth, among other antigrowth factors, inhibits the phosphorylation of pRb, maintaining it in the hypophosphorylated state. In this state, pRb inhibits the action of E2F, thereby preventing it from stimulating the expression of an array of genes involved with the passage of cells from the G1 phase into the S phase [22]. Instead, cells are induced into G₀ phase from an active proliferative phase, or into a more lasting postmitotic/differentiation state [23]. To sustain cell proliferation, tumour cells are required to develop measures to escape this regulatory mechanism. Upstream deregulation of TGF β or its receptors truncates this regulatory system, leading to the hyperphosphorylation of the pRb, and for that reason increased E2F action. Finally, this results in cells shifting from the G1 phase to the S phase [24]. Examples for TGF- β are TGF- β 1, TGF- β 2, and TGF- β 3, but, TGF- β 1 has been shown to be the most common expressed one in the immune defence mechanism. [25, 26].

1.1.3 Evading apoptosis.

Apoptosis is known to be a process by which cells undergo programmed cell death, and this is characterized by blebbing of plasma membrane, cell shrinkage, condensation of chromatin, and fragmentation of DNA. After this, there is rapid engulfment of the dead cells by adjacent cells (Fig. 1.3) [27, 28]. Two groups of key regulators are involved in the apoptosis pathway; sensors and effectors. The former play a surveillance role, both within and outside the cell for anomalies such as DNA damage / hypoxia and cell attachment, and triggering programmed cell death that is accomplished by “effectors”[29]. There is also directed or targeted cell killing by means of death ligands, for example, cells expressing Fas or TNF receptors trigger apoptosis by binding to death ligands and protein cross-linking [30, 31].

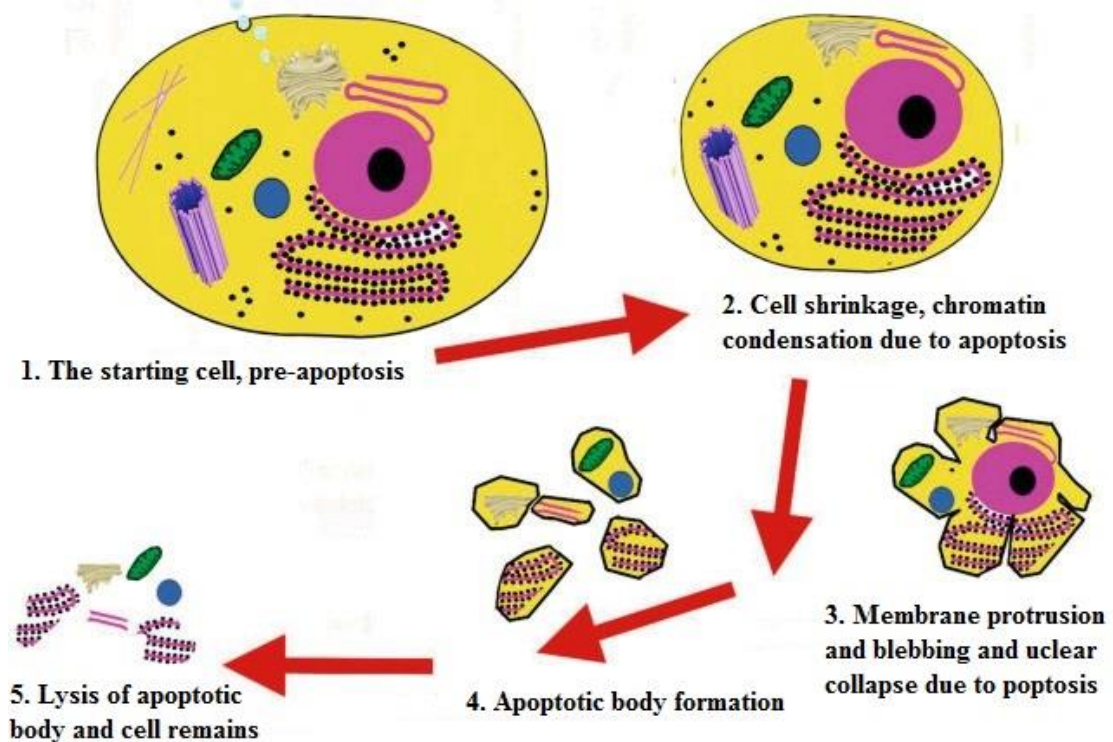


Figure 1.3. Apoptosis.

Diagram represents the different steps in the apoptosis that starts with the pre-apoptotic cell undergo cell shrinkage and chromatin condensation, followed by protrusion and blebbing of plasma membrane, formation of apoptotic bodies, and culminating by lysis of body and cell remains. Adapted from Laurence *et al* [32].

It is significant to note also that cells in general sustain their survival based on important cell-matrix and cell-cell interactions which produce signals required for normal cell function. Under normal circumstances, this inherent cell-cell / cell-matrix mechanism for supply of signal will have to be jeopardized for cell death to happen [9, 33, 34]. The mitochondrion is the power house of the cell. It is therefore no surprise that the majority of the apoptotic signals are targeted at this organelle which, in response, releases cytochrome C to herald cell destruction [35]. The Bcl-2 family controls this release, and they are either pro- or anti-apoptotic by means of their stimulation or inhibition of Cytochrome C release, respectively (Fig. 1.4) [36]. Late in the execution pathway there is creation of apoptotic bodies [30].

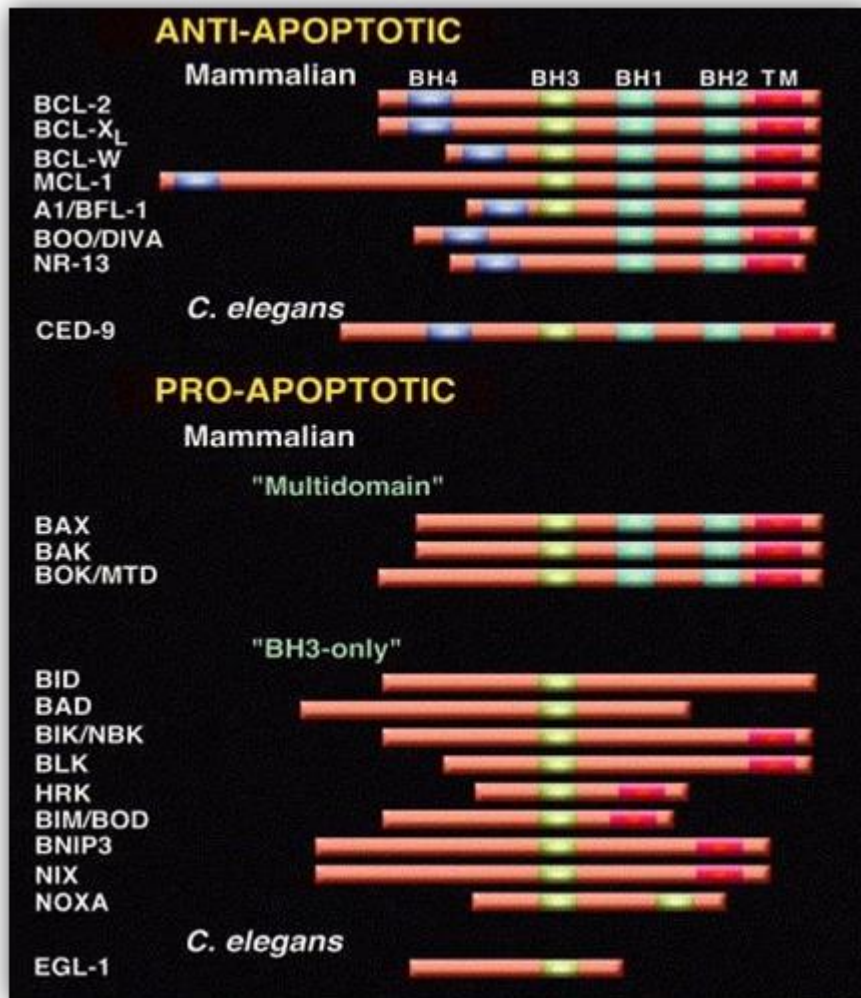


Figure 1.4. Members of the Bcl-2 family.

This diagram represents members of the Bcl-2 family of proteins. They are grouped into pro- and anti-apoptotic sub- groups by means of their stimulation or inhibition of Cytochrome C release, respectively. Also, it represents structural and functional classification of the Bcl-2 proteins. They are classified into three main groups based on conserved Bcl-2 homology (BH) domains. TM, transmembrane domain. Adapted from L. Scorrano *et al.*[36].

The caspases are the effectors of apoptosis, which ultimately generate well-ordered cell death through extrinsic and intrinsic pathways [9, 37, 38] (Fig. 1.5). They start this by commencing the execution pathway, triggered by cleavage of caspase-3. DNA fragmentation and other cellular events such as degradation of cytoskeletal and nuclear proteins, and cross linking of proteins are involved in this pathway [9, 37, 38].

Cancer cells have to develop a means of disabling the apoptotic pathway/machinery to survive and expand. Tumour cells are capable of this through a number of

mechanisms, the most frequently occurring being p53 inactivation, occurring in over half of cancer cases [39, 40]. This is no surprise, considering the transcriptional activities of p53 in general result in the activation / upregulation of downstream target genes such as MDM2. MDM2 in turn is an important negative regulator of the p53 tumour suppressor and CDKN1A (also known as p21/Waf1/CIP1), a downstream p53 effector [39, 41, 42]. These in turn are conferred with cellular activities that bring about cell cycle arrest, DNA repair, senescence and programmed cell death [39, 41, 42]. Inactivating mutations in p53 may lead to increased cell proliferation and possibly metastasis as is the case in human hepatocellular carcinoma and Kaposi's sarcoma [39, 41, 43]. It has been suggested that a variety of mechanisms involved in abrogate the apoptotic pathway are adopted by tumour cells. These mechanisms include those that bring about transcriptional / translational and post translational regulation. For example, transcriptional / translational alterations lead to overexpression of anti-apoptotic proteins and the inhibition of pro-apoptotic proteins expression [44]. The post-translational regulation on the other hand involve several mechanisms such as altered protein function, destruction of pro- apoptotic proteins and stabilization of MCL-1 [44]. For example, it has been revealed in colon and lung cancer cell lines that the presence of a false FAS receptor interferes with active FAS receptors for the pro-apoptotic FAS ligand, thus hindering apoptosis [45]. Because p53 can be activated by wide range of signals, this suggest that it is most likely the wild-type p53 has a function at different levels of tumour progression [46]. Binding of p53 as a transcription factor with DNA results in activation or repression of transcription FAS/APO-1 gene, a process that culminating in to induction of apoptosis [46, 47].

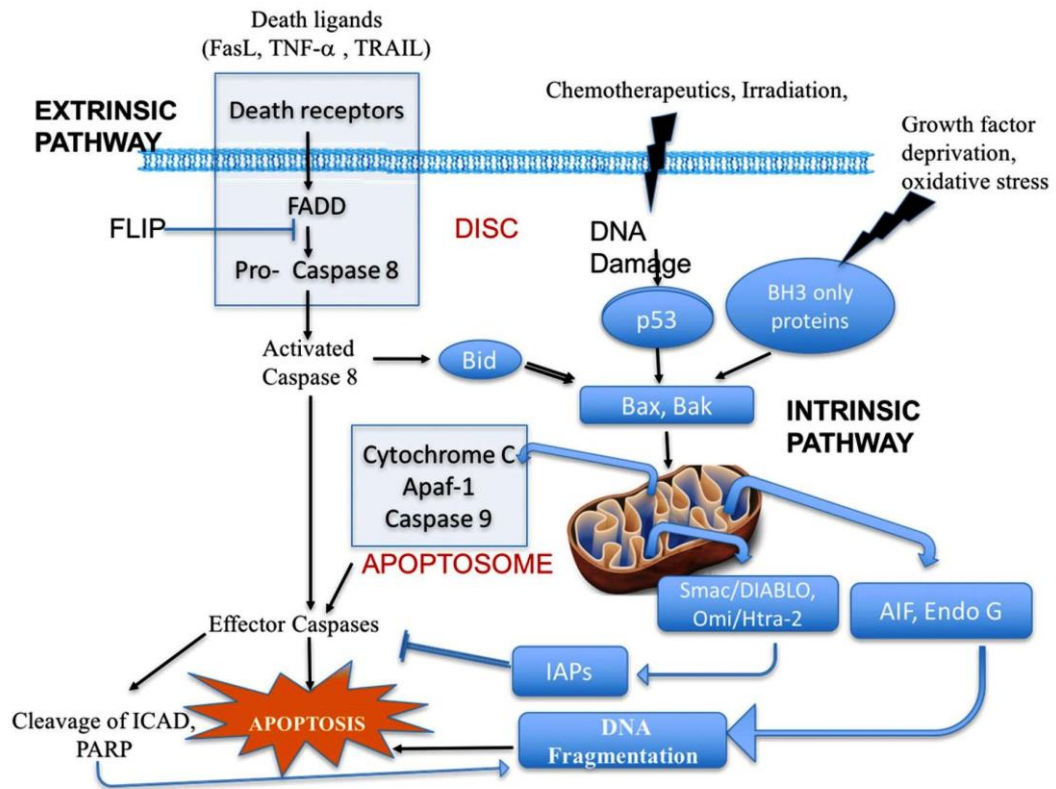


Figure 1.5. Diagram represents the intrinsic and extrinsic pathways of apoptosis. Extrinsic pathway, takes place through binding between death ligands and death receptors, leading to activation of caspase 8 and then activate the effector caspase-3 which in its turn cleaves and inhibits ICAD and PARP, results in DNA fragmentation and ultimate apoptosis. The intrinsic pathway, is mediated through growth factor deprivation and oxidative stress that stimulate BH3 only proteins, chemotherapeutics and irradiation that result in DNA damage and subsequent activation of p53, and mitochondrial ROS that induce oxidative modification of mitochondrial proteins. Such events of stimulation permeabilize the mitochondrial outer membrane and cytosolic translocation of pro-apoptotic factors comprising cytochrome c, Smac, Htra2 and CAD, activating caspase-3 and eventual DNA fragmentation. Adapted from Mishra *et al* [48].

1.1.4 Limitless replicative potential.

It is suggested that normal cells limit the number of cell divisions that they carry out by an inherent mechanism, this so-called Hayflick effect or Limit [49]. As an example, cells in culture often stop replicating after a certain number of duplications, rather than replicating endlessly. They therefore achieve a restricted range of replications and subsequently enter into a senescence stage [50]. Replication may be driven forward to a state known as the “crisis point”, where substantial cell death takes place [51]. It is believed that there is the chance for some cells to totally evade this rule and become

immortalised, replicating indefinitely, with 1 in 10^7 cells calculated to achieve this immortalised state [52]. It is hypothesised that the diversity of cell types that make up tumour masses comprise of a population of immortalised cells and cells that will eventually die [53, 54]. Limited replication that characterizes normal cells as a result of constant loss in telomere repeat length with each cycle of cell duplication. As a result of this loss, chromosomes become exposed and targets for DNA damage. Telomere maintenance is detected in malignant cells [55, 56], largely because of upregulation of the telomerase enzyme which maintains the number of telomere DNA repeats (TTAGGG) at the 3' ends of each chromosome, following cell replication [57]. By this approach, telomere shortening is not affected, cellular replication is conserved and DNA damage limited.

1.1.5 Sustained angiogenesis.

Cancer tissues are characterized by their ability to adopt angiogenic capability, thereby sustaining efficient nutrient and oxygen supply [58, 59]. For this purpose, signals are produced by soluble factors and their corresponding endothelial membrane bound receptors, typified by vascular endothelial growth factor (VEGF). VEGF in turn binds to its endothelial membrane bound tyrosine kinase receptors, neuropilin-1/2 [60]. In general, signalling by VEGF is needed for both vasculogenesis and angiogenesis. Vasculogenesis refers to formation of new blood vessels by the angioblasts [61, 62]. Angiogenesis on the other hand is formation of new blood vessels from pre-existing vasculature [63].

Endogenous inhibitors and stimulators to angiogenesis exist in reciprocal amounts, suggesting the process of vasculogenesis is tightly controlled to achieve a balance between both groups of stimulators and inhibitors [63]. Inhibiting the activity of those in favour of angiogenesis will consequently prevent angiogenesis [64]. A typical example of a powerful angiogenic inhibitors is Thrombospondin-1 (TSP-1) [65]. Synthesized, secreted and functioning in the ECM, this member of the thrombospondin family of proteins, controls angiogenesis in two ways: directly and indirectly [66]. Direct by means of physical impact on vascular endothelial cells, and indirect via modulating other angiogenic regulators [66]. Effects of inhibition exerted by TSP-1 on angiogenesis have been confirmed in several experimental models [66]. Investigators have been able to demonstrate the importance of angiogenesis or formation of new capillaries for the growth of tumours [67], and that tumours are

capable of a shift from a quiescent state of capillary formation to active angiogenesis [68].

1.1.6 Tissue invasion and metastasis.

Cancer cells invade adjacent sites and metastasise to more distant locations. Tumour metastasis is thus considered to be the setting up of secondary tumours at completely different site/sites from their primary location [69]. There are two theories with regard to tumour invasion and metastasis: the first suggests that tumours migrate from their original and primary site due to congestion, to therefore create more space [70, 71]. The other postulates that, even before crowding, and at the initial stage of tumour establishment and growth, invasion and metastasis of tumour cells may still occur [70-72] (1) to establish a distant tumour, cancer cells metastasise by first invading the surrounding stroma, then (2) travel to more distant sites via blood or lymphatic vessels before (3) moving out to create new settlements by seeding in ectopic microenvironment [73] (Fig. 1.6). According to the “seed and soil” hypothesis of tumour growth proposed by Paget, “remote organs cannot be altogether passive or indifferent regarding tumour cell embolism in blood vessels. He also concluded that cancer flourishes in a favourable environment suggesting the dependence of the seed upon the soil [74]. Invasion is a local migration through tissue into neighbouring tissue with normal/similar orthotopic microenvironment [75]. Tumour invasion and metastasis are both forms of tumour dissemination, and are considered the most lethal capabilities tumours acquire, making them more difficult to manage after spread to additional tissues [71, 76]. The most common places for tumours to metastasize involve the liver, brain, lungs, and bones. Organs such as the skin, adrenal gland, lymph nodes could also be involved. The lungs, liver and bone are the most common sites of metastases in SCC of head and neck [77]. Brain metastases is an infrequent consequence of head and neck cancers and occur most frequently in cases of breast cancer, advanced lung cancer and melanoma.[78-80]. Also, the central nervous system is another site that could be invaded by head and neck cancers through the base of the skull as a common route [81, 82] or via invasion of perineural tissue [83-85].

It has been suggested that the seeding process and the conditions of an entirely new environment will generally appear harsh on the seeded cells, but, as a result of genetic instability and heterogeneity of tumour cells, they are said to be able to generate a subset of cells with a phenotypic characteristic that enables them to withstand such

otherwise incompatible and new microenvironment [86]. Nature of tumour stroma is also a major factor for successful seeding [73, 74, 87]. It has been revealed that CAM expression (cell adhesion molecules), members of the immunoglobulin family, cadherins, and integrins by tumour cells, is a significant feature in the survival of metastatic tumours in their new location [88]. It is how the tumour cells avoid anoikis while circulating without cell-cell attachment. Anoikis is a physiological process for tissue homeostasis and development. It inhibits detached epithelial cells from recolonization in other places, thus preventing dysplastic cell growth or attachment to an improper matrix. Dysregulation of anoikis, such as anoikis resistance, is an important event in tumour metastasis. Acquiring anoikis resistance by cancer cells enable them to survive after being detached from the primary site and during their travel within the vascular system till they are able to colonise a distant location [89, 90].

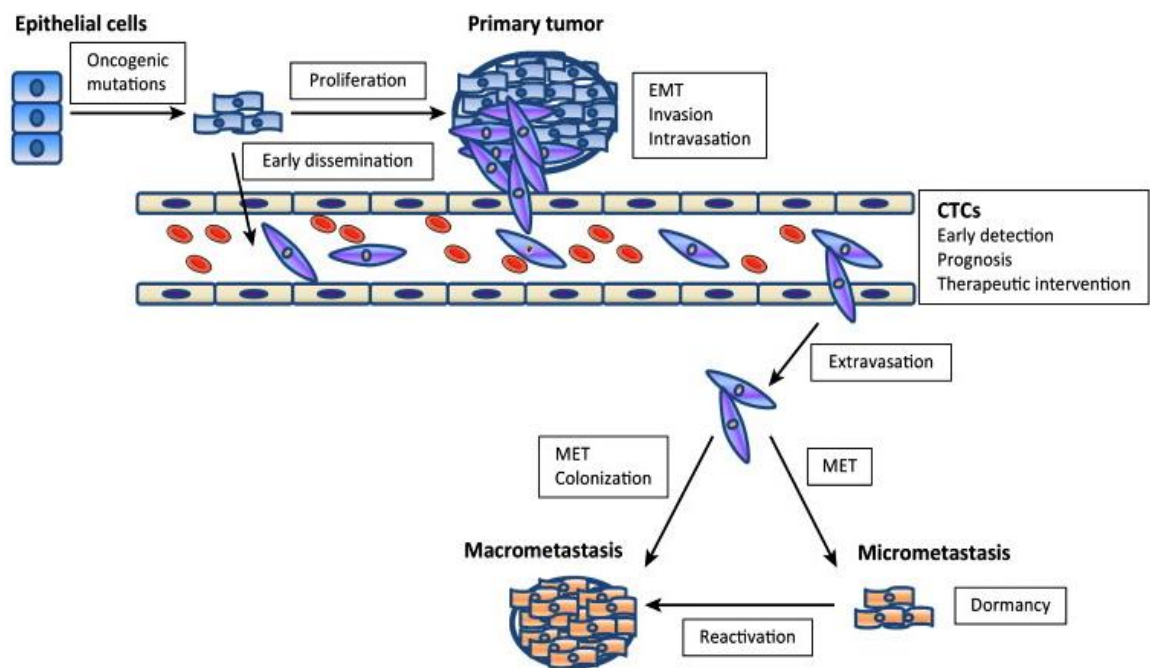


Figure 1.6. The tumour invasion–metastasis cascade.

Metastasis involves a series of discrete steps, starting with local invasion, followed by intravasation of tumour cells into blood as well as lymphatic vessels. There is thereafter transit of circulating tumour cells (CTCs) through the vasculature, followed by extravasation to the parenchyma of distant organs, and finally proliferation from micrometastases into macrometastases. Adapted from Yutong *et al* [91].

1.1.7 Reprogramming energy metabolism.

In general, neoplasia involves augmented tissue growth and proliferation. That way, the requirement for energy metabolism is increased. Physiologically, healthy cells under aerobic conditions are known to convert glucose into pyruvate through a metabolic process called glycolysis occurring mostly in the cytosol of cells [92, 93]. The resultant pyruvate is directed into the mitochondria for onward CO₂ production in the presence of a positive gradient in oxygen concentration which supports this mitochondrial reaction [94]. It is therefore the normal trend to have more pyruvate channelled into the mitochondria for conversion into CO₂, a process known as oxidative phosphorylation (OXPHOS), in aerobic conditions.

Tumour cells are subjected to unique physiological pressures of the tumour microenvironment, these stresses include hypoxia, acidosis and increased interstitial fluid pressure[95]. One of the adaptations tumour cells may undergo to survive under these unfavourable conditions is to alter their metabolic phenotype. It has been shown that tumour cells have the ability to act in the contrary, rather favouring reaction in the opposite direction- a condition termed as 'Warburg effect', first described by Warburg, and also known as aerobic glycolysis [96, 97].

OXPHOS will usually produce copious ATP, hence, a metabolic switch in favour of glycolysis will endure shortage in ATP, put at in the region of 18 fold less. To reimburse this reduction in the efficiency of energy production (ATP), cancer cells raise their glucose uptake to compensate by means of increased glycolysis. They attain this by the upregulation of glucose transporters like GLUT1 [98]. It has also been demonstrated that this increased glycolysis is associated with tumour suppressor genes such as p53 as well as oncogenes such as MYC and RAS[99]. As an example, p53 seems to oppose alterations of metabolism related to development of cancer, by this way it is neutralising the conversion to glycolysis. p53 inactivate the phosphoglycerate mutase (glycolytic enzyme) by increasing the activity of proteosomal degradation and the ubiquitylation [100, 101]. By means of this capability, cancer cells are able to cope with a hypoxic condition predominantly attributable to excessive oxygen demand and potential cell / tissue overcrowding. They are therefore able to upregulate transcription factors in favour of glycolysis such as HIF1 α and HIF2 α , as well as glucose transporters [102]. Under hypoxia, however, the HIF-1 α protein is stabilised and able to bind with HIF-1 β to form HIF-1, a potent transcription factor involved in the

regulation of glycolysis. HIF-1 binds to HREs (5'-RCGTG-3') in the promoter region of the MCT4 target gene. It is assumed that the amplified glycolysis offers essential substrates for the supply of amino acids, indispensable for the assembly of new cells and their organelles [103]. Metabolic symbiosis is another adaptive feature that tumour cells may undergo [104]. This model is discussed in details in (1.3.4 of this thesis). It may therefore be suggested that this hallmark may not exactly be applicable to all tumour cells and that the metabolic twist may simply be one of the routine adaptation features for cells in general, and maybe more with tumour cells.

1.1.8 Evading immune surveillance

To become established, tumour cells need to develop means by which they are able to escape immune surveillance, as there is always a constant surveillance for tumours by the immune system. The important surveillance role of the immune system against the development of cancer may be strengthened by the fact that the occurrence of certain types of cancer rises in patients with compromised immune system [105].

To demonstrate the importance of the immune system as it opposes tumour formation, an experiment using immunodeficient mice revealed that a deficiency in either T cells or natural killer cells (NK) increased susceptibility to tumour formation [106]. Also, transplantation research showed that, slightly immunogenic cancer cells arising from immunocompromised primary hosts fail to thrive when seeded onto immunocompetent secondary hosts, in contrast to when they are transplanted onto correspondingly vulnerable secondary hosts [107]. In the same way, patients who have organ transplants may grow donor-derived tumours because of their suppressed immunity, while their donors have had the cancer cells quiescent, probably due to their improved immunity [108]. Clinically and epidemiologically, colon and ovarian tumours are believed to be less aggressive after massive infiltration with both cytotoxic T lymphocytes (CTLs) and NK cells, in contrast to those that are deficient in the immune cells [109]. An apparent deviation in this emerging hallmark is the fact that there is currently no data indicating immunocompromised patients are forming a higher percentage of cancer cases.

1.1.9 Tumour-promoting inflammation

Immune / inflammatory cells infiltration to some extent does occur in every tumour [109]. It is believed that the infiltrating immune cells, chiefly those of the innate

immune system favour tumour growth, as against acting in the opposite which is more logical [110]. It is suggested that the mechanism by which they attain this is related to the inflammatory cells increasing the bioavailability of vital molecules, e.g. growth factors, survival factors, proangiogenic factors and probably ECM anchorage factors [110, 111]. Collectively, all of these function together to promote tumour invasion and metastasis [110, 111]. Furthermore, the inflammatory cells probably augment the release of reactive oxygen species (ROS) which favour establishment of cancer cells and induce malignancy [112].

During cancer development the immune cells play different regulatory roles [110]. It has been thought that presence of leukocytes in and around developing tumours signify the host's attempt to eliminate cancer cells. Actually, leukocytes such as CD8+ cytotoxic T lymphocytes (CTLs) and natural killer (NK) cells, perform an important function in limiting tumour progression (Anti-tumour programming) [110]. These anti-tumour systems can be restrained by a different subset of leukocytes that act to promote tumour progression (Pro-tumour programming) [110]. It has been indicated that these two antagonist functions of leukocytes are dynamic.

Tumour-immune surveillance programmes are induced through Type 1 T helper (TH1) cells, or alternatively by the activation of macrophages and dendritic cells (DCs), and neutrophils via regulatory T cells (TREGs) and Type 2 T helper (TH2) cells [110]. This programme has been shown to be implicated in supporting and enhancing tumour progression. Several studies about TREGs in humans revealed that they are a specialized type of T cell and are able to hinder macrophages from being activated [110]. Instead of that, TREGs promote immunosuppressive myeloid phenotypes via their ability to produce Interleukin 10 (IL10) and TGF β [110, 113]. A recent report about the role of neutrophils in tumour immunity showed that a lack of TGF β signalling by inhibiting activin receptor-like kinases (ALK4/5) leads to mobilisation of a subpopulation of neutrophils known as N1-polarized neutrophils, characterised by their bioactivities to destroy tumour cells [110, 114]. In the tumour microenvironment, production of TGF β by different cell types suggests that TREGs inhibit N1 tumoricidal actions by producing the TGF β and therefore, support pro-tumour N2 or immature monocyte (IMC) phenotypes. These information from different studies shows that the equilibrium state between TH1 and TH2/TREG effects

controls the pro-tumour programming against anti-tumour programming of tumour associated myeloid cells [110].

Programmed cell death protein-1 (PD-1), expressed on the surface of T cells, considered to be a vital immune checkpoint protein. Binding between PD-1 and its ligands, namely programmed cell death protein ligand 1 (PD-L1) and programmed cell death protein ligand 2, results in significant downregulation of T cell activity and cytokine production. Such kind of effect is contrary to the biological characteristics of treatments which aim to target cytotoxic T lymphocyte associated protein 4 (CTLA-4), and PD-1/PD-L1 blockage is currently regarded as “tumour site immune modulation therapy”. [115]. The PD-1 pathway blockage by means of monoclonal antibodies to PD-1 or PD-L1 is able to prompt the immune system to eliminate cancer cells, and this method has shown significant anti-tumour efficacy, in comparison with standard first-line and second-line chemotherapy for Non-small-cell lung carcinoma (NSCLC) in its advanced stage [115].

1.1.10 The p53 gene in relation to cell cycle and apoptosis.

This transcription factor activates numerous genes and leads to arrest of the cellular cycle and cellular repair or apoptosis [116]. The p53 as tumour suppressor gene is involved in different types of tumours where it serves both as a gene-specific transcription factor and as a specific inhibitor of the transcription of particular genes. The two outcomes of re-expression of wild type p53 in cancer cells not expressing wild type p53, are G1 arrest and apoptosis [116, 117]. In cases where p53 is activated as a transcription factor, there is the expression of p21 WAF1/CIP1/Sdi1, an inhibitor of the cyclin dependent kinases (CDKs)2, 3, 4 and 6, which contributes to the cellular arrest occurring between G1-S transition. Therefore, arrest of G1 can develop basically by the p53 induced expression of p21 WAF1/CIP1/Sdi1. BAX, a homologue of the BCL-2 gene is one of the other genes regulated by p53. Bax simply speeds up the rate at which apoptosis proceeds. P53 has also been shown to down-regulate the expression of cyclin A, producing a secondary break in cell cycle progression into / through the S phase [116, 117].

Eventually, the outcome of the diverse mechanisms of action of p53 is to preserve the cellular genomic stability. Therefore, lack of this protein results in genomic instability

of the cell, the build-up of mutations and increase in tumorigenesis [116]. It has been revealed that fifty to fifty-five percent of all types of human cancer appear as a result of mutations presented by p53 [116]. These mutations are primarily found in DNA binding domain of the protein and leads to lack of its biological activity. Often, tumours that show presence of wild type p53 have an improved response to therapy in comparison to those that demonstrate presence of p53 mutations [116]. Understanding of the role of p53 in cancer development and progression could provide new leads about gene therapy for cancer as a part of the general therapeutic strategies.

1.1.11 Genome instability

It is generally accepted that for cells to become cancerous, on the basis of genetic changes, mutations accumulate to trigger or sustain carcinogenesis [118]. Healthy cells under normal physiological conditions are therefore unlikely to become cancerous, having inherent checks against cell cycle aberrations in addition to mechanisms in place for repair of damaged DNA [119]. That cancer occurrence is generally more than expected does suggest that cancer cells may be more susceptible to mutations, for them to be able to acquire a sufficient number of mutations put together to trigger carcinogenesis [3].

Accumulation of mutations is a characteristic of cancer cells and may be an initiating factor (ie DNA damage and mutation occurs in normal cells and if inactivating mutations occur in DNA repair mechanisms then the cells are more likely to accumulate additional mutations that may then lead to cancer). For instance, in colorectal cancer (CRC), DNA repair is usually deviant, resulting in an accumulation of mutations [120]. Colorectal cancers could be categorised depending on the patterns of expression of Mismatch repair (MMR) proteins. MMR proteins are nuclear enzymes, important in base-base mismatch repair that arise throughout DNA replication in cells under proliferation. These proteins act by forming complexes (heterodimers) that in their turn bind to areas of abnormal DNA and initiate its elimination. A lack of these proteins result in an increase in DNA replication errors, especially where the genome has areas of short repetitive nucleotide sequences, an event called microsatellite instability (MSI). MSI has been observed in large proportion of colorectal cancers that occur in individuals with Lynch syndrome (above 90%), whereas in sporadic CRC it is seen in about 15% of patients [121]. An example

is the loss of function of the p53 DNA damage repair pathway, observed in many types of cancer [122, 123].

In BRCA1 and BRCA2, two genes commonly implicated in hereditary breast cancer, mutations are behind about 80-90% of cases, but less common in sporadic breast cancers [124]. Reduced expression of these tumour suppressors, BRCA1 or BRCA2, essential for an accurate repair of double-strand DNA breaks, render cells incapable to repair double strand breaks by homologous recombination pathway [125, 126] and as a result repair continues via error-prone pathways. These cells may acquire mutations during strand repair and often accumulate chromosomal rearrangements. This in turn leads to the emergence of a dominant cell lineage that acquires the capabilities of autonomous cell division and of metastatic potential [125, 126]. Following DNA damage, activation of both S- and G2/M-phase cell-cycle arrest requires BRCA1. It has been shown that the G2/M-phase cell-cycle arrest rely on preceding phosphorylation of BRCA1 via the master checkpoint kinase ATM (ataxia telangiectasia mutated) [127], which causes Ataxia telangiectasia (AT), an autosomal recessive genetic cancer syndrome. Carriers of this syndrome are heterozygous for ATM mutations and seem to be susceptible to develop breast cancer by age 50 (about 11%) and by age 70 (about 30%). Germline missense mutations result in a stable protein but functions abnormally in a dominant negative fashion and constrains the normal ATM protein. In contrast, truncating mutations gives rise to an unstable as well as abnormal ATM protein associated with high risk of developing breast cancer [124].

Polymorphisms in DNA repair genes results in attenuation in the capacity of DNA repair, particularly when they get exposed to endogenous and exogenous genotoxic factors, and this again can be classified as additional risk factors for breast cancer. Another gene involved in base excision repair, One XRCC1 399Q variant allele, has been demonstrated to augment risk of breast cancer in carriers from African-American ethnic group [124].

It has been found that the majority of cancer cells (70–90%) show presence of an abnormality in chromosome numbers, a state termed aneuploidy [128, 129]. Characteristically, aneuploidy indicates the gain or loss of entire chromosomes (whole chromosome aneuploidy), while structural (or segmental) aneuploidy signifies amplification or loss of fragments of chromosomes [129]. Frequency of aneuploidy in

cancer cells denotes a robust association between both mitosis and oncogenesis [129]. DNA damage and breakage is another example of generation of aneuploidy, which can cause chromosomal deletions, duplications and translocations, leading to partial aneuploidy [129].

Cells exposed to ionizing radiation producing numerous DNA damage demonstrate augmented frequency of structural chromosomal aberrations, for example dicentric chromosomes and chromosomal translocation, in relation to radiation dose. It has been revealed that aneuploidy is associated with reduced proliferation in many organisms and also has detrimental effect in cells, causing lethal developmental defects [129-131]. Aneuploidy leads to gene modifications which corresponds to the changes in gene copy number [129, 132, 133], with the resultant altered gene expression responsible for the decreased cellular fitness of the aneuploid cells [129, 134]. Because of altered expression of considerable number of genes (imbalanced gene expression) from the aneuploidy chromosomes, imbalance in vital proteins causes loss of control in the maintenance of protein homeostasis, a state that may have an effect on multiple cellular functions and signalling pathways, displaying gene-specific phenotypes that lead to proteotoxic stress [129, 135].

It has been proposed that proteotoxic stress has a significant function in the decreased cellular fitness in cells with aneuploid. The increase in expression of proteins leads to the titration (a loss) of chaperones necessary for proper protein folding. Aneuploid yeast strains are susceptible to form protein aggregates, signifying impaired folding [129, 133, 134]. Aneuploid yeast cells display not only increase in frequencies of chromosome loss, but also increase in frequencies of mutation [129, 136]. It has been described that in aneuploid yeast cells as well as in human cells, the DNA replication is impaired by DNA replication stress resulting in increase in the formation of DNA double-strand-breaks (DSBs) that lead to low degrees of DNA damage. Cell adapts to this type of damage and undergoing mitosis, might result in chromosomal translocations and deletions (chromosomal rearrangements) [129, 137].

Aneuploidy is thought to be implicated in many diseases e.g. Down syndrome and Alzheimer's disease. Down syndrome reveal a raised risk of leukaemia, but, remarkably, prevalence of solid tumours is lower compared with that of euploid individuals [129, 138]. Genes on chromosome 21 potentially implicated in the

suppression of tumorigenesis have been described [139]. Link between certain types of cancer and certain karyotypic patterns as cancer cells frequently demonstrate complicated karyotypes [129, 140]. Involvement of Aneuploidy in developing of neurodegenerative diseases e.g. Alzheimer's disease has also been pointed out [141-143]. Proteotoxic stress that is associated with aneuploidy is probably involved in the pathogenesis, as presence of a relationship between protein misfolding and neurodegeneration is acknowledged. Down syndrome increases susceptibility to Alzheimer's disease and age acceleration [129, 144].

Developments in the molecular-genetic analysis of cancer cell genomes have come up with the strongest explanations about mutations related to alteration in the function and of enduring genomic instability in the course of tumour progression. Comparative genomic hybridization (CGH) is one type of analysis that shows the gains/losses of gene copy number throughout the cell genome; in different types of tumours, the prevalent genomic aberrations disclosed by CGH afford obvious proof for loss of control of genome integrity [3]. Significantly, the reappearance of certain aberrations (both amplifications and deletions) at certain sites in the genome denotes that this kind of sites are likely to accommodate genes with alterations, leading to tumorigenesis [3, 145]

Accordingly, it is clear that genome instability enables the acquisition of hallmark capabilities [3]. The technique of CGH enable visualizing the present or missing chromosomes or parts of chromosomes in a tumour sample using fluorescence microscopy. Array CGH is analogous to CGH, with the exception of the labelled DNAs which are not hybridized to metaphase spreads, but to DNA molecules on a glass slide, resulting in an increase in the resolution. Genetic analyses in HNSCCs also strongly show the presence of other subclasses of this type of cancers. This first obvious distinction is the difference between HPV+ cancers (high-risk types of this virus), compared with HPV-. Furthermore, it was observed via karyotyping and ploidy investigation that subgroups of cancers are diploid or near-diploid, and most of them are aneuploid [146-148].

Recently, these findings have been confirmed by demonstrating that, at 1 megabase resolution, approximately 20% of HPV- HNSCCs appear to have only a few copy-number alterations, proposing presence of a near-normal chromosome number. [146,

149]. These reports show a separate group of cancers with an apparently near-normal genome. The few experiments with available data highlight the heterogeneity in HNSCC, at both the molecular as well as clinical levels [146, 147]. Aneuploidy is a condition that represents the karyotype of cell and can originate in several ways [150]. The preponderance of aneuploid tumours have chromosome numbers within the range of diploid cells i.e. 40–60 chromosomes preponderance. Because aneuploidy describes a condition associated with an abnormal number of chromosomes, it can be identified by any method that quantifies chromosome numbers, including karyotype analysis, fluorescence in situ hybridization, spectral karyotyping, or array-based comparative genomic hybridization analyses [150].

It has been reported that loss of heterozygosity (LOH) in HNSCCs is taking place at particular chromosomal loci, and a genetic progression model that is founded upon patterns of LOH in HNSCCs has been suggested [151]. For instance, several losses at chromosome arms 3p, 9p, and/or 17p, which are usually observed in precursor lesions, are regarded as early markers of carcinogenesis in HNSCC. They are likely to give rise to loss of tumour suppressor genes (TSGs) that have been mapped to these loci; such would be responsible for providing an advantage in growth for the cells [151-157]. LOH at 17p13 is believed to include TP53, while LOH at 9p21 is believed to include INK4a, the tumour suppressor gene encoding p16 [157]. The latter gene is regularly inactivated by chromosomal loss or by hypermethylation in the large proportion of HNSCC precursors [157]. Furthermore, inactivation of INK4a is the most frequent way of disrupting the pRb pathway in HNSCCs associated with tobacco as an etiological factor [158]. LOH have been used to detect regions on chromosomes that might have putative tumour suppressor genes (TSGs). TSGs are believed to encode proteins that adversely regulate cell growth and consequently suppress tumorigenesis, thus, loss of TSG function is crucial during carcinogenesis [159]. Genetic alterations associated with oral squamous cell carcinoma (OSCC) have been demonstrated, with allelic loss at certain chromosomal regions believed to also indicate the presence of TSGs [159].

Potential locations for these genes can be identified by means of the LOH analysis [159, 160]. The allelotyping investigations in OSCCs have revealed several chromosomal regions in which LOH was often seen. Indicating possible involvement of a number of TSGs in the carcinogenesis of OSCC. With the exception of X and Y

chromosomes, multiple LOHs were seen at different loci on the other chromosomes. For instance, in OSCC, LOHs were detected in high frequency on chromosome 3 in particular, the short arm (3p) [159, 161]. LOH has been shown to be more in regions, 3p13-p21.1, 3p21.3-p23, and 3p25, with as high as 2-3 TSGs on 3p already demonstrated [159, 161]. In OSCC, it has been observed that the FHIT gene is localized to 3p14.2 and shows an alteration with decreased or aberrant protein without presence of mutations and deletions [159, 162-164].

1.2 The cancer microenvironment

1.2.1 Cancer-Associated Fibroblasts (CAFs)/ myofibroblasts

The tumour microenvironment is the complex that accommodates intracellular and intercellular interactions involved with cancer metabolism. It is composed of stromal cells, immune/inflammatory cells, vessels and the ECM (Fig. 1.7) [3]. The immune /inflammatory and vascular components have been discussed above (see sections 1.1.5, 1.1.8 and 1.1.9). The stromal cells and matrix are examined here.

Cancer cells are able to influence the metabolism of the microenvironment so that a “niche” favouring their growth is established. CAFs have been shown to affect tumour cells, proliferation, angiogenesis, invasion and metastasis. [165]. Such events also involve hydrogen peroxide (H_2O_2), $HIF1\alpha$ and $NF\kappa B$ produced by the cancer cells [166, 167].

Recent research has drawn attention to the significance of the so called CAFs or myofibroblasts in the tumour microenvironment as they seem able to influence tumour progression and the invasion process in particular. CAFs appear morphologically spindle shaped, resembling conventional fibroblasts, and are not neoplastic [165]. They are now recognised as a significant cell type in the tumour microenvironment.

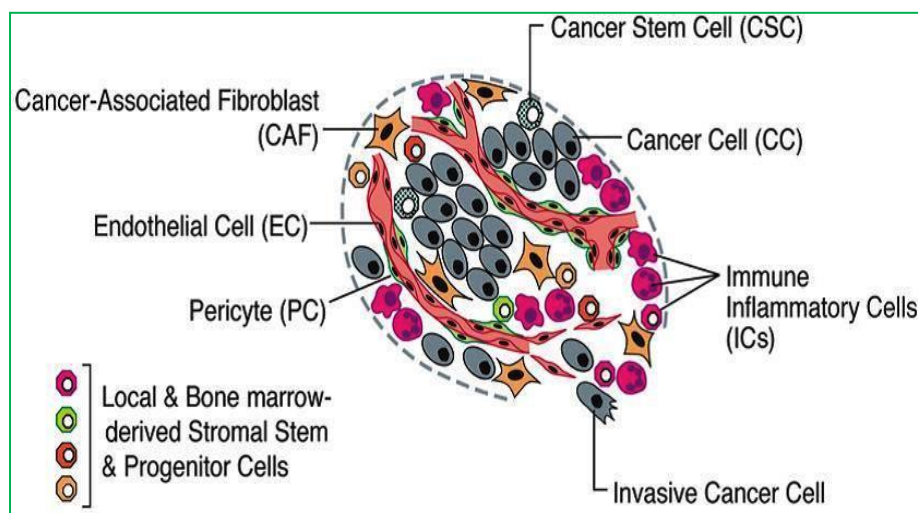


Figure 1.7. Showing a collection of distinct cell types that make up the tumour microenvironment in solid tumours.

Both parenchyma and the stroma of tumours have distinct cell types and subtypes which play important roles in the support of tumour growth and progression. The associated immune / inflammatory cells comprise two subclasses; tumour-promoting as well as tumour-killing. From Hanahan *et al* [3].

Despite the morphological resemblance, CAFs are distinct from fibroblasts as they express specific proteins. These proteins include alpha-smooth muscle actin (α SMA), cell-surface serine protease fibroblast-activation protein α (FAP α), fibroblast-specific protein 1 (FSP-1), neuroglial antigen-2 (NG2), platelet-derived growth factor receptor- β (PDGFR- β), fibroblast-associated antigen and prolyl 4-hydroxylase [165, 168]. Expression of these proteins can be immunohistochemically assessed and α SMA is a widely used, conventional marker for the routine detection of CAFs in the tumour microenvironment [169, 170]. However, caution should be exercised because none of these proteins is exclusively expressed in CAFs [165]. Together with α SMA, the expression of prolyl 4-hydroxylase, suggestive of ability to synthesis collagen account for the alternative designation of CAFs as myofibroblasts.

The origin of CAFs has not been proven. It has been suggested that throughout tumour formation and progression, a variety of cell types transdifferentiate to CAFs via the influence of local and distant signals [165, 171, 172]. Resident tissue fibroblasts and their variants as well as mesenchymal stem cells are possible candidates for the origin of CAFs [165, 173] [174]. Other possible sources are bone marrow-derived cells [165, 175]. α SMA+ myofibroblasts may even be derived from adipose tissues [175]. Finally, endothelial and epithelial cells may transform into CAFs via endothelial-mesenchymal transition (EndMT) and local epithelial-mesenchymal transition (EMT), in response to stimuli from surrounding cells [165, 176, 177]. The precise percentage of the contributing cells for CAFs in human cancers is unknown [165], but in an experimental setting this is influenced by the conditions of the experiment and thus may be manipulated [165].

At least two distinct groups of CAFs are now recognised: Those arising via reprogramming of fibroblasts and those arising from myofibroblasts, the latter being characterized by the expression of α SMA [165]. Although myofibroblasts may be inconspicuous in non-diseased tissue, they increase in wound healing and chronic inflammation and are of significance in pathological fibrosis affecting liver, lung, and kidney [165].

CAFs secrete various ECM components, and thus contribute to the formation of the desmoplastic stroma typifying several carcinomas (see 1.2.2). Throughout this thesis, the terms CAFs and myofibroblasts are used indiscriminately.

Another method of classifying CAFs is based on distinguishing active and senescent forms. Both seem capable of promoting tumorigenesis, though via different pathways. Fibroblast activation and senescence are two stress responses which commonly appear in CAFs [178]. It is believed that these two forms of stress responses are clinically significant and essential for the pathogenesis of OSCC [178]. Several investigations have focused on the importance of CAFs and showed that they occur in elevated levels in oral cancer and this is tightly linked to progression of cancer, invasion, recurrence and poor prognosis [178-180]. Also, a high degree of association has been found between fibroblast activation and patient mortality irrespective of the stage of the disease and it seems to be a preferable prediction factor for prognosis when compared to the TNM staging system [169, 178]. Therefore, from a diagnosis point of view, it has been shown that identifying activated CAFs in oral tumours is regarded as a significant indicator about how these tumour behave as well as about the patient's outcome [178]. Fibroblast senescence is known to be induced as a result of a number of primary risk factors related to oral cancer and these factors include agents such as alcohol and tobacco. Also, it has been reported that fibroblast senescence is precedent to dysplasia in cases of premalignant lesion oral sub-mucous fibrosis [178, 181].

It has been observed that human fibroblasts in culture are not able to keep proliferating indefinitely. In spite of their viability and being metabolically active, fibroblasts eventually lose the ability to divide [182] and thus reach a senescence, which may be induced by persistent DNA damage. Generally, senescence is a state characterised by a permanent stop to growth; it is distinguished from quiescence by the presence of an increased level of p16INK4A. Oxidative stress resulting from mitochondrial dysfunction, overexpression of oncogenes [183] and the effects of chemo-/radio-therapy, are known to cause DNA damage and thus indirectly effect senescence.

Severe and irreversible cell damage leads to senescence in tumours of epithelial origin. In this case, the cell damage overpowers the DNA repair process, and the resultant senescence plays the important role as tumour suppressor. Cancer cells are thought to bypass this suppression by means of inactivation processes of the p53 and p16INK4A/pRB signalling pathways [184]. Conversely, senescence of stromal fibroblasts act as promoter for the tumour. Investigations showed that growth of premalignant epithelial cancer cells, originating from human prostate or lung, can be stimulated by co-culturing them with senescent fibroblasts. This type of co-culturing

also results in stimulation of migration and invasion of tumour cells [185]. The importance of the stimulation of senescent cells on the progression of epithelial cancer cells has recently been highlighted. Notably, senescent cells produce different types of pro-tumorigenic proteins, named the senescence-associated secretory phenotype (SASP) [186].

The SASP proteins involve a number of soluble and insoluble factors. These factors have the ability to produce an effect on adjacent cells via stimulating different receptors on cell-surface and related signal transduction pathways which can result in several diseases such as cancers [187]. In general, SASP can be classified into the following three main groups:

(1) Soluble signalling factors that includes interleukins, chemokines and growth factors [187].

(2) Secreted proteases. This group can have three main functions [187]:

- Exfoliation of membrane-associated proteins, which leads to production of soluble forms of membrane-bound receptors.
- Degeneration of signalling molecules.
- Degeneration of the ECM.

(3) Secreted insoluble proteins/extracellular matrix (ECM) components [187].

These effects offer powerful means through them senescent cells can make modifications in the tissue microenvironment [187].

Fibroblast senescence has been demonstrated to play important roles in epithelial proliferation, differentiation, cellular metabolism and genetic instability, thereby promoting cancer cell invasion, metastasis and resistance to therapy. Fibroblast senescence also causes induction of the EMT in two nonaggressive human breast cancer cell lines (T47D and ZR75.1) [178, 188].

These interactions between senescent fibroblasts and cancer cells are reported to be mediated significantly by the TGF- β [189-191]. The tumour-derived epithelial TGF- β functions jointly with ROS in order to stimulate both activation and senescence of fibroblasts [189]. As a consequence of induction of CAF senescence, the CAF-derived TGF- β and MMP2 jointly mediate induction of EMT in tumour cells in association

with downregulation of a wide array of adhesion molecules of epithelial cells. Downregulation of adhesion molecules such as e-cadherin, desmoglein 1 and 3, desmoplakin, desmocollin, b-catenin and plakophilin) result in discohesion of keratinocytes and promotes epithelial invasion in vitro [192]. Also, lack of p53 has been demonstrated to augment at a minimum, a cohort of the SASP, including molecules such as the interleukins [188].

Some difference between active and senescent fibroblasts are:

In general, quiescent fibroblasts are extended and narrow in thickness (thin cells) with prolongations at both ends giving them a fusiform or spindle-like appearance, in contrast to activated fibroblasts which are cruciform or stellate in their shape [193, 194]. Quiescent fibroblasts are characterised by several features such as being metabolically inactive, having G0/G1 cell cycle arrest, not producing extracellular matrix as well as missing the ability to migrate. However, they are able to react with growth factors and be converted to activated fibroblasts [193]. Upon activation, quiescent fibroblasts display features of proliferation and migration and also production of ECM and growth factors [193]. It has been proposed that they are fibroblast-specific protein 1 (FSP1) and $\alpha1\beta1$ integrin positive [193, 195]. Quiescent fibroblasts are epigenetically stable and do not show active secretome. The differentiation property that quiescent fibroblasts possess is thought to enable them play a peculiar role [193]. Quiescent fibroblasts are able to differentiate initially into activated fibroblasts and afterward, according to receiving suitable stimuli, produce other varieties of mesenchymal cells, for example adipocytes, chondrocytes, and endothelial cells [193]. Based on this property quiescent fibroblasts could be regarded as adult tissue resident mesenchymal stem cells [193]. Activated fibroblasts are metabolically active and display abundant activities such as synthesis of proteins and contractility which is important for several vital functions, for example the wound closure and generation of connective tissue [193]. They express specific proteins including α SMA, FAP α and PDGFR- β [165, 168]. Compared to quiescent fibroblasts, they are epigenetically modified. These activated fibroblasts are regarded as very heterogeneous cells, with different patterns of expression based on the variant tissues of their origin [193, 196].

The process of fibroblast activation involves a group of metabolic changes to obtain an active state of functional and metabolic conversion resulting in sustained proliferation, cellular mobility and activated secretory functions [193]. Mitochondrial respiration of cancer cells may be supported by the increase in lactic acid, ketone bodies and fatty acid created by the glycolytic CAFs and accompanied with invasion and resistance features of cancer cells [193]. CAFs may have the ability to control the bioavailability of metabolites for immune cells due to an elevation in catabolism and autophagy pathways in CAFs. Such metabolic effects may lead to weakness in tumour immunity [193]. It has been shown that activated fibroblasts can be recruited by cancer cells and these activated fibroblasts are similar to fibroblasts that appear during the process of wound healing [193, 197-200]. In many types of cancer, the important mediators of fibroblast activation are fibroblast growth factor 2 (FGF2), PDGF and TGF β [193, 201-203]. Stimulated fibroblasts and cancer cells secrete PDGF which can result in activation and induction of fibroblast proliferation and is associated with cancer progression and invasion [193, 204]. It has been shown that the increase in expression of CAV1 or its loss in CAFs can also support invasion of a tumour through the remodelling of ECM [193, 205-207]. Several co-culture experiments showed that CAFs support the formation of tumours when compared with normal associated fibroblasts [193, 208, 209]. CAFs are able to induce tumour growth through their ability to prompt angiogenesis via bone marrow-derived endothelial cells and also by CAF-derived stromal cell-derived factor 1 (SDF1) [193, 208]. Several studies have shown that CAFs possess a pro-tumorigenic role through their ability to upregulate and deregulate a number of molecular regulators that result in further enhancement of their proliferation and support tumour invasion. Examples of these actions are: the heat shock factor 1 (HSF1) is upregulated [193, 210]; Yes-associated protein 1 is activated; supporting ECM stiffening tumour invasion [193, 211]; Notch and p53 signalling pathways are deregulated [193, 212]; secretion of ECM-degrading proteases, for example the MMPs that facilitate migration of cancer cells [193, 213-216]; production of TGF β receptor type II in FSP1 in invasive SCC [193] and fibroblast-derived exosomes as mediators in progression of cancer and remodelling of stroma. [193, 217-219]. Also, it has been reported that CAFs might promote the metastatic process via secreting cytokines and growth factors into the blood stream to induce the invasiveness and growth properties of tumour cells at a distant niche [193, 210, 220, 221]. The following are examples: (1) in colorectal cancer, CAFs secrete

IL-11 [193, 222] and stanniocalcin 1 (STC1) [193, 223] resulting in enhancement of the ability of cancer cells to colonise; (2) in breast cancer metastasis to the lung, metastasis associated fibroblasts secrete tenascin C and VEGFA [193, 224]; (3) in melanoma metastasis to the liver, the activated liver-resident fibroblasts facilitate angiogenesis [193, 225].

1.2.2 The desmoplastic reaction

Tumour invasion includes complex interactions between cancer and stromal cells, necessary for instance in the course of tumour invasion into the ECM [179, 226-228]. Stromal cells act by producing collagen and ECM proteins to start the “desmoplastic reaction” leading to the invasion process [179, 229, 230].

In desmoplasia there is a reaction of cells toward inductive stimuli released by the invasive epithelial tumour cells and this results in stromal changes that lead to formation of fibrous connective tissue. Desmoplasia may also be known as the desmoplastic response, desmoplastic stroma and the tumour-induced stroma (Fig. 1.8). In terms of morphological presentation, tumour stroma and granulation tissue resulting from wound healing processes have been shown to be similar [231]. Degradation of matrix component of tumour stroma by the action of proteolytic enzymes is crucial for tumour invasion and is associated with an inflammatory reaction.

Generation of granulation tissue continues with fibrous tissue formation, and these fibrous tissues consists of specialized mesenchymal cells with intermediate ultrastructural and biomechanical characteristics. There are similarities between these mesenchymal cells and myofibroblasts (Fig. 1.9) [179, 232], which are frequently detected by the presence of α SMA [179, 233]. Deposition of collagen by stroma cells during tumour invasion leads to formation of desmoplasia [179, 234].

Presence of desmoplastic stroma can be observed in the primary tumour as well as in the metastatic cancers and contains a remarkable number of stromal cells such as fibroblasts or myofibroblasts. These are frequently organized in a manner that is parallel to the structured tumour-cell-aggregates, and they are found mixed with fibrillary collagen or (GAGs) (Fig. 1.9) in a rather inconsistent manner. This arrangement may, or may not be associated with inflammation [235]. Although establishment of desmoplasia is crucial in tumorigenesis and in metastasis [236], it has attracted limited research attention with regards to OSCC and OPSCC.

Therefore, whether the stroma adjacent to tumour cells actually functions as a host defence mechanism, or, functions to speed up progression of tumour and thus negatively influencing the efficacy of therapy [179, 237], has become an important point.

The biological relevance of the desmoplasia is not completely clear. It was initially proposed that this reaction might function as a protective measure against tumour invasion and thus restrict its spread [238, 239]. More recently, it has been revealed that the molecular crosstalk taking place between stromal cells and cancer cells, and cancer-induced changes within tumour stroma, all result in modifications in the capability of tumour cells to differentiate, proliferate and metastasise [229, 239-242]. These data have been validated by different clinical cancer researches (breast, lung and skin), suggesting the possibility of a relationship between tumour invasion, desmoplasia, metastases, and recurrence [239, 243-245].

Conflicting results have been published from studies on desmoplasia in colon cancer, with a few proposing that the stromal desmoplastic reaction is an unfavourable factor of prognosis [239, 246, 247]. A few other studies have not been able to demonstrate the importance of desmoplasia as a prognostic factor [239, 246]. These discrepancies could be attributed to a number of factors such as the case volume, technical errors, for example a lack of objectivity in grading systems (involving semi-quantitative methods), inter and intra observer variation, or the sampling error.

Serpin E1, also known as plasminogen activator inhibitor-1 (PAI-1), regulates the urokinase as well as the tissue-type plasminogen activators, resulting in the activation of the pro-enzyme plasminogen to plasmin, which leads to the promotion of invasion via the degradation of the ECM; in addition to that, they activate the matrix metalloproteinases [248, 249]. Invasion can also be promoted via the plasminogen activation system by downregulating the cell–cell adhesion molecules, such as E-cadherin [248, 250]. This system plays a role in the metastatic cascade by influencing proliferation, migration, angiogenesis and extravasation, and it has been involved in different types of cancer such as breast and colorectal cancer (CRC) [248, 250-253].

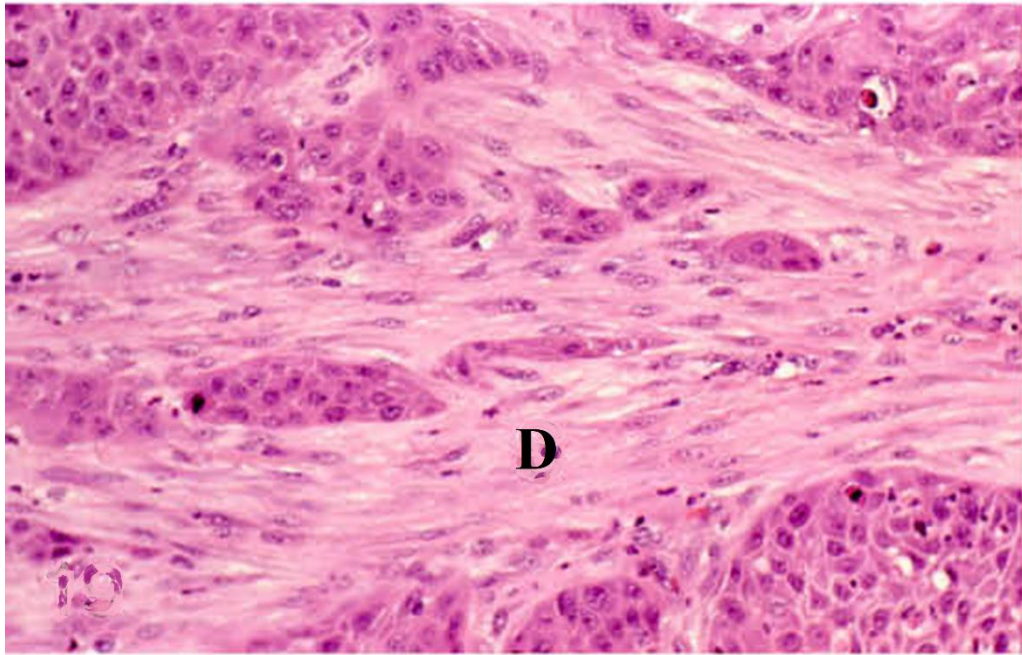


Figure 1.8. Typical histological desmoplasia (D) in OSCC. Shows sheathing of tumour aggregates and islets by stromal cells. Adapted from Woolgar *et al* [235].

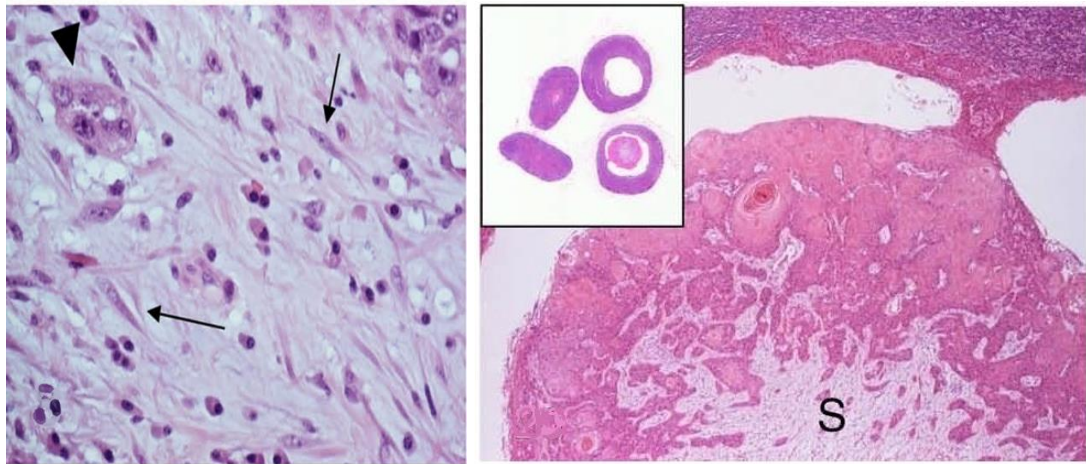


Figure 1.9. Myofibroblasts in stroma of a conventional SCC (Left, arrows); the arrowhead points to an islet of malignant keratinocytes. GAGs (right) gives the stroma its pale/‘oedematous’ appearance in desmoplastic stroma (S) of cystic SCC metastasis of a cervical lymph node. Adapted from Woolgar *et al* [235].

1.3 The metabolism of cancer

1.3.1 Glycolysis and conversion of pyruvate to lactate

Glucose enters the cell and is converted to pyruvate by the glycolytic pathway [92] which is a group of oxygen-independent reactions [92]. In addition to energy production, glycolysis plays an important role in the production of intermediate molecules which are channelled into the synthesis of lipids and nucleic acids.

In the absence of oxygen, pyruvate is converted into lactic acid and this process generates a lesser amount of energy than the complete oxidation of pyruvate. This also allows glycolysis to go on in conditions where the energy needs of a cell outpace the ability to transport oxygen [92].

1.3.2 Citric acid cycle and oxidative phosphorylation

The majority of ATP produced is via the citric acid cycle and OXPHOS by the electron transport chain (ETC) [92], a series of coupled reactions which take place in the mitochondria [254]. The key role of the cycle is to harvest the high energy electrons from pyruvate and is also a significant source of precursors for many building blocks of macromolecules, including amino acids, cholesterol and nucleotide bases [255].

The citric acid cycle (also known as the tricarboxylic acid cycle, TCA, or the Krebs cycle) involves a series of oxidation-reduction reactions that lead to the oxidation of an acetyl group to two molecules of CO_2 . Pyruvate enters the TCA as acetyl-Coenzyme A (acetyl-CoA) [92, 255], and its transfer into the mitochondria is via a pyruvate transporter. It is oxidatively decarboxylated by the pyruvate dehydrogenase complex to acetyl CoA. The TCA cycle does not actually require oxygen as a substrate and does not generate abundant ATP. Most of the ATP produced by aerobic respiration is by OXPHOS, through the ETC (Fig. 1.10) [254]. NADH and FADH₂ generated in glycolysis and the TCA contain a pair of electrons with a high transfer potential. Through OXPHOS, these electrons are used to reduce molecular oxygen to water, releasing a large amount of free energy, channelled into the generation of ATP.

Highly specialised transmembrane complexes act as electron carriers that contain multiple centres for oxidation-reduction reactions; these include complex I, which accepts energy from the TCA in the form of NADH, and complex II, which accepts electrons from FADH₂. Complex I and II donate these electrons to complex III,

followed by complex IV [254, 255]. At complex IV, electrons are used to reduce oxygen to water. During the flow of electrons via the protein complexes in the inner mitochondrial membrane, protons are pumped out of the mitochondrial matrix, causing an uneven distribution of protons, and this creates a pH gradient and an electrical potential across the membrane, producing a proton-motive force. Protons can flow back into the mitochondrial matrix through a protein complex termed ATP synthase, synthesising ATP from ADP in the process. This way, the proton gradient across the inner mitochondrial membrane couples the oxidation of fuels to ATP generation via the phosphorylation of ADP.

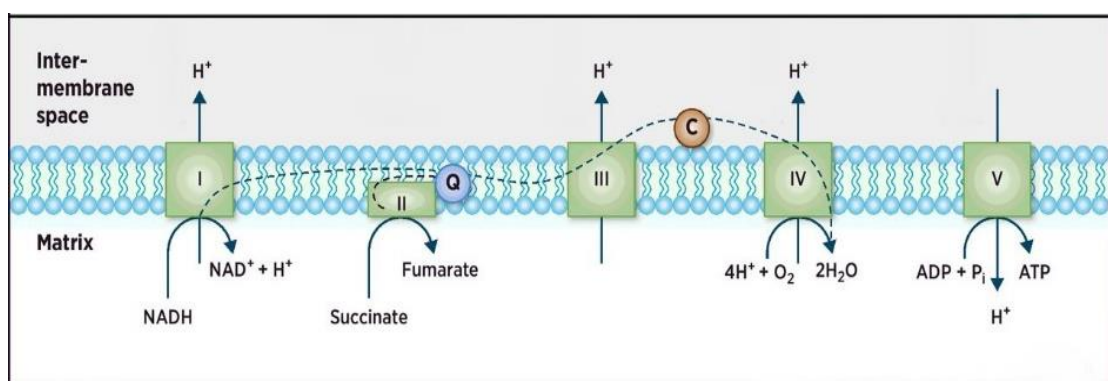


Figure 1.10. The oxidative phosphorylation metabolism.

The diagram represents: the process of ATP production by oxidative phosphorylation metabolic pathway in which electrons are transported from NADH or FADH_2 to O_2 through a chain of transmembrane protein complexes in the inner membrane of mitochondria, termed the electron transport chain. Movement of the electrons through the chain takes place as indicated by the dotted line: complex I, complex II, Coenzyme Q10 (Q), complex III, cytochrome c (C) and complex IV. O_2 functions as an acceptor for the terminal electron. From Ashton *et al* [254].

1.3.3 The Warburg effect

Tumour cells are subjected to unique physiological pressures from the tumour microenvironment, including hypoxia, acidosis and increased interstitial fluid pressure [95]. One adaptation tumour cells may make to survive under these unfavourable conditions is to alter their metabolic phenotype. Consequently, the metabolism within solid tumours is considerably altered compared to adjacent normal tissue. These alterations in tumour metabolism were first recognised by Otto Warburg in 1925 [99] [256]. Warburg observed that normal tissues exploit mitochondrial metabolism to generate 90% of the cell's ATP, with glycolysis accounting for approximately 10% of the ATP supply.

In normal or non-transformed cells, the presence of oxygen inhibits the energetically unfavourable glycolytic pathway in favour of mitochondrial respiration, this is termed the Pasteur Effect [257]. Warburg noted that tumour tissue was found to generate approximately 50% of the ATP by glycolysis. This shift towards the glycolytic pathway occurred even with the availability of sufficient oxygen to support mitochondrial function. This concept, observed in solid tumours, is named the Warburg Effect, or aerobic glycolysis. Glycolysis provide a more rapid ATP generation than OXPHOS, supplying cancer cells with the necessary substrates (biosynthetic) required for fast proliferation such as ribose 5-phosphate and NADPH [103, 258] [29,30], and cell growth support in case of hypoxic conditions [102]. Although initially overlooked in cancer research, aerobic glycolysis has become increasingly important and forms the basis of the clinical imaging technique 18fluorodeoxyglucose positron-emission tomography (FdG-PET). FdG-PET utilizes fluorodeoxyglucose, an analogue of glucose which becomes trapped in cells displaying high glucose metabolism. This technique is proving successful as a diagnostic tool in determining regions displaying the glycolytic phenotype [259-261].

1.3.4 Symbiosis of aerobic and anaerobic tumour cells

In 2008 a substantial input to the field of tumour metabolism was made by Sonveaux *et al* [262]. The presence of a “metabolic symbiosis” was identified to exist between aerobic and hypoxic tumour cells. In this partnership, lactate which is produced by hypoxic tumour cells as a waste product of glycolysis is taken up by aerobic tumour cells and used as the primary fuel for OXPHOS, thereby maximising glucose use. Hypoxic cells downregulate OXPHOS in favour of the glycolytic pathway, and this has two benefits; reduction in the use of OXPHOS maintains redox homeostasis and the consumption of glucose enables maintenance of energy homeostasis [262]. This is made possible by MCT1, which has been shown to transport lactate into tumour cells in an oxygen-dependent manner. MCT1 is then able to work in concert with lactate dehydrogenase B (LDH-B) which converts lactate to pyruvate, in an oxygen-dependent manner. The use of lactate as a fuel source in aerobic tumour cells is advantageous, signifying that aerobic tumour cells are not dependent on glucose availability, making glucose available for use by hypoxic tumour cells.

In general, researchers use the MCT1 inhibitor α -cyano-4-hydroxycinnamate (CHC) to inhibit MCT1. It is shown in in-vivo models of Lewis lung carcinoma (LLc) and

WiDr colorectal adenocarcinoma xenografts that CHC results in a tumour growth delay; this was not seen in a hepatocarcinoma model of transplantable liver tumour cells (TLT) which do not express MCT1 and which were insensitive to CHC treatment. Tumours treated with CHC also displayed an increase in necrosis which correlated with the hypoxic regions of the tumours. The results of this study suggested that upon MCT1 inhibition by CHC, the aerobic tumour cells which were importing lactate as a primary fuel source switched to glucose uptake, resulting in cell death in the hypoxic regions of the tumours due to deficiencies in glucose availability.

Also, it has been shown that the growth delay of LLc tumours following 6Gy irradiation is increased following concomitant treatment with CHC, although due to the experimental design, the size at which the CHC-treated tumours were irradiated was significantly less than that of the vehicle-treated tumours. Nevertheless, this novel indirect targeting of hypoxic tumour cells is an interesting therapeutic strategy, particularly for the sensitisation of hypoxic tumour cells to radiation treatment.

1.3.5 Metabolic interactions between tumour and stroma (reverse Warburg effect)

The contact between tumour cells and their microenvironment is multifaceted; involving metabolic events, close interaction with the ECM, cooperation with stromal cells, blood perfusion, and an interplay with the immune system. The significance of the association between tumour cells and the normal stroma has recently been highlighted. A model has been proposed by Lisanti and colleagues which describes the process by which proliferating cancer cells can take advantage from a “Reverse Warburg Effect” through prompting glycolysis in the adjacent CAFs in order to obtain metabolic fuels e.g. lactate from them (Fig. 1.11) [166, 263-265].

It has been suggested that activated CAFs can use aerobic glycolysis to produce pyruvate and lactate, which can be exported and used as high-energy metabolites for the highly proliferative aerobic epithelial cancer cells in oxidative metabolism [166, 263, 264]. Essentially, tumour cells could influence CAFs to turn into wound healing stroma, facilitating tumour growth and promoting angiogenesis, while also directly feeding the adjacent tumour cells, in a host/parasite type relationship [1].

This energy transfer network, described in a number of epithelial cancer types [1, 167, 266-269], consists of two metabolic compartments which are; the stromal fibroblasts

as catabolic compartment and cancer cells as anabolic compartment. This creates an environment favourable to growth, survival, and metastatic spread [263, 264, 270]. These highly proliferative and poorly differentiated cancer cells are thought to originate from basal stem cells [1]. In HPV- HNSCC, CAFs support and potentially induce a highly invasive and metastatic phenotype related to poor survival.[271-273].

The implications of this finding are widespread and represent a reversal of the metabolic symbiosis identified between aerobic and hypoxic tumour cells, which has been suggested by Sonveaux *et al* [262] in which lactate can be imported into tumour cells by MCT1, for conversion to pyruvate by LDH-B.

Trafficking of the metabolic substrates, lactate and ketone bodies from their sources (fibroblastic tumour stroma) to point of use (cancer cells), requires a specialised carrier system. This is performed by means of differential expression of monocarboxylate transporters (MCTs) on the cell surface i.e. this kind of expression depends on the cell type [274, 275]. For instance, the MCT4 that exports metabolic fuels such as lactate is upregulated by glycolytic cells (CAFs) [276] whereas MCT1 is upregulated by cancer cells as an importer of these metabolic fuels [266, 277, 278]. Figure 1.11 demonstrate the notion of reverse Warburg metabolic model.

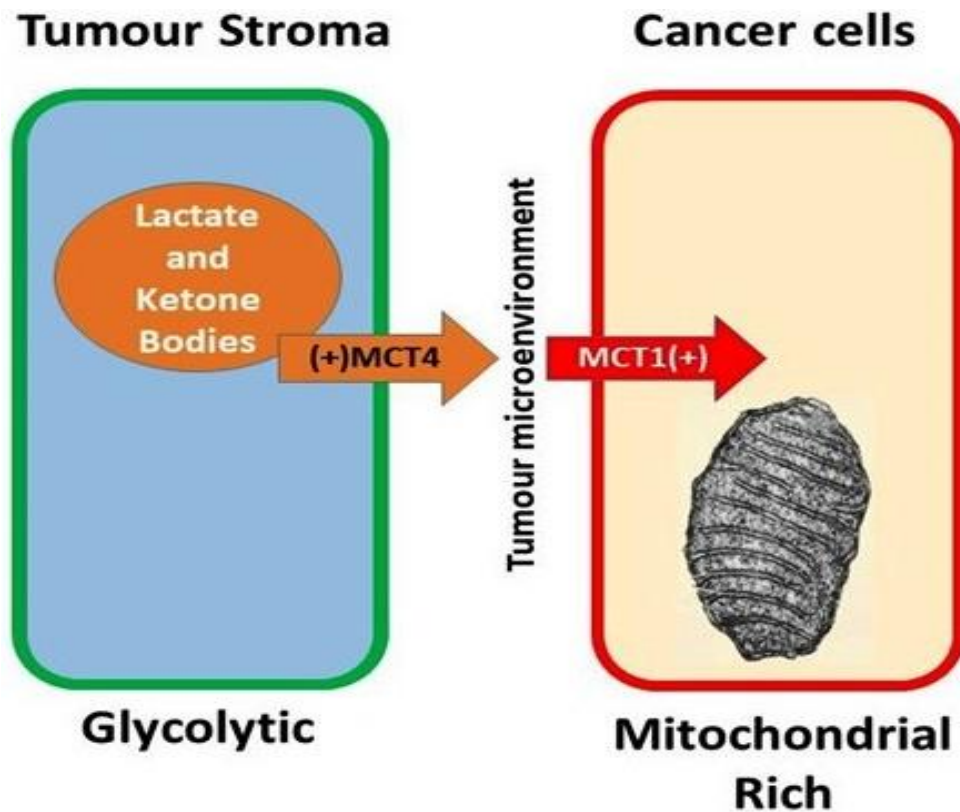


Figure 1.11. The reverse Warburg metabolic model.

This figure demonstrates the idea of reverse Warburg metabolic model where stromal cells (glycolytic) increase their generation of intermediate catabolites e.g. lactate, glutamine and ketone bodies and subsequently secrete them out into the tumour microenvironment using MCT4 as exporters, an event that stimulates OXPHOS in carcinoma cells which in their turn uptake these intermediate catabolites using MCT1 as importers. Adapted from Bovenzi *et al* [265].

This 'energy transfer' relationship between stromal and epithelial cells in human tumour is called stromal-epithelial lactate shuttle which is equivalent to the crucial lactate shuttle that takes place physiologically in skeletal muscles and brain tissues, where cells have dedicated MCTs to channel the lactate molecules from one cell type to another [270, 279, 280]. The glycolytic cells (fast-twitch fibres) in the skeletal muscle release lactate molecules which are subsequently used up by oxidative cells (other group of fibres called slow twitch fibres). In the same way as in the brain, this model of energy transfer is termed as a 'neuron-glia metabolic coupling', where the glycolytic fast-twitch fibres and astrocytes transfer lactate outside, which is then employed as a source of energy by neighbouring slow-twitch fibres and neurons (oxidative cells) [274, 281-285].

From a functional point of view, it has been shown that overexpression of MCT4 in CAFs occur as a result of oxidative stress, and can be stopped by the anti-oxidant action of N-acetyl-cysteine, and this can deliver a novel anti-cancer treatment, by engaging MCT inhibitors [270]. If the “Reverse Warburg Effect” is correct, one may predict that tumours containing a substantial quantity of stroma may have a worse prognosis due to increases in lactate production and secretion. In fact, a link between tumour progression and stroma has been carried out which indicated that a higher proportion of stroma correlated with an increase in tumour progression and a reduction in the survival of patients with colon cancer [286]. The implications of these findings would suggest that inhibition of lactate transport or glycolysis would directly kill CAFs, while indirectly starving tumour cells of lactate and pyruvate, metabolically uncoupling tumour cells from the fuel supplying stroma. This glycolytic feature is peculiar to tumours and forms the basis of fluoro-2-deoxy-glucose positron emission tomography (FDG-PET) imaging [265].

1.3.6 Causes of hypoxia in tumours

The major causative factors of tumour hypoxia are the abnormal structures and functions of the microvessels supplying the tumour, increased diffusion distances between the nutritive blood vessels and the tumour cells, and reduced transport capacity of the blood due to the presence of disease-related anaemia.

Dewhirst best explains the factors which are causative to tumour hypoxia in seven key points of regulation of tissue oxygenation [287]. The first point describes a steep longitudinal oxygen gradient; the radial distance that oxygen can diffuse from a vessel depends on how much oxygen is in the vessel. Therefore, as intravascular oxygen partial pressure (pO_2) drops, the extent of hypoxia surrounding a vessel will increase. Secondly, an increase in intravascular gradient means that red blood cells can lose oxygen leaving little to diffuse into the tumour. Thirdly, shunt flow can divert blood around the tumour. The fourth point of regulation is that, reduced vascular density produces hypoxia due to the limitations in oxygen diffusion. The fifth point of regulation is the unorganised vascular structure and orientation which are less functional at providing oxygen to all areas of the tumour. The sixth point is the imbalance between oxygen consumption and delivery rates. Lastly, the seventh feature is that of a slower blood flow due to intravascular hypoxia which results in a reduction in red blood cell deformability that increases blood viscosity [287, 288].

One may think that the enhanced proliferative capacity of tumour cells, distancing themselves from the oxygen- and nutrient-carrying vasculature would be their own Achilles' heel; however tumour cells activate adaptive responses in order to survive in such conditions. HIF-1 α is continually produced in cells but degraded rapidly under normoxic conditions. When the partial pressure of oxygen is reduced below 10mmHg, the HIF-1 α is stabilized and able to bind with HIF-1 β to form (HIF-1), a transcription factor which is then bound to hypoxia-response elements (HREs) in the promoter regions of target genes. This binding results in regulation of a multitude of downstream target genes implicated in an array of pathways involved in the promotion of cell survival in hypoxia, thus supporting the metastatic phenotype [289, 290].

1.3.7 Gene control of tumour metabolism with particular emphasis on hypoxia-inducible factors (HIF) and their regulations

For some time, many studies examining the effect of oncogenic alterations in tumour metabolism have suggested that the activation of oncogenes, e.g. PI3k, or loss of tumour suppressor genes, e.g. p53, are important factors for the driving of aerobic glycolysis. Several oncogenes and associated proteins including HIF-1 α , RAS, SRC, CMYC and p53 have been found to influence tumour cell metabolism, favouring cell survival, independent of cell proliferation. Initial studies which recognised the importance of oncogenes in the control of tumour metabolism demonstrated a relationship between Src- and Ras-transformation and increases in the expression of glucose transporters [291]. Further confirmation of a link between oncogenes and glycolysis came a decade later when it was noticed that the c-Myc oncogene was able to directly trans-activate the LDH-A gene [292]. It has also been shown that activation of the Akt oncogene is adequate to initiate the shift to aerobic glycolysis [293].

Moreover, the importance of p53 in the regulation of glycolysis and mitochondrial function has been elucidated [294]. [295]. For example, data have shown that target genes that are under the direct control of p53 contribute in several pathways of metabolism [296]. The TP53-induced glycolysis and TIGAR ,apoptosis regulator, acts in glycolytic metabolism by inducing degradation of fructose-2,6 bisphosphate, and by that means they function against the anaerobic glycolysis (Warburg effect) [294, 296].

An overview of the relationship between genetic alteration and the tumour microenvironment is given in Fig. 1.12.

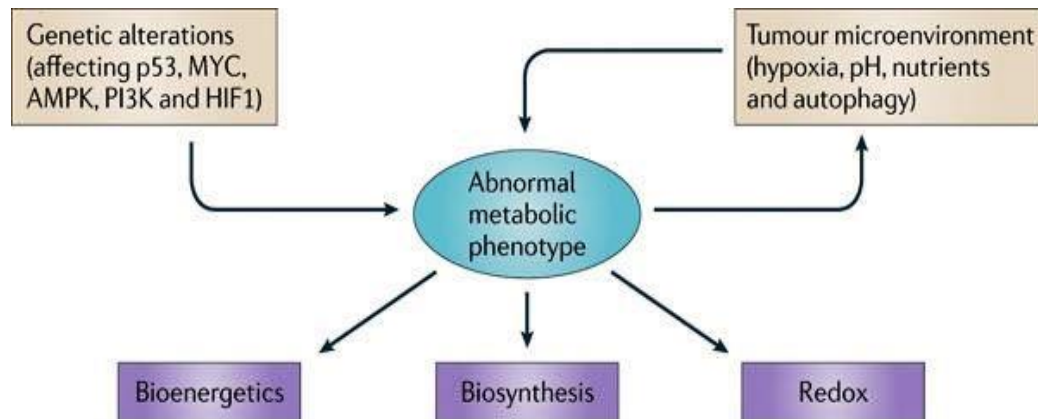


Figure 1.12. Determinants of the metabolic phenotype.

The metabolic phenotype is controlled by the tumour microenvironment as well as intrinsic genetic mutations. Oncogenic signalling pathways lead to the alteration in the metabolic phenotype of the cell. The abnormal metabolism then promotes proliferation by controlling the generation of ATP, maintaining redox homeostasis and ensuring the biosynthetic capabilities required by proliferating cells. Adapted from Cairns *et al.* [297].

Role of HIF-1 in the process of tumour metabolism regulation is twofold, first in responding to metabolic alterations, and second, in the regulation of metabolic reprogramming. The function of HIF-1 both upstream and downstream of tumour metabolism represents a feedforward mechanism which is crucial for tumour progression. One of the principal groups of genes regulated by the HIF-1 transcription factor is associated with glucose metabolism [298]. HIF-1 is responsible for the increase in the expression of transporters required for glucose entry to the cell. It also increases the expression of genes that encode enzymes implicated in glucose breakdown into pyruvate, and those involved in the clearance of pyruvate. In hypoxic conditions, pyruvate does not enter the mitochondria but is converted to lactate by means of lactate dehydrogenase (LDH) which can be produced by the tumour cell and released into the extracellular space. [299].

HIF-1 can regulate glycolysis at many stages. Firstly, HIF-1 induces the facultative glucose transporters GLUT1 and GLUT3 [300]. These are the main transporters of glucose in tumours and function in the transport of glucose down its concentration gradient. Increasing the quantity of the transporters therefore leads to an increase in

glucose flux into the cell. HIF-1 can increase the amount of glucose flux into the glycolytic pathway by increasing the expression of the glycolytic enzymes involved in this pathway including hexokinase 1 or 2 (HK). All glycolytic enzymes are at least in part directly regulated by HIF-1 [289, 301, 302]. It is the functional interaction of HIF-1 with other transcription factors that determines the subgroup of HIF-1 target genes activated in any particular hypoxic cell [303]. A number of HIF-1 target genes have been identified and implicated in an array of pathways (Fig.1.13).

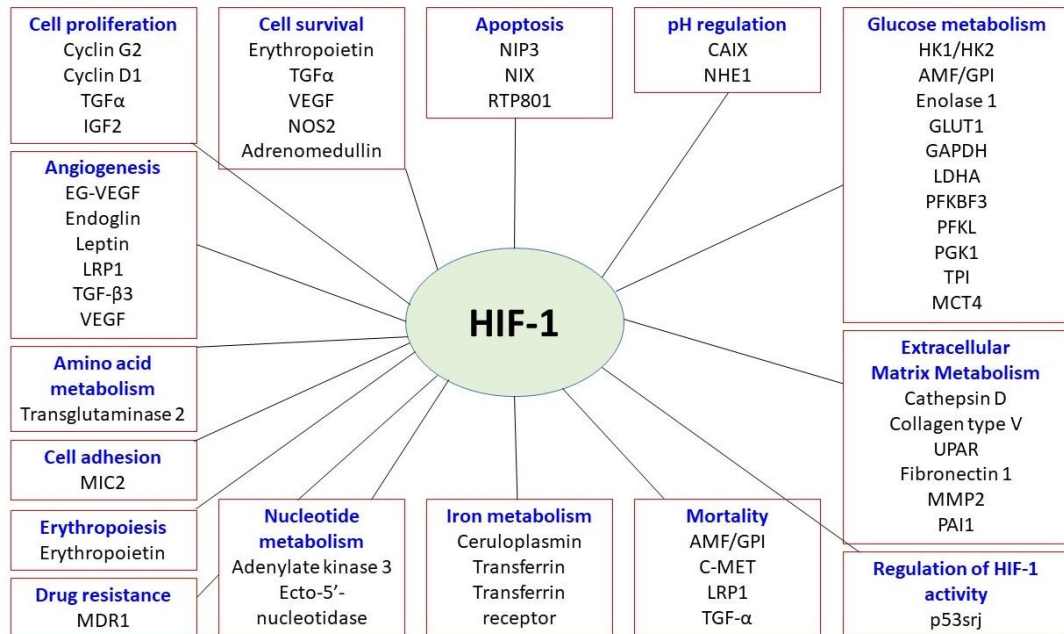


Figure 1.13. Examples of HIF-1 target genes.

An illustration of some of the examples of HIF-1 target genes recognised and implicated in a large array of pathways. HIF-1 binds to HREs (5'-RCGTG-3') in the promoter region of target genes. Adapted from Semenza *et al.*[303].

1.3.8 The clinical significance of hypoxia

1.3.8.1 Hypoxia and radioresistance

Several studies have been conducted to define the effects of oxygen concentration on cellular response to X-ray radiation [304-308]. The response of cells to the effect of ionising radiation is reliant on the amount of oxygen available for them. Tumour cells that are adequately oxygenated have a larger sensitivity to radiation when compared with cells living under hypoxic condition [307, 309]. In the absence of oxygen (anoxic conditions), cells are about two to three times more resistant to cell death as a result of radiation compared to the same cells that underwent irradiation at normoxic condition (physiological range of oxygen) or higher levels of oxygen concentration [304, 310, 311]. The proportion of X-ray dosages between two conditions; the absence of oxygen where the $pO_2 = 0$ mmHg and a particular pO_2 that are needed to destroy the equivalent numbers of cancer cells is generally termed the oxygen enhancement ratio. It has been shown that, in mammalian cells, the increase in radiosensitivity takes place only progressively when pO_2 rises into the normoxic range. This suggests that these cells are completely sensitized by oxygen molecules to ionizing radiation at utmost normoxic conditions [304, 310, 311]. The molecular oxygen has the ability to act as a powerful radiosensitizer and this feature is attributed to its chemical properties as an electrophile with high reactivity [304]. The generally admitted mechanism by which maximum radiation damage/injury happens under oxygen availability is called the oxygen fixation hypothesis [304, 312, 313]. This type of damage is also termed the oxygen-dependent promotion of ionizing radiation-induced damage [314].

As shown in Fig. 1.14, no direct substantial damage/injury to cellular macromolecules, especially the DNA, is taking place under the effect of X-rays. As an alternative, in biological systems, the ionizing radiation generates hydroxyl free radicals when it comes across copious water molecules [314]. Later, interaction takes place between hydroxyl free radicals and DNA strands which leads to generation of DNA-derived free radicals. At lower levels of oxygen concentration (absence of oxygen), it is possible to restore, with relative ease, the DNA free radicals via chemical reduction by means of reducing molecules such as sulfhydryl compounds [314]. Yet, when it interacts with oxygen molecules, the DNA-derived free radicals might be transformed into peroxides. Peroxides are compounds that cannot be returned back to their initial

structure via chemical reduction and that results in “fixation” of DNA damages [309, 314].

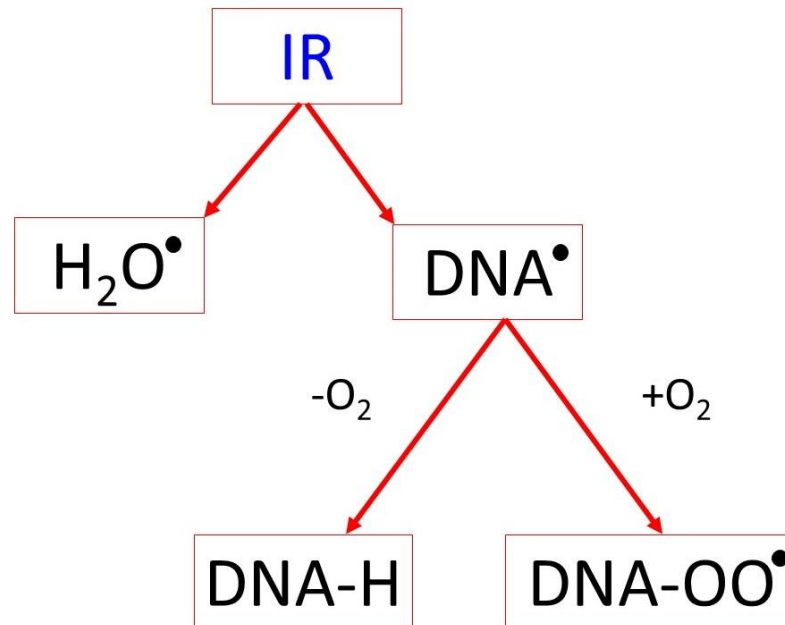


Figure 1.14. The oxygen fixation hypothesis.

Exposure of cells to IR generates free radicals in DNA or water ($\text{H}_2\text{O}\cdot$). Free radicals in DNA ($\text{DNA}\cdot$) can react with oxygen (O_2) to form a peroxy radical ($\text{DNA}\cdot\text{O}_2$). In the absence of O_2 , the DNA radical is reduced, restoring the DNA to its original state. Free radicals produced in water ($\text{H}_2\text{O}\cdot$) can damage adjacent DNA. Adapted from Bertout *et al.* [315].

1.3.8.2 Hypoxia and chemoresistance

In addition to hypoxia-induced radioresistance, hypoxia can also lead to chemoresistance due to various reasons. The poor vasculature common in hypoxic tumour regions together with decrease in drug diffusion makes drug delivery to hypoxic regions more complicated. Certain drugs, such as bleomycin and etoposide, show decreased drug activity in the absence of O_2 . Some agents have little effect on hypoxic tumour cells which may be non- or slowly proliferating or with altered pH gradients. This may be due to alkylating agents and antimetabolites, or due to the induction of gene amplification [316, 317].

1.3.8.3 Hypoxia and the metastatic phenotype

The most aggressive feature related to tumour development is the occurrence of distant metastasis. Invasion and metastasis are both forms of tumour dissemination, and are considered the most deadly acquired capabilities of tumours, as they render the tumours more difficult to manage following spread to other tissues [71]. Tumour metastasis in particular is put as the leading cause of mortality due to cancer [76].

In a variety of cancers, regardless of treatment type, patients with tumour hypoxia at the time of diagnosis are more highly expected to have local recurrence or distant metastasis. This may be due to hypoxia causing over-replication and gene amplification, which may in turn drive metastasis. This has partly been confirmed with further studies suggesting that hypoxia is associated with point mutations, gene amplifications and DNA strand breaks during acute hypoxia and reoxygenation [290]. It has also been shown that hypoxia may be involved in the driving of expression of genes implicated in the metastatic cascade, including lysyl oxidase (LOX), osteopontin, VEGF, and interleukin 8 (IL-8) which can be induced by HIF-1 α [318, 319]. In the case of LOX, it has been shown that LOX is in correlation with hypoxia in breast as well as HNSCC, and is linked to distant metastasis as well as poor overall survival. In addition, LOX inhibition in vivo resulted in the elimination of metastasis [318].

1.3.8.4 Hypoxia and treatment outcome

Hypoxia has been reported as a significant prognosticator in many tumour types independent of treatment type [320]. The impact of hypoxia on treatment outcome in HNSCC was demonstrated, using Eppendorf pO₂ measurements of 397 patients receiving radiotherapy. The five-year survival rate of patients with a pO₂ < 2.5mm Hg was shown to be 0-20%, with the most hypoxic tumours approaching 0% [321]. In head and neck cancer, hypoxia not only determines “disease-free” and overall survival, but also determines local control. This therefore proposes that hypoxia-induced radiation resistance is a major factor in relation to local failure, and there has been a multitude of studies which confirm the link between hypoxia and treatment outcome [320]. Multiple techniques for quantifying hypoxia have been used in such studies, including the use of pO₂ measurement, immunohistochemical analysis of HIF-1 α and HIF-1 target genes, and the use of exogenous bio-reductive compounds, including pimonidazole and EF5 [320].

1.4 Head and neck squamous cell carcinomas (HNSCC)

1.4.1 General features with emphasis on prognostic factors in HNSCC

HNSCC includes a heterogeneous group of malignancies originating from the upper aerodigestive tract with different anatomic subsites involving the oral cavity, oropharynx, nasopharynx, hypopharynx, and larynx. SCC originating from these different subsites are together regarded as the 6th most common malignancy across the world, amounting to 932,000 new cases and 379,000 deaths in 2015 [322, 323]. Remarkable epidemiological trends have been noticed in HNSCC over the past forty years, with the overall occurrence of HNSCC dropping marginally but a considerable shift seen in the relative involvement of each subsite to the overall prevalence of HNSCC [323, 324]. Tumours originating from subsites, rather than the oropharynx (oral cavity, hypopharynx and larynx) have seen rates of incidence decrease when compared with the incidence of OPSCC, which has progressively increased [323, 325, 326]. These subsite-specific epidemiological trends have been imputed to changes in societal factors that have caused changes in exposure to two different, but complementary classes of HNSCC risk factor: (1) tobacco and alcohol consumption, and (2) HPV infection [326].

Effective public health efforts in the developed world are generally credited with attaining population-level reductions in tobacco and alcohol intake [323, 327] and simultaneous drops in tumours due to tobacco consumption as for instance non-oropharyngeal HNSCC and lung cancer [328]. However, tendencies to sexual attitudes that increase the risk of picking up sexually transmitted pathogens, like HPV, have been connected with the increase in HPV+ cancers such as OPSCC and anal cancers [328, 329]. At the present time, HPV+ OPSCC cases are exceeding the incidence of HPV+ cervical cancer [325, 330] and this is may be because at present, there is no sign of prevention of HPV+ OPSCC, since research assessing the effect of vaccines on the development of oropharyngeal squamous cell carcinoma have not been shown. Currently, no screening exam exists for the oropharynx, comparable to the cervical clinical examination and Pap smear, though it is supposed that OPSCC also originates from a dysplastic lesion (not established) [331].

The prognosis in HNSCC has a massive range that extends from excellent to poor. For example, it has been reported to be excellent for verrucous squamous cell carcinoma, contrasting with a poor prognosis for small cell neuroendocrine carcinoma. Meanwhile, common squamous cell carcinoma prognosis is favourable [332]. To be more specific, 5-year survival rates are reported as the following from the higher percentage to the lower: verrucous squamous cell carcinoma has the higher survival rate (95%) followed by chondrosarcoma (90%) then mucoepidermoid carcinoma (80%) and (68%) for both squamous cell carcinoma and spindle cell carcinoma. The lowest percentages are reported for carcinoid tumour, atypical carcinoid tumour, melanoma, basaloid squamous cell carcinoma and small cell neuroendocrine carcinoma of the larynx with (20%), (48%), (46%), (17.5%) and (5%) respectively [332].

It is clear that the prognosis in HNSCC relies, to a large extent on the various biological behaviours of the different types of tumours (oncotype). So, the oncotype is the main factor in determining the type of treatment, and deciding the prognosis in HNSCC. Also, there are a number of factors of substantial prognostic value including an anatomical extension (stage of the disease), existence of an additional neoplasm, comorbidities, environmental aspects and a history of treatment previously carried out. Although not always the case, being the carcinoma associated with lymph node metastasis is typically regarded as the single most negative substantial factor in the prognosis of HNSCC. However, in the case of a primary adenoid cystic carcinoma, distant metastases may be identified in the liver, bones, brain or lung without cervical lymph nodes involvement [332].

Prediction of prognosis and the postoperative management depends also on the presence of extracapsular spread (ECS) and its extension, and on how the extracapsular spread can be accurately detected [333, 334]. Other factors are able to add additional value to the prognosis when the thin perinodal wall, or the capsular sinuses contain an emboli of tumour cells or ITCs [335]. Ninety percent of patients who present with pN2 or pN3 according to the pathological TNM stage, particularly if they are associated with the presence of ECS, are considered to be at risk and expected to die within 24 months [333]. A considerable percentage reach to 25% of OSCC cases have clinical evidence of metastases (distant, not locoregional) within 24 months of initial diagnosis [336]. A worse prognosis is usually associated with early

local relapse caused by a true recurrence, compared with a relapse caused by a metachronous primary tumour [337]. Furthermore, in the neck region, relapse caused by the growth of occult metastases outside the original field of treatment, or in the contra lateral neck, shows a better prognosis than a relapse occurring due to recurrence or persistence in a field treated with surgery or radiation [337].

Another robust prognostic factor in OSCCs is the reconstructed tumour thickness (depth of invasion), which, in the case of endophytic tumours, corresponds to the actual thickness. It is regarded as compensation for an exophytic growth component or ulceration and tissue destruction [235]. As an important prognostic factor, it is important that tumour size, which has an effect on both the treatment choice and outcome, is considered [235]. In previous investigations, the patients were divided into two groups: surgery associated with neck dissection, or surgery not associated with neck dissection, and important differences between both the clinical T stage and the diameter of the tumour, as well as pT stage versus overall survival, were observed [235]. Histologically, tumour thickness is considered to be more accurate as a predictor for occult nodal metastasis, local recurrence, and survival than tumour diameter [235, 336]- tumour diameter and thickness have a relationship with ‘tendency to be graded as poor’ [235, 336]. Although it is difficult to determine the critical tumour thickness due to its variability from site to site, but 4 mm is a useful average for OSCC with thicker tumours having a fourfold increased risk of nodal metastasis than thinner tumours [235, 338]. A pattern of invasion has a predictive value in a clinical setting, and is regarded as the single most significant feature since it gives a reflection of cellular cohesion. Moreover, the pattern of invasion is considered to be a surrogate to the group of malignancy biomarkers used in vitro, including the loss of contact inhibition, and tumour cell motility [336], and can be seen as a histopathological appraisal of surgical margins in OSCC and OPSCC resection samples [339]. The Anneroth score can be used as a regular diagnostic factor, and as a factor for predicting metastasis to the lymph node, and has been reported to be more informative than other systems such as TNM staging system and Broder's grading system [340]. Anneroth's system is a multi-factorial grading system was developed to achieve a more accurate morphologic assessment of the growth potential of HNSCCs, particularly in the tongue and floor of the mouth. It is composed of six histological variables having the same importance when used to determine the grade of tumour.

Three of these variables are associated with the tumour cellular population including differentiation, proliferation and mitosis. The other three variables are related to tumour-host relationship and involve pattern and stage of invasion and cellular response [341]. Studies have shown that the presence of CAFs in the tumour-associated stroma is a significant prognostic factor and is related to poor prognosis in a variety of cancers [169, 342-344]. Their presence has been revealed to anticipate disease recurrence in numerous cancers [342, 344], and it has been shown that the robust independent risk factor of early OSCC death is a feature of the stromal cells, rather than cancer cells. Increased stromal α SMA expression gave rise to the uppermost hazard ratio and the likelihood ratio of any variable investigated. It was highly associated with mortality, irrespective of disease stage [169], and such data propose that an increased α SMA expression in the stroma can be exploited to detect aggressive OSCC, irrespective of disease stage, and could be important in both the treatment and follow-up [169].

1.5 Oropharyngeal squamous cell carcinoma (OPSCC)

1.5.1 Structural and functional aspects of oropharynx

The oropharynx occupies the area at the back of the oral cavity, which extends from the soft palate to the epiglottis and also includes the palatine tonsils and base of the tongue. Fig. 1.15 shows the location and different anatomical boundaries of the oropharynx and tonsils [345]. The entrance to the throat is guarded by aggregates of lymphoid tissue, which form Waldeyer's ring. The aggregates include: 1) the palatine tonsils, the most prominent and recognisable with naked eye; 2) the pharyngeal tonsil (hyperplasia of which corresponds to the well-known adenoids); and 3) the lingual tonsils [346] (Table 1.1).

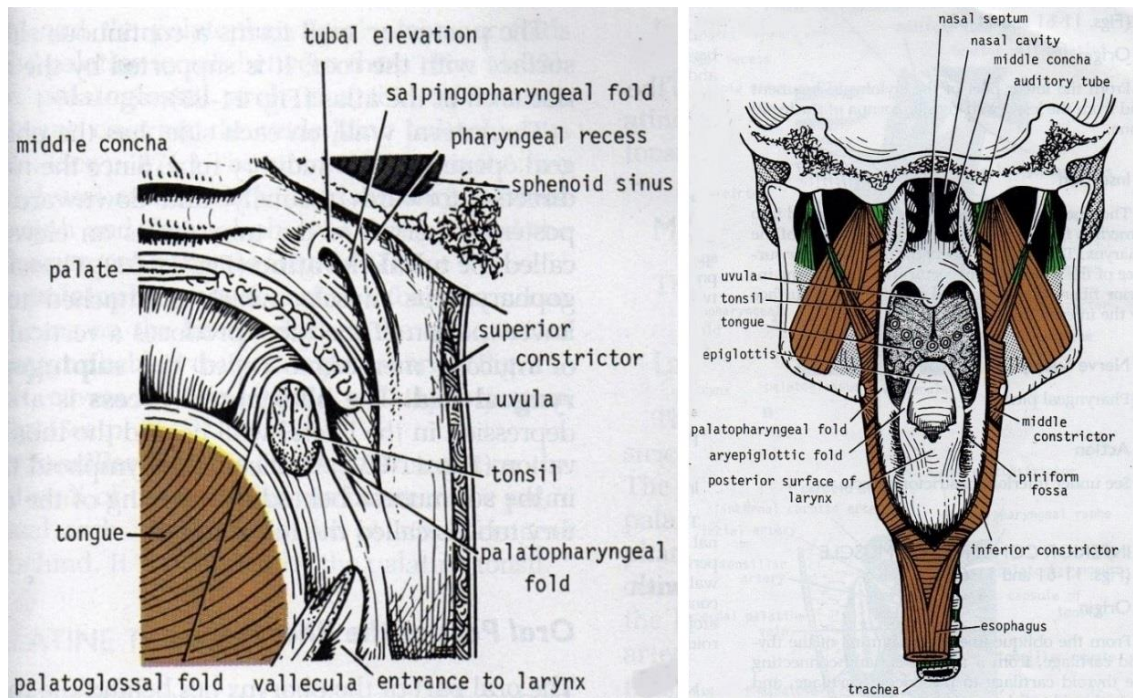


Figure 1.15. Boundaries of oropharynx. Adapted from Junqueira *et al.* [346].
 The circumvallate papillae of the tongue and the anterior tonsillar pillars are the anterior boundaries of the oropharynx separating it from the oral cavity. The pharyngeal constrictor muscles form the posterior boundary whereas superiorly bounded by the soft palate. Inferiorly, the oropharynx is separated from the larynx by the epiglottis and glossoepiglottic fold and from the hypopharynx by the pharyngoepiglottic fold. Oropharynx includes base of the tongue, soft palate, palatine tonsils, and oropharyngeal mucosa and constrictor muscles from the level of the palate to the hyoid bone.

Tonsil	Location	Surface epithelium	Crypts
Palatine	Lateral walls of the oropharynx.	Stratified squamous non-keratinising.	10-20, prominent, elongated and ramifying.
Pharyngeal	Superior nasopharyngeal wall.	Mixture of ciliated pseudostratified columnar epithelium, and stratified squamous epithelium.	Short folds but no true crypts.
Lingual	Base of tongue	Stratified squamous non-keratinising.	Short folds

Table 1.1. Histological differences between tonsils.

The lymphoid aggregates of the oropharynx show follicles with germinal centres and interfollicular areas, and is permeated by the tonsillar crypts. The crypts are invaginations of the surface epithelium; expand the available surface area for antigenic recognition and stimulation; and may contain cellular debris, shed epithelial cells, lymphocytes and bacterial colonies [346, 347]. The epithelium lining the crypts, is described below. Table 1.2 summarises the differences between tonsils and lymph nodes.

Feature	Tonsils	Lymph nodes
Capsule	Absent or incomplete	Present
Sinuses	Absent	Present
Antigenic delivery	Direct via transport from the environment to the tonsillar lymphocytes [347]	Indirect via afferent lymphatics [347]

Table 1.2. Differences between tonsils with lymph nodes.

This crypt epithelium is stratified, squamous and non-keratinising with sponge-like patches accounting for its characterisation as 'reticulated'. The reticulated arrangement allows lymphocytes and macrophages to migrate easily through the epithelium [348]. This migration is facilitated by the incomplete basal lamina of the crypt epithelium and is of immunological significance [348]. In addition, the reticulated arrangement enables an increased area of contact between antigens from the pharynx and migrating lymphocytes [347]. The crypt epithelium is the first barrier to foreign particles entering the crypts, which may be successfully removed by the migrating macrophages, and microorganisms including viruses. Despite the advantages increased area of contact between antigens and lymphocytes, the reticulated arrangement breaches in the continuity of the epithelium barrier. This in turn facilitate entrance of viruses and renders the tonsils vulnerable to corresponding infections [349]. Some of the surface epithelial cells are known as M cells because of micro-villous/-folded surface [350]. Intraepithelial dendritic cells and subepithelial IgA-producing plasma cells, are also present [350].

1.5.2 Human papillomavirus in OPSCC

The human papilloma virus (HPV) family is a subset of viruses, characterised by their double-stranded circular DNA, in which the capsid is icosahedral. About 150 HPV types have been isolated and entirely sequenced [351], and according to the homologous nucleotide sequence of the major capsid protein (L1), the HPV types are categorised into different genera (alpha genus, beta genus, gamma, mu, and nu) and HPV types with a skin tropism that appear to be linked with the growth of benign cutaneous lesions [352]. There are approximately 30 HPV types included in the alpha genus, characterised by their ability to cause an infection to the genital mucosa, oral tract and many benign cutaneous HPV types, associated with the growth of common skin warts. The (alpha) HPV types are divided, according to their oncogenic potential, into two groups: low-risk (LR) HPVs, mainly related to benign genital warts (e.g. types 6 and 11), and high-risk (HR) HPVs containing viruses considered to be the etiological agents of cervical cancers and cancers in the head and neck region [353]. The International Agency for Research on Cancer (IARC) has considered twelve different types of high-risk human papillomavirus as carcinogenic to humans. These are: 16, 18, 31, 33, 35, 39, 45, 51, 52, 56, 58, and 59, [354].

The genomic organisation of all HPV family members is similar, with 8 or 9 open reading frames (ORFs) found on the same DNA strand.

The genome of human papillomavirus can be dissected into three different regions: Early region, late region and long control region (LCR) (Fig. 1.16). The early region includes open reading frames (ORFs) that encodes the non-structural proteins which have been labelled from E1 to E8 [355]. The late region contains two late genes termed L1 and L2 that encode the structural viral capsid proteins required for creation of virion and its transmission and spread [355]. The human papilloma virus' early gene products play a significant role in regulating the life cycle of virus and manipulating cell machinery resulting in replication, transcription and translation of viral proteins (through the action of E1 and E2), regulating early viral gene products, inducing cytoskeleton rearrangements (through the action of E4), and this gives rise to deregulation of the cell cycle (through the action of E6 and E7) [355-359]. The long control region (LCR), a non-coding region, localised between ORFs L1 and E6. This contains the majority of the regulatory elements associated with the replication and transcription of viral DNA. This region encloses binding sites for host transcription

factors such as SP1 and the TATA box, as well as for the viral E1 and E2 proteins that control viral replication and gene expression.

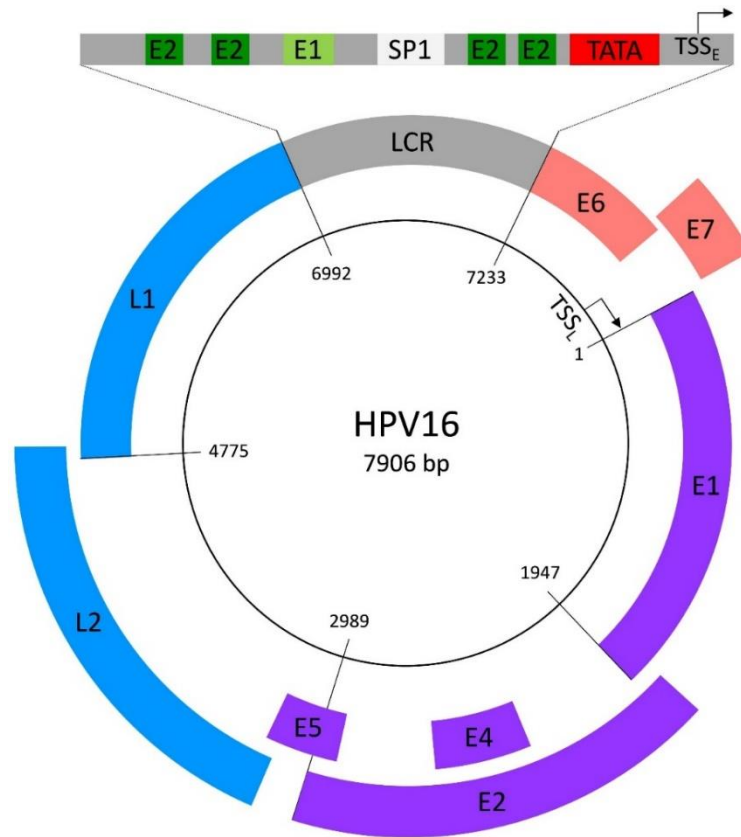


Figure 1.16. Genomic organisation of HPV16. From Faraji *et al.* [323]. The genome organisation of HPV16 is representative of the HR alpha genus HPVs. The diagram represents: (1) the viral genes; early (E1, E2, E4, E5 coloured in purple, E6, and E7 coloured in light red) and late (L1 and L2 coloured in blue) that are required for various phases of the virus life cycle. These genes encode a greater range of gene products due to mRNA splicing. (2) The long control region (LCR); comprises binding sites for transcription factors of the cell such as SP1 and the TATA box (coloured in red), and also for the viral E1 and E2 proteins (coloured in green) that regulate the processes of replication and gene expression of the virus. TSS_E and TSS_L are transcription start sites for viral early genes and viral late genes respectively.

The life cycle of the high risk HPV has a tight link with differentiation series of stratified epithelia [360]. The different important steps involved in carcinogenesis of HPV+ are shown in figure 1.18. These multiple steps are:

The normal productive life cycle

Infection with the virus:

In this stage the virus particles consisting of viral DNA and two capsid proteins, namely L1 and L2, that make icosahedral capsid [361, 362] enter the epithelial basal lamina, and interact with its important components such as heparin sulphate proteoglycans and laminin [363-366].

Virus internalisation:

Structural alterations in the virion capsid enable transfer to a secondary receptor on keratinocytes present in the basal layer of the epithelium [367-369]. After the internalisation has been completed, virions pass through several steps including endosomal transport followed by an uncoating process and cellular sorting. The complex of L2-DNA guarantees the accurate entrance of the viral genome to the nucleus, whereas the L1 protein remains in the endosome and is eventually degraded under the action of lysosomal enzymes [370, 371].

Maintenance of the genome and epithelial cell proliferation in the lower layers:

The infection process is succeeded by a preliminary phase of genome amplification and is followed by a phase in which the viral episome is maintained at a low copy number [372-374]. The copy number is retained at approximately 200 copies per cell [374].

Amplification of the genome in the upper layers of the epithelium:

Proliferation is mediated by E6 and E7 at the basal and para-basal cells and subsequent infection by the human papilloma virus enables an increase in size of the lesion.

Packaging of viral genomes and virus release:

For the HPV life cycle to be completed it should include a number of steps to permit the process of genome packaging. These steps are: (1) Expression of the minor coat protein (L2) (2) The cell leaves the cell cycle (3) Expression of the major coat protein

L1. Genome encapsidation needs the L2 to be recruited into replication sites through E2 [375, 376]. Maturation of the virus takes place in the keratinocytes present in the most superficial layers. These keratinocytes are characterised by passing through a change from a reducing to an oxidizing environment prior to virus release. This allows a gradual gathering of disulphide bonds between the L1 proteins, resulting in formation of infectious virions with high stability [362, 377].

Deregulation of life cycle and progression of cancer:

It has been described that in HPV+ tumours, the well-controlled expression of viral gene products that results in production of virus particles is disordered. The increase of E6 and E7 expression in HPV infection disposes the cell to accumulate genetic errors, which progressively participate in progression of cancer. Also, viral deregulation assists the viral episome integration into chromosomes of the host cell, resulting in additional deregulation of E6 and E7 expression genes [360]. Integration can lead to disturbance in viral genes that control normal transcription from LCR. An example of that is E2, a virally-encoded transcription factor that normally acts as a regulator for E6/E7 availability [378]. The site of viral integration is often present within the E1 or E2 genes [379]. Integration and deregulated E6/E7 could promote stable and elevated expression of these genes [380], which gives rise to a build-up of genetic alterations that ultimately results in cancer [381]. Data has shown that it is the overexpression of E6 and E7 for prolonged periods of time and the progressive accumulation of genetic changes, which are significant in the progression of cancer [382, 383].

Clearance and regression of lesion:

It has been reported that in a large proportion of cases infected by HPV, eliminate the infection without showing obvious symptoms and ultimately acquires an efficient cell mediated immune response resulting in regression of the lesions. The inability to have an effective cell mediated immunity to eliminate or inhibit the infection leads to persistence of the infection, with an increasing possibility of progressing to advanced grade intraepithelial neoplasia followed by invasive carcinoma [360]. It is becoming obvious that, efficient avoidance of innate immune recognition is a characteristic of HPV infections [358, 360]. Studies on animal models have shown that in cases where lesion regression appears, the lesion is eliminated by replacing the active infected cells

with 'seemingly normal cells' as the basal cells carry on their division [360]. However, these cells that seem to be normal may still incorporate the viral genomes with an absence of associated expression of viral genes. It is important to mention that reactivation of the virus life cycle can take place in cases where the immune system is suppressed [360]. This has been supported by a number of immunosuppression studies which revealed that reactivation could happen at a site that was previously infected. Also, persistence of infection in the epithelial basal layer subsequent to regression has also been proposed in humans [384-386]. It has been reported that, for cancer to progress and develop, evasion of immune detection by the virus over a long duration is required with the aim of accumulating genetic changes [387, 388].

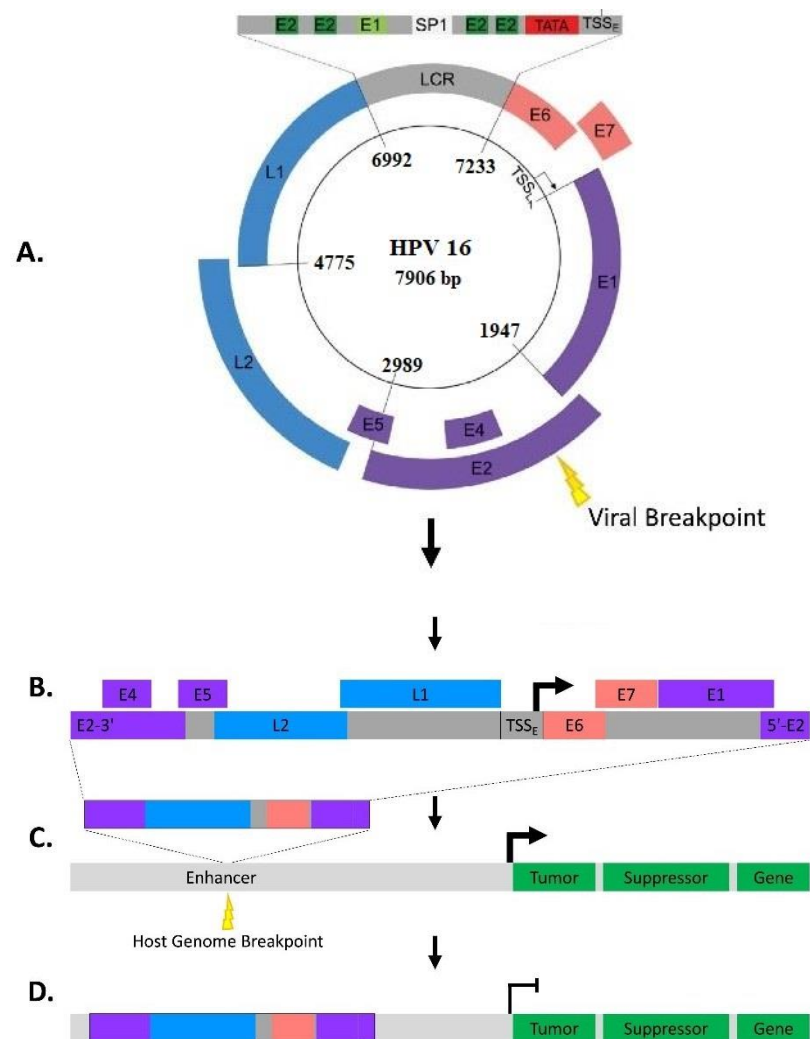


Figure 1.17. Steps of HPV integration and promotion of tumorigenesis. (A) The viral genome with breakpoints frequently arise in the E2 gene. (B) Viral linearization, via interruption of the E2 gene, results in an unregulated expression of E6 and E7 viral oncogenes, symbolised by the bold arrow at TSS_E. (C) The linearized viral genome inserts into a segment of open chromatin. (D) Viral DNA integration may result in disruption in the expression of nearby genes. From Faraji, *et al.*[323].

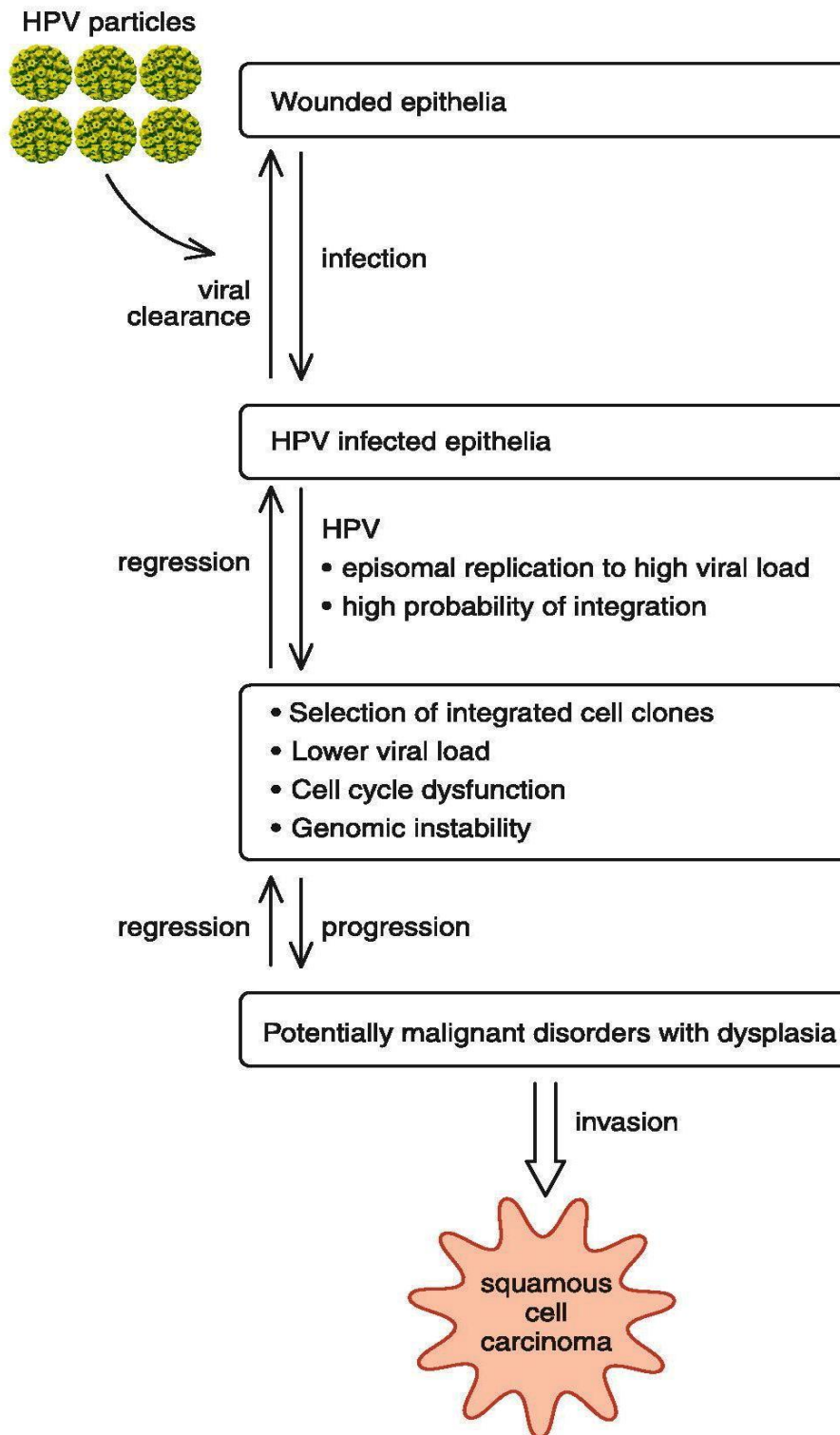


Figure 1.18. Events of cancer progression in infected keratinocyte with HPV. This diagram represents the different important steps involved in carcinogenesis of HPV+ cancer starting from the normal life cycle of the HPV and passing through the cancer-causing events and to end by the invasion. These steps include: infection, regression, progression and finally the invasion. Adapted from Rautava, *et al* [349].

The expression of E6 and E7 in a continuous way is considered to be essential for the maintenance of the malignant phenotype [323]. The integration of viral DNA into the host genome most frequently takes place with oncogenic HPV types [323, 389], and is often observed in HPV+ OPSCC [323, 351, 390]. In fact, 50% of HPV+ HNSCC (39-71%) showed that the virus integrated into the human genome [323, 391-393]. The steps of HPV integration and promotion of tumorigenesis are demonstrated in Fig. 1.17. It is important to state that integration is not a part of normal HPV life cycle and is an extremely rare event.

The E6 and E7 proteins from HR HPVs play an important part in the process of carcinogenesis. E6 is a basic and cysteine-rich protein of about one hundred and fifty amino acids, and has the capability to associate with an enormous number of cellular proteins [394] due to the existence of two zinc-binding regions, denoted as E6N and E6C. These are considered to be the main structural peculiarity of E6, and the same structural features are applicable to E7.

E6 and E7 oncoproteins amend the regulation of central functions in the cell, for example cell cycle, apoptosis, differentiation, senescence, cell polarity, and activate immune-response-related pathways via interacting and inactivating p53 and pRb, respectively.

HPV E6 oncoprotein binds with p53 causing its degradation and consequently lack of G2/M checkpoint regulation. HPV E7 oncoprotein connects with Rb leading to its degradation and causing the nuclear translocation of E2F and stimulates transition to S-phase. Furthermore, downregulation of Rb leads to loss of feedback inhibition and upregulation of p16INK4 expression. These events lead to the perturbation of cell cycle, proliferation, and eventually malignant transformation [323, 351, 395]. More details about the mechanism of E6 inactivation of p53 protein and the mechanism of E7 inactivation of RB protein and their consequences are demonstrated in Fig 1.19.

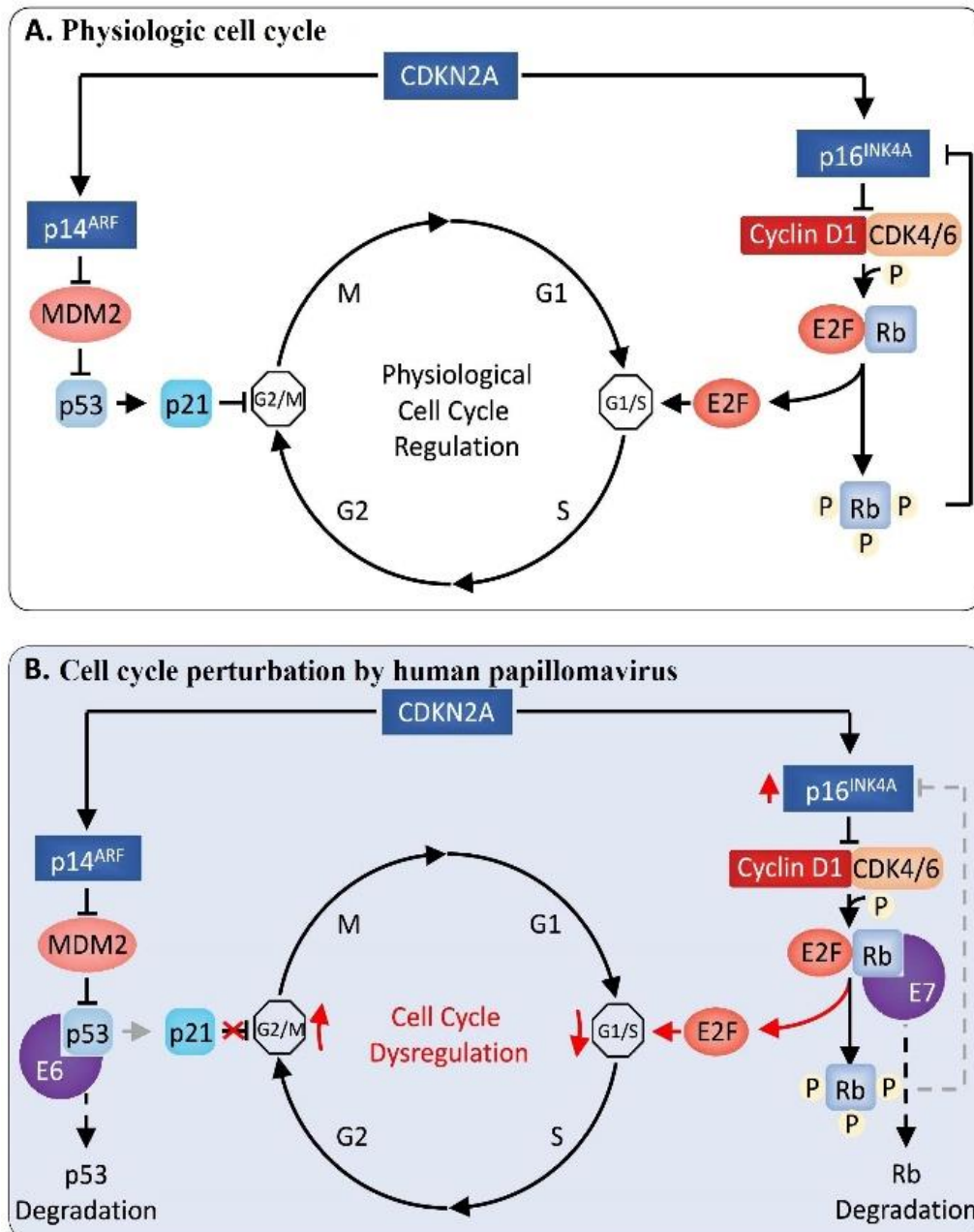


Figure 1.19. Perturbation of cell cycle by HPV.

Upper diagram represents: normal regulation of cell cycle by controlling the G2/M and S-phase transition checkpoints. The first pathway: p14^{ARF} hinders MDM2, thus activating p53 to stimulate p21 and arrest cell cycle to progress into mitosis. The second pathway: p16^{INK4A} suppresses the CyclinD1/CDK4 and CyclinD1/CDK6 complexes, thereby accelerating phosphorylation of the retinoblastoma protein (Rb), prompting it to release E2F family transcription factors to enter the nucleus and stimulate transcription of S-phase inducing transcripts. Phosphorylation of Rb also leads to feedback inhibition of p16^{INK4A} expression.

The lower diagram represents: Destruction of p53 through its binding with HPV E6 oncoprotein, leads to deregulation of G2/M checkpoint. Downregulation of Rb oncoprotein through its binding with HPV E7, leads to translocation of E2F into the nucleus and fostering transition to S-phase. Also, degradation of Rb causes loss of feedback inhibition and upregulation of p16^{INK4A}. From Faraji *et al.* [323].

Data from multiple studies has shown that the E7 proteins are greatly able to bind with the Retinoblastoma (Rb) protein (pRb) family, and also are capable to associate with and destroy both p105 and p107 that regulate cell cycle entry in the basal layer of the epithelium. In the upper layers of the epithelium E7 proteins are capable of associating with p130 that is implicated in cell cycle re-entry[360]. The E7 proteins are able to induce host genome instability, by deregulating the centrosome cycle in the proliferative epithelial cells in the basal layer [359, 360, 396-400]. E6 proteins have the ability to interplay with multiple PDZ targets via the PDZ-domain-binding motif that is situated at the C-terminus of all the E6 proteins affecting different cellular activities such as cell polarity control, cell proliferation and cell signalling [360, 401, 402]. It has been described that the E6 proteins have the ability to mediate an upregulation of telomerase activity [360, 403-405] and also to preserve the telomere integrity throughout the continual division of the cell [360]. Furthermore, E6 proteins deactivate different aspects of p53's role, with the capability to degrade p53 in the cell, and prompt its ubiquitination and degradation, for example proteasome-dependent degradation, suggesting that it has a significant life-cycle role [360, 394, 406, 407]. It has been reported that, it is essential to recall that a major role of the E6 and E7 proteins in HPV is not to support proliferation, of basal cell but on the contrary, to induce re-entry into cell cycle of epithelial cells located in the middle layers of the epithelium for the purpose of permitting genome amplification [360]. The E6/E7 expression in the upper epithelial layers permits the re-entry to S-phase for cells with infection and further increases in the viral genome copy number [360, 408].

1.5.3 Epidemiology and clinical presentation of HPV+ and HPV- OPSCC

Recording data about the HPV+ OPSCC incidence varies from place to place across the world, which may be a consequence of many contributing factors. For instance, the increase in HPV+ OPSCC is well-researched in North America and Europe, as well as in Australia [325, 409-411]. Incidence of HPV+ OPSCC is significantly increased. Around 85,000 cases of OPSCC appeared across the world in 2008, with a quarter of this number being HPV+ (at least 22,000 cases) [412]. The annual percentage rate keeps increasing, seen in, for example, the United States (5% annual percentage rate expansion in the frequency of oropharyngeal cancers) and Finland (6% increase) [325, 413]. Chaturvedi et al. expected that by 2030, 50% of all cancers in the head and neck region will be linked to human papillomavirus [325, 326].

The presence of a strong predilection of HPV+ HNSCC for the oropharynx has been documented by several researches [414-416]. The HPV+ OPSCC are acknowledged as a distinct neoplastic entity, characterised by unique epidemiological, histopathological, molecular, and clinical features [323, 417, 418].

The representative patients with HPV+ OPSCC are middle aged (present at a younger age in comparison with their counterparts of head and neck cancer, they are more often younger than 60 years), white, have a high socioeconomic position, often lack a significant history of smoking and drinking, have a history of multiple sexual partners (more than 8–10) and most likely to have greater than four oral sex experience with different partners [419-423]. It is less likely that patients with HPV+ OPSCC will consume alcohol in comparison with HPV- OPSCC patients, or those with other types of HNSCC [418]. HPV is considered to be the most frequent infection among the infections transmitted sexually in the United States, and the main source of infection of HNSCC [424, 425]. Despite the spread of HPV infection being prevalent, this high-risk virus is cleared by most people within around eighteen months [323, 426], and it is thought that persistent infection is indispensable for the establishment of HPV+ cancers [323].

Most HPV+ OPSCC patients present with, more likely, small primary tumours associated with advanced nodal disease [427]. These small primary oropharyngeal tumours are likely to be asymptomatic and a large proportion of patients request

medical care by reason of symptoms related to nodal disease [428]. HPV+ OPSCC manifests obvious sensitivity to therapy, including first line surgery, and a considerably better prognosis and survival is seen than in those patients with HPV- OPSCC, in spite of their presentation with advanced nodal disease [417, 427, 429, 430]. This survival improvement has led to intense enhancements in the 5-year survival rates for OPSCC, and despite the fact that overall recurrence rates are less for patients with HPV+ OPSCC (when compared with patients with HPV- OPSCC), the former presented a greater proportion of their recurrences at distant sites. These disseminated metastases are most likely to grow in unconventional locations (that is, other than in the lungs) [431-433]. Distant metastases, associated with HPV+ OPSCC, may also occur more than 24 months following initial treatment, contrary to distant metastases in patients with HPV- OPSCC, which characteristically develop within 24 months. Nevertheless, patients with HPV+ OPSCC that present metastases, again have a better treatment outcome in comparison with HPV- head and neck metastatic cancers [431, 433]. Second primaries are less likely to occur in HPV+ OPSCC cases when compared with their counterparts of HPV- OPSCC [434, 435].

Several explanations can be used to help clarify the reason behind the improvement in survival of HPV+ OPSCC. They could involve causes related to the epidemiology of this disease; for instance decreased consumption of chemical carcinogenic agents such as alcohol and tobacco, indicating the presence of an improvement in the medical status for the category of patients where HPV is regarded as a contributory cause for establishment of cancer [436]. Also, it has been proposed that the absence of mutations of p53 observed in cancers that show expression of HPV E6 such as HPV+ OPSCC could be an important cause behind the better responses to radiation treatment [436]. An additional potential interpretation is related to histopathological features that may include the more proliferative, non-keratinizing and less differentiated features of HPV+ OPSCCs that might render them more vulnerable to radiation treatment [436]. Epidemiologically, at the present time, the HPV+ OPSCC exceeds the rate of cervical cancer [437, 438]. In comparison to cervical cancer, HPV+ OPSCC pathologically originates from the tonsillar crypts, characterised by its potency to metastasize and this is attributable to the breached basement membrane of the crypt epithelium or may be due to the intraepithelial vessels that are present in this category of cancer [348, 439]. Furthermore, an absence of field cancerisation and premalignant regions in the

overlying epithelium is regarded as a point of difference when compared to cervical cancer [416, 439-441]. Also, the human papilloma virus copy numbers seen in head and neck squamous cell carcinomas are frequently lower than that found in cervical cancers. Moreover, by contrast to cervical cancer in which large proportions of tumours display viral integration, HPV+ oropharyngeal squamous cell carcinoma frequently shows episomal HPV DNA [323]. Either way, such explanations indicate presence of variations in the mechanisms of HPV+ carcinogenesis in head and neck squamous cell carcinoma, with more answers required [323].

It is obvious that the HPV+ OPSCC has distinct molecular, epidemiological and clinical features, regarded as a reflection for unique underlying biology [442]. These observations resulted in the creation of a new staging system more appropriate to this distinct entity [443] and changes in therapy paradigms [323, 444]. HPV 16 is the main cause for more than ninety percent of HPV+ OPSCC cases, while small number of OPSCC can be ascribed to the other HPV types [445]. At present, there is no sign of prevention of HPV+ OPSCC, since research assessing the effect of vaccines on the development of oropharyngeal squamous cell carcinoma have not been shown. It has been revealed by Herrero and his group that vaccination against HR HPV reduces the incidence of oral infection in the cases that received the vaccine, with 93.3% (95% CI = 62.5% to 99.7%) as an estimation for the efficiency of the vaccination [331]. Currently, no screening exam for the oropharynx, comparable to the cervical clinical examination and Pap smear, exists though it is supposed that OPSCC also originates from a dysplastic lesion (not established).

1.5.4 Histopathology of OPSCC

HPV+ OPSCCs are regarded as originating from the tonsillar crypts epithelium [415]. The tonsillar crypts likely trap infectious agents simply via lowering mechanical clearance [446]. This could explain why the oropharynx has higher levels of HPV+ cancer compared with the oral cavity (Fig. 1.20 A and B).

Areas of transition between tumour and normal epithelium are regarded as less frequent than in HPV- OPSCCs [415]. The latter occasionally may show histological progression from dysplasia into an invasive growth via carcinoma in situ [415]. However, molecular investigations of HPV+ OPSCC suggest progressive genetic alterations of the infected tonsillar epithelium, which influence aberrant basal cell

differentiation, dysplasia, carcinoma in situ and, eventually, invasive carcinoma (Fig. 1.20 C and D) [323].

The invasive component of HPV+ OPSCCs is in the form of sheets, lobules or ribbons of malignant keratinocytes [415]. Central necrosis or cystic degeneration and tumour infiltrating lymphocytes (TILS) can be seen [415]. In contrast to OSCC, desmoplasia is often inconspicuous [415].

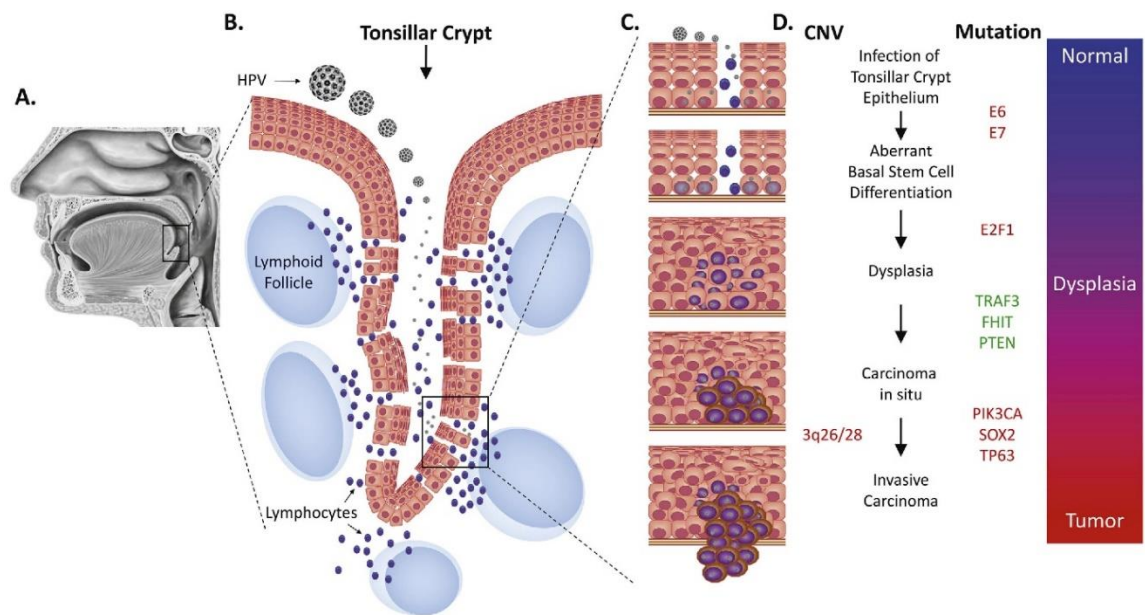


Figure 1.20. Tumour progression in HPV+ OPSCC. From Faraji *et al* [323]. This diagram represents: (A) The presence of a strong predilection of HPV+ HNSCC for the oropharynx, comprising lingual tonsils, the palatine tonsils and base of the tongue. (B) In tonsillar crypt, HPV obtains entrance to keratinocytes in the basal layer passing through breaches in the reticulated epithelium. (C) Peculiar differentiation of basal cells of the tonsillar epithelium as a result of infection followed by dysplasia, carcinoma in situ, and eventually invasive carcinoma. (D) Model for somatic mutations proposing that tumour development pass through several stages. This occurs as a result of (1) upregulation or increased copy number of certain genes and loci (E6, E7, E2F1, PIK3CA, SOX2, TP63 and 3q26/28) (2) deleted or mutated genes namely TRAF3, FHIT and PTEN. (3) CNV, show variations of copy number.

Cytologically, the HPV+ OPSCC tumour cells often show a basaloid phenotype with a high nuclear-to-cytoplasmic ratio; there are syncytial appearances, whereas intercellular bridges and keratin pearls / keratinisation of single cells are often lacking

[415]. It is controversial whether this morphology simply reflects the origin from the tonsillar crypts or in HPV related phenomenon [415].

As in other forms of squamous cancers, the earliest sign of invasion in HPV+ OPSCC is expected to be a breach in the continuity of the basal lamina followed by irregular extensions of the transformed epithelial cells into the subepithelial stroma. This qualifies as micro-invasion. Eventually, frank invasion is established and accompanied by desmoplasia, angiogenesis and inflammatory/immune reaction. Nevertheless, and in contrast with OSCC, the distinction between dysplasia, carcinoma in-situ and micro-invasion is more difficult in HPV+ SCC. Possibly, reflects the poorly defined junction between the reticulated epithelium and the underlying lymphoid tissue, attributable in turn to the incomplete basal lamina (see 1.6.1) and the abundant sub-/intra-epithelial lymphocytes; the aforementioned inconspicuous desmoplasia adds to the difficulties [415]. Immunohistochemical staining for cytokeratins would allow the difficulties to be overcome, but its routine application is unrealistic. The difficulties may also account for the notion of occult, tonsillar carcinomas, metastasis to cervical lymph nodes being often the first clinical manifestation [415].

The popular belief that HPV+ OPSCCs are poorly or undifferentiated, seems inappropriate in view of their origin from the crypt epithelium. In this vein, they can be regarded as highly differentiated tumours instead [415]. Accordingly, the degree of keratinization which is one of the histopathologic features traditionally considered to influence prognosis of conventional OSCC [447] is of little or no use in OPSCC. Nevertheless, the presence of anaplasia and multiple tumour-cell nuclei in non-keratinizing p16+/small-cell HPV+ OPSCC, has been regarded as influencing prognosis [415, 448].

Persistent, integrated HPV infection is essential for the cellular transformation [349]. The particular structure of tonsillar epithelium allows HPV to escape immunological surveillance and effects persistent infection in turn. This is coordinated by E6, and E7 [323]. In addition, the replicating HPV affects the differentiation of keratinocytes in the crypt epithelium [349]. The entrance of the virus into keratinocytes likely depends on receptors present on the surface of the latter; $\alpha 6\beta 4$ integrins may act as such receptors [349]. Recent investigations on the interaction between HPV and receptors

on the surface of basal and supra-basal keratinocytes also suggest that the binding process involves a single or group of receptors; the initial process is centred on single receptor, whereas its completion depends on different receptors. Accordingly, entrance of HPV to keratinocyte may start with $\alpha 6\beta 4$ integrin and completed by surface heparin sulphate proteoglycans (HSPGs), such as syndecan-1 [349]. The virus preferentially enters basal keratinocytes; this is supported by investigations on HPV-associated carcinomas of the cervix [446].

The pathology of nodal metastases in HPV+ OPSCC, is characterised by cystic degeneration of the tumour deposit. It is a common finding and its recognition via the MRI pre-operative of a neck swelling is an indicator of an occult HPV+ OPSCC [415].

1.5.5 Prognostic features

Being the oropharyngeal carcinoma infected with HPV is a good prognostic feature. The improved prognosis associated with positive HPV status steadily trumps conventional prognostic features based on morphology of the tumour, including tumour grade and histologic subtype [415]. Further, the presence of anaplasia, as well as cell multinucleation in the tumour, are predictors for poor outcomes in patients diagnosed with non-keratinising p16 positive OPSCC [415]. However, the HPV positivity is superseded if the tumour presents the phenotype of the small cell variant, which is an unfavourable prognostic feature [415].

1.6 Hypothesis, aims and objectives

The contact between tumour cells and their microenvironment is multifaceted; comprising metabolic events, close interaction with the ECM, stromal cells and blood cells. The HPV+ OPSCC is a neoplastic entity characterised by unique epidemiological, histopathological, molecular, and clinical features including extensive nodal disease, and is of significantly better prognosis than HPV- OPSCC [323, 417, 418].

We hypothesized that the difference in the prognosis of the two types of OPSCC (HPV+ and HPV-) is due to a difference in their levels of interaction with one or more of the aforementioned components (ECM, stroma and blood).

- 1) The desmoplastic reaction as a difference between the two types.

In HPV- HNSCC, stroma support potentially induces a highly invasive and metastatic phenotype related to poor survival [3, 165, 270]. Glycosaminoglycans (GAGs) and myofibroblasts are components of the desmoplastic stroma that characterizes many advanced carcinomas. Currently, there is only limited published work showing the relevance of CAFs / stroma in HPV+ HNSCC. We hypothesised that this difference in the intensity of desmoplasia and/or in one or two of its components, is responsible for the difference in aggressiveness between these two groups (HPV+/-). This investigation may be by the study of desmoplasia as a whole (histological desmoplasia), by the study of its components, GAGs and α SMA+ myofibroblasts, or by the study of serpin E1 which is a marker for invasion. The difference between the two groups is mirrored on prognosticators such as the depth of invasion, outcome and recurrence, which would have an impact on both choice and outcome of treatment.

Depth of invasion is considered to be one of the more significant prognosticators in cases of head and neck squamous cell carcinoma [449-451]. The invasion process to adjacent tissues is multifaceted and involves a dynamic array of events that takes place biologically in the tumour. Previous studies have shown that a greater stromal invasion was more frequent in HPV+ tumours when compared to HPV- cases of cervical cancer [449, 452]. Also, in another study conducted on OPSCC cases, the depth of invasion in HPV+ was investigated and it was found to be deeper than in cases of HPV- [449]. Yet, it has been reported that limited research has been done to investigate the factors that have a direct effect on the process of tumour invasion [449]. Therefore, more details associated with HPV activity during the invasion process is still being unravelled [449]. More research about the influence of HPV infection on tumour invasion of OPSCC could help in making decisions for a more suitable therapy in oropharyngeal cancer cases [449].

2) The metabolic events as a difference between the two types

We hypothesised that the metabolic events in HPV+ OPSCC are different from those of their counterpart, and that these metabolic variations lead to varied prognosis, likely as a result of a difference in oxygen concentration in both. We have therefore decided to repeat the previous metabolic studies, this time using a better matched cohort of OPSCC from similar site but different HPV status. Whether the metabolic

compartmentalisation related to the lactate transporters present in OPSCC or not was chosen for investigation.

HPV+ OPSCCs cases showed a lower percentage of risk of death (about half) compared to HPV- OPSCCs [417, 453, 454]. Such improved outcomes indicates that there is need to put in action a new system of staging devoted to such types of cancer [453, 455] and to assess the opportunities of treatment de-escalation. The reason behind this is that the present treatment regimen could expose patients with HPV+ to the risk of over-treatment and also to be exposed to needless toxicity. It has been suggested that less intensive treatment for patients with HPV+ cancers could attain same degree of effectiveness with less toxic effects and a better life quality [453].

Metabolic conversion towards anaerobic glycolysis instead of mitochondrial respiration is believed to be one of the hallmarks of cancer so as to meet the increase in energy demand for intermediate catabolites and metabolic fuels to sustain rapid proliferation of cancer cells [456-458]. Anaerobic glycolysis has been shown to provide a survival advantage for cancer cells without relying on the availability of oxygen. Also, glycolysis offers cancer cells another advantage by rendering them able to have a detoxification action on chemotherapeutic drugs/agents as well as reactive free radicals [456, 458]. Furthermore, by-products of glycolysis, for example lactate and pyruvate were reported to provide resistance to radiation and to support progression of cancer [456, 459, 460]. Studies have shown that blocking of the glycolytic pathway results in hindering cancer cell proliferation and increases their response to radiation [456, 461-463]. This data indicates that metabolic activity is a determining factor of cell reaction to radiation in OPSCC and also a potential prognosticator that might aid in more stratification of patient outcome [456, 464].

Accordingly, aims and objectives of the study

- a) To characterise the desmoplasia in OPSCC and its relation to clinicopathological features, particularly depth of invasion and outcome in relation to HPV status,
- b) Assess the impact of HPV status on metabolic events in OPSCC,
- c) To determine whether or not, oxygen levels of tumour microenvironment is connected to tumour-cell phenotype, by investigating HIF-1 α and GLUT-1

expression. And to determine if the levels of HIF-1 α and GLUT-1 are influenced by the HPV infection in OPSCC.

- d) Identify the differences between HIF/ angiogenic proteins expression (VEGF and VEGFR2) in HPV+ and HPV- OPSCC to better understand the biology of HPV tumorigenesis.

Chapter 2

General methods

2.1 Introduction

This study was split into two main sections. These were the investigations with the use of clinical specimens, in the form of tumour tissue samples, and the scoring of full sections and TMAs (tissue microarray), while the second involved the use of cell lines and determination of cellular functional changes, following environmental changes and co-culturing. Study of histological desmoplasia, hypoxia, glucose transportation and vascular distribution in the two types of OPSCC were done on whole sections whereas the distribution of myofibroblasts, glycosaminoglycans and metabolic events were performed on TMAs. The rationale behind this is the best use of the available material where in the desmoplasia study pre-existed Heamatoxin and Eosin stained sections were available. Use of triplicate cores in the TMAs is representative and reduce consuming large amount from the precious tissue samples. Hypoxia and vasculature study was pilot study, so use of smaller number of selected cases was sufficient to accomplish the target of this investigation.

2.2 Subjects

A retrospective cohort and pathological review of 45 cases of HPV+ and 63 cases of HPV- OPSCC were identified, in which the well-known primary tumour sites and lymph node statuses were treated during a twenty two years period from June 1992 to March 2014. It is a cohort of convenience, there was no selection process, included patients who are available in our consented database. All specimens were gathered after informed consent was obtained from patients in accordance with an ethical approval (refs nos: EC 47.01 & 10/H1002/53) [465]. The patients received treatment in the Liverpool hospital, department of Head & Neck Oncology [465]. OPSCC Cases were selected firmly according to tumour site carried out at the diagnosis and admission to the tissue bank [465]. Cases that could not be surely classified as OPSCC were ruled out [465]. Demographic and clinicopathological data was obtained from the institutional databases and patient records, as shown in Tables 1, 2 and 10.

2.3 Histopathological assessment

Paraffin-embedded specimen blocks and their Haematoxylin and Eosin (H&E) sections were retrieved from pathology archives, together with pathology reports. New sections, 5µm thick, were cut in cases where there were no available slides for the selected specimen, or where the available slide was not representative of the block specimen and the section H&E stained. A set of slides for each case (ranging from 5 to 50 slides), containing primary lesions and their positive and negative lymph nodes, were examined and analysed with light microscopy with the sections showing an invading front, normal mucosa and a larger tumour core, were selected for study of the histological desmoplasia.

2.4 Scoring matrices

Our definition for histological desmoplasia is the presence of myofibroblasts, as well as areas that show absence of cells that would suggest the presence of ECM. The following pathological data was collected: direction of growth (expophytic, endophytic or exo-endophytic), histological subtype, growth pattern (cohesive or non-cohesive), the presence of desmoplasia and its distribution/intensity, and finally the depth of invasion, determined from pathology reports. A systematic scanning of the whole section, using a medium power objective, was undertaken. The tumours were categorised, based on their microscopic features, into: keratinising squamous cell carcinoma, and non-keratinising squamous cell carcinoma. Desmoplasia, at the tumour advancing front and in the tumour core, were scored for distribution and intensity on H&E stained sections. Scoring was done by KBS (study researcher) under control and supervision of TA. A composite score system was used to score the different intensity and distribution groups, rather than using separate groups that are small, or contain too few samples to provide accurate statistical analysis on their own. These scores are presented in Table 2.1. Finally, these four grades were clustered into two main groups; sparse group included the cases that showed absence or presence of little amount of desmoplasia (grades 0 and 1) and prominent group included the cases that showed presence of large amount of desmoplasia (grades 2 and 3).

Score	Groups of intensity and distribution included	Binary scoring
0	No desmoplasia	Sparse
1	Uniform widespread grade 1 and/ or Multifocal grade 1(Single focus)	
2	Uniform widespread grade 2 and/ or Multifocal grade 2	Prominent
3	Uniform widespread grade 3 and/ or Multifocal grade 3	

Table 2.1. Desmoplasia composite score system.

2.5 TMA production

TMA construction done by KBS. By means of a manual tissue arrayer from Beecher Instruments, tissue microarrays (TMAs) were constructed using cores, carefully chosen from FFPE blocks of primary OPSCC tissue. These cores of 1-mm diameter and 4-mm depth were taken from the previously determined histopathologic areas of interest on each primary tumour's H&E sections. These areas of interest included the tumour advancing front, tumour core and normal epithelium, and connective tissue, and were relocated in recipient array blocks in a randomised arrangement. The cores were cut, arranged in triplicate with each replicate positioned on a different location in the same array block, and the accuracy of tissue sampling was confirmed by microscopic examination of H&E sections of these TMAs.

2.6 Histochemistry

Sections (5 micrometre thick) were cut from each TMA block. Alcian blue stain at pH 2.5 was used to stain acidic polysaccharides, such as glycosaminoglycans, a component of ECM.

2.7 Immunohistochemistry

Immunohistochemistry staining is performed by KBS. A group of markers has been employed to determine the metabolic and stromal events in OPSCC specimens by studying the expression of monocarboxylate transporters (MCTs), namely MCT1, MCT4 and TOMM20. MCTs are membrane proteins that transport metabolic substrates including lactate, pyruvate and ketone bodies from and into the cells [466]. A correlation has been found between expression of MCT1 and lactate and ketone body uptake and employment of these catabolites for oxidative phosphorylation (OXPHOS) metabolism [262, 466, 467]. MCT1 upregulation and expression occur conspicuously in several types of cells that have elevated mitochondrial OXPHOS, for instance heart and red muscle, proposing a significant function in oxidation of metabolic intermediates such as lactate and ketone bodies [466, 468]. MCT4 is regarded as the major transporter (an exporter) of lactate and ketone bodies from the cells to the tumour microenvironment. Also MCT4 is considered as a marker of oxidative stress [466, 469]. The upregulation and expression of MCT4 is taking place via the major glycolytic transcription factor HIF-1 α , which is prompted by both hypoxia and oxidative stress [278, 470].

Translocase of Outer Mitochondrial Membrane 20 (TOMM20) is a protein detected in the outer mitochondrial membrane and is acting by recognising and sorting precursor proteins in the cytosol that are essential for the process of mitochondrial biogenesis, so it is regarded as an important translocase [471, 472]. Expression of TOMM20 is linked to oxidative phosphorylation metabolism and mitochondrial mass [473]. In immunohistochemistry, TOMM20 shows cytoplasmic location, and is associated with a granular appearance [1].

Ki-67 is an antigen upregulated and expressed in all the phases of the cycling cells, but is absent in the G0 and the early G1 phases [474], and to be specific during G1, S and G2 phases. It is commonly used as a biomarker of nuclear proliferation to evaluate the growth fraction of cancer cells and also to be able to offer data about the fraction of actively cycling cells. It has been demonstrated to be a valuable prognosticator in breast cancer [475-477]. It's use has become widespread because it appears to be a correct and reliable method of measuring tumour growth rate and in identification of tumour cells with high levels of proliferation [475]. The proliferation activity is

revealed by the Ki-67 antibody through its recognition of nuclear antigen which is upregulated and expressed importantly in the G2 and M phases [478, 479].

Plasminogen can be converted to the wide-ranging protease plasmin through receptor-tethered urokinase-type plasminogen activator (uPA), an event that starts a cascade of serine and matrix metalloproteinase (MMP) that enables both invasion and metastases in cancer [480-482]. The major biological adverse controller of the above mentioned proteolytic network, is the serine protease inhibitor, clade E member 1 (SERPINE1; plasminogen activator inhibitor-1), associated with aggressiveness of tumours. An increase in SERPINE1 level is regarded as a poor prognosticator and indicates decreased disease-free survival in multiple types of cancer including lung, ovarian, breast and oral cancers [480, 483-485]. SERPINE1 is frequently found in cancer cells and CAFs at the tumour advancing front of squamous cell carcinoma (SCC). It has been suggested that SERPINE1 immunoreactivity could be employed for the purpose of stratification of cases in relation to the risk of metastases. [481, 486-488].

It has been reported that one regular characteristic of fibroblasts in the tumour-induced stroma is a myofibroblastic phenotype. This feature is founded on the production of markers of smooth muscles, particularly α SMA [489]. The α -SMA expression has become the marker with a high reliability in assessing differentiation of myofibroblasts [489]. In immunohistochemistry, the α -SMA expression in myofibroblasts exhibits a cytoplasmic location. Positive correlation was reported between the presence of myofibroblasts in the tumour-induced stroma and tumour invasion [489-491].

HIF-1 α has been researched widely as a possible indirect indicator of hypoxia in tumours and a large proportion of these studies have reported that an elevated level of HIF-1 α expression is a negative factor for prognosis in cases receiving radiotherapy [492-495]. Cells constantly produce HIF-1 α , but it gets degraded quickly in the presence of normal levels of oxygen (normoxia). In cases of decreased oxygen levels (hypoxia) the HIF-1 α is stabilized and gets bonded with HIF-1 β to procedure HIF-1, a powerful transcription factor implicated in the control of several events and activities in the cell including oxygen transport, pH control, angiogenesis and glycolysis. The activity and level of HIF-1 α is accurately regulated by the oxygen concentration inside the cells [492, 493, 495].

Vascular Endothelial Growth Factor (VEGF), also called VEGF-A, is a member of bigger family of proteins [496] and considered to be the main mediator of angiogenesis in diseases [497]. VEGFs stimulate angiogenesis through their binding with three main subtypes of tyrosine kinase receptors (VEGFRs) [498]. Hypoxia that occurs as a result of tumour proliferation denotes a main driver of VEGF processing via stimulation of the HIF pathway in tumour cells and in the tumour microenvironment [498]. VEGFRs are principal mediators that regulate activities of blood vessels in physiological as well as pathological conditions. VEGFR2 is the major receptor implicated in the promotion of angiogenesis [499]. The binding that occurs between VEGF and VEGFR2 supports proliferation of endothelial cells via stimulation of RAS/RAF/ERK/MAPK pathway [500, 501] and, simultaneously, prompts the expression of antiapoptotic protein extending their survival [502].

Deparaffinisation and antigen retrieval were performed on a Dako cytomation IHC machine (Dako PTLINK) using FLEX Target Retrieval Solution, High pH (50x Tris/EDTA buffer,pH 9)(Dako Denmark A/S, Produktionsvej 42, DK-2600 Glostrup, Denmark). Sections were placed in a preheated PT-LINK at 65°C, heated to 96°C for 20 minutes, and returned to 65°C. Sections were then cooled to room temperature by immersing them in a Tris-buffered saline with 0.05% Tween-20 (TBST) for 10 min and processed in an autostainer (Dako) programmed with the following steps: (1) 2-min wash with Tris-buffered saline; (2) peroxidase block with 3% hydrogen peroxide for 5 min to quench endogenous peroxidase activity; (3) Incubation with a primary antibody against the specific protein at recommended dilution for 60 mins, followed by two washes with TBST; (4) incubation with peroxidase-conjugated secondary antibody against mouse (cat# DM824) and rabbit (cat# DM825) immunoglobulins using EnVision™ FLEX+ Dual Link System Peroxidase (Dako) for 30 min, followed by two washes with TBST; (5) development of the sections with 3,30-diaminobenzidine tetrahydrochloride (DAB) solution (cat# DM823, EnVision™ FLEX+ from Dako) and counterstaining with Harris hematoxylin from SIGMA-ALDRICH. All sections were then dehydrated and mounted with DPX mountant.

Optimisation of primary antibody

The staining quality of immunohistochemistry may be affected by means of numerous variables/factors that must be taken into consideration to obtain accurate and

invariable information. Concentration of primary antibody, diluent, time of incubation, and temperature employed in the staining procedure, all of these variables/factors could influence the quality of staining. These variables/factors were optimised with samples used to obtain good quality staining with minimum background noise. The optimisation procedure for the above mentioned antibodies was addressed by keeping a fixed incubation time (30 minutes) and temperature (room temperature), while changing concentration of the antibody to define when a best signal is attained with minimum background staining. Preliminary optimisation studies were conducted using a broad range of antibody concentrations. Time and temperature are left unchanged for the incubation step when comparing samples stained with different concentrations of the same antibody (Fig. 2.1).

Controls procedures

Different normal tissues types with well-defined expression of the antigen were used for positive and negative controlling, where expression of the antigen is, in general, fairly constant among the different tissue specimens. Based on information provided in the antibody datasheet and/or IHC tissue atlas, the best tissue control is then chosen. Fig. 2.2 presents an example of the positive and negative staining for each antibody used in the immunohistochemistry studies.

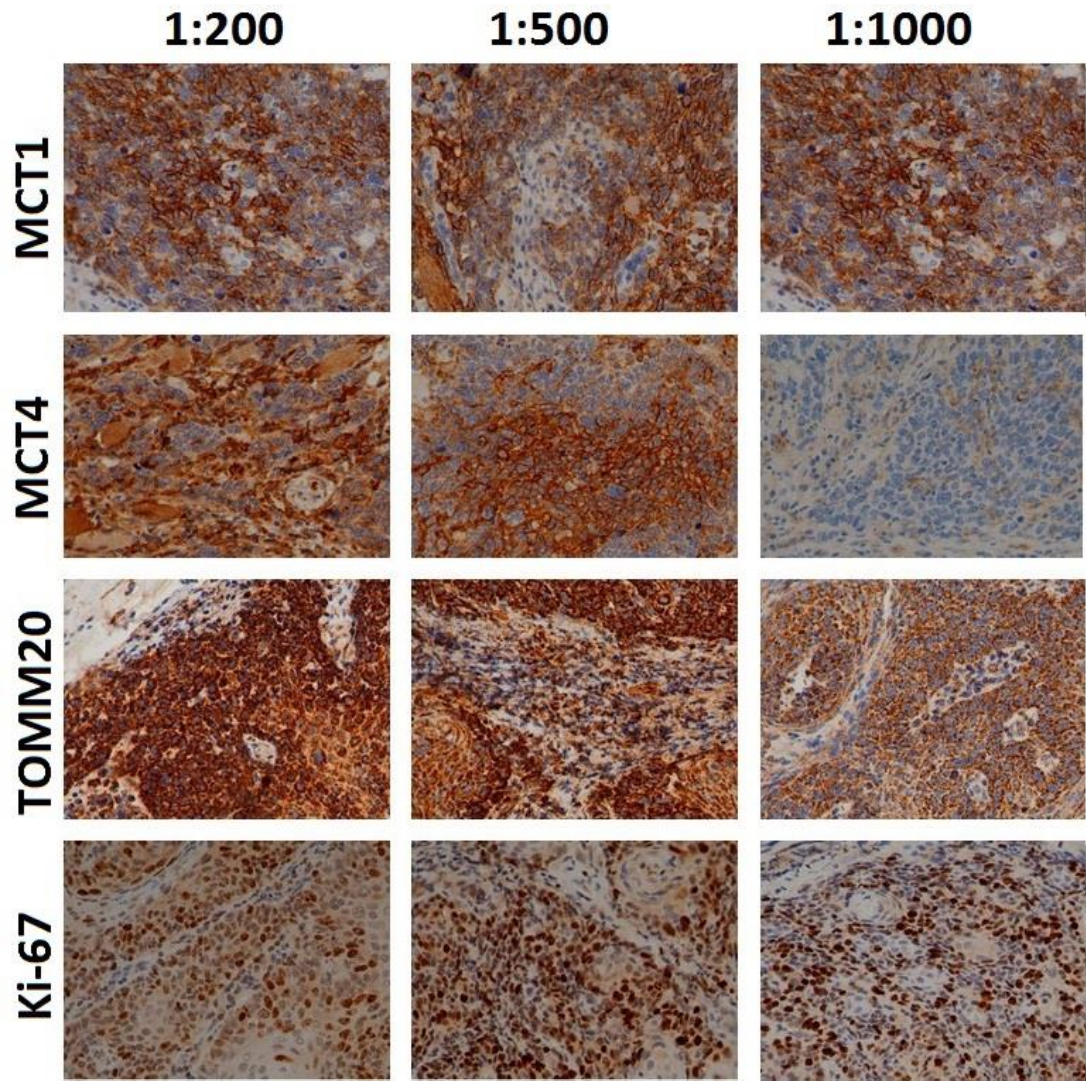
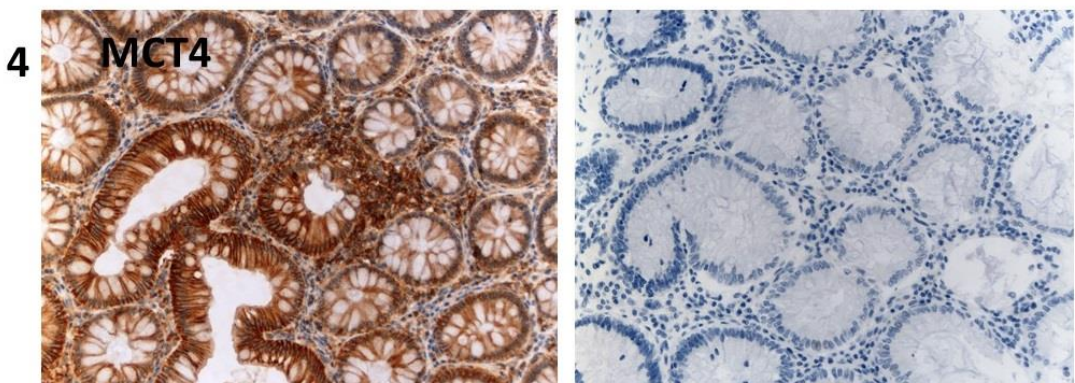
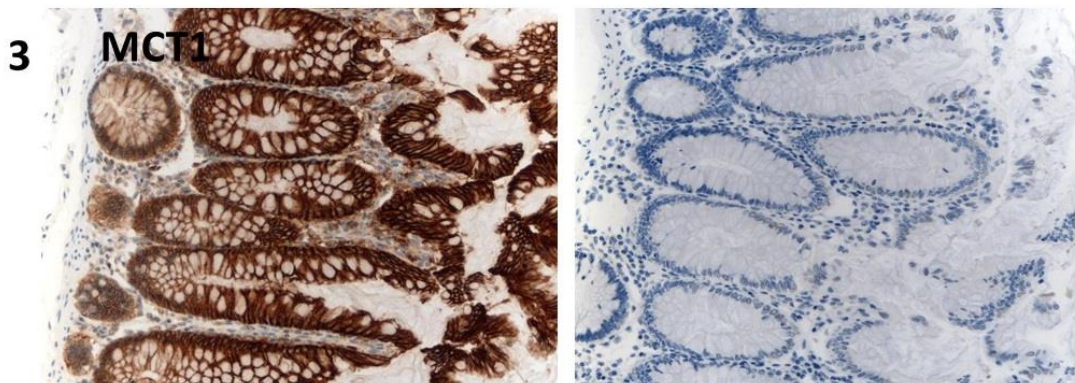
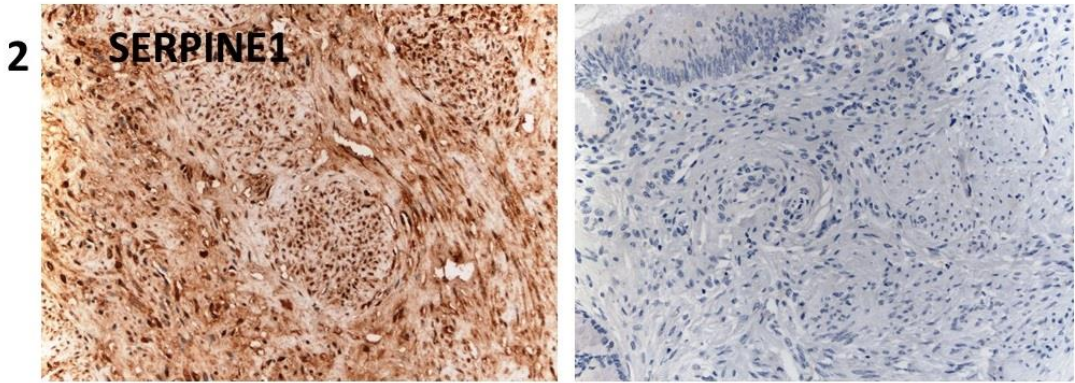
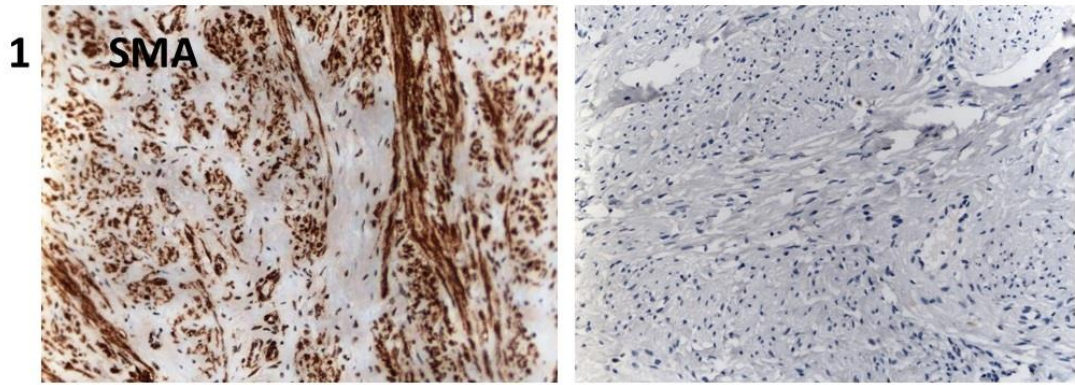


Figure 2.1. An example for primary antibodies optimization.

Optimization procedure for primary antibodies is approached by maintaining a constant incubation time (30 minutes) and temperature (room temperature), while varying the antibody concentration; 1:200, 1:500 and 1:1000 to determine when an optimal signal is achieved with low background noise. Concentration of 1:500 was used for MCT4 whereas 1:1000 was chosen for MCT1, Ki-67 and TOMM20.



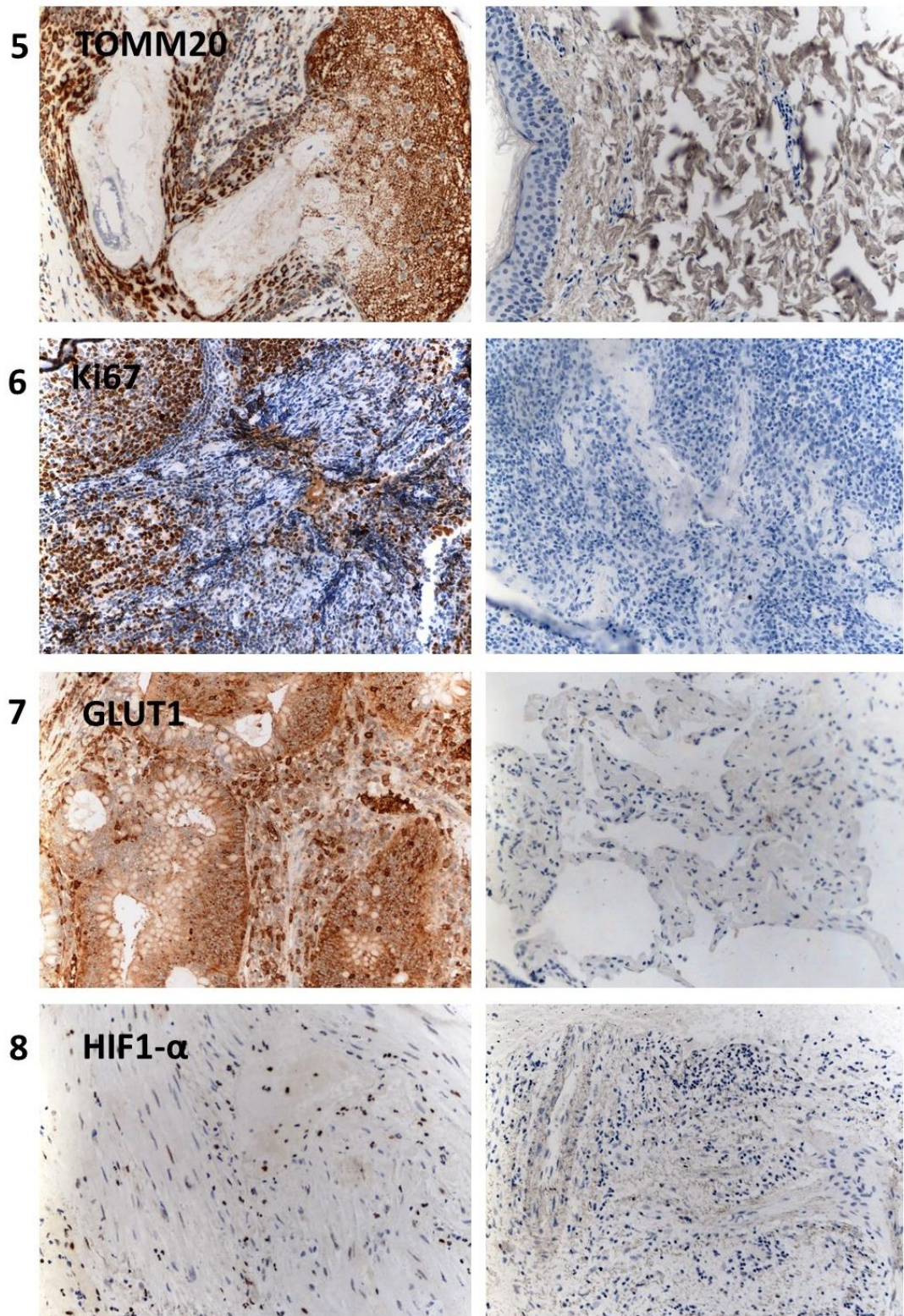


Figure 2.2. Typical examples for positive (left) and negative (right) IHC staining. Panel of FFPE tissues were used for this purpose; Cervix (1&2), Colon (3, 4 & 7), Skin (5), Placenta (6) and Gall bladder (8). Original magnification 20x.

2.8 Slide scanning

All slides used for the histochemical and immunohistochemical studies were digitalised using an Aperio CS2 slide scanner system (Digital Pathology Scanner: Leica Biosystems, Buffalo Grove, IL, USA). Image viewing and analysis was performed using the Aperio Imagescope v.10.2.2.2352 software package (Aperio Technologies, USA). Analysis was conducted blindly to the related clinical information. Aperio CS2 is a highly reliable workhorse for medium-volume sites, and delivers high-quality digital slides with 20X and 40x magnification capabilities from the desktop.

2.9 Scoring

Immunohistochemistry stained TMA sections were scored by KBS using a semi-quantitative binary scoring system, looking at the intensity and distribution of reactivity. The pattern of distribution of the staining was attributed to one of the following forms: focal, multifocal or widespread (Fig. 3.1 A) and the intensity of staining was graded as high (+++), intermediate (++) or low / sparse (+ or -) (Fig. 3.1 B & C), hence giving a total of 9 possible staining patterns. The histochemical and immunoreactivity was determined separately at core and the front of the tumour. Several of the potential staining patterns were present at low frequency, so cases were clustered into two groups, namely high expression, including cases with both multifocal and widespread patterns with strong staining (for example, widespread x strong staining, widespread x moderate staining, multifocal x strong staining, multifocal x moderate staining, focal x strong staining and focal x moderate staining), and low expression, including weak staining in focal patterns (focal x negative staining, focal weak staining and multifocal-widespread x negative or weak staining) (Fig. 3.1). In the literature, the Ki67 cut-offs in oropharyngeal cancer studies is not yet determined [503], so we analysed distribution in the percentage of cancer cells found to be Ki67-positive and found them to be gathered into two distinct groups: the first group has a percentage of staining equal to or less than 30% and called as the low rate proliferative index group and the second group has a percentage of staining equal to or above 30 % and called as the high rate proliferative index group.

2.10 Statistical analysis

All data were tabulated, and statistical analyses were performed with the Statistical Package for Social Sciences (SPSS) for Windows version 22.0 (SPSS statistics 22). The frequencies and statistics for the different parameters were studied by using a descriptive analysis. The association of desmoplasia at the tumour core, desmoplasia at the advancing front, α SMA, serpin E1 and Alcian Blue with depth of invasion were represented by its log, and was studied by an independent t test, from which boxplot graphs were generated. The Chi-square test was used for studying the relationship between desmoplasia at the tumour core, desmoplasia at the advancing front, α SMA, serpin E1 and Alcian Blue, and the other different clinicopathological factors. $P \leq 0.05$ were considered statistically significant. Most of our data was categorical (except for the depth of invasion), so contingency tables were the most appropriate test. Multivariate analysis was not undertaken, the groups were generally too small to make this valid.

Chapter 3

Desmoplasia in HPV+ and HPV- oropharyngeal squamous cell carcinoma

3.1 Introduction

Despite the fact that HPV+OPSCC is accompanied by extensive nodal disease, it has significantly improved treatment outcome and patient survival to low overall recurrence rates [325, 504, 505]. ECS in metastasis in cervical lymph nodes is regarded as the most important clinical prognosticator for the recurrence of and the death due to OSCC [248, 506-509]. It has been proposed that molecular features that have an impact on prognosis should often be associated with the characteristics of the tumour cells [169]. It has become more and more obvious that the 'normal' components of the stroma, including myofibroblasts, inflammatory/immune cells, and endothelial cells, perform a vital function in supporting tumour advancement [169, 240, 510]. GAGs and CAFs, the two components of desmoplastic reaction, are involved in the construction of the desmoplasia which characterizes different advanced tumours [235, 511]. Several types of solid tumours have myofibroblasts ('activated' fibroblasts, peritumour fibroblasts, and CAFs) as constituents of their stromae [169, 248, 343, 512]. Alpha smooth muscle actin (α SMA) expression by myofibroblasts identifies their presence in the tumour stroma [169, 170]. Alcian Blue is a routinely used histochemical stain for demonstration of GAGs [513-515]. It has been revealed that CAFs influence the invasion of cancer cells in OSCC [169, 516] and that the different types of aggressive basal cell carcinoma of the skin have a considerable amount of desmoplasia [169, 517].

Studies have shown that the presence of CAFs in the stroma of the tumour is an important prognostic value, also related to poor prognosis in many types of tumour [169, 342-344]; in addition, their presence has been revealed to anticipate disease recurrence through various types of tumours [342, 344]. It has been shown that the robust independent risk factor related to early OSCC death is a characteristic of tumour stroma, instead of cancer cells. High levels of stromal α SMA expression gave rise to the uppermost hazard ratio and the likelihood ratio of any feature investigated, and

was significantly related to mortality, irrespective of stage of the disease [169]. Such data propose that high α SMA expression in the stroma may be exploited to recognise aggressive OSCC, irrespective of disease stage, and could be an important factor in both the treatment and the follow-up [169].

It is becoming obvious that the classification of cervical lymph node is significant in prognosis and also this significance is not restricted only to recurrence in the neck region. Extra capsular spread is generally a mirrored image of the biological events in tumours [509]. There is limited use of molecular biomarkers in the treatment of head and neck squamous cell carcinomas compared with other types of cancer [509]. Extra capsular spread has been suggested to have prediction capacity and would be of significant value in the therapy of oral squamous cell carcinoma [509]. It is possibly beneficial for this group of patients to be predicted precisely by employing such a measure prior to making a decision about the final therapy, for the reason that imaging investigations are not adequately precise [509]. The extra capsular spread group is known to be associated with poor prognosis and thus might render this group eligible for other different types of treatments such as monoclonal antibody, immunotherapy or neoadjuvant measures in cases where this can be achieved [509].

It has been shown that grading of oral cancer has a valuable importance for prediction of the prognosis and making a decision on an efficient treatment plan [518, 519]. The TNM classification for example, which is founded mainly on anatomical site, is significant for total efficient clinical care and also to assist in defining cases for clinical trials, for stratification, clinical and research at molecular level, as well as policy making [519]. Staging has been described to be of great value, with cases receiving different treatments based on stage, and has been successful [520]. Oral cancer can be classified based on primary site and also based on the pattern of the tumour invasion or according to the degree of cancer cell differentiation [521, 522]. The staging system of oral cancer takes into consideration multiple features including clinico-pathological features and overall, the tumour stage providing information about tumour extension and its prognosis [523]. The TNM staging system takes into account the size of tumour (T), regional lymph nodes involvement (N) and metastasis (M) [524].

In HPV- HNSCC, the stroma support potentially induces a highly invasive and metastatic phenotype related to poor survival [3, 165, 270], however to date there has not been any published work relating to the importance of CAFs / stromae in HPV+ HNSCC. We hypothesize that in HPV+ OPSCC there is an association between the intensity of desmoplasia (as evidenced by Alcian Blue staining and presence of α SMA+ myofibroblasts) and the outcome or other prognostic indicators such as recurrence that would have an impact on both the choice and outcome of treatment. Here, the aim of this project was to investigate the presence of GAGs and myofibroblasts in a well-annotated cohort of HPV+ and HPV- OPSCC as well as study their correlations with clinicopathological features, using α SMA, Alcian Blue and serpin E1 biomarkers.

So, in summary, the overall aim of this chapter is to characterise the desmoplasia in OPSCC and its relation to clinicopathological features, particularly depth of invasion and outcome in relation to HPV status. In order to achieve these aims, these are the objectives

- a- Examination of histological desmoplasia in H and E stained sections
- b- Examination of GAGs
- c- Examination of α SMA
- d- Examination of SerpinE1

3.2 Materials and methods

3.2.1 Reagents

Three reagents are used in this research, namely Antibodies to α SMA, which is a biomarker for presence of myofibroblasts, Serpine E1, a biomarker for invasion and Alcian blue which is a water soluble basic dye related polyvalent to group with blue colour used to detect GAGs at pH 2.5. Details of antibodies used in this study are described in Table (3.2).

Marker	Clonality	Pretreatment	Dilution	Source	Control tissue
α SMA	Polyclonal	See Chapter 2.7	1:600	Abcam, Cambridge, UK (5694)	Colon
Serpin E1	Monoclonal		1:400	Sekisui Diagnostics, LLC, Stamford, CT (37852)	Breast

Table 3.1. Details of antibodies.

3.2.2 Evaluation

Histochemistry (for Alcian Blue) and immunohistochemistry (for α SMA and serpin E1) stained TMA sections were analysed and scored using a semi-quantitative binary scoring system, looking at the intensity and distribution of reactivity. The pattern of distribution of the staining was attributed to one of the following forms: focal, multifocal or widespread (Fig. 3.1 A) and the intensity of staining was graded as high (+++), intermediate (++) or low / sparse (+ or -) (Fig. 3.1 B & C), hence giving a total of 9 possible staining patterns. The histochemical and immunoreactivity was determined separately at core and the front of the tumour.

Several of the potential staining patterns were present at low frequency, so cases were clustered into two groups, namely high expression, including cases with both multifocal and widespread patterns with strong staining (for example, widespread x strong staining, widespread x moderate staining, multifocal x strong staining, multifocal x moderate staining, focal x strong staining and focal x moderate staining), and low expression, including weak staining in focal patterns (focal x negative staining, focal weak staining and multifocal-widespread x negative or weak staining) (Fig. 3.1).

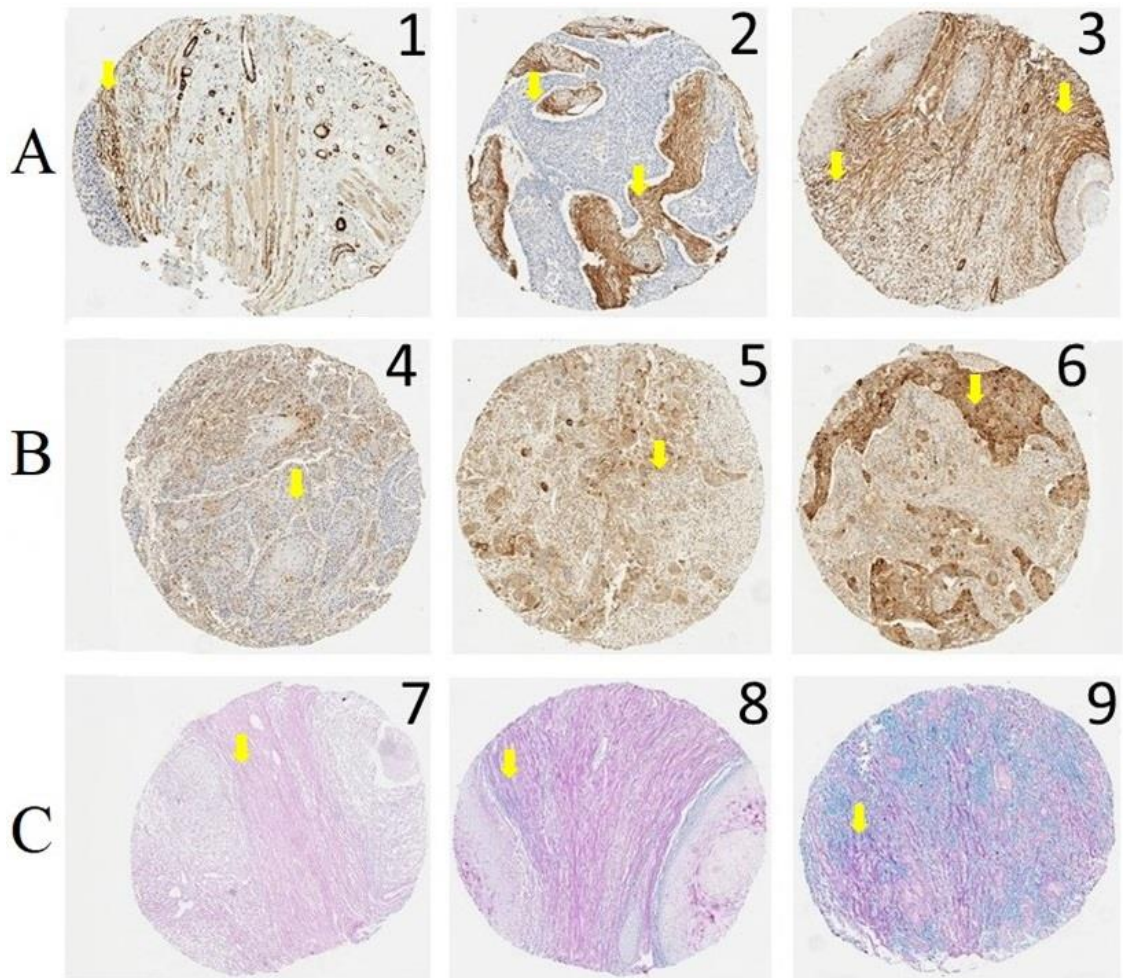


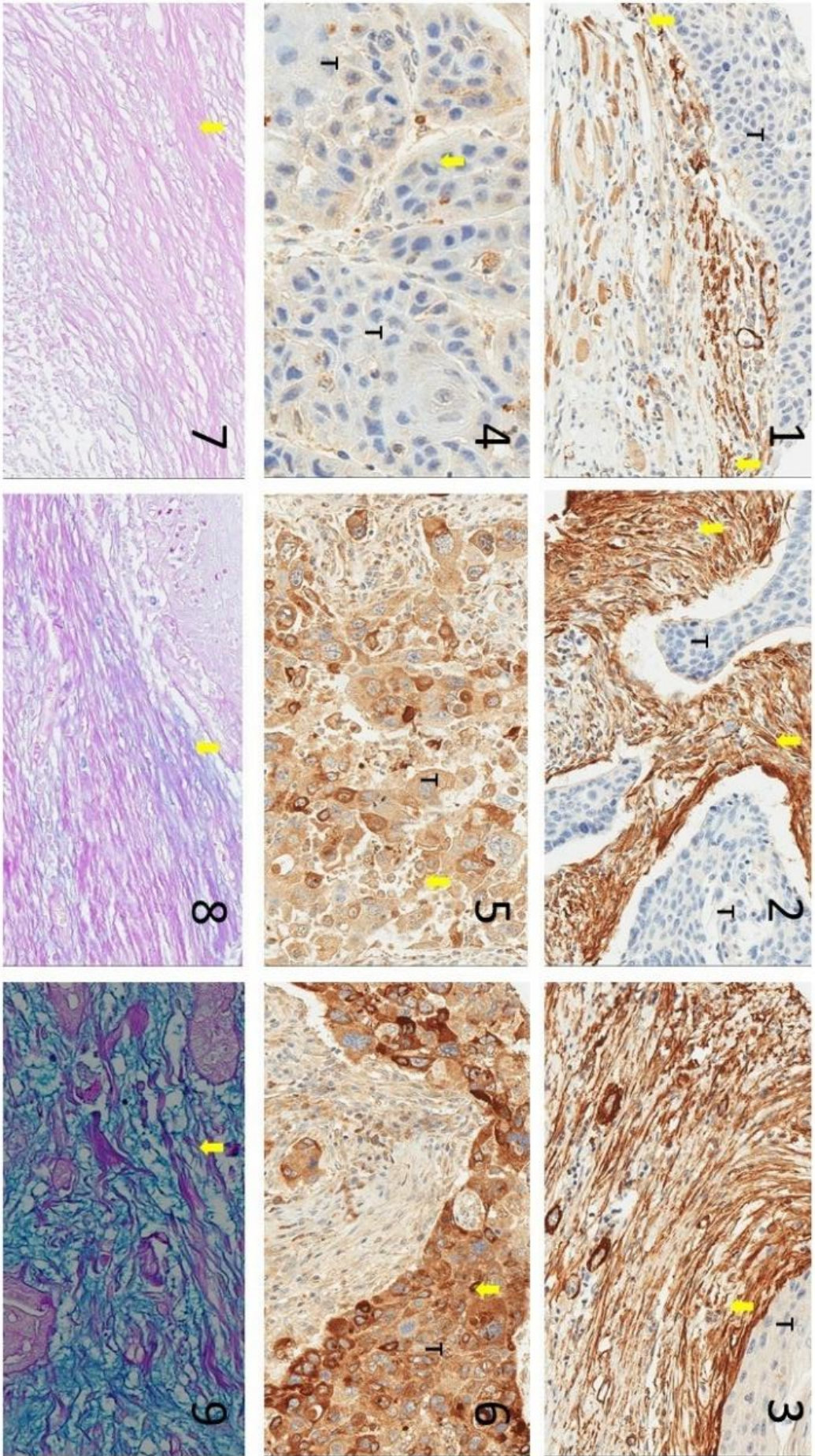
Figure 3.1. A typical example of scoring for expression of α SMA and serpin E1, and presence of GAGs in OPSCC performed on TMA sections.

A: IHC for α SMA: 1, focal pattern; 2, multifocal pattern; 3, widespread pattern.

B: IHC for serpin E1: 4, weak; 5, moderate; 6, strong staining.

C: Alcian Blue staining: 7, weak; 8, moderate; 9, strong.

Areas of interest indicated by arrows are magnified in the below panels.



3.3 Results

In HPV+OPSCC, the tumour spreads to different subsites of oropharynx, meaning that it was not always possible to precisely define the subsite. Nine cases out of 42 (21%) were unclassified, in fact reported as oropharynx in their site, but without a precise origin. However, in 33 of the total number of cases it was possible to define the precise site of the tumour: 17/33 (51.5 %) were located in the tonsils, 9/33 (27.2 %) at the base of the tongue, 2/33 (6 %) in the soft palate, 2/33 (6 %) in the pharyngeal wall and 3/33 (9 %) were mixed (appendix 1). The majority of cases 36/43(84%) were purely non-keratinizing SCC, with 3/43 cases (7%) purely keratinizing SSC and 4/43 (9%) mixed SCC (Fig. 3.2). In twenty-one cases out of 41 (51%), the tumours' pT were classified as T2 and 14 cases (34%) as T3, while most tumours, namely 33/43 (79%), showed nodal involvement (appendix 1). The tonsil and the base of the tongue were the frequent sites, with the majority of the tumours pT2 or pT3. 27/42 (64%) showed pN2, 6/42 (14%) pN1, while 9 cases (21%) with pN0. About half of the cases, namely 22/41 (53%), did not show any extra capsular spread. These subjects involved in these cases included were predominantly male, however further details on the clinical and pathological characteristics of the sample used in this study are presented in appendix 1.

In HPV- OPSCC, nine cases out of 62 (14.5%) were unclassified, in other words reported as oropharynx in their site, but without any precise origin. However, in 53 of the total number of cases it was possible to define the precise site of the tumour: 29 (55 %) were located in the tonsil, 11 (21 %) at the base of the tongue, 13 (24 %) in the soft palates (appendix 2), all keratinising differently. Differentiation was determined from pathology reports. Data available from 15 cases showed that 11 of them (73%) are moderately differentiated, 3 cases (20%) are well differentiated and one case (7%) is acantholytic. In 11 cases out of 29 (38%) the tumours' pT were classified as T2, 9 cases (31%) as T3, 7 cases (24%) as T4 and one case (3%) as T1 and 65% of tumours (22/34) showed nodal involvement. 17/30 (56.6%) showed pN2, 6/30 (20%) pN1 and 7/30 cases (23%) with pN0. About half of the cases did not show any extra capsular spread 18/35 (51%), but further details of the clinical and pathological characteristics of the sample used in this study are presented in appendix 2. The two groups of OPSCC showed significant difference in age ($p = 0.029$). The majority of cases classified as non-keratinising for the histological subtype in HPV+ OPSCC meanwhile the majority

of HPV- OPSCC where classified from moderate to well differentiated, which is in fact a reflection of their high degree of keratinisation. The site and the presence of lymph node metastasis were also significantly different between the two types ($p = 0.020$ and 0.001 respectively).

In HPV- OPSCC, the histological desmoplasia at the front of the tumour was significantly correlated with pT-stage ($p = 0.047$). The histological study of desmoplasia in both HPV+ and HPV- OPSCC has not shown any significant correlation between desmoplasia at the centre and at the periphery of the tumour. Moreover, the depth of invasion (DOI) in HPV+ OPSCC was significantly correlated with histological desmoplasia at the core and advancing front of the tumour with p value of 0.001 and 0.045 respectively (Fig. 3.3). In contrast with HPV- OPSCC, histological desmoplasia in its two locations did not show any correlation with the depth of invasion (Fig. 3.3). Furthermore, there was not any correlation observed between the depth of invasion and the outcome in either HPV+ or HPV- OPSCC.

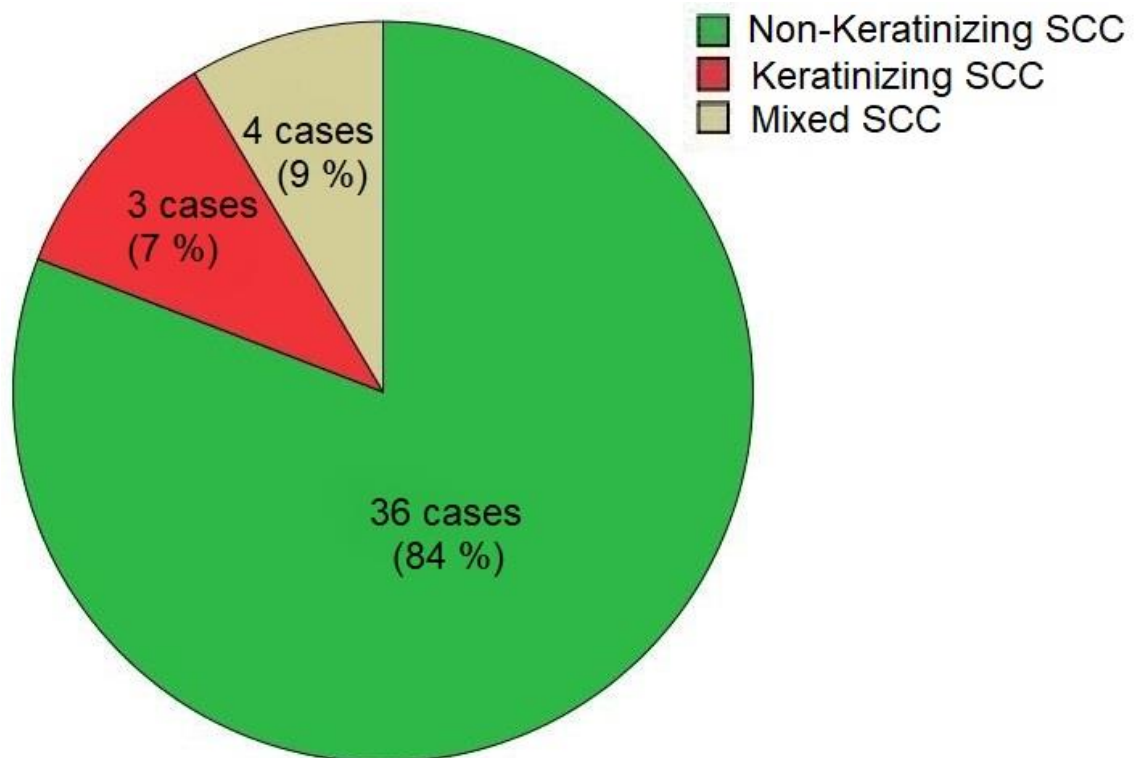
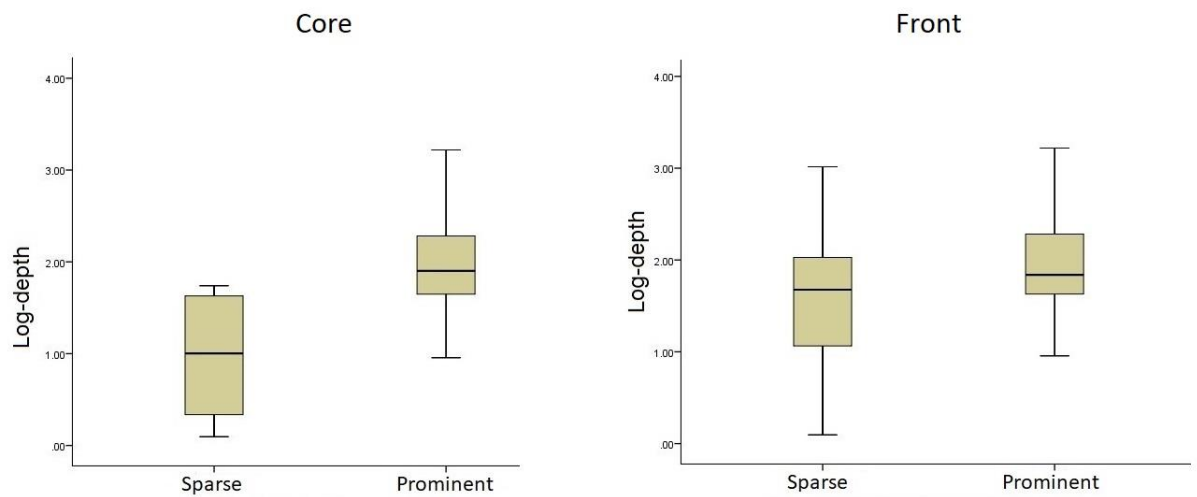


Figure 3.2. Histological subtype of 43 cases of HPV+ OPSCC. The majority of cases 36/43(84%) were purely non-keratinizing SCC, with 3/43 cases (7%) purely keratinizing SSC and 4/43 (9%) mixed SCC.

HPV+ OPSCC



HPV- OPSCC

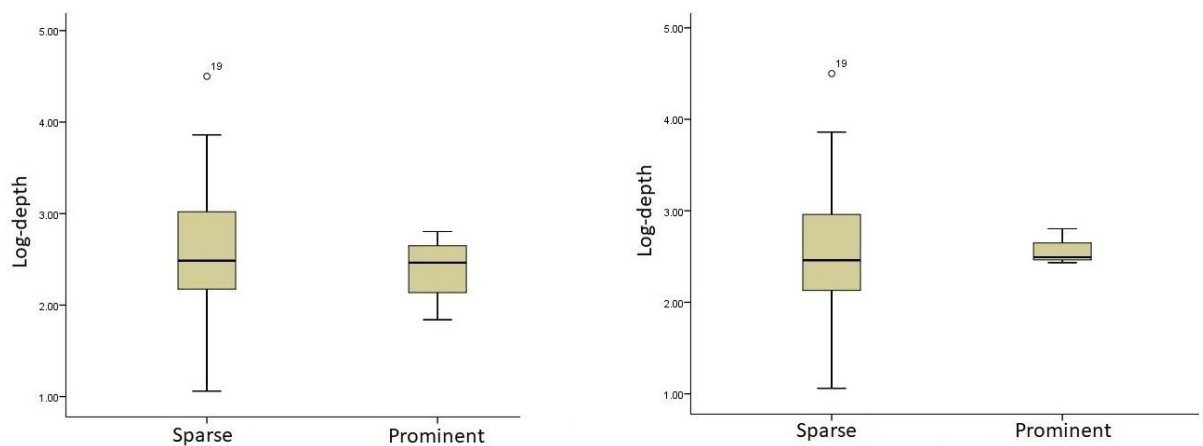


Figure 3.3. Correlation between desmoplasia and depth of invasion in OPSCCs.

The depth of invasion (Log-depth) in HPV+ OPSCC was significantly correlated with desmoplasia at the core and advancing front of the tumour with p value of 0.001 and 0.045 respectively. In contrast with HPV- OPSCC, desmoplasia in its two locations did not show any correlation with the depth of invasion.

Staining results of Alcian Blue, α SMA and serpin E1

In HPV+ OPSCC

Alcian Blue

The front stained more strongly with Alcian Blue, representing ECM, than the tumour core (Fig. 3.4), where it was also generally less prevalent (48% vs. 65%, respectively; $p = 0.008$, Table 3.3). A significant association was seen at the tumour core between Alcian Blue and histological desmoplasia ($p = 0.027$). Similarly, Alcian Blue staining at the tumour front also correlated significantly with desmoplasia at the front of the tumour ($p = 0.006$).

α SMA staining

Interestingly, high levels of α SMA expression were observed at the core as well as at the front of tumour (Table 3.3 and Fig. 3.4). A significant relationship was observed between desmoplasia at tumour core and α SMA at the tumour core ($p = 0.001$), as well as between desmoplasia at tumour front and α SMA at the tumour front ($p = 0.021$; Table 3.5).

Expressions of the two components of desmoplasia, namely GAGs and myofibroblasts, were strongly correlated at the front of the tumour ($p = 0.009$) (Table 3.4), but not at the core of the tumour, where Alcian Blue staining was generally less prevalent (Table 3.3).

Serpin E1

The serpin E1 was expressed at high level at the tumour core, as well as at the tumour advancing front (97% and 84%, respectively, see Table 3.3, Fig. 3.6). Significant correlation was seen in the carcinoma between serpin E1 expression at the tumour core and Alcian Blue staining at the front ($p = 0.019$).

Biomarker	HPV+ OPSCC		HPV- OPSCC	
	Tumour core	Advancing front	Tumour core	Advancing front
Alcian Blue	14/29 (48%)	17/26 (65%)	41/57 (72%)	19/31 (61%)
α SMA	27/32 (84%)*	26/31 (84%)*	37/53 (70%)	22/32 (69%)
Serpin E1 tumour	31/32 (97%)*	26/31 (84%)	31/59 (53%)	12/33 (36%)
Serpin E1 stroma	16/30 (53%)	11/27 (41%)	26/59 (44%)	8/30 (27%)

Table 3.2. Expression of Alcian Blue, α SMA and serpin E1 in HPV+ and HPV- OPSCC cases at the core and front.

Serpin E1 tumour: presence of serpin E1 staining of carcinoma cells; serpin E1 stroma: presence of serpin E1 staining of stroma cells. * Indicates statistically significant values.

		α SMA at tumour front		
		Low expression	High expression	Total
Alcian Blue at tumour front	Low expression	10	6	16
	High expression	4	16	20
Total		14	22 p = 0.009*	36

Table 3.3. Strong correlation between Alcian Blue reaction and α SMA expression at the tumour front in HPV+ OPSCC.

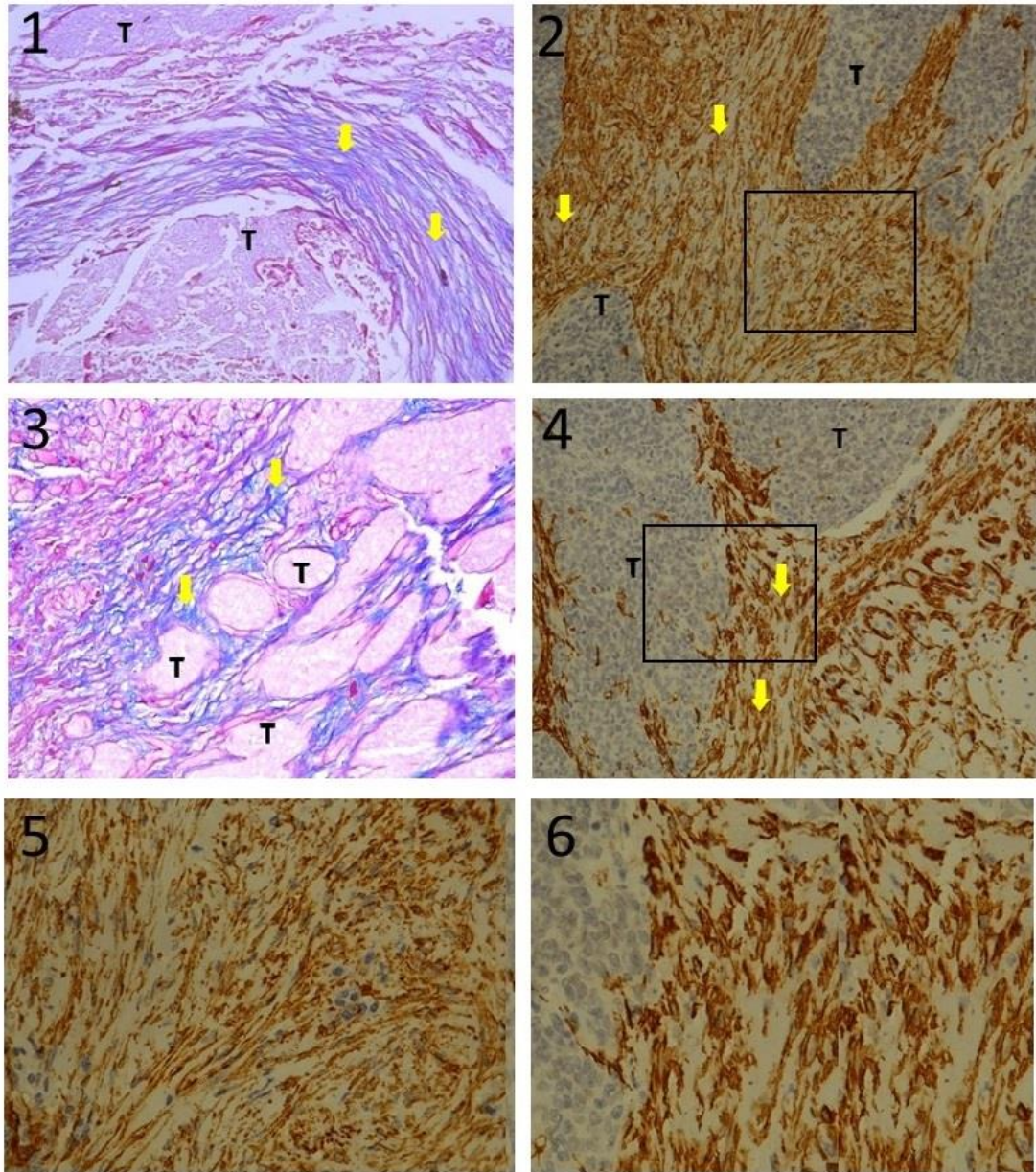


Figure 3.4. A typical example of staining for GAGs and myofibroblasts/CAFs in the stroma of HPV+ OPSCC performed on TMA sections. Alcianophilic GAGs (arrows) in the core (1) and front (3) of the same tumour (T). α SMA+ spindled cells (arrows) in the core (2) and front (4) of the same tumour (T). The rectangled areas are magnified in panels (5) and (6) respectively. Note that myofibroblasts are arranged in parallel to contour of the tumour (arrows in panels 2 and 4)

In HPV- OPSCC

Alcian Blue staining

Alcian Blue staining is more often found at the tumour core, while it was generally less prevalent at the front (72% v 61%, respectively; Table 3.3 and Fig. 3.5). However, the strength of staining was the same at both the core and the front. Alcian Blue staining at the tumour core correlated significantly with desmoplasia at the tumour core as well as at the front ($p = 0.004$ & 0.022 , respectively; Table 3.5).

α SMA expression

High levels of α SMA expression were observed at the core as well as at the front of tumour (Table 3.3 and Fig. 3.5). There was not any association noticed between desmoplasia and α SMA in HPV- OPSCC. There was not any association noticed between the two elements of desmoplasia in HPV- OPSCC.

Serpin E1 expression

A lower level of serpin E1 expression was seen both at the tumour core and the front, where the expression was less prevalent (53% vs 36%, respectively). Carcinoma cell serpin E1 expression in the tumour core correlated significantly with desmoplasia at both the core and the front of the tumour ($p = 0.003$ and 0.017 , respectively), while stromal serpin E1 in the same location correlated significantly with the α SMA expression ($p = 0.051$). Serpin E1 expression by carcinoma cells at the front correlated significantly with desmoplasia at tumour core ($p = 0.038$) and with α SMA expression at the tumour front ($p = 0.030$), while stromal serpin E1 expression at the front correlated with α SMA and Alcian Blue staining ($p = 0.021$ and 0.040 respectively).

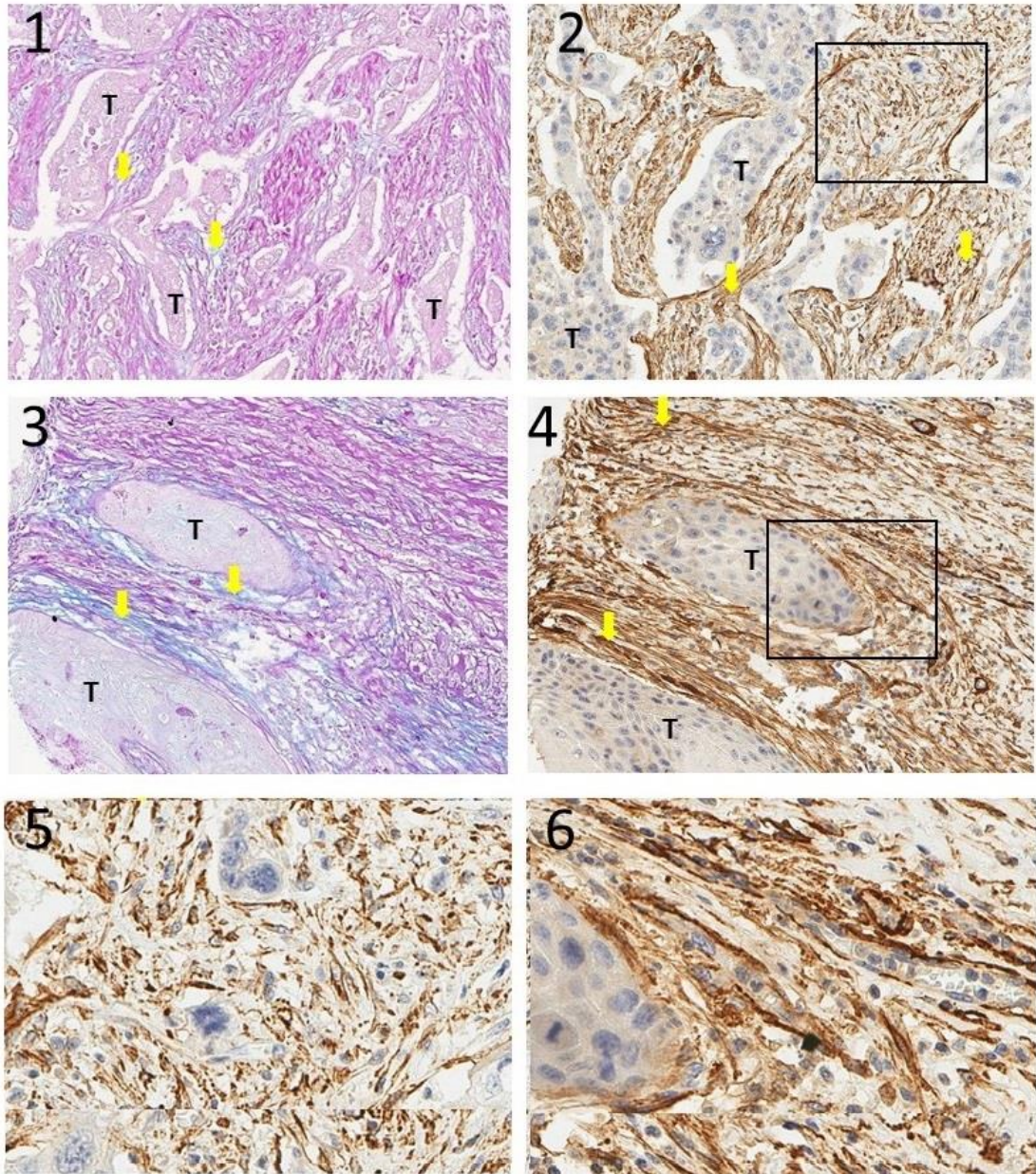


Figure 3.5. A typical example of staining for GAGs and myfibroblasts/CAFs in the stroma of HPV- OPSCC performed on TMA sections. Alcianophilic GAGs (arrows) in the core (1) and front (3) of the same tumour (T). α SMA+ spindled cells (arrows) in the core (2) and front (4) of the same tumour (T). The rectangled areas are magnified in panels (5) and (6) respectively.

A		Tumour core						Tumour front						
			Alcian Blue			αSMA			Alcian Blue			αSMA		
			Low	High	Total	Low	High	Total	Low	High	Total	Low	High	Total
HPV-	Desmoplasia at tumour core	Low	5	23	28	10	15	25	9	15	24	8	19	27
					p (0.004)*			p (0.083)			p (0.917)			p (0.660)
	High	4	1	5	0	5	5	2	3	5	1	4	5	
	Total		9	24	33	10	20	30	11	18	29	9	23	32
HPV+	Desmoplasia at tumour core	Low	11	1	12	6	6	12	6	5	11	4	6	10
					p (0.027)*			p (0.001)*			p (0.367)			p (0.702)
	High	15	12	27	2	28	30	10	16	26	10	20	30	
	Total		26	13	39	8	34	42	16	21	37	14	26	40
HPV-	Desmoplasia at tumour front	Low	6	23	29	10	16	26	9	16	25	8	20	28
					p (0.022)*			p (0.129)			p (0.592)			p (0.882)
	High	3	1	4	0	4	4	2	2	4	1	3	4	
	Total		9	24	33	10	20	30	11	18	29	9	23	32
HPV+	Desmoplasia at tumour front	Low	17	4	21	5	18	23	13	8	21	11	11	22
					p (0.056)			p (0.571)			p (0.006)*			p (0.021)*
	High	10	9	19	3	17	20	3	14	17	3	16	19	
	Total		27	13	40	8	35	43	16	22	38	14	27	41

B		Tumour core		Tumour front	
		Alcian Blue	αSMA	Alcian Blue	αSMA
H	Desmoplasia at core	p (0.004)*	p (0.083)	p (0.917)	p (0.660)
HPV	Desmoplasia at core	p (0.027)*	p (0.001)*	p (0.367)	p (0.702)
HPV-	Desmoplasia at front	p (0.022)*	p (0.129)	p (0.592)	p (0.882)
HPV	Desmoplasia at front	p (0.056)	p (0.571)	p (0.006)*	p (0.021)*

Table 3.4. Details of different groups (High and Low) of desmoplasia and its two components; the Alcian Blue and αSMA in both HPV+ and HPV- OPSCC are shown in table (A). Summary of the statistically significant correlations between the three variables are shown in table (B). * Indicates statistically significant values.

Interestingly, the lower level of serpin E1 expression seen in HPV- OPSCC cases both at the tumour core and the front, was significantly different to the serpin E1 expression by HPV+ OPSCC carcinoma cells ($p < 0.005$). Expression of serpin E1 by carcinoma cells was always stronger and more prevalent than the expression by stromal cells and this was significant in HPV- OPSCC at the tumour core (53% v 44%: $p = 0.007$). For stromal expression of serpin E1, there was not a statistical difference between the two types of OPSCC, either at the tumour core or at the front.

Moreover, there is significant statistical difference in the presence of GAGs at the tumour core between the two types of OPSCC ($p = 0.031$, Table 3.6).

The comparison between the expression of α SMA, the presence of GAGs and the expression of serpin E1 in the core and front of OPSCCs are shown in Figs 3.7 and 3.8. See appendix 3 for the correlation between serpin E1 expression and desmoplasia at the tumour core and the front in HPV+ and HPV- OPSCC.

Negative immunostaining for α -SMA in stromal cells in HPV+ and HPV- OPSCC is shown in Fig. 3.9.

		p16/cISH		
		HPV-	HPV+	Total
Alcian Blue at the core	Low	16	15	31
	High	41*	14	55
Total		57	29	86

Table 3.5. The GAGs reaction at the tumour core between the two types of OPSCC. *Presence of significant statistical difference, $p = 0.031$. p16/cISH indicates that positivity of HPV infection is based on positivity of both p16 and chromogenic in situ hybridization tests .

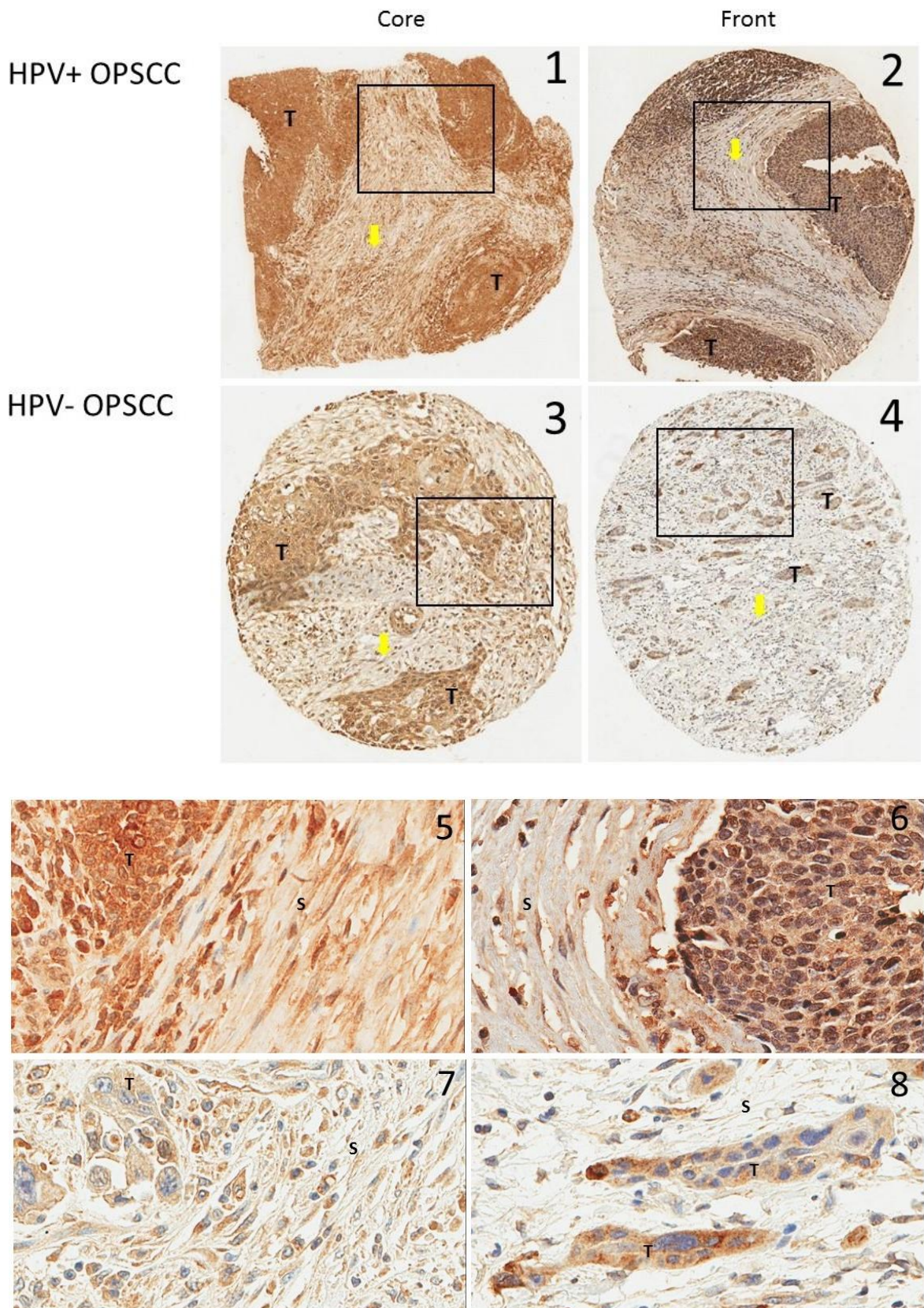


Figure 3.6. A typical example of serpin E1 staining performed on TMA sections showing expression at tumour core (1 and 3) and front (2 and 4) in HPV+ and HPV- OPSCC done on TMA sections. Tumour (T); stromal cells (arrows). The rectangled areas in panels 1, 2, 3 and 4 are magnified in panels 5, 6, 7 and 8 respectively. Tumour (T); stroma (S).

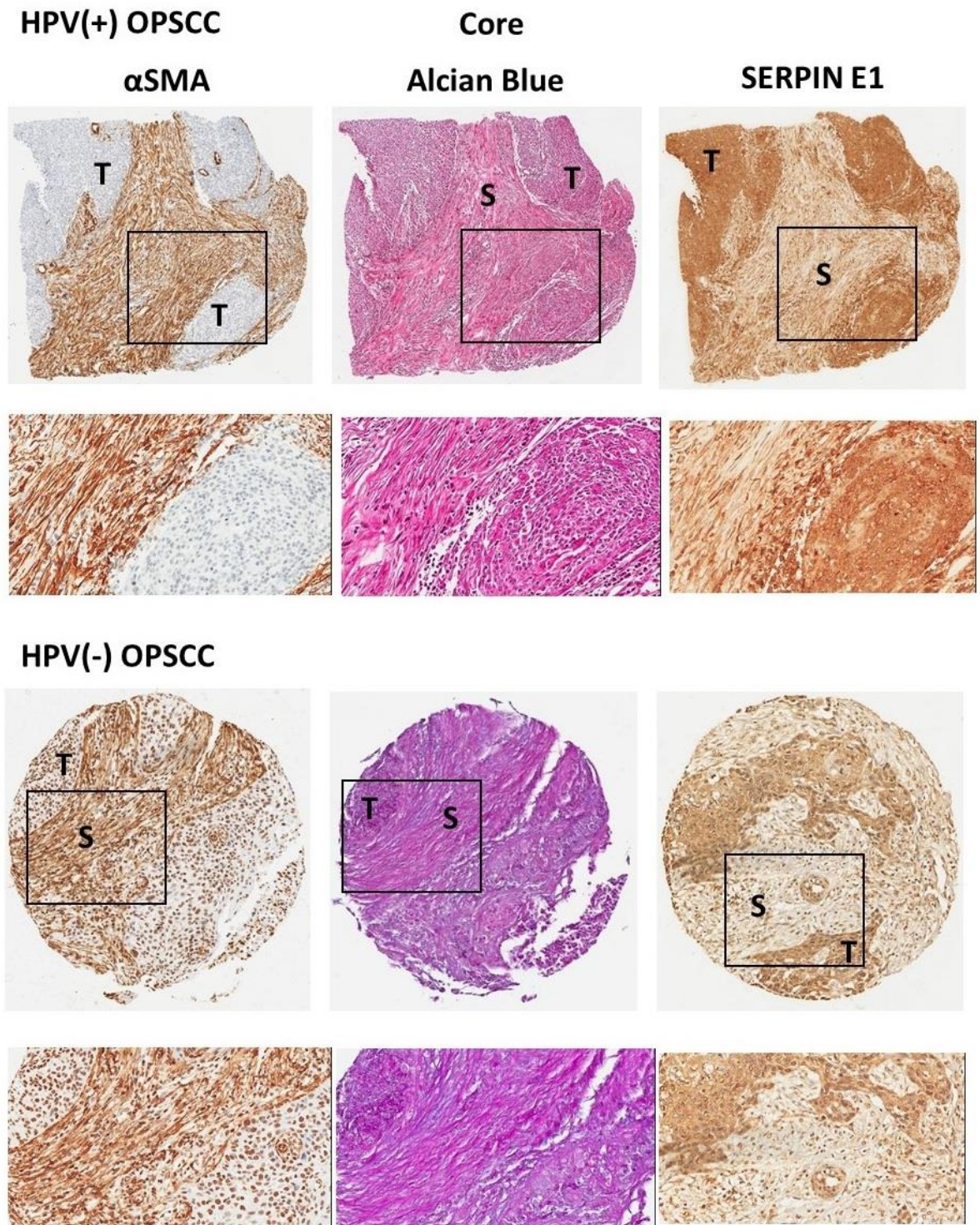


Figure 3.7. Step sections done on TMAs allowing comparison of expression of α SMA, presence of GAGs and expression of serpin E1 in the core of OPSCCs (two cases). Tumour (T); stroma (S). Note that the immunoreactivity of serpin E1 in HPV+ is stronger than HPV- OPSCCs. Also, expression of serpin E1 by carcinoma cells was always stronger than the expression by stromal cells. For stromal expression of serpin E1, there was not a statistical difference between the two types of OPSCC at the tumour core.

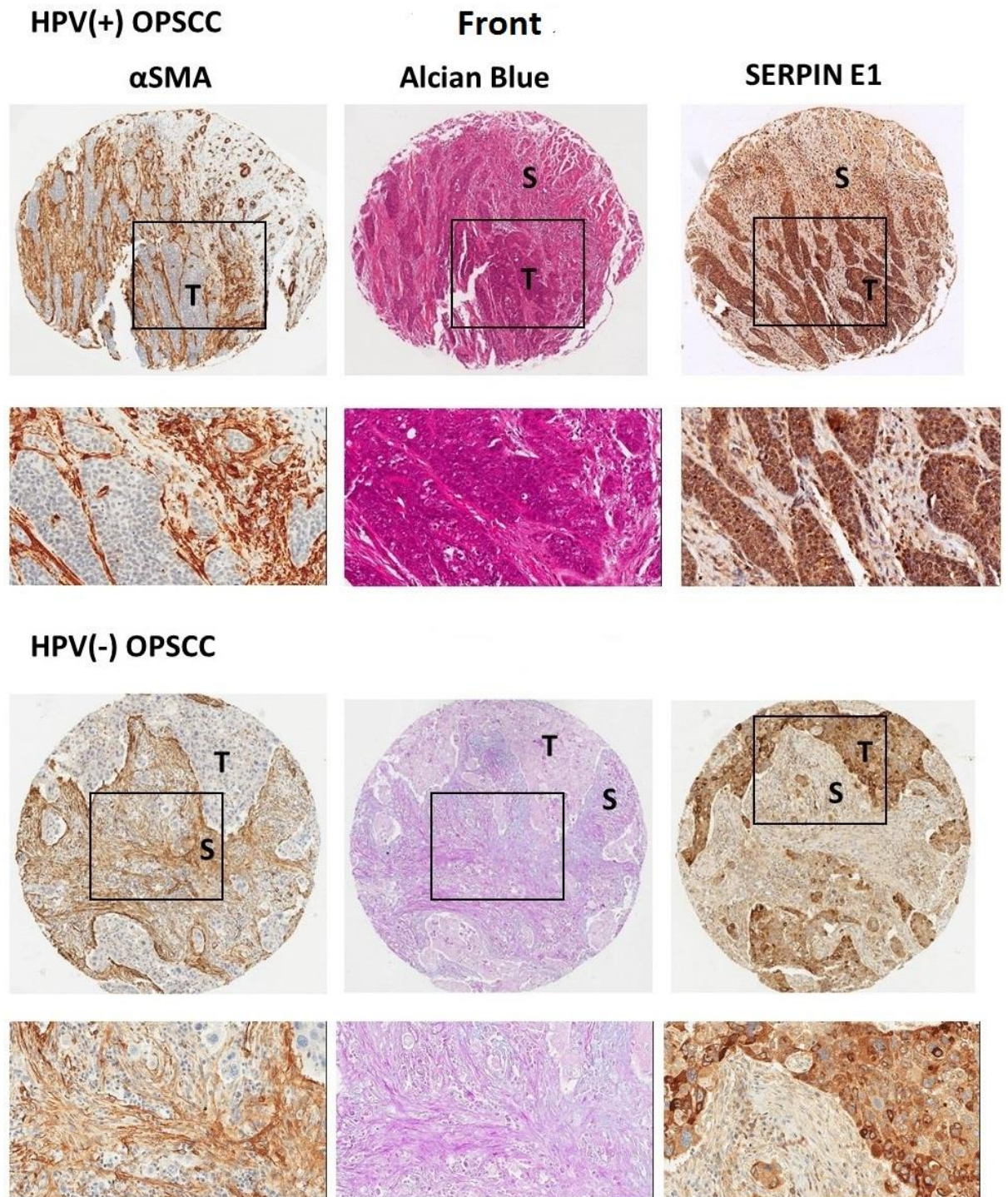


Figure 3.8. Step sections done on TMAs allowing comparison of expression of α SMA, presence of GAGs and expression of serpin E1 in the front of OPSCCs (two cases). Tumour (T); stroma (S). Note that the immunoreactivity of serpin E1 in HPV+ is stronger than HPV- OPSCCs. Also, expression of serpin E1 by carcinoma cells was always stronger than the expression by stromal cells. For stromal expression of serpin E1, there was not a statistical difference between the two types of OPSCC at the tumour front.

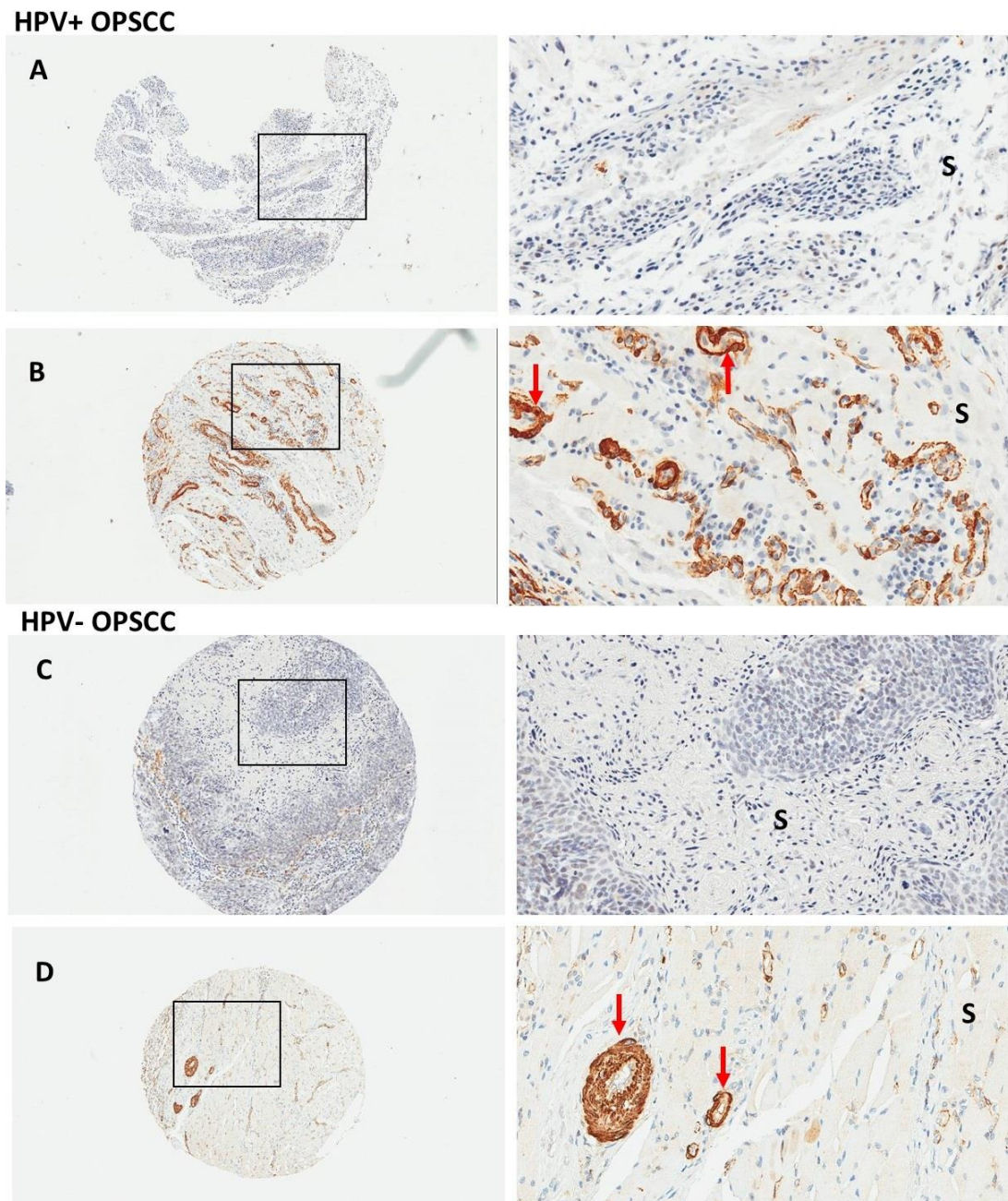


Figure 3.9. Negative immunostaining for α -SMA in stromal cells in HPV+ and HPV- OPSCC.

Representative TMA photomicrograph showing negative immunostaining for α -SMA in stromal cells in HPV+ and HPV- OPSCC at tumour core (A & C) and advancing front (B & D). The rectangled areas in the panels of the left column are magnified in the right column. Tumour (T); stroma (S). Strong positive staining of blood vessel walls is seen (red arrows) (original magnification x100).

Correlation of α SMA, Alcian Blue and serpin E1 expression with clinicopathological variables.

In HPV+ OPSCC

α SMA expression

α SMA expression at the tumour core correlated significantly with extranodal metastatic spread (0.047). Also, the α SMA expression at the core correlated significantly with the histological subtype ($p = 0.050$).

Serpin E1 expression

The level of serpin E1 expression in cancer cells at the front is related to the presence of nodal metastasis, as well as ECS ($p = 0.040$) (Table 3.7), the expression in cancer cells at the core correlated with the tumour site ($p = 0.016$).

In HPV- OPSCC

Alcian Blue staining

The Alcian Blue staining at the tumour core showed a significant correlation with the survival status ($p = 0.009$) (Fig. 3.10) and age ($p = 0.046$).

α SMA expression

The α SMA expression at the front correlated significantly with the survival status ($p = 0.004$) (Fig. 3.11), while α SMA tumour core expression has exhibited a strong correlation with the tumour site ($p = 0.017$).

Serpin E1 expression

The tumour cell serpin E1 expression at the front correlated significantly with the histological subtype ($p = 0.046$), as well as the site of the tumour ($p = 0.029$), while stromal expression correlated with the tumour site ($p = 0.008$).

α SMA expression at the tumour core correlated significantly with extranodal metastatic spread (0.047), however this correlation was not seen in the HPV- OPSCC.

Alcian Blue staining and α SMA expression did not correlate with the depth of invasion, either in the HPV+ OPSCC or in the HPV- OPSCC, however the combination where both α SMA and serpin E1 were expressed was prognostic ($p =$

0.043) (Table 3.8). A strong statistical difference has been found between the survival data of HPV+ and HPV- OPSCC ($p = 0.001$). The percentage of people who are still alive is higher in HPV+ 65% (24/37) than HPV- 43% (16/37), however further details are described in Table 3.9. At the front of HPV- OPSCC, α SMA individually or in combination with stromal serpin E1 correlates strongly with survival status ($p = 0.004$ and 0.016 respectively) (Table 3.10).

See appendices 4 and 5 for the actual data on the correlations between α SMA, Alcian Blue and serpin E1 expressions, with clinicopathological variables at the core and the front of the tumour in HPV+ and HPV- OPSCC.

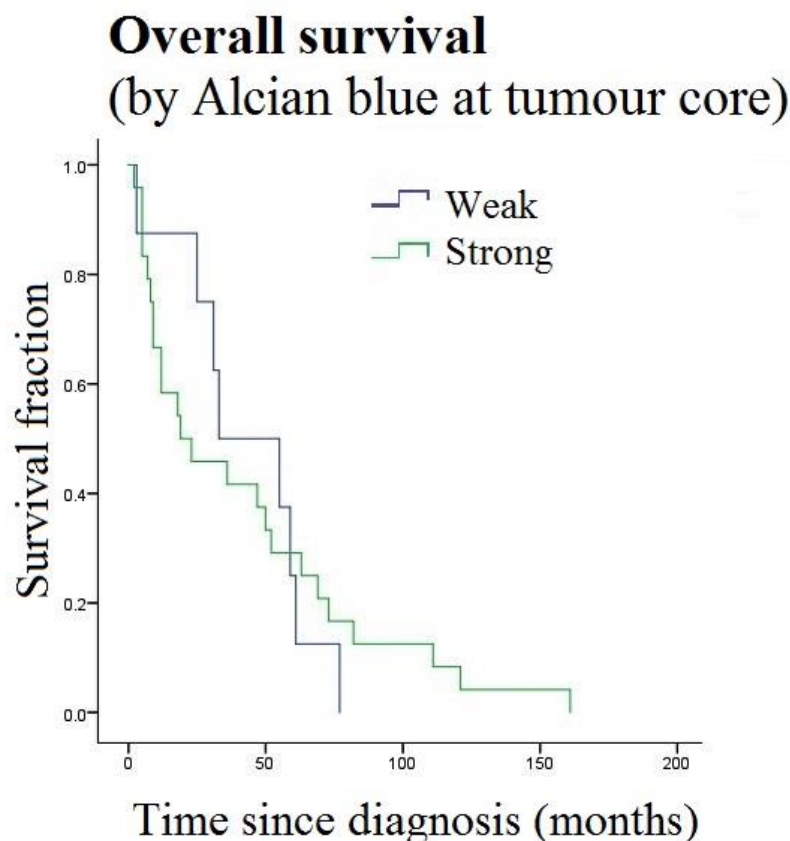


Figure 3.10. The Alcian Blue staining at the tumour core showed a significant correlation with the survival status ($p = 0.009$) in HPV- OPSCC.

Overall survival (By α SMA at tumour front)

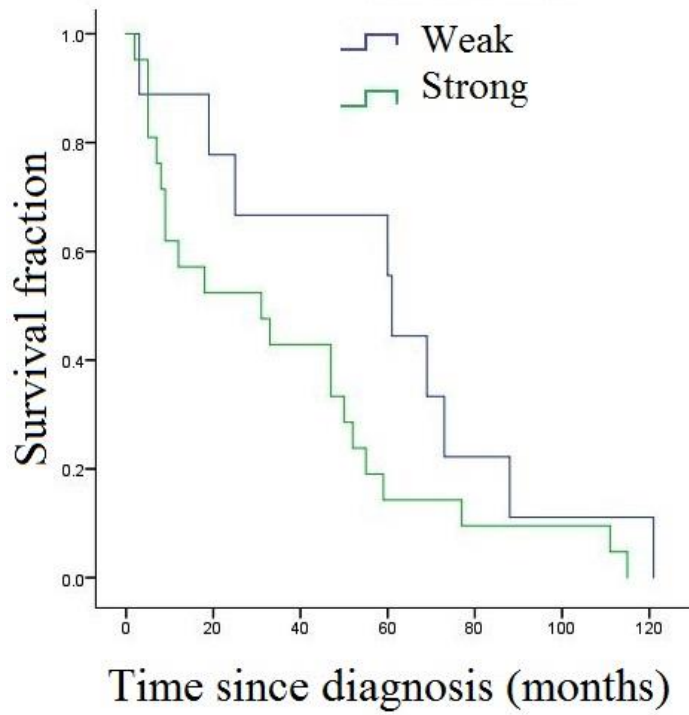


Figure 3.11. The α SMA expression at the front correlated significantly with the survival status ($p = 0.004$) in HPV- OPSCC.

	HPV+ OPSCC		HPV- OPSCC	
	Tumour core	Tumour front	Tumour core	Tumour front
α SMA	p = 0.047*	p = 0.971	p = 0.505	p = 0.778
Serpin E1 tumour	p = 0.0206	p = 0.040*	p = 0.392	p = 0.233
Serpin E1 stroma	p = 0.619	p = 0.558	p = 0.388	p = 0.843
α SMA and Serpin E1 stroma	p = 0.844	p = 0.961	p = 0.507	p = 0.928
α SMA and Serpin E1 tumour	p = 0.525	p = 0.637	p = 0.479	p = 0.197
α SMA and Serpin E1 stroma and Serpin E1 tumour	p = 0.945	p = 0.961	p = 0.507	p = 0.518
Serpin E1 tumour and Serpin E1 stroma	p = 0.751	p = 0.453	p = 0.966	p = 0.481

Table 3.6. Correlations of α SMA and serpin E1 expressions with ECS in HPV+ and HPV- OPSCC.

Presence of significant correlation between tumour serpin E1 and ECS at the front (p = 0.040), but this effect was not observed in the HPV- OPSCC.

	HPV+ OPSCC		HPV- OPSCC	
	Tumour core	Tumour front	Tumour core	Tumour front
α SMA	p = 0.173	p = 0.232	p = 0.931	p = 0.343
Serpin E1 tumour	p = 0.853	p = 0.851	p =	p = 0.426
Serpin E1 stroma	p = 0.324	p = 0.183	p = 0.617	p = 0.367
α SMA and Serpin E1 stroma	p = 0.043*	p = 0.184	p = 0.876	p = 0.327
α SMA and Serpin E1 tumour	p = 0.223	p = 0.180	p = 0.834	p = 0.426
α SMA and Serpin E1 stroma and Serpin E1 tumour	p = 0.043*	p = 0.184	p = 0.876	p = 0.774
Serpin E1 tumour and Serpin E1 stroma	p = 0.332	p = 0.171	p = 0.617	p = 0.774

Table 3.7. Depth of invasion and α SMA and serpin E1 expression in HPV+ and HPV- OPSCC.

Serpin E1 tumour: presence of serpin E1 staining of carcinoma cells; serpin E1 stroma: presence of serpin E1 staining of stroma cells.

Survival status	HPV+	HPV-
Alive	24/37 (65%)	16/37 (43%)
Died of disease	11/37 (30%)	15/37 (41%)
Died other	2/37 (5%)	6/37 (16%)

Table 3.8. Survival data in both HPV+ and HPV- OPSCC.

	HPV+ OPSCC		HPV- OPSCC	
	Tumour core	Tumour front	Tumour core	Tumour front
α SMA	p = 0.649	p = 0.649	p = 0.609	p = 0.004*
SerpinE1 tumour	p = 0.850	p = 0.649	p = 0.747	p = 0.951
Serpin E1 stroma	p = 0.343	p = 0.197	p = 0.912	p = 0.080
α SMA and	p = 0.947	p = 0.277	p = 0.059	p = 0.016*
Serpin E1 stroma				
α SMA and	p = 0.486	p = 0.529	p = 0.296	p = 0.622
Serpin E1 tumour				
α SMA and	p = 0.929	p = 0.277	p = 0.059	p = 0.451
Serpin E1 stroma				
and Serpin E1 tumour				
Serpin E1 tumour	p = 0.792	p = 0.708	p = 0.141	p = 0.417
and Serpin E1 stroma				

Table 3.9. Survival and α SMA and serpin E1 expression.

Summary of findings

- a) Histologically, more invasion has been seen in HPV+ OPSCC, when was more desmoplasia present, suggesting that the HPV infection could affect the relation between desmoplasia and depth of invasion.
- b) Presence of GAGs more often at the tumour front HPV+ OPSCCs suggests that the invasion process is probably driven more by GAGs rather than myofibroblasts.
- c) In contrast to published data from OSCC, presence of CAFs was observed at the tumour core as well as the front of OPSCCs.
- d) Presence of desmoplasia is not a suitable marker for survival in HPV+ OPSCC.

3.4 Discussion

The pathological study of the resected tumour specimens can provide important information which can be highly useful in the diagnosis, treatment, and prognosis of the disease. In other words, several histological features such as the grading of malignancy, the invasion pattern, the distance from the tumour to the resection margins, as well as the cohesion at the invasive tumour advancing front have been used for this purpose in OSCC [525]. This study has examined clinical and histological features in HPV+ and HPV- OPSCC with special reference to depth of invasion and desmoplasia, both at the core and front of the tumour. The cohort of samples of this study was of convenience and determination of clinico-pathological was one of the aims of the study.

HPV+ OPSCC typically presents with patients who are younger than 45 years old [442, 526]. However, these data contradict our results where we have found that 75% (24/32) present in older age (>50). Nevertheless, the study conducted by Schache et al. (2016) demonstrated a statistical difference in the mean age between the two categories of OPSCC (mean age 54.2 for HPV+ versus 61.3 years of age at diagnosis for HPV-, $p = 0.003$), meaning that HPV+ patients are younger than their counterparts [527].

In our HPV- OPSCC cohort, 83% of cases (50/60) are older than 50, with 18 cases in the 60-70 age group, however both groups of OPSCC showed significant difference in the age.

We found that 81% (34/42) of the HPV-positive tumours occurred in men, while only 19% (8/42) affected female patients, which is in agreement with previous studies underlining that men are three to four times more likely to suffer from this form of cancer than women [329, 528, 529]. However, the relatively small size of the cohort, the low percentage of female cases, as well as the manner in which the cases have been collected could all be the factors that affected our study results as far as age and gender are concerned.

We observed that the largest portion of our OPSCC cases (17 cases) were located in the tonsil, followed by the base of the tongue as a common site, and these data agree with the literature which shows that the primary lesion in HPV + oropharyngeal SCC is more commonly located in the tonsil and the base of the tongue [395, 422, 465, 528,

530, 531]. On the other hand, data from our HPV- OPSCC were somewhat different to its counterpart, with higher frequency in tonsil, followed by soft palate; however, these data are still consistent with various other sources which in fact demonstrate that HPV- OPSCC can occur in all anatomical sites [419, 531].

Several researches revealed that HPV+ OPSCC are more likely to manifest with small tumour sizes (T1-T2) [433, 526] and advanced nodal stage, namely more often cystic and multilevel [526, 532]. Also, they are characterised by distinctive histological pathological features, for example poor-to-moderate tumour differentiation and non-keratinising or basaloid cell morphology [433, 526, 533, 534]. However, not only was the occurrence of distant metastasis described to be encountered less often in this type of OPSCC but also the fact that this metastasis appears late and has a different pattern from that one seen in patients with HPV- tumours [526, 535]. Moreover, some authors have reported that over 2/3 of cases presented with nodal disease of N2 or N3 [454, 536, 537].

About half of our HPV+ OPSCC were classified as T2 and approximately a third as T3, while associated with a high rate of nodal metastasis. Distribution of the morphologic subtypes in our HPV+ OPSCC was mostly non-keratinizing (81%), and these data concur with previous results in the literature [528, 538]. However, several researchers show different data in which the only subtype that characterize HPV + OPSCC is purely non-keratinizing SCC [539], which does not agree with our result. In HPV- OPSCC, more than one-third of the cases were T2, while the rest classified as T3 and T4 with a large proportion associated with nodal involvement. Most of these cases were moderately-to-well differentiated, which means that they are keratinising, our results confirming other findings in the literature as well.

One of the clinical/pathological variables being investigated is tumour thickness, which has previously been shown to provide the most useful information about the grade of malignancy and tumour aggressiveness [235, 337, 540]. Many investigations in OSCC at different subsites and stages emphasised the vital role played by tumour thickness as an important predictor for metastasis to lymph nodes associated with poor outcome [540-557], however with conflicting data described [547, 558].

Furthermore, tumour thickness also demonstrated to be potent post-surgery predictor for cervical nodal metastasis and disease-free survival [541, 549]. There was not any

correlation observed between the depth of invasion and outcome in either HPV+ or HPV- OPSCC. Our initial hypothesis was that the degree of desmoplasia would be related to the increased level of cancer invasiveness. In the current study, we have used desmoplasia as a marker for tumour thickness. Our data from HPV+ OPSCC have shown that tumour thickness is of high prognostic value as it strongly correlates with desmoplasia at the core and the front of the tumour, a result which suggests that the HPV infection could have an impact on the relation between desmoplasia and tumour thickness. Therefore, the presence of HPV infection in HNSCCs could provide a partial answer for the previous important question on whether the stroma adjacent to tumour cells actually functions as a defence mechanism in favour to the body or it rather speeds up the progression of the tumour, thus indirectly influencing the efficacy of therapy? [179, 237]. The second part of the answer regarding the uncertain function of desmoplasia could be attributed to the presence of complex crosstalk mechanisms between stromal and cancer cells. The later argument has been used to explain the differences in the previous results in other types of carcinoma which showed contradictory data and proposed a different role of the desmoplastic reaction. It is believed that desmoplasia starts to increase when carcinoma cells begin their invasion beyond the muscularis mucosae in colorectal carcinoma [247, 342, 559]. Conversely, Martin and his group described that the dense desmoplasia has the ability to restrain tumour progression and play a part in regression of the tumour in colon cancer [560].

In HPV+ OPSCC, the median tumour thickness in the tonsil was 6.6 mm (ranging from 3.6 to 14.5), compared with 3.2 mm (ranging from 1.2 to 25.0) in the BOT, $P = 0.003$. The median tumour thickness in the soft palate was 3.5 (1.4 to 5.7), in the pharyngeal wall was 7.8 (5.9 to 9.8), in the mixed group was 5.1 (1.1 to 6.4). In HPV- OPSCC, the median tumour thickness in the tonsil was 16 mm (ranging from 3 to 35) 16.1 mm for BOT (ranging from 7.9 to 22). The median tumour thickness in the soft palate was 10.1 (ranging from 9 to 11.4). Compared with various researches on related sites in HNSCCs, a wide range of variations could be observed. For instance, the following measurements for the median of tumour thickness have been recorded: 5 to 7.8 mm for the tongue, 5.0 mm /14.6 mm in cases associated with lymph node metastasis /8.6 mm in cases not associated with lymph node metastasis for the floor of the mouth [525, 541, 561], 1.53 ± 1.08 cm for the tonsil [562] and 3 mm for the soft

palate [563]. These variations could be attributed to the different techniques and approaches used to obtain these values.

In the present study, the amount of desmoplasia has been measured in primary HPV+ and HPV- OPSCCs, performed through a semiquantitative analysis of the histological desmoplasia using H & E technique, commonly used by most laboratories of routine pathology. Although it is overwrought and lengthy, it is easy to apply, and it does not need complex equipment. However, some studies prefer to use ‘computerassisted image analysis’ to measure desmoplasia due to the fact that it is reliable and allows desmoplasia to be evaluated more precisely. Their results displayed that the technique of semi-quantitative scoring for desmoplasia is an undependable means, because quantitative values of desmoplasia were not significantly different between the different semi-quantitative scores of desmoplasia. Even though the univariate analysis of survival exhibited both semi-quantitative desmoplasia grades and percentage of desmoplasia to be related to prognosis, only desmoplasia scoring conducted via quantitative methods possessed an obvious relationship with the overall survival [239].

With a comprehensive understanding of involvement of stroma in cancer development, the inhibition of the crosstalk that occurs between stromal and tumoral cells might become a target for new therapeutic agents as an anti-stroma treatment [229, 239, 564]. For example, the transforming growth factor b, a cancer cell-derived cytokine, stimulates the stroma and directly results in transdifferentiating the fibroblasts into myofibroblasts [229, 239].

Apoptosis and its mechanism of induction in CAFs, factors related to antiangiogenesis, as well as inhibitors of matrix metalloproteinase are other examples of potential therapeutic targets [229, 239, 564, 565]. Furthermore, the ECM may take part in drug resistance that appears in solid tumours through the inhibition of the therapeutic agents by penetrating the tumour or decreasing apoptosis in cancer cells as a result of the chemotherapy effect [239, 566, 567]. Netti and his colleagues identified an extended collagen network in tumours that showed high resistance to drug penetration, and detected collagen as a possible target of therapy in order to increase the penetration of therapeutic agents [239, 566].

We showed that measuring the amount of desmoplasia is an independent prognosticator in primary HPV+ OPSCC but not in HPV- OPSCC. Due to the recent progress achieved in our comprehension of the involvement of stroma in the process of tumour development, for both diagnostic and therapeutic aims, pathologists may possibly be asked to evaluate the 'extent of desmoplasia' in their pathology reports in relation to surgical treatment. In addition to being easy to use, consistent approaches for desmoplasia evaluation as described in the current investigation should be considered for clinical trials in the future.

The limitations of this investigation include a small cohort size of HPV+ OPSCC. Therefore, further expansion and validation of these data is necessary to support the association between depth of invasion and desmoplasia. Based on data from literature and the given number of patients/cases in many studies, we suggest increasing number of cases to the double would be considered an optimal cohort size.

In conclusion, the association between tumour depth and desmoplasia appears to be one of the most significant predictors of tumour aggressiveness. The evaluation of the tumour thickness in HPV +/- OPSCC in its early stage at the time of presentation may permit suitable therapy to be offered accordingly. A larger review of tumour thickness/desmoplasia/ inflammation relationship should also be considered for patients with HPV positive OPSCC.

Tumour heterogeneity is a significant characteristic of HNSCC, mirrored in its clinical and molecular features [169, 248, 568]. For instance, it has been reported that OSCC is a heterogeneous disease and has a considerably larger tendency for dissemination associated with poor outcomes in comparison with OPSCC [248, 569-577]. Currently, the classification and indices of prognosis are established exclusively based on the morphological appearance of tumour. Patient management is influenced to a large extent by the staging system tumour/node/metastasis (TNM), enhanced with supplementary pathological data on the tumour per se and the involved lymph nodes [169, 336]. Although cases with a disease in its advanced stage frequently display a poor survival rate, this is not always the case. However, no particular pathological or molecular feature can detect aggressive tumours at their initial stage [169, 578], therefore identifying the proper biomarker could help in making a decision about escalation or de-escalation of therapies.

The target of the staging systems is to make reliable data regarding prognosis available. However, HPV as an important prognosticator was not involved in the 7th version of UICC; in fact, in numerous studies a weakness in the differentiation of UICC 7th edition in HPV+ carcinoma was systematically described, while satisfactory data were reported for HPV- carcinoma [455, 579-581]. The 8th UICC edition put in consideration HPV status for greater power of differentiation concerning stages and anticipation of survival in OPSCC on the basis of cohorts primarily received chemo-radio therapy [455] or surgery-radio therapy [581, 582].

The presence of a myofibroblastic stroma has been described as related to local recurrence, metastasis and poor prognosis in several tumour types, such as breast, colorectal, oesophageal and tongue carcinomas [169, 180, 342-344, 583]. Moreover, positive α SMA expression in a tumour stroma could function as a marker for aggressive tumours, although it has not been yet clarified the reasons why the formation of stroma appears only in certain tumours, but not in others [169]. Further comprehension of the biological mechanisms controlling the stromal response may provide some indication that could explain the aggressive behaviour of the tumours and may also permit the development of novel therapeutic strategies [169, 584].

We examined three molecular markers related to the presence of myofibroblasts (α SMA), GAGs and tumour invasion (serpin E1) and correlated them to the typical pathology features that are generally seen in OSCC and OPSCC patients.

Our histopathological data in HPV+ OPSCC showed that GAGs were more often found at the tumour front and were generally less prevalent at the tumour core in contrast to HPV- OPSCC, where GAGs were more prevalent at the tumour core and generally less apparent at the advancing front. Furthermore, the amount of glycosaminoglycans at the tumour core was significantly different between the two types of OPSCC [585].

Previous investigations have shown that the distribution of stromal α SMA expression shows a wide discrepancy both between various tumours, as well as between various regions in the same tumour, and this mirrors tumour heterogeneity [248, 512]. However, it has been reported that the use of triplicate cores in TMAs construction, as applied in the current research, may give a top level of concordance (up to 98%) being descriptive of their whole sections [248, 586, 587]. Hence, comparatively large size

cores were cut at the front of tumour (1 mm) to ensure that sufficient tumour tissue as well as nearby stroma are available for scoring.

Our immunohistochemical data in HPV+ OPSCC as well as in HPV- OPSCC showed that α SMA was expressed in a high proportion of tumours in the stroma at the tumour advancing front. Interestingly, a high frequency of α SMA expression was also observed at the core in these tumours, regardless of the HPV status, which was contrary to our expectations that suggested that α SMA expression would be highest at tumour front where the tumour and the stromal cells lie in contact, as is the case for OSCC [248, 588-591] or in other tumours [592, 593]. This is can be explained as a reflection to regions related to desmoplasia at chronologically earlier sites, which became integrated within the growing tumour, as myofibroblasts are found to be present throughout these tumours.

In HPV+ OPSCC, the presence of GAGS and myofibroblasts were correlated at the advancing front, but not at the tumour core, where Alcian Blue staining was generally less prevalent. However, there was a significant association between Alcian Blue staining and the histopathological observation of desmoplasia at the tumour core and Alcian Blue staining at the tumour front correlated significantly with desmoplasia at tumour front. In HPV- OPSCC, Alcian Blue staining at the tumour core correlated significantly with desmoplasia at the core as well as the front.

α SMA staining at tumour core in HPV+ OPSCC correlated significantly with desmoplasia at tumour core, while α SMA at the advancing front correlated with desmoplasia at tumour front. These Alcian Blue and α SMA data suggest that the histopathological identification of desmoplasia relies more on the presence of GAGs than on the identification of myofibroblast populations in H&E stained slides. However, there were not any correlations between the presence of desmoplasia and α SMA staining observed for HPV- OPSCC. The presence in our OPSCC samples of the two components of desmoplasia, namely myofibroblasts and GAGs, could explain the aggressive and invasive nature of this type of tumours, these data being in agreement with other data that demonstrate that the formation of desmoplasia is essential in tumorigenesis and metastasis [235, 236, 594]. Established metastases are often associated with desmoplasia and their recognition is straightforward [595, 596].

Various co-culturing experiments have shown that CAFs can promote the carcinogenesis of tumour cells [193]. One of these experiments showed the formation of tumours resembling prostatic intraepithelial neoplasia in mice when inoculated with a mixture of Simianvirus 40 (SV40)-transformed prostate epithelial cells and CAFs. However, this was not the case when these mice were inoculated with same mixture, but with NAFs instead of CAFs [193, 209].

CAFs can secrete many molecular regulators that have a pro-tumorigenic function. The HSF1-driven pro-tumorigenic programme in tumour cells might be complemented by the upregulation of the heat shock factor 1 (HSF1) in CAFs. This event supports the pro-cancer influence of the TME [193, 210], and activates the Yes-associated protein 1 (YAP1) in CAFs which consequently promotes ECM stiffening and tumour invasion [193, 211]. In addition, CAFs proliferation can be enhanced via deregulation of Notch as well as p53 signalling pathways in these cells [193, 212]. Production of ECM-degrading proteases such as the MMPs by activated fibroblasts facilitates motility and invasion of cancer cells [193, 213-215], for example MMP1, which induces invasiveness [193, 213]. MMP3, also known as Stromelysin-1, is also released by CAFs and cleaves E-cadherin resulting in the promotion of epithelial to mesenchymal transition (EMT) and invasiveness in neighbouring tumour cells [193, 216]. EMT is a process taking place in embryos of vertebrates and through which their cells produce new types of tissues, resulting in production of what is so called the third germ layer or mesoderm [193]. It has been described that these mesenchymal cells have an important role in the differentiation process of epithelial cells. Also, studies have shown that the EMT process has a function in organising development of different organs and pathological remodelling. Lung development is regarded as an obvious example for that [193, 597]. EMT also includes the process by which primary mesenchyme give rise to secondary epithelial cells throughout the period of development, as in the case of meso-endodermal structure formation. Furthermore, EMT can take place in variable types of injuries as a result of inflammation, fibrosis, wounds and cancer, where the secondary epithelium goes through EMT to produce fibroblast-like cells [193, 598]. It has been reported that EMT has a valuable role in tumour cell metastasis, where cancer cells go through EMT, enabling them to move and reach distant organs [193, 598-600].

Furthermore, invasive phenotype of many cancers can occur as a result of deletion of TGF β receptor type II (Tgfr2) in FSP1+ fibroblasts. Examples of these cancers are SCC of the forestomach and prostatic intraepithelial neoplasia which rely on fibroblast-produced hepatocyte growth factor (HGF) [193, 601]. Another example for cancer progression mediators is the Fibroblast-derived exosomes. They mediate development of cancer and stromal remodelling positively through their regulation of fibroblast activity and chemoresistance [193, 217-219, 602]. The lack of members of the tissue inhibitor of metalloproteinases (TIMP) family can lead to generation of exosomes characterised by enhanced expression of MMP and disintegrin and metalloproteinase domain-containing protein 10 (ADAM10) activity, such as the fibroblasts which lack four members of the TIMP family. This case is characterised by enhancement in tumour cell motility, metabolic reprogramming as well as stimulation of cancer stem cell features [193, 603].

With our data on HPV+ OPSCC, the α SMA expression at tumour core is correlated significantly with extra nodal metastatic spread. This would suggest that: (1) tumour deposit metastasis into lymph nodes, and (2) extranodal metastasis into neck region, in particular the soft tissues, are regularly encircled by an obvious desmoplastic reaction and myofibroblastic stroma. Moreover, at tumour core, the expression of α SMA is correlated significantly with the histological subtype.

In HPV- OPSCC findings, the α SMA expression at tumour core has strong correlation with the tumour site. Also, the high expression of α SMA at the tumour front is correlated significantly with survival and this finding is consistent with data from previous investigations in OSCC which showed that poor outcomes are associated with an elevated expression level of α SMA in stromal cells. Furthermore, the high α SMA expression at the tumour front, was in significant correlation with both lymph node stage and the presence of nodal metastasis [134, 177, 260, 261, 427]. However, the Alcian Blue staining at tumour core correlates significantly with survival status and age, while desmoplasia at the tumour front correlates with the pT-stage.

Recently, studies in OSCC have shown a greater prognostic significance for stromal α SMA expression compared with the presence of ECS [169, 248]. Our study in HPV- OPSCC, however, suggests that presence of either myofibroblasts (α SMA staining) or the presence of GAGs is of greater diagnostic value as they are individually highly

significantly associated with adverse outcomes ($P = 0.004$ for Myofibroblasts and 0.009 for Alcian Blue).

Several IHC studies in OSCC have identified that the presence of serpin E1 is associated with metastasis [248]. In fact, our study HPV+ OPSCC frequently demonstrated serpin E1 expression at the tumour core as well as at the tumour front, but this was not mirrored in HPV- OPSCC.

In the tumour core of HPV- OPSCC, the expression of serpin E1 by cancer cells was always stronger than its expression by stromal cells; moreover, stromal expression was observed in significantly fewer cases than carcinoma cell expression. There was also a significant difference in the serpin E1 expression by cancer cells between the two types of OPSCC. Tumoral serpin E1 expression in the tumour core of HPV- OPSCC correlated significantly with both desmoplasia at the tumour core and front while stromal serpin E1 at the same location correlated significantly with the α SMA expression. Serpin E1 expression by cancer cells at the advancing front in this cohort of OPSCC correlated significantly with desmoplasia at tumour core and α SMA expression at the same location. At the tumour advancing front, serpin E1 stromal expression correlated with the α SMA and Alcian Blue expression. In HPV+ OPSCC, the only positive correlation was found between serpin E1 expression at tumour core with Alcian Blue at the advancing front.

HPV+ OPSCC tumour cell serpin E1 expression at the front associated with the presence of nodal metastasis and ECS, whereas its expression in cancer cells at the core and stromal cells at the front was not significantly correlated with any clinicopathological parameters. These data are in agreement with the biological function of serpin E1 in tumour invasion and metastasis [248, 604].

Serpin E1 expression by cancer cells at the tumour core only correlates with the tumour site. In HPV- OPSCC, tumoural expression of serpin E1 at the tumour front correlates significantly with the histological subtype as well as site of the tumour, meanwhile stromal expression correlated with the tumour site.

Previous study about expression of serpin E1 in human melanoma suggested that its expression correlates with metastases. Also, expression of SerpinE1 has an amplitude that may influence melanoma site-specific dissemination, with cutaneous metastases represents a tumour subtype presenting elevated levels of Serpin E1 [604]. Serpin E1,

through its different interactions with vitronectin (VN) and cellular receptors, and also through its central position feature is coordinating the duration and location of both intracellular (signal initiation) and extracellular (detachment/re-adhesion cycles, receptor binding) events that manage the intricate process of cell movement in both physiologic and pathologic contexts. Obviously, the binding of serpin E1 with its several targets including VN, uPA, uPA/uPAR, and LRP1 has the potential to affect the motile program on multiple levels [605]. Other data demonstrated that addition of exogenous serpin E1 stopped HT1080 cell adhesion (IC₅₀ 180 nM) and has the ability to promote cell detachment from vitronectin. HT1080 is a fibrosarcoma cell line which has been used extensively in biomedical research. The cell line was created from tissue taken in a biopsy of a fibrosarcoma present in a 35-year-old human male. Furthermore, melanoma cells transfected with a uPA variant, which had an impaired interaction with PAI-1, were not invasive and had impaired binding to vitronectin. These data emphasise the significance of a balanced proteolysis and suggest an additional role for Serpin E1 distinct from its role in proteolysis. These data also suggest that Serpin E1 could have a role in the migratory process by facilitating the detachment from, vitronectin in the ECM [606].

In a study about expression and role of the two elements of the plasminogen activator (PA) system; proteases and of integrins, in a panel of cell lines of malignant melanoma in humans having different abilities to invade and metastasise, variation between metastasizing cell lines and nonmetastasizing cell lines has been shown to be present. This difference between the different cell lines occurs due to the presence of variation in their upregulation and expression of urokinase-type PA (uPA) and type 1 and 2 PA inhibitors (PAI-1 and -2). The two elements were upregulated and expressed only in the cell lines that possessed great capability of invasion and metastasis. Investigations about expression of plasminogen activator elements in malignant melanomas in humans, showed that the elements of plasminogen activator were expressed only in primary tumours of melanoma in their advanced stage as well as in metastatic lesions of melanoma [607].

It has been reported that serpin E1 and α SMA expression are more significantly correlated with the presence of ECS and nodal stage at the front rather than the core in oral cancer, suggesting the importance of achieving an in-depth understanding of the biological approaches to and prognosis of ECS with methods concentrating on the

interface between the tumour and the stroma [248]. Our data from HPV- OPSCC is not consistent with expression of serpin E1 and α SMA in oral cancer where there has not been any association found between these two biomarkers and ECS neither in tumour centre nor in the advancing front. In contrast, data obtained from our study in HPV+ OPSCC shows that ECS was in association with expression of both α SMA and serpin E1 proteins at the core and front respectively.

A previous study has highlighted the inadequate predictive ability of the TNM system, which is currently used to stage and co-ordinate treatment plan for OSCC patients [169]. Marsh et al. recognised four prognosticators that collectively had a good performance in predicting OSCC mortality, namely α SMA expression, metastasis, tumour cohesion, and age. Of these, only metastasis is a part of the current TNM system [169]. It is important to state that the TNM status is also unable to accurately predict OPSCC outcome. However, our data in HPV negative OPSCC could suggest the coexistence of the following biomarkers as predictors for mortality; SMA expression, GAGs, metastasis, serpin E1 expression.

To sum up, we have shown that presence of myofibroblasts throughout OPSCC tumours is not consistent with data from oral cancer [169]. The presence of myofibroblasts within the tumour core is distinctive for HPV + OPSCC and may indicate that this cell type plays a different role in these tumours compared with in HPV- OPSCC and HPV- oral SCC, where high α SMA expression in tumour stroma is a strong predictor for mortality in OSCC patients [169] regardless of disease stage.

Observations from multiple studies have shown that expression of α SMA and serpin E1 at the tumour advancing front has greater prognostic value compared with their expression at the tumour core [248, 343, 608-610]. Therefore, it is important to include the tumour invasive front (the leading edge) in the incisional biopsy for diagnostic purposes. Also, data has demonstrated that the simultaneous presence of serpin E1 and myofibroblasts in tumour tissue has an important role in tumour invasion [169].

Validation of these data, as future work, in a prospective cohort with larger size, deep biopsy could be used to decide the possibility for this approach to be used in future biomarker detection and layering of a disease in OPSCC. Further new opportunities for research have arisen due to the stronger recent interest in tumour microenvironment; moreover, the effects of CAFs in invasion and metastasis have also

led towards further research in biological comprehension and possible metastatic cascade therapies.

Nodal metastasis/ECS are not prognostic markers in HPV+ OPSCC, so alternative biomarkers are required for this subgroup e.g. serpin E1 and α SMA. However, associations between the front and nodal metastasis/ECS reiterate the significance of this leading edge for detection of proper and applicable biomarkers in OPSCC.

Chapter 4

Metabolic events in HPV+ and HPV- Oropharyngeal Squamous Cell Carcinoma

4.1 Introduction

The recent views suggest that reprogramming energy metabolism is a dynamic system implemented by tumour cells to meet their demands for continual cell proliferation [100]. Several studies have shown that glycolytic metabolism can support biosynthetic activity which fan out from the intermediates of glycolysis, for instance amino acids, nucleic acids and phospholipids, essential building blocks for cells with high rate of proliferation, and also regulate the cellular redox potential to reduce the damage that results from the impact of ROS using NADPH [100, 103, 611-613]. These metabolic events advocate the presence of glycolytic phenotype in tumour cells [100]. However, a recent metabolic model in head and neck squamous cell carcinoma, has hypothesised that a sort of metabolic symbiosis exists between non-proliferative glycolytic stromal and cancer epithelial cells that produce catabolites which are transferred into the tumour microenvironment and afterward retaken up and exploited by a population of proliferative and rich in mitochondria cancer cells, to mediate a process of energy generation and proliferation via OXPHOS [1, 100]. In more detail, this metabolic model proposes the presence of three cell populations with different metabolisms be recognised: (1) a population of epithelial cancer cells with high rate of proliferation using OXPHOS associated with high lactate and ketone body uptake; (2) a population of epithelial cancer cells with low rate of proliferation, poor in mitochondria and characterised by increased lactate and ketone body production (highly glycolytic); and (3) non-proliferative CAFs poor in mitochondria with increased lactate and ketone body generation (highly glycolytic) [1, 100]. Moreover, both highly glycolytic populations/compartments have been noticed to form an important percentage of tumour cells [1, 100].

Investigations into HNSCC (mix of oral, oropharyngeal, larynx, hypolarynx and nasopharynx cancers) have reported that increased lactate levels are related to the nodal, as well as distant, metastases [614, 615]. The study of Walenta, S. et al. (1997) described the relationship between lactate status and metastasis in HNSCC, and saw that low lactate concentrations within a relatively narrow concentration range were recorded in cancers of patients without metastasis. Lactate concentrations found in patients with metastasis, meanwhile, were scattered over a wide concentration range [614]. The frequency distributions of the measured pixel values of lactate obtained from patients without metastasis were tilted toward low lactate concentrations, rarely exceeding 15 $\mu\text{mol/g}$. The frequency distributions of lactate concentrations in tumours with metastatic spread, however, were often extended between 0 and 40 $\mu\text{mol/g}$, and even more with a Gaussian or a multimodal shape [614]. Data from a second study tested the association between lactate concentration and the survival status in HNSCC. It revealed that a better survival-rate was found in patients with tumours in which the concentration of lactate was low, when compared with patients with tumours with an increased concentration of lactate [615]. In this study, using the technique for metabolic imaging (Bioluminescence imaging), the median concentration of lactate in the tumour was 7.1 $\mu\text{mol/g}$, and according to this median value, tumours were classified into two groups: low and high. The values of lactate concentration in the low group were below the median mean, while the high group had values above the median. The median follow up time of survivors was twenty seven months, while the two-year survival was 90% for those patients with primary tumours with a decreased concentration of lactate but 35% for those patients with tumours characterised by increased concentration of lactate (<0.0001). There was a negative correlation between the two-year metastasis free survival and an increased tumour lactate concentration (90% vs 25%, $p < 0.0001$). The median value of the lactate concentration for tumours with later metastasise was 12.9 mmol/g , and 4.8 mmol/g for those who continued to stay disease free ($p < 0.005$).

Carcinoma cells have elevated bioenergetic demands required to preserve cell growth. Glycolysis with production of intermediates (e.g. lactate) and decreased OXPHOS is frequently observed in cancer cells [1, 271, 616]. A two compartment tumour metabolism model has been suggested, employing the theory of “seed and soil” that might clarify the issue of metabolic heterogeneity observed in the various cancer types

and even between different parts in the same tumour. Several studies have shown that, to support tumour growth and its metastasis, carcinoma cells need a microenvironment that is rich in intermediate catabolites and permits their exchange between tumour cells, that is to say, a metabolically permissive microenvironment. This model of metabolism suggests that cancer cells produce H_2O_2 to prompt oxidative stress within surrounding fibroblasts (stromal cells). These fibroblasts afterwards increase their generation of ROS, which prompts glycolytic metabolism and this leads to an increase in the level of intermediate catabolites including lactate, glutamine and ketone bodies. Subsequently, the fibroblasts secrete these intermediates into the tumour microenvironment, an event that stimulates OXPHOS in carcinoma cells. Metabolic coupling with aerobic glycolysis in part of the epithelial cancer cells and OXPHOS in other parts supports tumour properties such as proliferation and resistance to apoptosis [617] (Fig. 4.1).

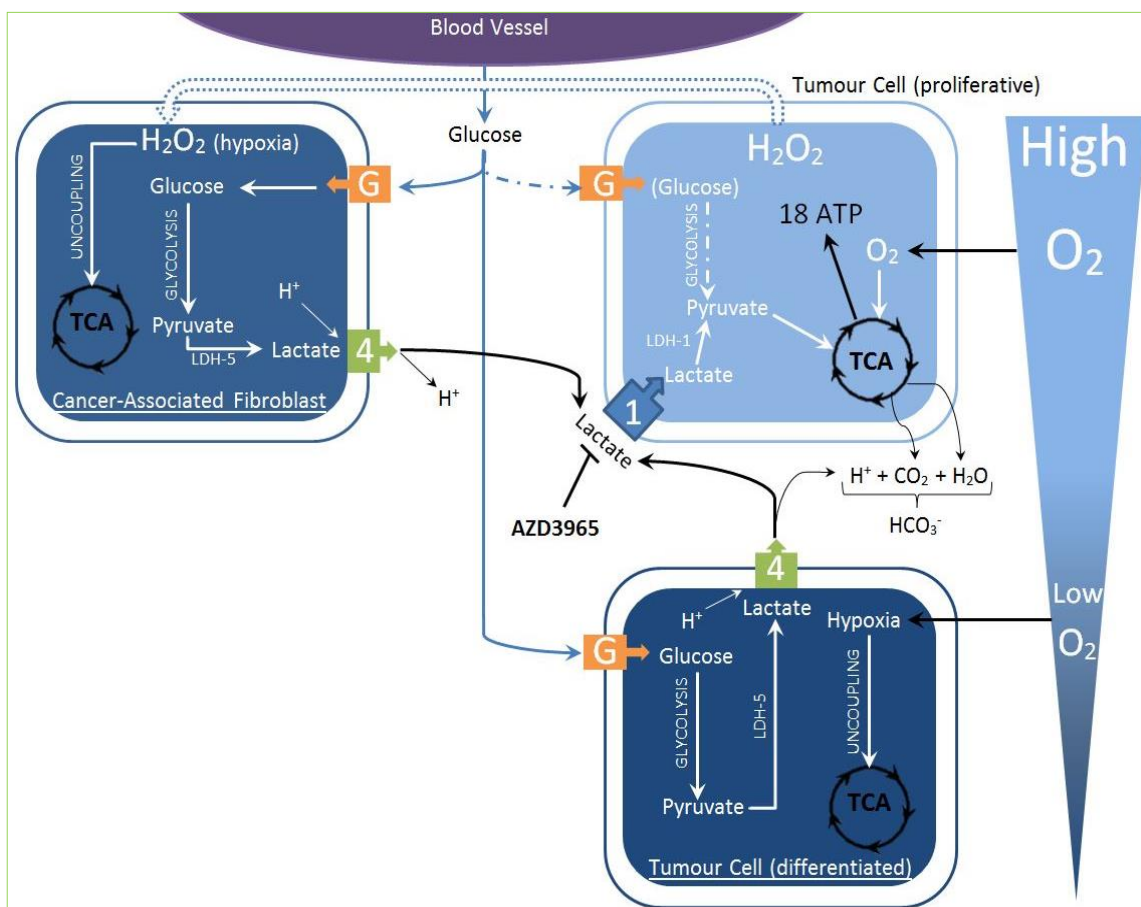


Figure 4.1. Lactate shuttle in tumour.

This diagram represents lactate shuttle that takes place between differentiated tumour cells (non-proliferative and low oxygenated), CAFs and the proliferative tumour cells. In this ‘energy transfer’ relationship, cells have dedicated MCTs to channel the lactate molecules from one cell type to another. Using MCT4 as exporter, the glycolytic cells release lactate molecules which are subsequently used up by oxidative cells employing MCT1 as importer. Acknowledgement to Tom Pearson, BSc Honours dissertation 2015.

Cell proliferation is regarded as a significant biological hallmark of tumourigenesis and has been reported to be of prognostic value in HNSCC [503, 618, 619]. In Walenta’s study, a multivariate logistic regression was performed to identify the relevant parameters for predicting metastasis. The fraction of Ki67-immunolabeled cancer cells ($p= 0.035$) was one of four significant parameters able to predict the presence of metastases [614]. The Ki67 expression in OPSCC had a tendency to be in negative relationship with prognosis, that is, cases of cancer that expressed Ki67 at a level of <25% were observed to have a considerably improved clinical outcome when

compared with the other group of cases, expressing Ki67 at levels of $\geq 25\%$ ($p = 0.0188$). The HPV+ OPSCC subset showed a highly positive outcome in relation to the Ki67, with a score of expression under the cut-off value of 25%. The survival benefit noticed in these cases, equal to a 2.48 relative mortality decrease at 5 years, occurred regardless of tumour stage. In a different way, all HPV- cases recorded a score of expression over 25%, with a survival curve of no more than 5 years. Likewise, a score of expression under 25% in the OSCC displayed a solid association with an improved follow-up ($p = 0.0240$). Contrarily, a Ki67 positivity of below 25% did not correlate with the survival benefit in the larynx carcinoma group ($p = 0.2467$).

Ritta *et al* demonstrated in their study that, for a cohort of 59 primary tumours of HNSCC that included 22 OPSCC, 25 OSCC and 12 from the larynx, HPV+ OPSCC had a better clinical outcome over the HPV- group. The Kaplan Meier analysis revealed that patients with HPV+ tumours had a considerably better overall survival in comparison with those with HPV- tumours ($p = 0.0211$). Contrastingly, in the OSCC and carcinomas of larynx, HPV positivity give the impression of being a negative prognosticator, although the Kaplan Meier analysis was not high in its significance ($p = 0.2802$ and $p = 0.5439$, respectively) [503].

De Petrini, *et al.*'s study aimed at defining the prevalence of HPV DNA in a cohort of forty seven cases of OSCC and OPSCC, and to associate the clinical behaviour of HPV+ and HPV- carcinomas. They examined the proliferation index, as assessed through the positivity of Ki67 in the immunohistochemistry assay. The DNA of HPV was found in fifty percent of OPSCCs, and thirty six percent of OSCCs. However, although such figures are in the range described in the previous investigations [620-622], a percentage of 36% of HPV DNA found in oral carcinomas is considered to be high for the subset of cancers supposed to be HPV-. The only genotype detected was HPV 16. The HPV+ carcinomas belonging to both sites showed a decreased proliferative index, as demonstrated by the ratio of cells that were positive for Ki67 immunoreactivity, with a poorer outcome in the HPV- subgroup. An increase in the rate of proliferation has been associated with aggressiveness of carcinomas from different anatomical sites. Cases with HPV+ tumours had a superior overall survival rate in comparison with HPV- tumours ($P=0.04$ and $P=0.02$ for OPSCCs and OSCCs, respectively). Data in this proposes that HPV+ OPSCC has a distinct disease entity related to an improved prognosis [623].

It has been hypothesised that cells with low intracellular lactate rates have increased lactate uptake through the MCTs, permitting them to produce considerable quantities of ATP molecules through OXPHOS [624]. In a subset of human breast cancers, Lisanti and his group were able to demonstrate upregulation of both MCT4 in CAFs by oxidative stress and MCT1 in epithelial cancer cells. Therefore, the previously described ‘lactate shuttle’ might be present in human tumours for transporting energy between two locations; from the tumour stroma to epithelial cancer cells [270]. Recently, a three metabolic tumour compartments was delineated in head and neck cancers, where two non-proliferative different groups of cells (Ki-67- & MCT4+) in a tumour can determine the clinical outcome. This is probably through making available for use a supply of high energy metabolic substrates as mitochondrial fuels for the proliferative (Ki-67+) cancer cells [1]. However, head and neck cancer samples used in the later research were sourced from different sites and without any indication to their HPV status. This could have a strongly negative impact on any investigative result. To date, there is no data about the metabolic differences between HPV+ and HPV- OPSCC.

So based on these data from the above mentioned research in head and neck cancer and also on our data of the previous chapter showed that the stroma in HPV+ OPSCC is different from that one of HPV- OPSCC suggesting that this difference might has an effect on the tumour metabolism, makes the whole tumour behave differently, the overall aim of this chapter was to characterise the metabolic compartmentalisation related to the lactate transporters present in OPSCC. In order to achieve this aim, these are the objectives:

- a- Undertake observational metabolic studies using a better matched cohort of OPSCCs, with HPV status being the only difference between the cohorts.
- b- Conducting a comparative metabolic study between the two types of OPSCC (HPV+ and HPV-).
- c- Investigating presence/absence of the three compartment tumour metabolism model in OPSCC.

4.2 Materials

4.2.1 Reagents

The antibodies used in this study are described in table 4.1.

Marker	Clonality	Pretreatment	Dilution	Source	Control tissue
MCT1	Monoclonal	See Chapter 2.7	1:1000	Santa Cruz Biotechnology, Inc. (365501)	Colon
MCT4	Polyclonal		1:500	Santa Cruz Biotechnology, Inc. (50329)	Colon
Ki67	Monoclonal		1:1000	abcam, Cambridge, UK (92742)	Tonsil
TOMM20	Monoclonal		1:2000	Santa Cruz Biotechnology, Inc. (17764)	Breast

Table 4.1. Details of antibodies.

4.2.2 Evaluation

See chapter 2

4.3 Results

Ki-67

A high level of Ki-67 immunoreactivity was observed in both HPV+ and HPV- OPSCC carcinoma cells, located at both the core and front of the tumour. The highly differentiated tumour cells, however, did not show an expression of Ki67 and the stromal cells were largely negative (Fig. 4.2). A variation in the frequency of HPV+ and HPV- carcinoma cell in the core staining was observed, but was not significant (Tables 4.2 & 4.3). This could be considered as indicative of more differentiated cells being present in the HPV- than the HPV+ tumours.

TOMM20

The expression of TOMM20 was strongly positive in the cancer cells as well as CAFs in both the core, and at the front of HPV+ tumours. However, the TOMM20 expression was only observed in CAFs at the core in 58% of HPV- OPSCCs ($p = 0.005$) (Tables 4.2 & 4.3, Fig. 4.2). However, the difference between the frequency of TOMM20 staining of CAFs in HPV- OPSCC at the core and at the front of the tumour is not statistically significant ($p = 0.433$).

MCT1

An expression of MCT1 was observed in both HPV+ and HPV- OPSCC in about 60-70% of carcinoma cells, irrespective of their location in the tumour, but was negative or weak in the stroma (Tables 4.2 & 4.3, Fig. 4.2).

MCT4

A strong MCT4 immunoreactivity was found in almost all carcinoma cells, and yet a significant difference in the MCT4 expression was seen at the front between the two types of OPSCC ($p = .023$) but not at the core. However, the difference in the frequency of staining between carcinoma cells in the core and at the front were not statistically significant for the two types of OPSCC ($p = 0.823$ for HPV+ OPSSC and no value computed for HPV- OPSSC). This strong MCT4 immunoreactivity was also present at a high intensity in the CAFs present in both HPV+ and HPV- tumours. However, the proportion of HPV- OPSCCs demonstrating a high MCT4 CAF staining was statistically lower than that in HPV+ OPSCCs at both the core and the front ($p = 0.031$ and $.002$ respectively). There was no statistical difference in the MCT4 stromal

expression at either the core, or the front, in the same type of OPSCC ($p = 0.318$ for HPV+ OPSSC and 0.668 for HPV- OPSSC (Tables 4.2 & 4.3).

Biomarker	HPV+		HPV-	
	Tumour	Stroma	Tumour	Stroma
Ki-67	33/33 (100%)	0/32 (0%)	26/41 (63%)	0/47 (0%)
TOMM20	33/33 (100%)	33/33 (100%)*	42/43 (98%)	25/43 (58%)
MCT1	31/45 (69%)	1/45 (2%)	26/45 (58%)	2/46 (4%)
MCT4	44/45 (99%)	43/45 (96%)*	37/41 (90%)	32/42 (76%)*

Table 4.2. Frequency of strong immunoreactivity of each biomarker in HPV+ and HPV- OPSCC in the tumour core.

The expression of TOMM20 was strongly positive in the cancer cells as well as CAFs of HPV+ tumours. However, the TOMM20 expression was only observed in CAFs in 58% of HPV- OPSCCs ($p = 0.005$). A strong MCT4 immunoreactivity was found in almost all carcinoma cells. High intensity of MCT4 was also present in the CAFs in both HPV+ and HPV- tumours. However, the proportion of HPV- OPSCCs demonstrating a high MCT4 CAF staining was statistically lower than that in HPV+ OPSCCs ($p = 0.031$).

* Numbers in bold indicate statistical significance.

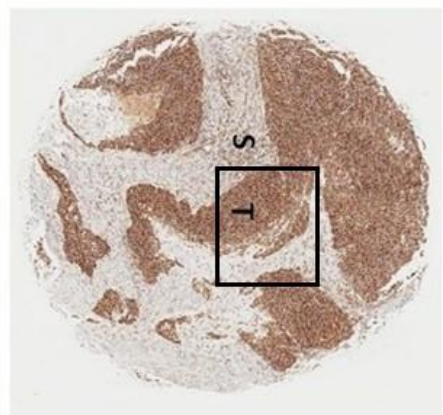
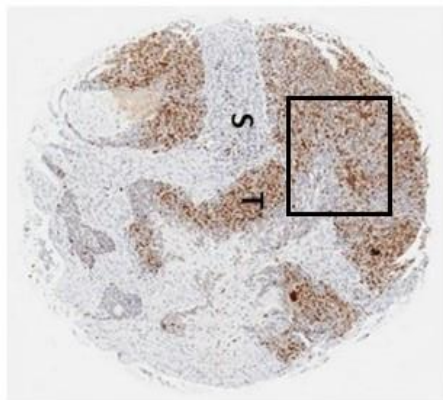
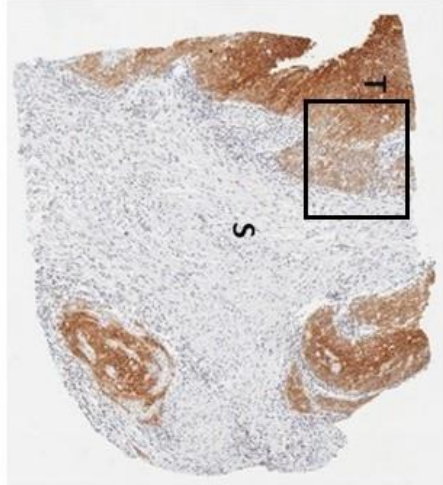
Biomarker	HPV+		HPV-	
	Tumour	Stroma	Tumour	Stroma
Ki-67	34/43 (79%)	0/33 (0%)	25/32 (78%)	3/31 (10%)
TOMM20	42/43 (98%)	43/43 (100%)	31/31 (100%)	28/29 (97%)
MCT1	25/38 (66%)	0/39 (0%)	16/27 (59%)	0/28 (0%)
MCT4	40/41 (98%)*	42/42 (100%)*	26/34 (77%)*	26/37 (70%)*

Table 4.3. Frequency of strong immunoreactivity in HPV + and HPV- OPSCC at the advancing front.

A strong MCT4 immunoreactivity was found in almost all carcinoma cells, and a significant difference in the MCT4 expression was seen between the two types of OPSCC ($p = .023$). This strong MCT4 immunoreactivity was also present in the CAFs in both HPV+ and HPV- tumours. However, the proportion of HPV- OPSCCs demonstrating a high MCT4 CAF staining was statistically lower than that in HPV+ OPSCCs ($p = 0.002$).

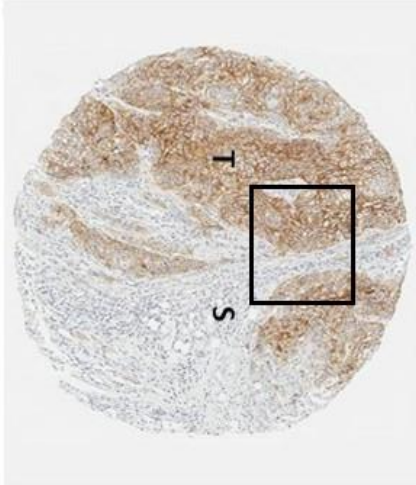
* Numbers in bold indicate statistical significance.

HPV+ OPSCC



HPV- OPSCC

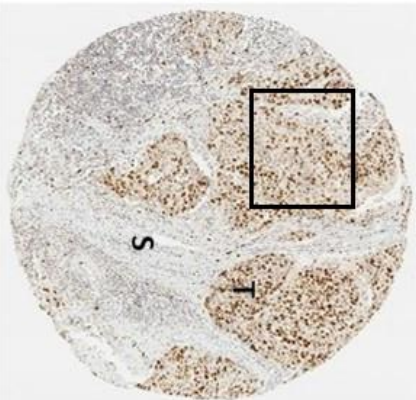
MCT1



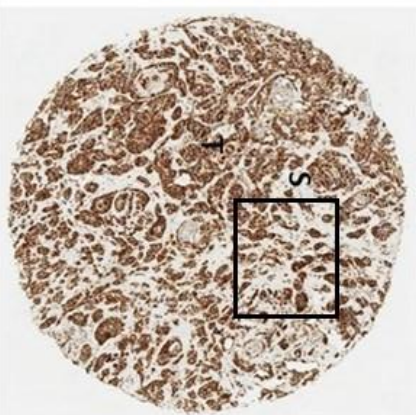
MCT4



Ki-67



TOMM20



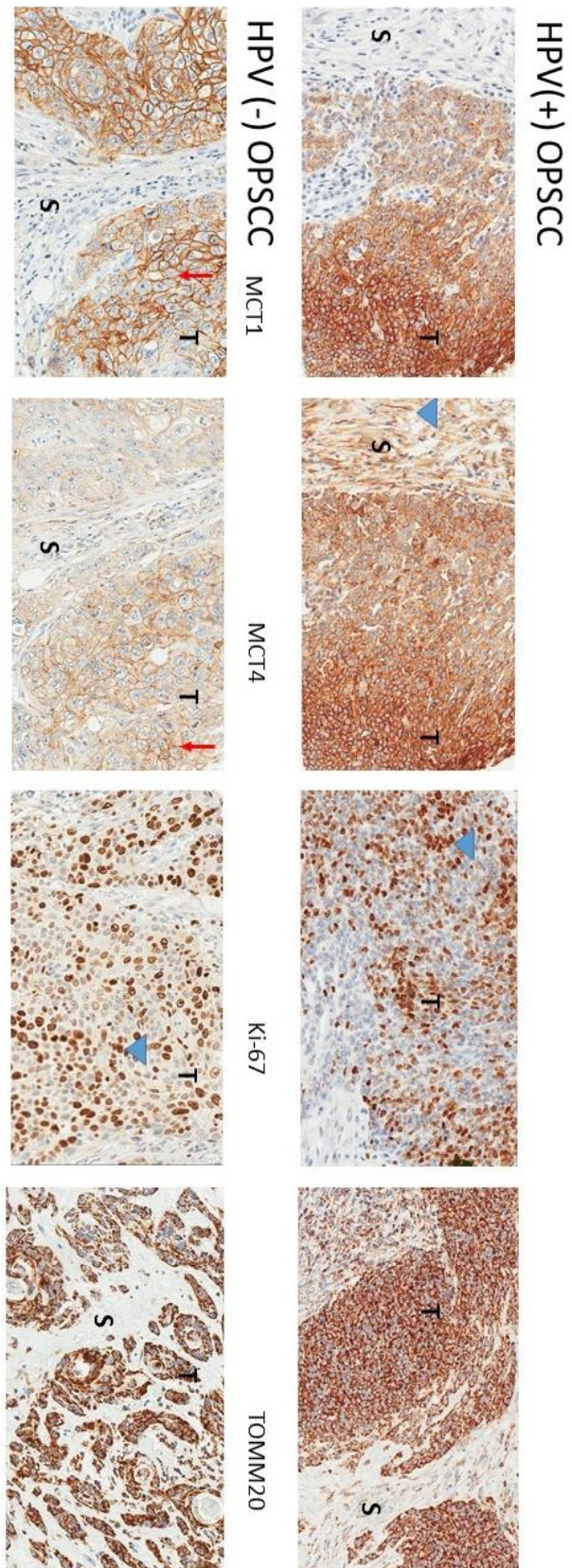


Figure 4.2. A typical example of immunohistochemical staining showing expression of Ki-67, TOMM20, MCT1 and MCT4 in HPV+ and HPV- OPSCC performed on tissue microarray sections.

Rectangled areas of interest in the upper panels are magnified in the lower panels respectively. The magnified pictures show obvious membranous expression of MCT1 and MCT4 in epithelial cancer cells (red arrows). Stromal expression is negative in MCT1 and positive in MCT4 (blue arrow head). Obvious nuclear expression of Ki-67 in tumour cells (blue arrow head) suggesting that they are proliferating. Group of tumour cells are negative for Ki-67 staining suggesting that they are not dividing. Cytoplasmic expression of TOMM20 by epithelial cancer cells suggestive of high mitochondrial mass implies that they have switched to oxidative phosphorylation. Tumour (T); stroma (S).

In 85% (18/21) of HPV+ tumours, a co-expression of all four markers was observed in carcinoma cells at the tumour core with 15% (3/21) of tumours demonstrating additional metabolic compartments (Fig 4.3). By contrast, only 50% (11/22) of HPV- OPSCCs demonstrated co-expression of MCT1 and MCT4, with the other 50% of tumours demonstrating additional, metabolic compartments (Figs. 4.3 and 4.4).

Co-expression of membranous MCT1 and MCT4 at the advancing front was observed in 84% (16/19) and 30% (6/20) of the HPV+ and HPV- tumours, respectively ($p=0.001$).

In a newly suggested tumour metabolism model, the Reverse Warburg metabolism is more divided to involve variant populations of epithelial cancer cells. These different epithelial cancer cells are (1) cancer cells with a high rate of proliferation and (2) cancer cells with a lower rate of proliferation [1]. This model is called the multi-compartment or three compartment tumour metabolism model (Fig. 4.5). It is suggested that the highly proliferative cancer cells obtain their metabolic fuels such as lactate substrate not only from the surrounding stromal cells, but also from the adjacent non-proliferative cancer cells (additional metabolic compartment). Thus, the tumour front with highly proliferative cancer cells expresses MCT1 benefits from the suitable microenvironment afforded by both stroma (MCT4+ CAFs) and the less proliferative cancer cells (a deeper population of MCT4+ cancer cells). These less proliferative cancer cells have low rate or absence of Ki-67 expression, a biomarker for proliferation; this population is also well differentiated and mitochondrially poor, which functions as the motivating force for cancer cells to proliferate through a lactate shuttle [1] (Fig. 4.5).

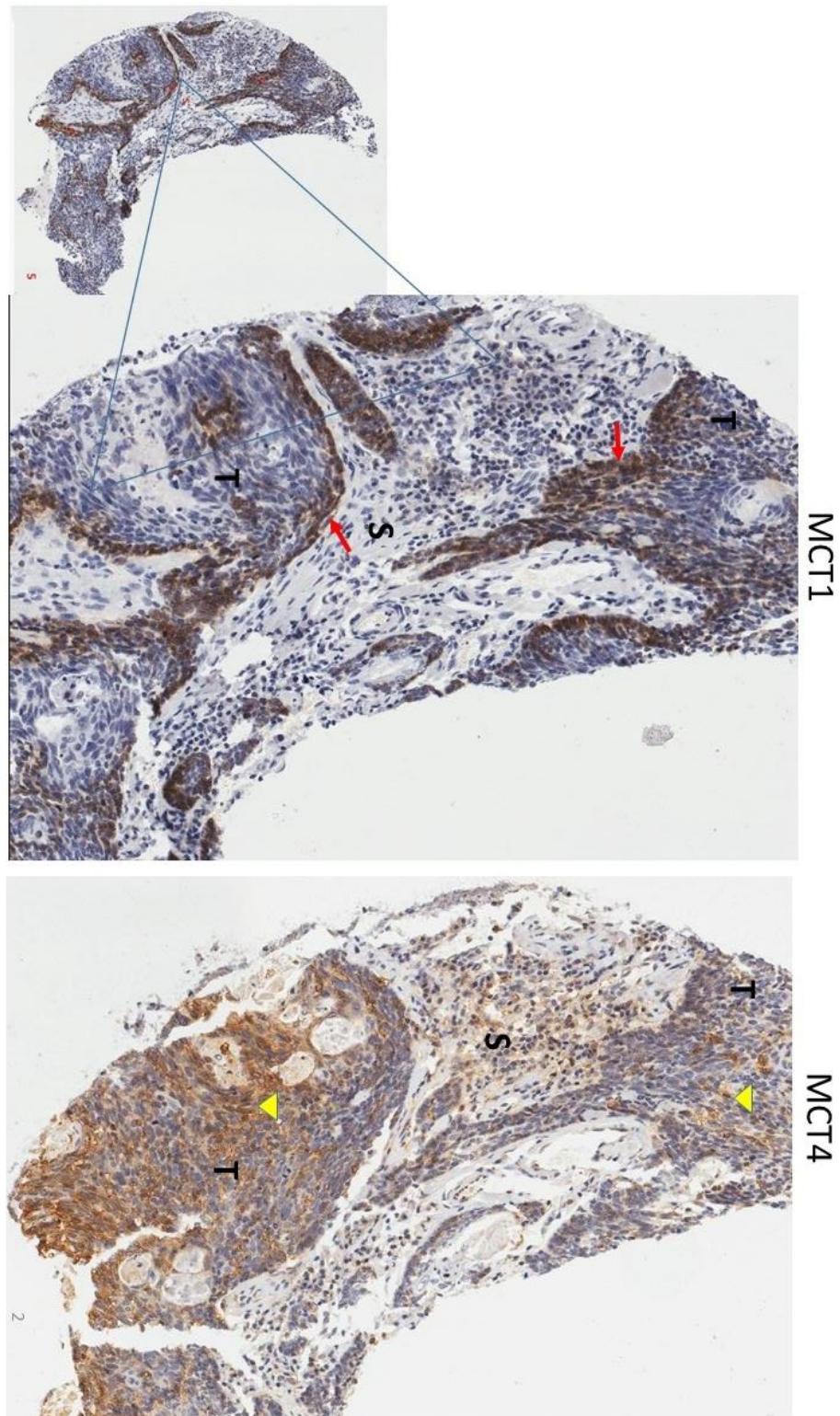


Figure 4.4. A typical example of metabolic compartmentalisation in HPV+ OPSCC. Population of highly proliferative cancer cells, at the advancing front of the tumour (red arrows), derive their lactate substrate not only from stromal cells (S), but also from surrounding nonproliferative cancer cells (yellow head arrows) that form the additional metabolic compartment. Thus, the highly proliferative cancer cells which expresses MCT1 (upper panel) takes advantage of the favourable microenvironment

provided by both stroma, MCT4+ CAFs, and a population of MCT4+ less proliferative cancer cells at the core of the tumour (lower panel).

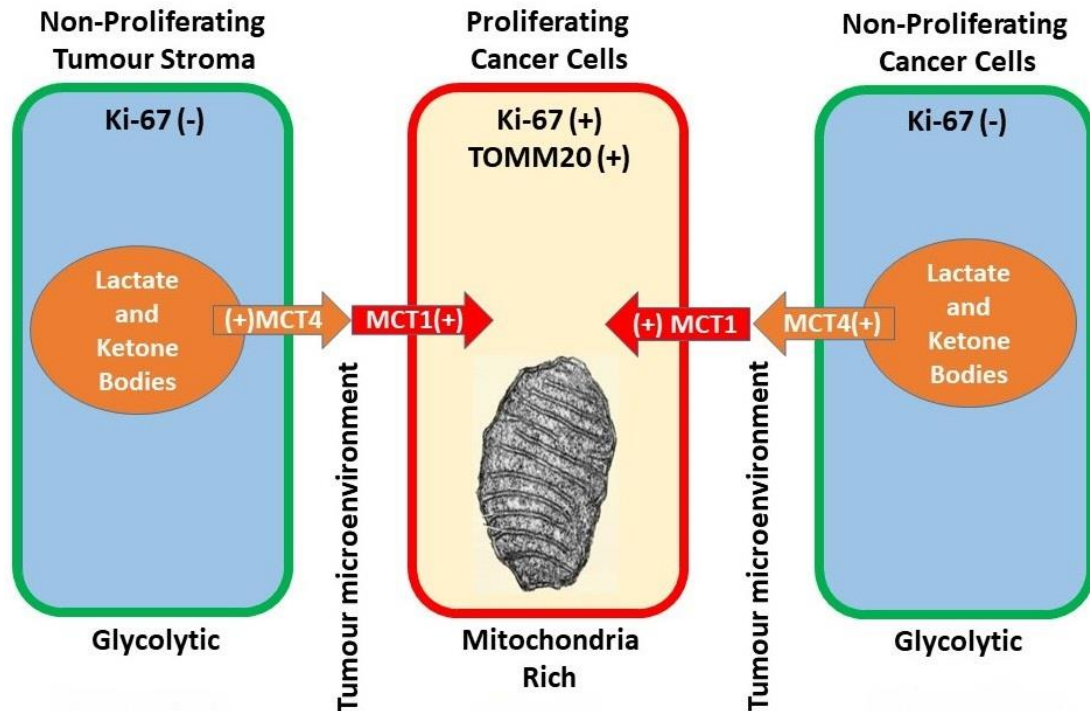


Figure 4.5. Three (Multicompartment) Metabolism Model.

This represents presence of three cell compartments, with different metabolism: (1) a compartment of highly proliferative epithelial cancer cells uses OXPHOS associated with high lactate and ketone body uptake; (2) a compartment of nonproliferative epithelial cancer cells poor in mitochondria and characterised by increased lactate and ketone body generation (highly glycolytic) (3) compartment of nonproliferative CAFs poor in mitochondria with increased lactate and ketone body generation (highly glycolytic). MCTs used to transport lactate and ketone bodies between these compartments. Adapted from Curry *et al.* [1].

4.4 Discussion

Recently, a three compartment model has been proposed where the Reverse Warburg Effect is more detailed, so as to involve different populations of cancer cells: cancer cells with high proliferation rate and cancer cells with a low proliferation rate [1, 625]. This model of metabolism with multi-compartments proposes that the highly proliferative cancer cells obtain lactate molecules, not merely from stromal cells, but also by means of adjacent non-proliferative cancer cells [1, 265, 625]. Although the study producing the three compartments tumour metabolism model had a sample with

good baseline characteristics, the problem lay with the small sample size. Confirmation of the existence of a model of such kind, the most important idea in this study, has been built on data from only 12 subjects. It has been reported that small investigations are vulnerable to estimations of inflated impression size, in addition to the impact of publication bias. Therefore, it is hard to believe in the proof of a large effect when a small analysis is the only foundation of that proof [626]. A larger sample would have aided in the data analysis, particularly when looking for possible interactions between the different metabolic biomarkers and their distribution in tumours compartments.

In this present research, we found that the markers related to a metabolic activity and the reverse Warburg metabolism (MCT1, MCT4, Ki-67 and TOMM20) are expressed in the carcinoma cells in the majority of both HPV+ and HPV-OPSCC cases. In HPV+ OPSCC cases, cancer cells located at the tumour core, as well as at the tumour front (by gross histology), are proliferative, rich in mitochondria and use mitochondrial fuels (Ki-67+ / TOMM20+ / MCT1+). Furthermore, the majority of these cells demonstrated high levels of MCT4 expression which signifies that they are undergoing glycolysis and exporting lactate. These epithelial cancer cells are surrounded by stromal cells that are undergoing oxidative stress and glycolysis (as demonstrated by a high MCT4 expression) but presented low levels of MCT1 expression and low proliferative indices. Aside from the low expression of MCT1 in the stroma compartment, we were able to show clear existence of metabolic activity in both the tumour and stromal compartments.

Multiple studies have shown that acidification of the tumour microenvironment and also different intracellular downstream pathways can perform a function in tumour progression with expression of MCT4 by carcinoma cells [44]. Moreover, it has been submitted that the lactate efflux has other impacts via affording substrates that support the proliferation of cancer cells [44]. Actually, a number of investigations concerning the Warburg metabolism proposed that expression of MCT4 by cancer cells can enrich cancer stem cells [26, 29, 30] and subsequently peripheral tumour cells can uptake this lactate and import it via MCT1 [44].

Our metabolic data is not completely consistent with the pattern of the three compartment tumour metabolism model suggested in head and neck cancer [627]. In

our metabolic data, the three compartment model is more compatible with data from HPV- OPSCC. We found that about 85% of HPV+ OPSCC tumours co-express MCT1 and MCT4 in the same tumour cells, while only 50% of HPV- OPSCC do so.

The reason behind this difference is probably because the tumour samples that we used are poorly differentiated while the three compartment arrangement is demonstrated in, predominantly, well differentiated tumours (eight were well-moderately differentiated while four were poorly differentiated). Purity of the sample is another important point that can affect the investigation considerably. The effect of diversity in the site of origin (different subsites) of involved tumours has not been taken in to account in the three compartment tumour metabolism study, where the result was given to the group as a whole and not specified to be from a certain subsite. All of our samples are from oropharynx, in contrast to the cases used for the three compartment tumour metabolism study where they are sourced from different subtypes, including oropharynx, hypopharynx, larynx and oral.

Another point needing clarification is that the stromal compartment, in the first experiment of this multi compartment model, has been shown to be highly catabolic with a strong level of MCT4 expression. However, a different picture of MCT4 expression was given in the second experiment where a third of these cases ($14/40 = 35\%$) of well-moderate subjects demonstrated a low level of expression.

Also, the second part of the study was retrospective and was conducted on a cohort of (42) oral subjects, the majority (40) of them were well-moderate while the other two were poorly differentiated. The sample size here is acceptable and the cohort has good baseline characteristics, but the issue lies with the availability of data about the four metabolic biomarkers (MCT1, TOMM20 and Ki-67). The available data was about MCT4, only and this is unable to provide evidence about the nature of metabolic activities and their compartmentalisation in these tumours, simply because no data was provided for the other metabolic biomarkers.

In another recent cross-sectional study carried out by Jensen et al., and tested the reverse Warburg effect in OSCC, and included (30) subjects. The majority of these were from floor of mouth (21) and the other (9) were from the tongue. With regard to the tumours' differentiation, (6) were well differentiated, (23) were moderately differentiated and (1) was poorly differentiated. It was shown that there were increased

expressions of MCT1 and MCT4 in both the epithelial and stromal compartment [625]. It has also been presented that the markers (MCT1 and MCT4) related to the reverse Warburg metabolism present in OSCCs, with three distinct compartments participating: tumour, stroma and differentiated cells. Although all the samples in this study belongs to one subtype (OSCC), our data is again not parallel to metabolic results presented in this study. The heterogeneity in the two metabolic results could be again attributed to either the difference in subtypes and origin of the carcinoma where one is from the oral cavity and the other is from the oropharynx. HPV status appears to be an important factor in affecting metabolism in OPSCC tumours.

Although all of the cases were OSCC and the sample size is acceptable, there are three main weak points: the researchers confirmed presence of the three compartments model in their OSCC cohort. However, they summarised their data in (Fig. 1) under a title of ‘Reverse Warburg metabolism in OSCC’. It would be better if they titled Figure 1 as ‘The three compartments metabolism model in OSCC’. This is because the Reverse Warburg Effect depicts a metabolic relationship among carcinoma and stromal cells where glycolysis accomplished by stromal cells generates lactate, molecules of which are transferred through a vectorial system of MCTs to cancer cells as metabolic fuel supply to produce energy via OXPHOS. On the other hand, the multi-compartment metabolism model dissected the cancer cell compartment into two compartments with two distinct populations; one with a high proliferation rate and one with a lower proliferation rate. These non-proliferative cancer cells with stromal cells make nutrients available for proliferative cancer cells [265]. Moreover, the author did not provide enough explanation about the method by which the immunohistochemistry was performed. Immunohistochemistry staining can be performed using full sections, or tissue microarrays, but neither of these was mentioned in the study. While HPV status has an effect on tumour metabolism, carcinogenesis, radiotherapy resistance and clinical outcome, no data was provided about the HPV status in these two previous studies.

The absence of consistency in the calculation of ‘expression positivity’ of the biomarker is another point behind the presence of discrepancies between results of the included studies. Considerable disparity was observed in the methodology used by these studies, and by which they labelled samples as positive or not for a particular biomarker. Some of these methodologies used a spectrum of grades, meanwhile others

used a binary system. Moreover, the categorisation of immunohistochemical staining in relation to its intensity and density was also subjected to inconsistency, with some investigations employing a computer-based algorithm and others depending on the grades-based observations by one, or a number, of pathologists [1, 625].

It was shown that well differentiated cancer cells in well differentiated OSCCs displayed a low proliferative index (\downarrow Ki67) contrary to the poorly differentiated cancer cells at the advancing front. In that case, proliferative index presented its highest reactivity rate (\uparrow Ki67) were situated at the boundary between the stroma and epithelium [1, 265, 270, 625]. Numerous studies have assessed the connection between proliferation activity and prognosis in several types of cancers. A relationship between high proliferative activity and poorer prognosis has been found in both HPV+ and HPV- of OSCCs as well as OPSCCs [503, 619, 623] [628]. A study tested the prognostic value of a Ki67 expression in relation to the HPV status in OPSCC, and revealed that HPV- and Ki67 positive oropharyngeal cancers are linked with a poorer outcome [628]. This study also reported that positivity of Ki67 in HPV+ was more frequent (57 %) when compared with HPV- cancers (33 %). This result might explain the correlation between HPV positivity and the presence of higher nodal status at the time of diagnosis. Nevertheless, a better survival rate has been noticed in the HPV positive + Ki67-negative group [503]. Our data from the proliferation index in HPV+ OPSCC cohort is consistent with the aforementioned data in the literature, and we were able to demonstrate that proliferation rate in HPV+ OPSCC has a tendency to be higher than its counterpart HPV- OPSCC.

As presented earlier (page 163), metabolic data from the present study showed that the markers related to a metabolic activity and the reverse Warburg metabolism (MCT1, MCT4, Ki-67 and TOMM20) are expressed in the carcinoma cells in the majority of both HPV+ and HPV-OPSCC cases, can be a centre of attention from a therapeutic point of view and could result in MCT1 becoming the object of investigation for metabolic anticancer therapies. Using inhibitors that can inhibit lactate uptake and decrease the amount of mitochondrial fuel to proliferative cancer cells, the OXPHOS and ATP production required for cell division and tumour growth could be diminished. Alternatively, achieving a stage of energy uncoupling between the anabolic carcinoma cells with high proliferation rate and the catabolic epithelial cancer and stromal cells with less proliferation rate, could stop mitochondrial fuel feeding to the highly

proliferative cancer cells, rendering them dependant on glycolysis as their main source of ATP production [467, 629].

The anticancer α -cyano-4-hydroxycinnamate, is a powerful MCT1 inhibitor that has an antineoplastic effects in vitro, as well as in vivo, with marginal toxicity [262, 630]. In vivo investigations in mice displayed that α -cyano-4-hydroxycinnamate considerably diminished tumour load [262]. A recent study undertaken by Amorim and his group demonstrated the various effects of inhibiting lactate transport system on cell lines from human CRC by means of different reagents known to have the ability of inhibiting lactate transport, such as α -cyano-4-hydroxycinnamate, DIDS (a stilbene derivative), and quercetin, a bioflavonoid. This study also revealed that in a dose-dependent manner, the inhibition of mono-carboxylate transport activity has the capability of preventing CRC cells biomass, reducing proliferation and augmenting their death. Furthermore, their results showed that pre-treatment of CRC cells with the mono-carboxylate transport inhibitors heighten the cytotoxicity of 5-fluorouracil [265, 631]. Nevertheless, MCT inhibitors are potent compounds, characterised by a lack of specificity and their use as inhibitors for lactate transport through plasma membrane extend to inhibit other functional activities inside the cell.

In a study performed in cervical, breast, and bladder cancers that express MCT1 and MCT4, Draoui and his group examined the effect of 7-aminocarboxycoumarin (7ACC) in xenograft models of these cancers[265, 632]. They demonstrated that the 7ACC was able to inhibit the influx of lactate, but not its efflux in cells with MCT1 and MCT4 expression. The study also showed that 7ACC diminished xenograft tumour growth. AR-C155858 is another anticancer drug that has been reported to be an efficient inhibitor in cancer of the prostate, by means of inhibiting MCTs (MCT1 and MCT2). Also, AR-C155858 has the ability to significantly decrease proliferation of cancer cells, increasing their apoptosis within tumour tissues from mice without substantial cytotoxicity on non-malignant tissues [265, 633]. At present, a new oral inhibitor for MCT1 and MCT2 (a second generation) called AZD-3965, is going through first phase clinical trials and could show a therapeutic effect against solid tumours in their advanced stage, in particular PCa, gastric cancer, and diffuse large B cell lymphoma, and could be used as anticancer drug in HNSCC [265, 634].

Metformin is one of the biguanides, and is known to act as an inhibitor for mitochondrial OXPHOS. Its action is attributed to its numerous cross reactivity with the system of lactate transport as OXPHOS inhibitors. It is efficient at prevention as well as therapy of HNSCC in both vitro and vivo [262]. Due to their synergistic effect against cancer, in cases of combined treatment with MCT1, MCT4, or CD147 inhibitors, these biguanides recently became the focal point in anticancer therapy [265, 635-637]. Now, there are numerous clinical trials assessing the effect of metformin on cancer development, particularly its ability to interfere with the metabolic coupling that takes place between stromal and epithelial cancer cells in HNSCC [265].

In advanced solid tumours, including head and neck cancers, hypoxia is regarded as a key feature associated with an adverse influence on prognosis [321, 638, 639]. We hypothesise that the difference in metabolic compartmentalisation found between the two types of OPSCC appears as a result in the difference of oxygen concentration in both. In Chapter 6, we have evaluated this hypothesis in the HPV+/-OPSCC setting, examining the expression of HIF-1 alpha, an established hypoxia marker and relating this expression to that of metabolic state. We have also investigated GLUT-1 as glucose transporter since GLUT-1 expression might also be in relation to the cellular metabolic state and mitochondrial activity (Chapter 6).

Conclusion

Results shown in this chapter suggest that:

- 1- Markers known to be associated with the reverse Warburg metabolism (MCT1 and MCT4) are expressed in both HPV+ and HPV- OPSCC but does not coincide with the presence of myofibroblasts. We therefore speculate that the mechanism leading to an induction of the myofibroblast phenotype of CAFs is separate from the induction of the reverse Warburg effect.
- 2- Three compartment tumour metabolism model is HPV dependant rather than site dependent based on OPSCC.
- 3- It is difficult to explain why tumour cells export and import lactate. But it is a common observation that needs a further work.
- 4- Presence of MCT4 expression are not suitable markers for survival in HPV+ OPSCC.

Chapter 5

Functional studies

5.1 Introduction

Metabolic adaptation towards glycolytic metabolism instead of OXPHOS is assumed to be one of the hallmarks of cancer so as to meet the rise in energy requirement for intermediate catabolites and metabolic fuels to sustain rapid proliferation of cancer cells [456-458]. Glycolytic metabolism has been reported to offer an advantage for cancer cells to survive without relying on the availability of oxygen, and also offers cancer cells another advantage by supporting the biosynthetic activities which fan out from the intermediates of glycolysis, for example amino acids, nucleic acids and phospholipids, essential building blocks for cells with high rate of proliferation [100, 103, 611-613]. Furthermore, by-products of glycolysis, for instance lactate and pyruvate were reported to provide resistance to radiation and to support progression of cancer [456, 459, 460]. Multiple studies have described that blocking of the glycolytic pathways results in hindering cancer cell proliferation and increases their response to radiation [456, 461-463]. This data indicates that metabolic activity is a determining factor of continual proliferation of cancer cells and carcinogenesis. It has recently become apparent that for multiple cancer cell types, metabolism of the mitochondrial substrates (e.g. glutamine and pyruvate) is essential for sustaining a rapid rate of proliferation. Also, a functional relationship between mitochondrial respiration and the capacity of cancer cells to proliferate has been identified in different types of cancers [640, 641].

Inadequate accessibility of glucose is considered to be a main feature of the tumour microenvironment [642-644]. This depletion in glucose from the surrounding tissues may be as a result of the heavy use of glycolysis by cancer cells (the hyperactivity of glycolysis) in the hypovascular microenvironment. The preferential use of glucose (a high glucose consumption) by cancer cells is likely due to their intrinsic metabolic characteristics, and other factors such as hypoxia [643]. Furthermore, a very low

concentration of glucose in tumours can occur as a result of poor blood supply. Data from a study by Hirayama *et al* proposed that the concentration of glucose in tumour tissues is only ~1 of 45 or 1 of 13 (in the colon and stomach respectively) of the ideal concentration of blood glucose (1 mg/mL or 5.6 mmol/L) [643].

Tumour cells increase their use of glycolysis to maintain continuous energy production under hypoxia and uncontrolled cell proliferation in the absence of oxygen [644], thereby offering an advantage to tumours [644]. It is apparent that the most obvious outcome of this glycolytic shift are accomplished in tumour areas that have a copious amount of glucose, and from which lactate, the final product of glycolysis, is removed competently [644].

The causes and explanations of the high use of glycolysis include:

1. Damage to the mitochondria i.e. cells cannot push pyruvate into Krebs's cycle.
2. Adaptation to hypoxia- as krebs's cycle requires abundant oxygen
3. Cancer cells evolve to inhibit mitochondrial activity to avoid apoptosis (mitochondria play a key role in co-ordinating apoptosis).
4. Glycolysis supports biosynthetic activities which fan out from the intermediates of glycolysis, for example amino acids, nucleic acids and phospholipids, essential building blocks for cells with high rate of proliferation.
5. Overexpression of mitochondrially bound hexokinase (key regulator of glycolysis).
6. Mutations of Pyruvate kinase muscle isozyme M2 (PKM2) are found in Bloom's syndrome. PKM2 is only found physiologically in very rapidly growing cells such as wound healing. PKM2 has been used as a diagnostic biomarker i.e. in stools for CRC.

One of the strategies that permit tumour cells to adapt to unsuitable conditions for glycolysis is to shift back to an oxidative metabolism, on account of proliferation, and on condition that an adequate amount of oxidative substrates and oxygen are available. An alternative is to move into more suitable soils, or, thirdly, to ameliorate the process of glucose delivery and that of lactate removal. The latter approach chiefly relies on the lactate to act as a paracrine molecule to affect signalling in the neighbouring stroma [644, 645].

In spite of the fact that MCT1 has appeared as a new target for anticancer therapy, there is limited data on the molecular mechanisms controlling its activity and expression [644]. At the posttranslational level, the membranous expression of MCT1 and transport activities necessitate its direct interaction with its auxiliary protein CD147 [104, 646, 647]. Their complex formation provides a stabilising effect, which is required for their localisation on the cell surface, the trafficking, and function of both of the proteins as a complex [644].

Due to the critical role of MCTs in the transportation of multiple monocarboxylate molecules across cell membranes, in particular lactate and pyruvate [466, 648], we investigated the effect of its glucose deprivation on the MCT1 expression. We also examined the effect of replacing glucose by pyruvate as an exogenous metabolic fuel.

Based on metabolic observations in fixed tissues suggesting that a high proportion of epithelial cancer cells in HPV+ tumours co-express MCT1 and MCT4, we decided to confirm them in an experimental model, where the experimental conditions can be changed and see whether affects how the tumour grow and react. So, the overall aim of this chapter is to develop a model enabling a functional investigation of these observations. In order to achieve these aims, these are the objectives

- a- Examination of baseline expression MCT1 and MCT4 in monoculture of epithelial cancer cell lines and fibroblasts from different HPV status.
- b- Examination of MCT1 and MCT4 expression in co-culture system of epithelial cancer cell lines and fibroblasts.

5.2 Materials and methods

5.2.1 Reagents

Antibodies were purchased from Santa Cruz Biotechnologies as follows: rabbit anti-MCT4 (cat #sc50329), mouse anti-MCT1 (cat #sc-36550), mouse- anti- β -Actin (1:1000: Santa Cruz, sc-47778), polyclonal Rabbit Anti-wide spectrum Cytokeratin antibody (cat # ab9377) purchased from abcam and monoclonal mouse anti-human Cytokeratin antibody (Code M3515, clones AE1/AE3) purchased from DaKo. Other reagents were as follows: Glucose-deprived DMEM was from gibco® by life technologies™ (UK, cat #11966-025) and reconstituted without glucose, L-Glutamine solution Bioextra G7513-100ML, 200 MM, from Sigma, serum FBS South American (CE) 500ml from Life Technologies, Sodium Pyruvate (100 mM) from Gibco®/Thermo Fisher Scientific (Cat#: 11360070), Glucose Solution contains D-glucose at a concentration of 200 g/L from Gibco®/Thermo Fisher Scientific (Cat#: A2494001) and 4,6-diamidino-2-phenylindole (DAPI) mounting medium reagent from Invitrogen.

5.2.2 Cell lines.

Five epithelial cell lines namely UMSCC4, UMSCC104, UMSCC 74A, UPICSCC 154, UPCISCC152, and four fibroblasts namely Liv99, Liv88, Liv60 and Liv91, were used for this experiment, and after optimisation experiments, the cohort was reduced to four cell lines consisting of two each of epithelial and fibroblast. The two epithelial cancer cell lines, namely UMSCC 74A (HPV-)[649] [650] and UPICSCC 154 (HPV+) [651, 652], and two fibroblasts, namely Liv 99F (originated from HPV- tumour) and Liv60F (originated from HPV+ tumour), were grown from biopsies following approval from the ethical committee (REC number 10/H1002/53), and written informed consent was obtained from subjects. The UMSCC 74A cells were maintained in DMEM, with 10% Fetal Bovine Serum (FBS) and 5% L-Glutamine meanwhile UPICSCC 154 grew in Eagles minimum, essential medium supplemented with 15% FBS, and L-Glutamine. The two fibroblasts were cultured in Dulbecco's modified Eagle medium (DMEM)-F12 medium supplemented with 10% Fetal Bovine Serum (FBS) and 5% L-Glutamine. Cells grown at 37°C in 5% CO₂ and were passaged using trypsin-EDTA when they reached 80-90% confluency.

5.2.3 Expression of MCT1 & MCT4

5.2.3.1 Protein extraction

Cell pellets for onward protein extraction and western blot analysis were prepared by scraping cell monolayers into 6ml PBS, followed by centrifugation at 1330g for 5 minutes to recover the pellets. These were stored at -80°C prior to protein extraction.

Harvested cells were re-suspended in 300µl of protein extraction buffer (50 mM Tris–HCl, pH 6.8, 1% SDS, 1% EDTA, 0.25% glycerol, 0.25% β- mercaptoethanol) with protease inhibitor (Roche Diagnostics), and the total protein was extracted with the use of a sonicator (Sonics and materials INC, 40-50 amplitude for 30 seconds) and stored in aliquots at -80°C until use. The total protein was quantified using the Bradford assay. The used additives, their concentrations, and their general role are listed in table 5.1.

Additive	Concentration	Role
Tris–HCl, pH 6.8	50mM	Buffering reagent, maintains the Ph at 6.8 Maintain ionic strength of medium
Sodium Dodecyl sulfate (SDS)	1%	Detergent Solubilisation of poorly soluble proteins
Glycerol	0.25%	Stabilization
EDTA	1%	Metal chelator Reduce oxidation damage, chelate metal ions Inhibits metallo-proteases
β- mercaptoethanol	0.25%	Reducing agent, reduce oxidation damage Breaks sulphide bonds of the protein Work as protease inhibitor

Table 5.1. The used additives, their concentrations, and their general role.

5.2.3.2 Western blotting

40µl of protein preparation, containing between 20µg and 50µg of total protein, were mixed with a half volume of sample loading buffer from SIGMA, and boiled for 5mins prior to being loaded into 10% SDS/PAGE gels (Appendices 6 and 7). Electrophoresis was carried out at 125V / 700 mA for 110 minutes, with the total protein from NOK,

a normal oral keratinocyte cell line known to express MCT1 and MCT4, used as a positive control.

Following electrophoresis, gels were transferred to 0.45µmm nitrocellulose blotting membranes (GE Healthcare Life Sciences) by using electroblotting for 1 hour at 20 V/700 mA. Components of the running and transfer buffer are shown in Appendices 8 and 9 respectively.

Prior to probing with primary antibodies, the blocking of membranes was carried out for one hour at room temperature using a blocking solution (PBS + Licor Blocking Buffer, ratio 1:1).

Primary antibodies were diluted in the blocking solution plus 2% Tween20, and incubated at 4°C overnight: rabbit-anti- MCT4 (1:500: Santa Cruz, cat #sc50329), mouse anti-MCT1 (1:1000 Santa Cruz, cat #sc-36550) and mouse-anti-β-Actin (1:1000: Santa Cruz, sc-47778). Membranes were washed in PBS with 2% Tween20 (Sigma Aldrich), for 5 minutes x 3, prior to incubation with secondary antibody. Fluorescent secondary antibodies; IRDye@800 goat anti-mouse, (926-32210) or goat anti-rabbit, (926-32211, both Licor) or Alexa Flour@680 goat anti- mouse or goat anti-rabbit, A21088, were used at a concentration of 1:10,000 for 2 hours incubation at room temperature. Membranes were rinsed in 1 x PBS solution, three times for 5 minutes, and then either scanned immediately or stored.

5.2.3.3 Data collection and Analysis

Western blot membranes were scanned before a visualisation of fluorescent secondary antibody localisation was undertaken on a Licor Odyssey scanner (3.0 Model) from LiCor, INC Lincoln USA. Densitometry was used to normalise and semi-quantitate the levels of protein expression, in comparison with the actin control. Briefly, the intensity of the β-Actin band in each lane was measured and compared to the internal control (NOK), with a ratio of control intensity divided by the sample intensity calculated and used to normalise the MCT1 and MCT4 protein expression levels for each sample. Raw data presented in Figs. 5.5, 5.6 and 5.7 is an example demonstrates how the graphs were generated based on the western blot analyses.

5.2.4 Proliferation assays

Both a crystal violet, and an MTT (MethylThiazolTetrazolin), assay were used for estimating cell proliferation, and to establish a survival curve for the cell lines.

5.2.4.1 Crystal violet assay

Crystal violet is a triarylmethane dye that can bind to Deoxyribonucleic acid (DNA) in a nucleus. The Crystal violet assay measures proliferation by estimating the amount of the DNA or nuclear particles. In a cell culture, dead adherent cells detach from plates and will be removed from viable cell population during washing steps. Crystal violet staining can be used to quantify the total DNA of the remaining population, and thus determine cell viability. The Crystal violet staining is directly proportional to the cell biomass and can be measured at 570 nm. Cells were grown in 12 well plates and seeded so that the wells were confluent after 4 days with proliferation determined every 24 hours. At each time point (every 24 hours), cells were washed briefly with PBS and air-dried for 5 minutes, before being incubated with crystal violet (Sigma) solution (0.05% in PBS) at room temperature for 30 minutes. The crystal violet solution was withdrawn, and cells were washed under running tap water for a few minutes and left to air-dry overnight at room temperature. The following day, 200µl of 10% acetic acid was added to solubilise the crystal violet and 100µl transferred in duplicate into 96 well plates. Absorbance was read at 570nm using a Spectramax-Plus284 absorbance microplate reader (Molecular Devices), against a 10% acetic acid blank, with the experiment carried out in 2 replicates.

5.2.4.2 MTT assay

The MTT assay measures the reduction of a tetrazolium compound (MTT) into insoluble Formazan product via the mitochondria of viable cells. Viable cells with active metabolism convert MTT into a purple coloured formazan product.

Cells were grown in 12 well plates and seeded so that the wells were confluent at 4 days, with proliferation determined every 24 hours. At each time point (every 24 hours), cells were washed briefly with PBS, then incubated in fresh culture medium containing 0.5mg/ml MTT solution at 37°C for 2 hours. MTT solution was withdrawn and the cells fixed with 500µl of chilled 3.7% formalin (pH 7.4) for exactly 12 minutes at room temperature. Formalin was withdrawn, and MTT solubilised with 400µl of

DMSO. 100µl of the resultant solution was transferred in duplicate to 96 well plates with the absorbance read at 570nm, using the microplate reader against a DMSO blank. The experiment was carried out in 2 replicates.

5.2.5 Effect of availability of metabolic fuel on MCT1 expression

We investigated low glucose concentration as a potential modulator of MCT1 and also tested whether the delivery of oxidative metabolic substrates could change the MCT1 protein expression, in both the presence at low concentration, or complete absence, of glucose. Two epithelial cancer cell lines were used: the HPV+ cancer cell line, UPICSCC 154, and the HPV- cancer cell line, UMSCC 74A. Each cell line was supplied with high glucose only (5.56 mM), low glucose only, pyruvate only (1 mM), or low glucose and pyruvate together in DMEM and grown in flasks for protein extraction, 12 well plates for proliferation assays. Cell proliferation was determined every 24 hours for four days.

5.2.7 Statistical tests

Data is presented as the mean value \pm standard deviation (S.D.), and the study was conducted in at least three independent runs. The statistical analysis was performed with SPSS statistics, version 22. Protein expression data from the tumour and normal tissue was analysed using a box plot analysis, and paired sample T test (SPSS statistics, version 22).

5.3 Results

5.3.1 Baseline expression of MCT1 and MCT4 in cell lines

MCT4 was expressed in both carcinoma cells but was absent to weak in the fibroblasts (Figure 5.1). MCT1 expression was weak in carcinoma cells and absent in fibroblasts (Figure 5.2).

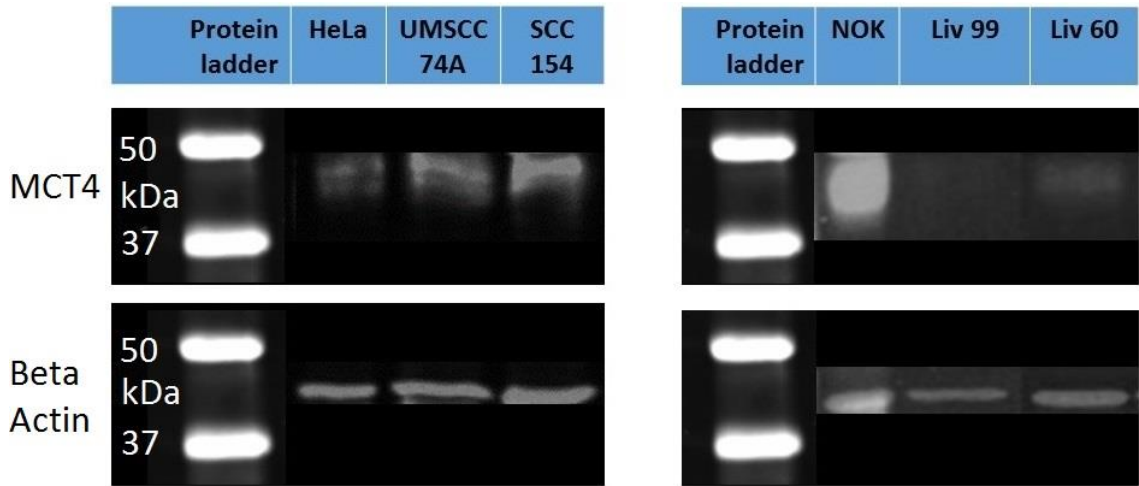


Figure 5.1. Baseline expression of MCT4 in cell lines. Western blot showing MCT4 expression in carcinoma (left) and cancer-associated fibroblast (right) cell lines. HeLa cells and NOK cells are used as a positive controls and Beta Actin as a loading control.

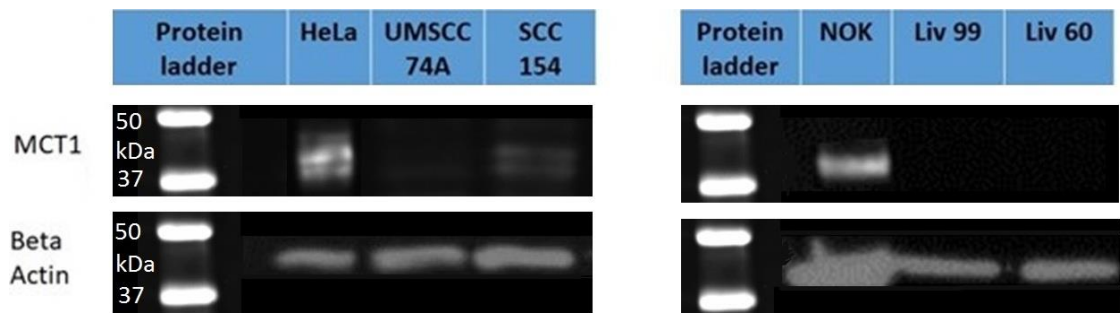


Figure 5.2. Baseline expression of MCT1 in cell lines. Western blot showing MCT1 expression in carcinoma (left) and cancer-associated fibroblast (right) cell lines. HeLa cells and NOK cells are used as a positive control and Beta Actin as a loading control.

5.3.2 Effect of metabolic fuel availability on MCT1 expression

Low glucose concentration induces MCT1 protein expression in HPV positive cancer cells

Using Western blot, we observed an increase in the MCT1 protein expression in HPV+ UPIC SCC 154 cells with decreasing glucose concentrations (Fig. 5.3, brown line). Conversely, there was no induction of MCT1 expression by HPV- UMSCC 74A in low glucose media (Fig. 5.4). However, crystal violet assay showed a decrease in the proliferation rate when compared with high glucose media, but manifested the same rate with the other two types of media. The same assay did not show remarkable change in proliferation rate when HPV- carcinoma cells grown in low glucose compared to high glucose media or to pyruvate-only media. In contrast, these cells showed an increase in their proliferation when pyruvate was delivered to low glucose media. Pyruvate, in the presence of low glucose concentration as well as in the absence of glucose, induces a MCT1 protein expression in HPV- cancer cells.

MCT1 expression for SCC154 in different media

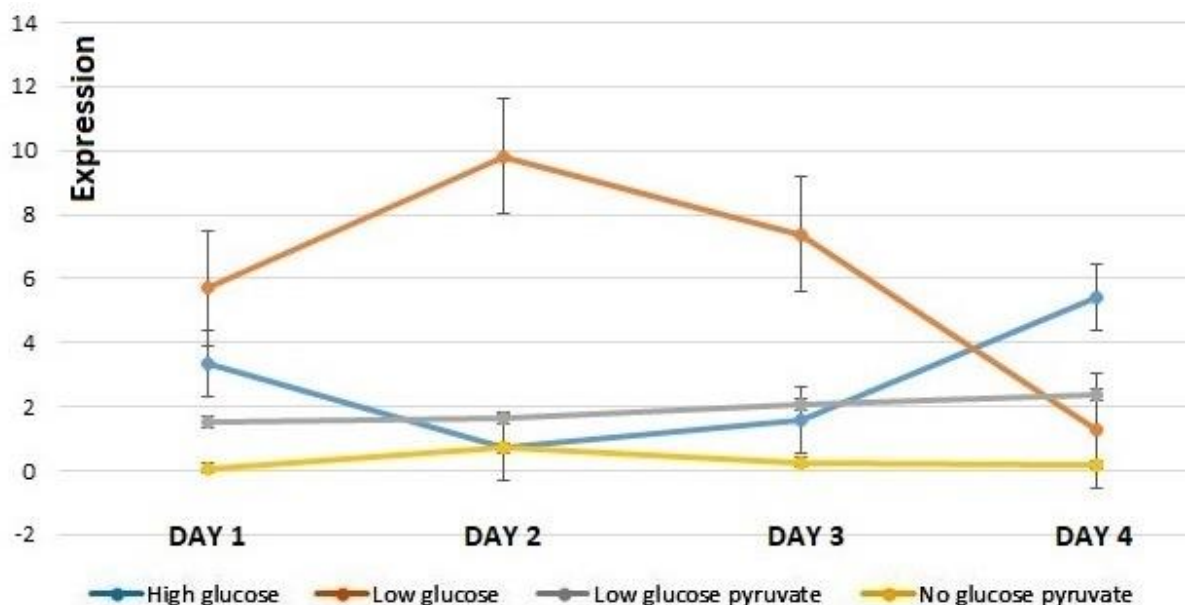


Figure 5.3. Line graph shows MCT1 expression in the four different media by the HPV+ cancer cells.

Using Western blot analysis, an increase in MCT1 protein expression has been observed in HPV+ UPIC SCC 154 cells with decreasing glucose concentrations

(blown line). In contrast to that, there was no MCT1 expression in the other three types of media (blue, grey and orange lines).

MCT1 expression for UMSCC74 in different media

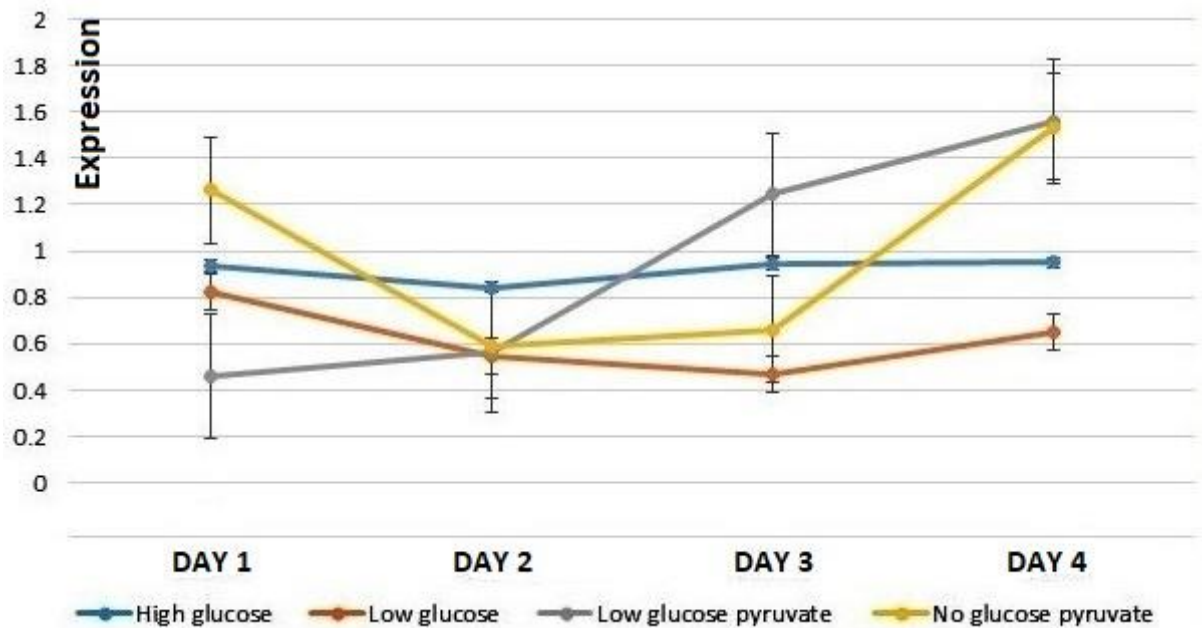


Figure 5.4. Line graph showing MCT1 expression by UMSCC74A (HPV-) cancer cells in four different metabolic media. There was no induction of MCT1 expression by UMSCC 74A in low glucose media. In contrast to that, there was MCT1 expression in both low glucose with pyruvate media and no glucose with pyruvate media (grey and yellow lines).

Western blots showed that pyruvate, a metabolite well-known to competently substitute glucose as an oxidative fuel for cells, [653] upregulated the expression of MCT1 UMSCC74 (HPV-) cells in the presence, or absence, of low glucose level (Fig. 5.4, grey and yellow lines). In UPCISCC154 (HPV+) cells, the MCT1 expression was unchanged by the addition of the TCA cycle substrate pyruvate to the media, in either the presence or complete absence of glucose (Fig. 5.3). However, the supplementation of pyruvate with glucose clearly promoted proliferation in the HPV- carcinoma. A more rapid proliferation was seen for those cells supplied with glucose + pyruvate

media when compared with glucose-only or pyruvate only, and the delivery of pyruvate to the media in association with glucose /without glucose did not show a clear effect on proliferation of the HPV+ carcinoma. A summary of MCT1 profile is given in table 5.2.

	Cell line	UMSCC 74A (HPV-)	SCC154 (HPV+)
Media	High glucose	No	No
	Low glucose	No	Yes
	Low glucose pyruvate	Yes	No
	Pyruvate only	Yes	No

Table 5.2. Summary of MCT1 upregulation profile in the four different types of media by the two epithelial cancer cells.

Days	Normalisation reading of first experiment	Normalisation reading of second experiment	Normalisation reading of third experiment	STDEV.P	Average	Number of experiments
High Glucose media Day 1	1.956426	0.1593	0.690036	0.755042213	0.934130667	3
High Glucose media Day 2	0.956593	0.437345	1.138402	0.297051046	0.844113333	3
High Glucose media Day 3	0.600508	0.247495	1.986057	0.750330448	0.944686667	3
High Glucose media Day 4	1.351161	0.27036	1.226099	0.482724714	0.949206667	3
NOK	1	1	1	0	1	3
Low Glucose media Day 1	0.961084	0.299901	1.210053	0.384060931	0.823679333	3
Low Glucose media Day 2	0.741387	0.166431	0.72009	0.266159153	0.542636	3
Low Glucose media Day 3	0.837811	0.298447	0.260771	0.263588098	0.465676333	3
Low Glucose media Day 4	0.521767	0.48482	0.946715	0.209574403	0.651100667	3
NOK	1	1	1	0	1	3
Low Glucose pyruvate media Day 1	0.776169	0.046505	0.559306	0.305941893	0.46066	3
Low Glucose pyruvate media Day 2	1.195574	0.021287	0.478852	0.483276561	0.565237667	3
Low Glucose pyruvate media Day 3	2.440712	0.034067	1.259679	0.982564891	1.244819333	3
Low Glucose pyruvate media Day 4	0.378804	2.747182	1.550163	0.966905186	1.558716333	3
NOK	1	1	1	0	1	3
No Glucose pyruvate media Day 1	1.039075	0.092211	2.651753	1.056647582	1.261013	3
No Glucose pyruvate media Day 2	0.657479	0.139441	0.974657	0.344246523	0.590525667	3
No Glucose pyruvate media Day 3	1.500646	0.10996	0.370674	0.603583379	0.660426667	3
No Glucose pyruvate media Day 4	4.130479	0.130043	0.346976	1.836828277	1.535832667	3
NOK	1	1	1	0	1	3

Figure 5.5. Detailed raw data of densitometry analysis of western blotting for different media over four days with average value of three experiments.

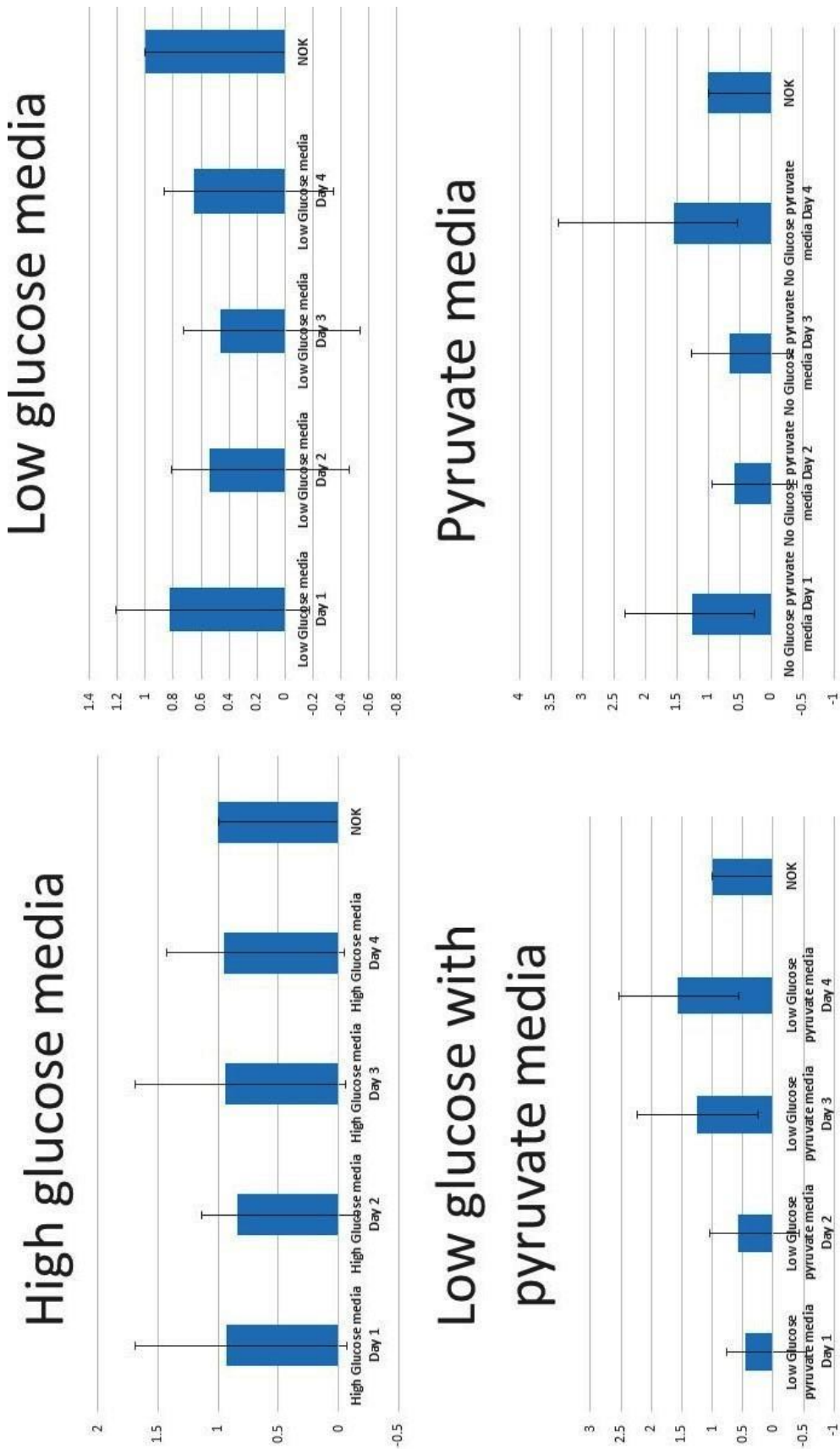


Figure 5.6. Bar graph generation from raw data of densitometry analysis of western blotting for different media over four days with average values of three experiments.

Type of media	DAY 1	DAY 2	DAY 3	DAY 4
High Glucose	0.934130667	0.844113333	0.944686667	0.949206667
Low Glucose	0.823679333	0.542636	0.465676333	0.651100667
Low Glucose with pyruvate	0.46066	0.565237667	1.244819333	1.558716333
No Glucose pyruvate	1.261013	0.590525667	0.660426667	1.535832667

Figure 5.7. Average values of densitometry analysis of three experiments of western blotting for different media over four days. The line graphs used in this study are generated from these average values using charts function in Excel 2013.

5.3.3 Effect of metabolic fuel availability on cell proliferation

Delivery of metabolic substrates promoted proliferation of the HPV- epithelial cancer cell

The crystal violet proliferation assay for HPV+ carcinoma showed a decrease in the proliferation rate in low glucose media when compared with high glucose media. The same assay did not show a remarkable change in proliferation rate when HPV- carcinoma cells were grown in low glucose compared to high glucose media. In order to determine if the availability of metabolic fuels affected the proliferation rates supplementation of pyruvate with glucose clearly promoted proliferation in the HPV- epithelial cancer cell line, and a more rapid proliferation was seen for those cells supplied with glucose + pyruvate media when compared with glucose-only or pyruvate only (Fig 5.8). Further, the growth of cells on pyruvate only was comparable with that of the cells supplied with glucose only media. The results obtained by the MTT assay were not exactly the same as that of the crystal violet assay, particularly those related to a low glucose with pyruvate and pyruvate-only media, where there were variations in the outcome at different points of time. In general, a part of low glucose with pyruvate media, carcinoma cells show nearly similar proliferation rates in the other types of media.

The discrepancy between crystal violet and MTT assay results can be attributed to differences in the mechanism of action of both of them. The crystal violet assay is a non-enzymatic assay, so its mechanism of action is based on the presence of attraction between both the dye and the external surface of the DNA [654-656]. The absorbed quantity of dye is related to the total amount of DNA in the cell culture which allows the number of living cells to be estimated [654-656]. By contrast, an MTT assay is an enzymatic assay; its mechanism of action is founded on the notion that tetrazolium salt is reduced to formazan product and this takes place in the mitochondria of surviving cells because of the action of mitochondrial dehydrogenases [654-656]. Because of that the MTT assay is affected greatly by agents that change cellular metabolism through rising levels of lactate dehydrogenase [657-660]. The crystal violet assay does not have this shortcoming that weakens the precision of MTT assay with its reliance on enzymatic reactions [654-656]. Also, different studies have

mentioned other factors that have been described as affecting and undermining the precision of the MTT assay as an enzymatic assay. These factors include: (1) The MTT assay can produce false negative results and this occurs because generation of formazan can be increased by the effect of Rotterlin compound that decouples the mitochondrial respiratory chain [654, 655]; (2) Reduction mechanism of tetrazolium can occur in other places in the cell rather than the mitochondria. These possible locations are: cell surface, lysosome membranes, endosome, or inside the cytoplasm, or even extracellularly [657-661] and this also has an adverse effect on the assay accuracy and in this way the assay provides inaccurate results; (3) Reduction process of tetrazolium is subjected to the impact and influence of different variables involved in the reaction of the MTT assay. These influencing variables include: phase of cell cycle, current growth phase and conditions affecting the reaction, for example pH and concentration of D-glucose [654, 655] which may lead to inaccurate results from the MTT assay.

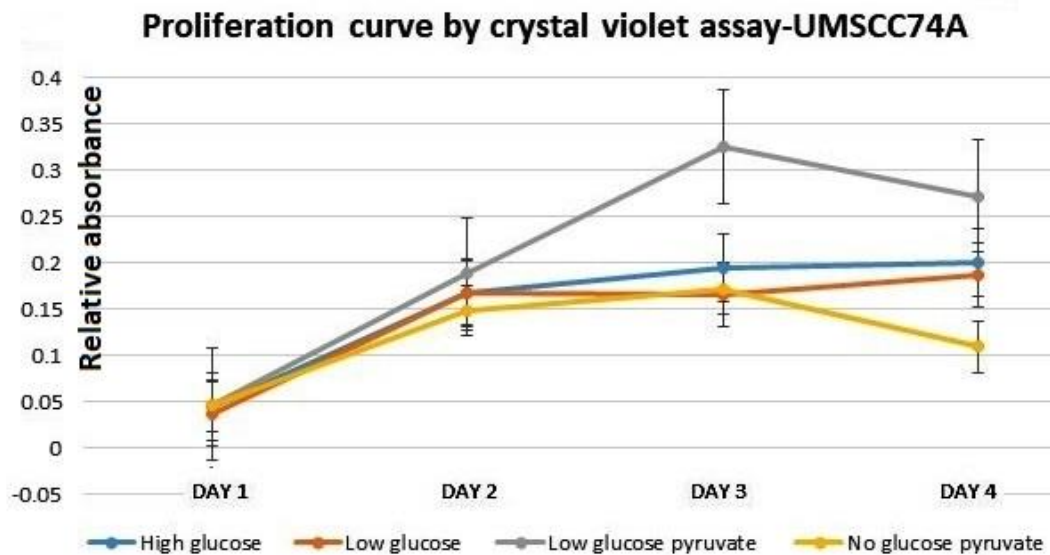
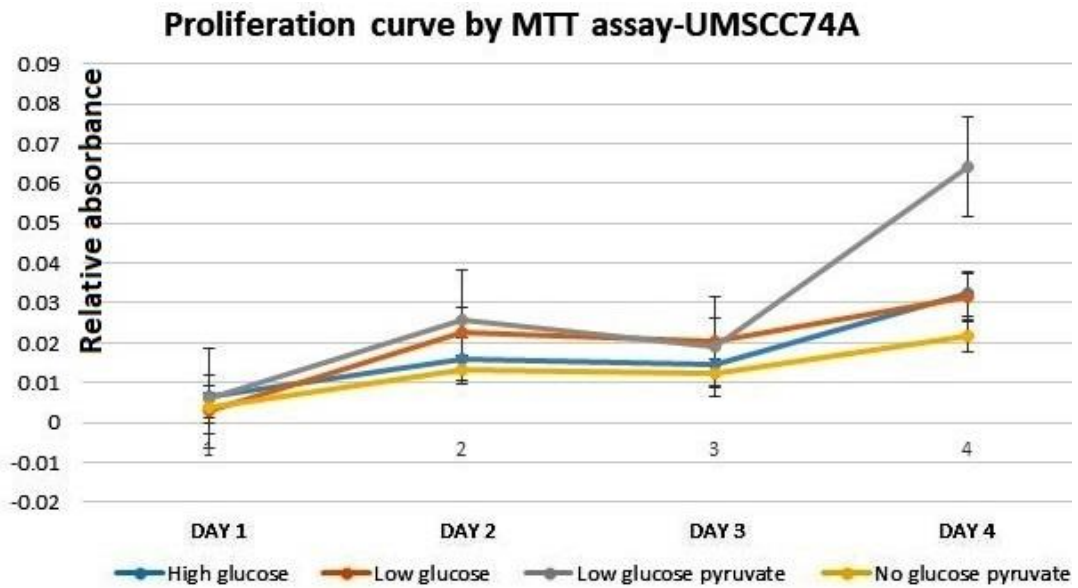


Figure 5.8. Effect of metabolic fuel availability on proliferation of (HPV-) cancer cells (UMSCC74A).

Line graph showing proliferation of UMSCC74A cancer cells by MTT assay (upper) and crystal violet (lower) in four different metabolic media cells. Over four days, cells proliferated most rapidly when supplied with glucose + pyruvate media (grey line) when compared with the low glucose only or pyruvate only condition.

The delivery of pyruvate to the media, in association with glucose or without glucose, did not show a clear effect on the proliferation of the HPV+ cancer cell line, UPCISCC154 (Fig. 5.9). Cells provided with pyruvate media, with or without glucose, showed an increase in their proliferation rate, followed by a rapid decrease.

Meanwhile, when supplied with glucose only at low concentration media, the growth in these cells was more rapid and for a longer time, with a steeper slope of the graph. However, the crystal violet assay showed the presence of a period of re-increase in the proliferation following that of the slope.

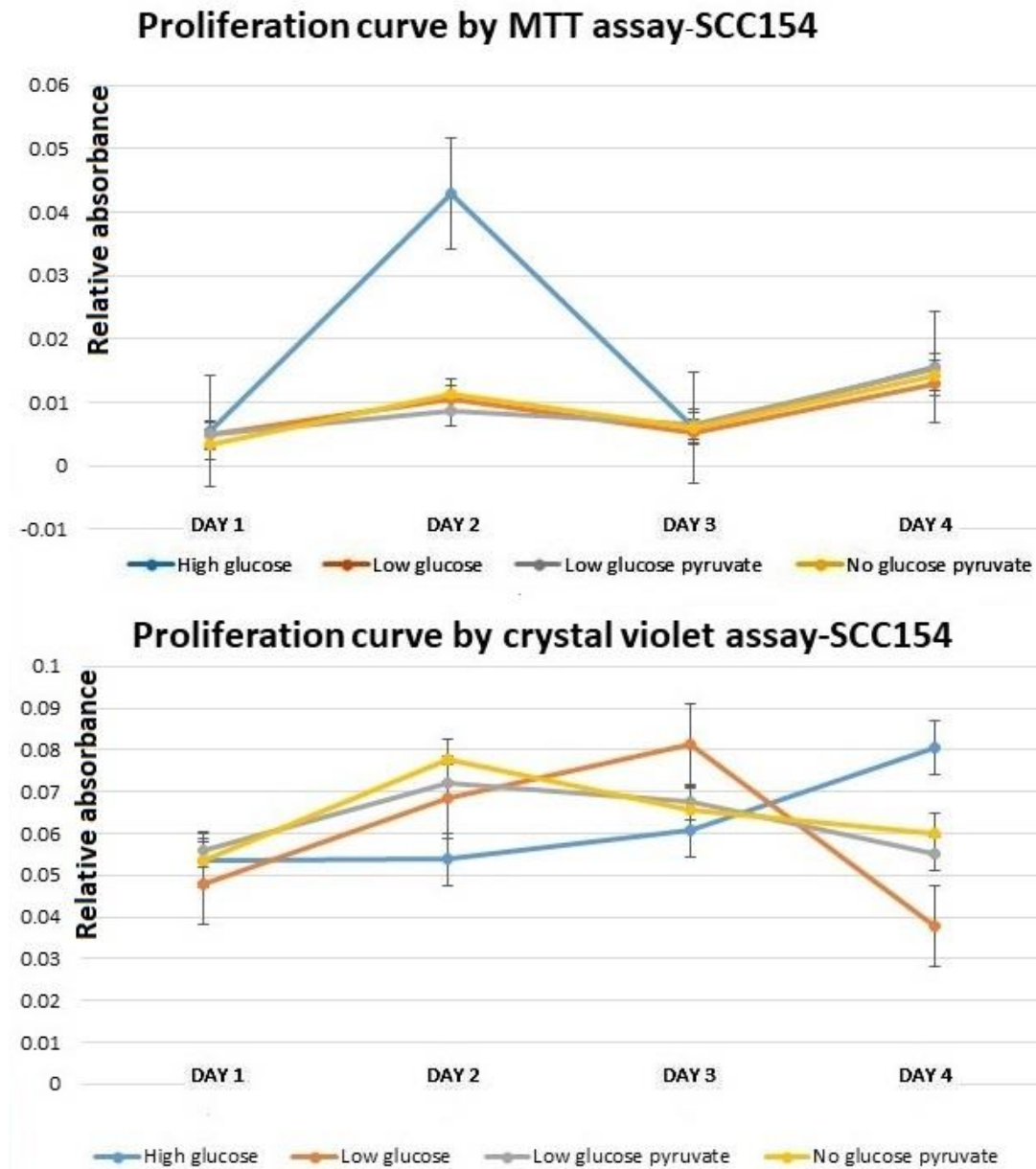


Figure 5.9. Effect of metabolic fuel availability on proliferation of (HPV+) cancer cells (UPCISCC154).

Line graph showing proliferation of UPCISCC154 cancer cells by MTT assay (upper) and crystal violet (lower) in four different metabolic media cells. Cells provided with pyruvate media with or without glucose (grey and yellow lines) show increase in their proliferation rate followed with rapid decrease meanwhile these cells when supplied with glucose only at low concentration media, the growth was more rapid and for longer time with steeper slope of the graph (brown line).

Effect of metabolic substrates on epithelial cancer cell viability and colony formation

The largest effect on proliferation was observed in HPV- epithelial cancer cells growing in a glucose-pyruvate combination, when compared with low glucose alone or pyruvate alone. Our proliferation results suggest that glucose with pyruvate may be a more preferable metabolic substrate than glucose alone or pyruvate alone in the promotion of cell proliferation in this cell line. However, the HPV+ cancer cells did not demonstrate any clear proliferation changes, and it is likely that alterations in metabolic substrates may cause cytotoxicity. A result of previous research done on MCF7 examining this effect, however, concluded that these alterations do not lead to obvious cell death [653].

5.4 Discussion

In spite of the fact that MCT1 has been identified as a potential target against cancer with a MCT1 inhibitor already under clinical trials [645, 662] (discussed earlier in more details in pages 166, 167 and 168), its mode of operation is yet to be fully understood, particularly in terms of its regulation by the tumour microenvironment [104, 663, 664]. Additional information is required by scientists for the design of effective combination therapies [644]. A recent study demonstrated that the mitochondria serves as both a glucose sensor and signalling organelle, thereby keeping the MCT1 expression in low levels, and operating in the OXPHOS mode through stimulation of its expression upon OXPHOS deficiency (directly or indirectly) [644].

In this study, we report that limited glucose availability induced an MCT1 expression in human HPV+ carcinoma cells, but not in the HPV- cells. Interference with the functional coupling, present between the tricarboxylic acid cycle and OXPHOS, is an essential characteristic of cancer metabolism [665], and occurs when tumour cells expand their supply of oxygen and nutrients, marking the shift to a glycolytic metabolism state. The Warburg Effect is also a typical feature of tumour cells constitutively dependent on glycolysis [662]. Such kinds of responses to low glucose give more explanation about the metastatic stimulation that is connected with the upregulation of MCT1 expression in metastatic lesions, when compared to primary lesions [666]. In the lack of other nutrients, the restricted availability of glucose renders mitochondria deprived of indispensable fuels resulting in stimulation of oxidative stress [667]. Consequently, the survival of cancer cells then depends on autophagy and their capability to counter extreme production of ROS. Recently, it has been demonstrated that overexpression of MCT1 by survivor cells can take place independently of clonal selection (two clones namely A and B isolated from the total population of wild-type of SiHa cells). Therefore, it may be regarded as an essential component of cell adaptation toward limited availability of glucose [644]. We have shown an upregulation in MCT1 protein expression by HPV- epithelial cancer cells when we added pyruvate; a metabolic fuel, to low glucose media. The same cells were able to use pyruvate in the absence of glucose and induce the MCT1 expression. In contrast to HPV- epithelial cancer cells, the HPV+ epithelial cancer cells were unable to use pyruvate either in the existence of glucose or in its absence. Other recent studies have shown that when the mitochondria is refuelled, it stops the reaction toward

glucose shortage, irrespective of the molecular nature of the fuel- that is, these oxidative metabolic substrates block the MCT1 induction in the absence of glucose. The delivery of the oxidative substrate in the presence of glucose also did not modulate/change the expression of MCT1 meaning that these compounds did not modify the basal expression of MCT1 in the presence of glucose. The overexpression of MCT1 in tumour cells, starved from glucose, was suppressed with substitution of oxidative fuels [644]. An indirect influence from the MCT1 expression cannot be ruled out, forming super-complexes with molecules such as CD147 and MCT4 [668]. Moreover, additional control would be required in the case of hypoxic conditions [669-671], and a reason hypoxia could be unsuccessful at inducing (or possibly inhibiting) the expression of MCT1 in vivo [262, 672] while it stimulates the expression of MCT1 in vitro [673]. It may also be the reason the upregulation of MCT1 expression is identified at early time points in certain studies [644], while other researchers did not find this induction of MCT1 when hypoxia increased for a longer duration (forty eight hours) [278]. In fact, modifying ROS can influence the response of MCT1 to hypoxia [644].

It became evident, though, that glycolytic metabolism is a less efficient way of producing ATP in comparison to mitochondrial OXPHOS; 2 ATP molecules are produced for each glucose molecule via glycolysis in comparison with 38 ATP molecules by means of oxidative phosphorylation, and glycolysis offers an advantage in growth via numerous diverse mechanisms [297]. The different advantages involve a more rapid ATP generation than OXPHOS, supplying cancer cells with the necessary substrates (biosynthetic) required for fast proliferation such as ribose 5-phosphate and NADPH [103, 258] [29,30], and cell growth support in case of hypoxic conditions [102]. Recently, literature has shown that mitochondria perform a significant part in proliferation cancer cells via glutamine metabolism in the Krebs cycle, providing supplementary metabolic substrates needed for cell proliferation and growth. This mechanism, however, is not fully understood [103, 674]. To a large extent, the metabolic reprogramming is a general cancer phenotype, and as a result, the metabolism of cancer cells nowadays is believed to be a significant potential target in the therapy of many cancers [675]. Our current investigation demonstrated that the HPV- epithelial cancer cells UMSCC 74A proliferated in a more rapid way when supplied with glucose/pyruvate as a metabolic substrate when compared with glucose

alone or pyruvate alone, and this takes place without the presence of an obvious death of cells. Given that cancer cells favourably upregulate glycolysis in comparison with normal cells [676], our result is, to some degree, surprising and thus suggests that glycolysis by itself is not enough to promote cancer cells proliferation in a rapid way. This thought is in line with recently published studies that show more rapid cancer cells growth can be achieved when these cancer cells are supplemented with energy substrates, such as pyruvate. Also, its metabolism can be carried out via the mitochondrial pathways of citric acid cycle and OXPHOS, comparing to glucose in many types of cancer cells such as glioblastoma and K-Ras-transformed HCT-116 from colon cancer cells [640, 641]. We also related the responses of proliferation following supplementing with pyruvate only, in comparison with glucose with pyruvate. Although the supplementation with glucose pyruvate resulted in a rise in proliferation, Pyruvate alone was unable to enhance the growth of cells. These diverse effects occurring between these two varieties of fuel may appear as a result of variations in their intracellular metabolism, or the way used to uptake these fuels inside the cells.

Neither of these observations explains why pyruvate alone was unable to support proliferation, and more investigation will be required for this. Further potential elucidations comprise that it is not easy to transport pyruvate alone into HPV- cancer cells UMSCC 74A or the pyruvate metabolism takes place at insufficient rate to supply mitochondrial respiration with the required fuel. Recent literature focused on the importance of ‘biosynthetic activity’ of mitochondria in cells that undergo rapid division and produce substrates aimed at biosynthesis of protein, lipid and nucleic acid [103]. A recent research [653] examined the effect of pyruvate in MCF7 cells; as pyruvate is considered to be a metabolic substrate for the tricarboxylic acid cycle, and accordingly drives mitochondrial function, on respiration.

In breast cancer cells, the distribution of MCT isoforms intracellularly demonstrated the presence of different patterns of expression and different distributions to the two membranes; a plasma membrane as well as a mitochondrial membrane [653, 677]. Moreover, MCT1 was described to be present in the mitochondria, and therefore it is clear that the regulation of monocarboxylate transport intracellularly takes place at various levels [653, 678]. Our results are supported by the ‘metabolic symbiosis’ relationship, originally reported by Sonveaux and his group, in the tumour

microenvironment [262]. It has been proposed that in solid tumours, the two molecules, glucose and lactate, are considered to be metabolic substrates used by carcinoma cells; yet, this use is spatially distinct (location dependent) [262].

Conclusion

Results shown in this chapter suggest that:

- 1- Based on metabolic data shown in Chapter 4 and preliminary functional data, there may be some differences in metabolism in HPV+ and HPV- tumours. We suggest that fibroblast population rather than epithelial cancer cell population results in this effect even though it is the cancer cell that is infected with HPV.
- 2- We therefore speculate that the mechanism leading to an induction of the myofibroblast phenotype of CAFs is separate from the induction of the Reverse Warburg Effect.

Limitations

Our results, based on two cancer cell lines with different HPV status produced results that need to be further verified as the case, in two or three additional cell lines. Recruiting in similar fashion, one with a significant level of baseline expression of MCT1, one with a moderate expression level, and a non-cancer cell line with any level of MCT1 expression. Probing for more partners will also open a window into understanding mechanism by which MCT1 is involved with tumorigenesis. Further optimisation of the Western blot experiments is required. Emphasis will be towards being able to precisely detect MCT1. Firstly, it will be important to employ cell lines obtained from tumours similar to those ones used for IHC. This way, a close correlation between both should be expected and serve as a means of validation of results on both sides (western blot and use of TMA). Also, very key will be the use of highly specific primary antibodies. Antibodies specific enough to select between the two forms of MCT1 (mature and immature) when used for the Western blot.

Chapter 6

Hypoxia in in HPV+ and HPV- oropharyngeal squamous cell carcinoma: preliminary investigations

6.1 Introduction

A hypoxic microenvironment is common in advanced solid tumours, including head and neck cancers [679]; adversely affects prognosis [321, 638, 639]; and is attributable to an imbalance between oxygen consumption and delivery [679]. The major causative factors of tumour hypoxia in advanced solid tumours are the abnormal structures and functions of the microvessels supplying the tumour, increased diffusion distances between the nutritive blood vessels and the tumour cells, and reduced transport capacity of the blood due to the presence of disease-related anaemia.

Oxygen tension (pO_2) in solid tumours, although cannot be precisely measured, depends on their location and size. Techniques used to assess hypoxic status in tumours, include immunohistochemistry for HIF-1 α and HIF-1a target genes, and pO_2 measurement. Before 1990, relevant data were mainly obtained by means of immunohistochemistry. The availability of Eppendorf electrode however, enabled measurement of pO_2 directly in the tumour per se [680], and has been applied to head and neck cancers and their cervical nodal metastases [679]. Other techniques depend on injecting a probe able to bind to hypoxic tissues, obtaining a biopsy and examining the latter via immunohistochemistry for the probe-binding protein; the most common probe is pimonidazole [681, 682].

The threshold of hypoxia in a solid tumour corresponds to a pO_2 of 10mmHg [679, 683]. Below that level, oxygen consumption or ATP production in tumour cells decrease progressively [684].

The hypoxic microenvironment in tumours should be examined in conjunction with the angiogenic events therein. Angiogenesis is a requisite for sustained cancer growth and metastasis [685]; and VEGF is the typical proangiogenic factor in most tumour types, including head and neck cancer [685, 686].

VEGF induces angiogenesis by binding to receptors (VEGFRs) expressed on endothelial cells in blood vessels adjacent to the tumour front [687, 688]. Overexpression of VEGF in head and neck cancers is associated with a higher tumour stage, lymph node and distant metastases, poor distant metastasis-free and overall survival, and increased risk of death [679, 688, 689]. In a previous study of 133 HNSCC, serum VEGF levels were significantly correlated with hypoxic tumour volume; the latter being calculated as the product of the absolute tumour volume and the hypoxic (< 5 mm Hg) measurement [690]. It seems thus likely that a hypoxic status influences VEGF expression; genes involved in the metastatic cascade, are also thus expressed [318, 319]. A significantly higher expression of VEGF mRNA and protein levels has been described in three human OSCC lines under hypoxic conditions [679, 691], and in-situ in laryngeal SCC and nasopharyngeal carcinoma [493, 679, 692]. In the in-situ studies, higher expression of VEGF was also associated with increased nodal metastases and higher recurrence rate [493, 679, 692].

VEGFs and VEGFRs have drawn attention because of their significance in the pathogenesis of colon, ovarian, lung and other cancers [693-695]. Anti-VEGF agents, such as the monoclonal antibody bevacizumab, have shown noticeable patient benefit in clinical trials and are commercially available [695, 696]. VEGF and VEGFR2 were found to be highly co-expressed in cancer cells in a cohort of HNSCC and this was associated with a high rate of proliferation of tumour cells and worse survival outcome [697]. The interesting co-expression of VEGF and VEGFR1, VEGFR2 has also been found in HNSCC cancer cells in vitro [698]. It suggests an autocrine mechanism for tumour growth in response to VEGF that complements the paracrine proliferative effect of the factor on endothelium [698]. There is also evidence that OSCC cells co-express VEGF isoforms and their receptors, strengthening the notion of autocrine and a paracrine functions in head and neck cancers [695, 697-702].

Only a few studies explored VEGF expression in HNSCC, in relation to the HPV status. While two studies reported an association, another two did not [685, 688, 703, 704]. There are no data available for VEGFRs.

Because of their known activity and implication in the lymphangiogenesis signalling pathway, multiple types of vascular endothelial growth factor including VEGF-C and -D and VEGFR-3 have become attractive targets for the treatment of cancer [705-707].

The data regarding VEGF expression in oropharyngeal squamous cell carcinoma and its importance in prognosis are inconsistent and conflicting [705]. However, an immunohistochemical study investigated the expression of angiogenic proteins in FFPE samples of oropharyngeal squamous cell carcinoma showed the presence of an association between VEGF and clinico-pathological parameters included tumour grading, tumour staging and angiogenesis [705]. Furthermore, another study examined the expression of VEGFA-C, and VEGFR1-3 in oropharyngeal squamous cell carcinoma using an immunohistochemistry technique and by means of multivariate analysis, results revealed that the expression of VEGF-C and lymph node metastasis were the only independent factors associated with locoregional recurrence and distant failure and they also have an influence on the overall survival [705]. Also, VEGF expression was shown to have an importance in disease prediction. A previous study performed on oropharyngeal squamous cell carcinoma cases that received surgical treatment as well as radiotherapy postoperatively showed an increase in the level of VEGF expression [705]. In addition, this elevated level of VEGF was the most important factor in the prediction of poor disease free and overall survival rate with a significant value in prognosis [705, 708].

The diversity in the anatomical sub-site of origin of tumour in the aforementioned HNSCC studies is notable and effects difficulties in extracting precise information related to OPSCC. Except for the study of Fei *et al.* [704], who examined a pure cohort of tonsillar SCC, the other studies are based on cohorts of HNSCC originated from different sub-sites. Examination of cohorts from a single sub-site, as in the present thesis, are desirable.

In cervical carcinoma, the HPV16 oncoproteins E5, E6, and E7 seem able to induce VEGF expression directly, via a p53 independent manner [709], or indirectly via epidermal growth factor receptor (EGFR) [710] or HIFs [711]. This has not been explored in HNSCC [685].

Data from a previous study conducted on mouse fibroblasts and human keratinocytes investigated whether HVP-16 E6 oncoprotein upregulates VEGF expression, suggested that it is likely that the HPV oncoprotein E6 might play a role in tumour angiogenesis through direct induction of the VEGF gene [709]. Researchers found that (HPV16) E6 positive cells commonly express significant rates of VEGF and also the

E6 oncoprotein has upregulated the promoter activity of VEGF when the VEGF promoter luciferase (Luc) reporter gene and E6 are co-expressed and makes the same in a p53 independently [709]. Furthermore, the same study has shown that an E6 responsive region that includes four Sp-1 sites, located within the VEGF proximal promoter, is essential as well for VEGF to be transcribed constitutively. E7 upregulates expression of VEGF via the effect of telomerase reverse-transcriptase (hTERT) as well as the action of telomerase activity [712, 713]. So, it is apparent that upregulation of VEGF by the E6 and E7 oncoproteins of HPV is tightly commanded, which denotes the significance of VEGF for HPV+ cancers and also shows its value as a potential therapeutic target [709].

In Chapter 4, differences in the metabolic compartmentalisation between HPV+ and HPV- OPSCC were shown. It seems sensible to hypothesize that those differences may reflect differences in tissue oxygen levels. To test this hypothesis, the present chapter aims at exploring whether OPSCCs express hypoxic phenotypes; and whether such expression relates to the metabolic events, angiogenesis and HPV status. To date, no endogenous marker has been found that strongly and consistently shows a relationship with hypoxia. Although GLUT-1 has been proposed as a hypoxia indicator [321, 672]. We decided to evaluate this concept in the HPV+/-OPSCC setting, examining the reliability of GLUT-1 as a hypoxia biomarker by relating its expression to that of HIF-1 alpha, an established hypoxia marker.

6.2 Overall aim and specific objectives of the chapter

- a) To use HIF-1 α and GLUT-1 expression as markers of oxygen levels in tumour microenvironment and to determine if their expression is influenced by the HPV infection status of OPSCC.
- b) Identify the differences between HIF/ angiogenic proteins expression (VEGF and VEGFR2) in HPV+ and HPV- OPSCC to better understand the biology of HPV tumorigenesis.

6.3 Materials and methods

6.3.1 Cohort selection

Full 5µm sections from 10 HPV+ and 10 HPV- OPSCCs (Appendix 10), included in the general cohort (Chapter 2.5), were sectioned from archival FFPE blocks of tissue and examined by immunohistochemistry for hypoxic phenotypes (hypoxia-inducible factor 1 alpha, HIF1 α), transport of glucose (glucose transporter 1, GLUT1) and angiogenic phenotypes (vascular endothelial growth factor, VEGF and vascular endothelial growth factor receptor 2, VEGFR2) (Table 6.1). The reason behind not using the same cohort as in Chapter 4 is due to the heterogeneity of staining on full sections that made them give a better picture compared with TMAs and accordingly it was decided to use this as a pilot study. The selection of samples used in this study from the main cohort was based on their MCT4 expression/staining pattern. Samples with high expression of MCT4 were chosen. The MCT4 perform lactate exportation from cells that are reliant on glycolytic pathway for their energy production. It has been described that MCT4 is upregulated by hypoxia through a HIF-1 α -mediated mechanism [278]. Based on this we expect to see a mirrored expression of HIF-1 α in our samples that showed expression of MCT4.

6.3.2 Antibodies

Marker	Clonality	Pretreatment	Dilution	Source	Control tissue
HIF-1 α	Monoclonal	See Chapter 2.7	1:50	BD Transduction Laboratories™ (610959)	Gall bladder
GLUT-1	Monoclonal (EPR3915)		1:500	Abcam, Cambridge,	Lung

				UK (ab115730)	
VEGF	Monoclonal		1:100	Thermo SCIENTIFIC (M7273)	Tonsil
VEGFR2	Monoclonal		1:100	Abcam, Cambridge, UK (ab9530)	Placenta

Table 6.1. Details of antibodies.

6.3.3 Assessment of staining

The stained sections were assessed in a blinded fashion by two observers; (AT) the study pathologist and KBS. Immunoreactivities were assessed in cancer cells and CAFs, and intensity (weak, moderate, strong) and localisation (membranous, cytoplasmic, and nuclear) of staining were recorded.

6.3.4 Statistics

The immunoreactivities of GLUT-1, HIF-1 α , VEGF and VEGFR2 of the 10 HPV+ and 10 HPV- OPSCCs were compared to their corresponding MCT4 and TOMM20 immunoreactivities as assessed in the TMAs (Chapter 4). For analysis, the statistical Program for Social Sciences (SPSS), Windows version 22.0 (SPSS statistics 22) was used. Relationships between the different parameters were assessed by the χ^2 test. $p \leq 0.05$ was considered statistically significant.

6.4 Results

6.4.1 HPV positive samples

Expression of HIF1 α

This was moderate to strong in 4/10 (40%) HPV+ OPSCC. The staining was nuclear (Fig. 6.1). The localisation of staining in the tumour cell aggregates did not show an obvious pattern; the aggregates showed staining variously localised at their centre or periphery only; diffuse staining of the entire aggregate was also seen (Fig. 6.1).

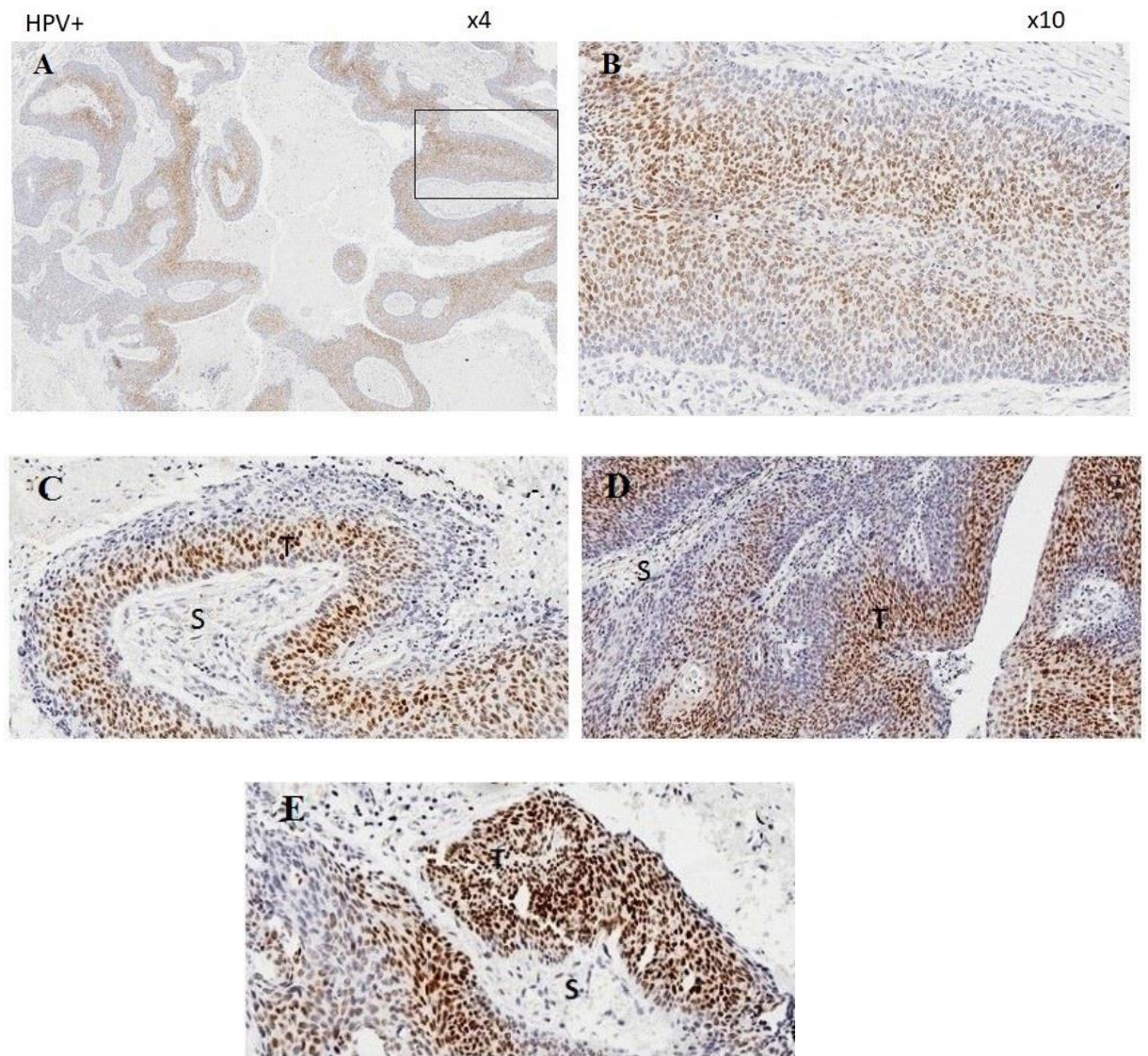


Figure 6.1. A typical example of HIF-1 α expression in HPV+ OPSCC.

The first row shows distribution of the immunoreactivity; A, widespread immunoreactivity; B, is a magnification of the rectangled area in panel A: the expression is typically nuclear. The second row shows variable localisation of the immunoreactivity; C, preferentially toward the periphery of tumour cell aggregates;

D, preferentially toward the centre of tumour cell aggregates; E, diffuse. Tumour (T); stroma (S).

Expression of GLUT1

All tumours of HPV+ OPSCC showed diffuse expression of GLUT1, and in both cancer cells and CAFs. While staining of CAFs was cytoplasmic only, variable membranous staining was also seen in the cancer cells (Fig. 6.2).

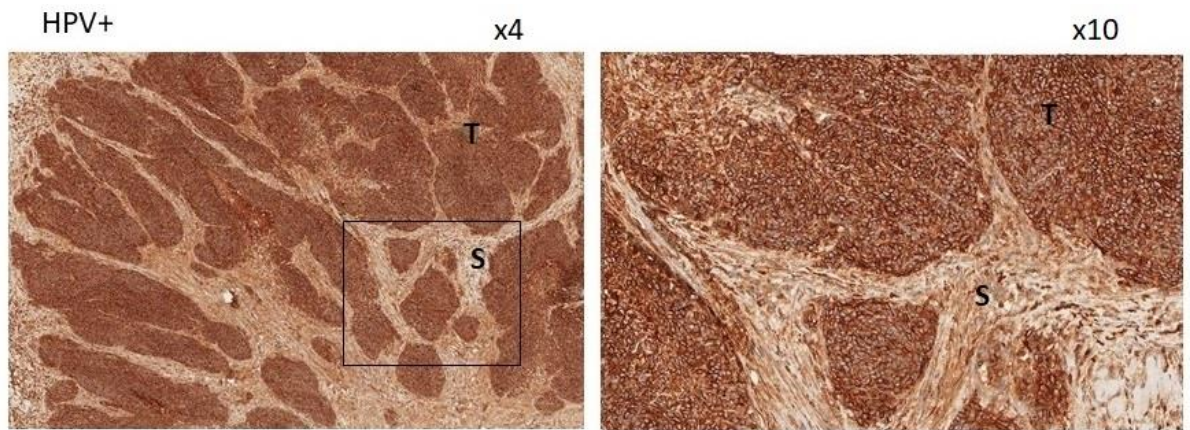


Figure 6.2. A typical example of GLUT1 expression in HPV+ OPSCC.

The left photomicrograph shows widespread immunoreactivity. The rectangled area in the left is magnified in the right showing a cytoplasmic expression of GLUT1 in cancer cells and CAFs. Tumour (T); stroma (S). Objective magnification as shown.

Expression of VEGF

Moderate to strong cytoplasmic VEGF staining was seen in all HPV+ OPSCCs, (10/10). It was present in both cancer cells and CAFs (Fig. 6.3).

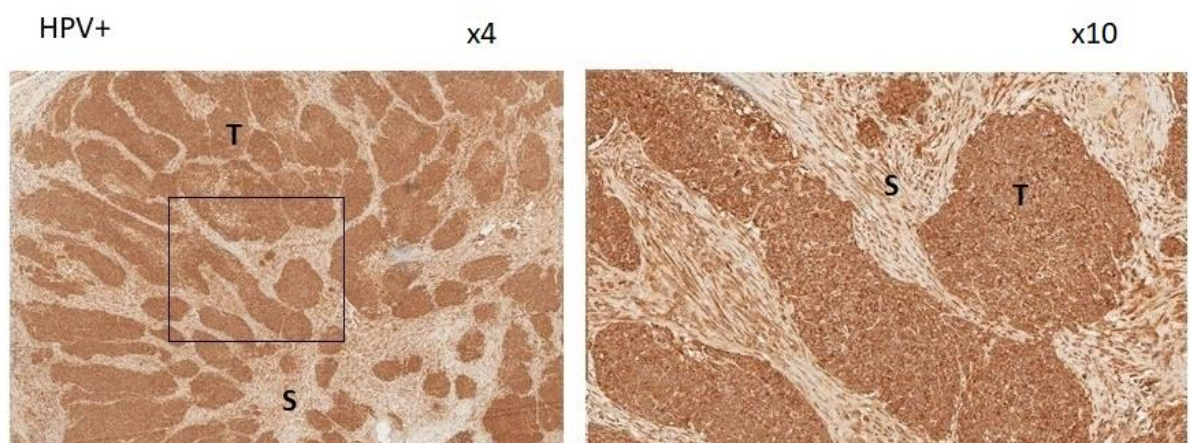


Figure 6.3. A typical example of VEGF expression in HPV+ OPSCC.

The left photomicrograph shows widespread of immunoreactivity. The rectangled area in the left is magnified in the right showing cytoplasmic expression of VEGF in both cancer cells and CAFs (right). Tumour (T); stroma (S). Objective magnification as shown.

Expression of VEGFR2

In the HPV+ OPSCC, 8/10 tumours expressed VEGFR2. The staining was largely diffuse, cytoplasmic, and mild to moderate in intensity (Fig. 6.4). The remainder tumours showed little or no staining. Both cancer cells and CAFs were stained, although staining was more intense in the former. Generally, staining appeared stronger in the core than the front of the tumours.

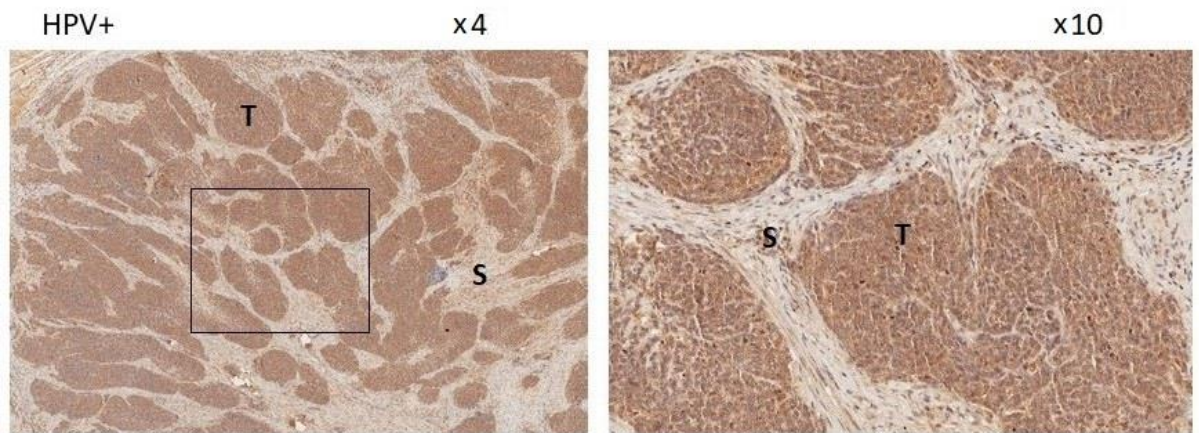


Figure 6.4. A typical example of VEGFR2 expression in HPV+ OPSCC.

The left photomicrograph shows widespread immunoreactivity is easily seen. The rectangled area in the left is magnified in the right showing cytoplasmic staining in both cancer cells and CAFs. Tumour (T); stroma (S). Objective magnification as shown.

6.4.2 HPV negative samples

Expression of HIF1 α

This was moderate to strong in 8/10 (80%) HPV- tumours OPSCC. The staining was nuclear (Fig. 6.5). The localisation of staining in the tumour cell aggregates did not show an obvious pattern; the aggregates showed staining variously localised at their centre or periphery only; diffuse staining of the entire aggregate was also seen (Fig. 6.5).

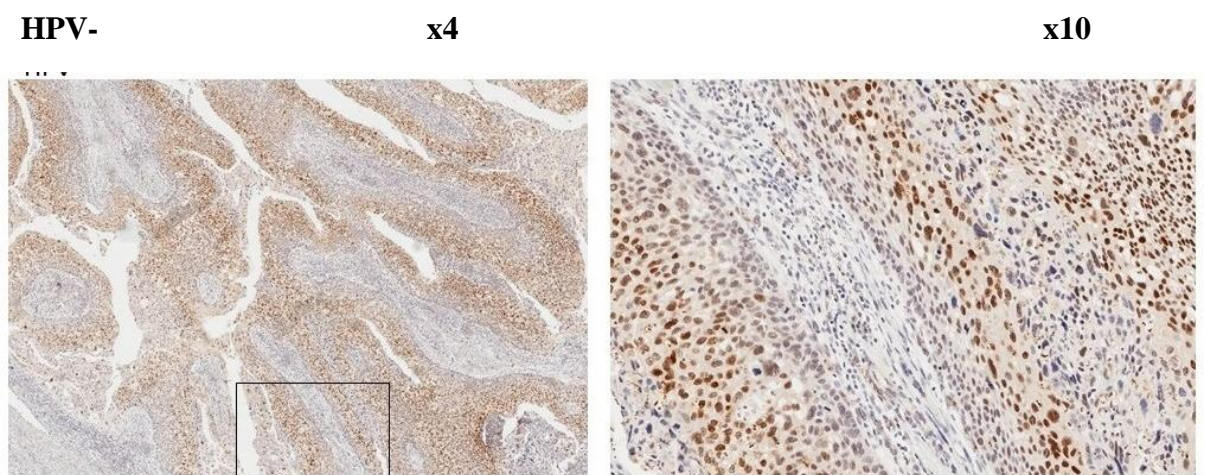


Figure 6.5. A typical example of HIF-1 α expression in HPV- OPSCC.

The left photomicrograph shows widespread immunoreactivity of HIF-1 α . The rectangled area on the left is magnified in the right showing typical nuclear expression. The localisation of staining in the tumour cell aggregates did not show an obvious pattern; the aggregates showed staining variously localised at their centre or periphery only; diffuse staining of the entire aggregate was also seen Tumour (T); stroma (S). Objective magnification as shown.

Expression of GLUT1

All tumours of HPV- OPSCC showed diffuse expression of GLUT1, and in both cancer cells and CAFs. While staining of CAFs was cytoplasmic only, variable membranous staining was also seen in the cancer cells (Fig. 6.6).

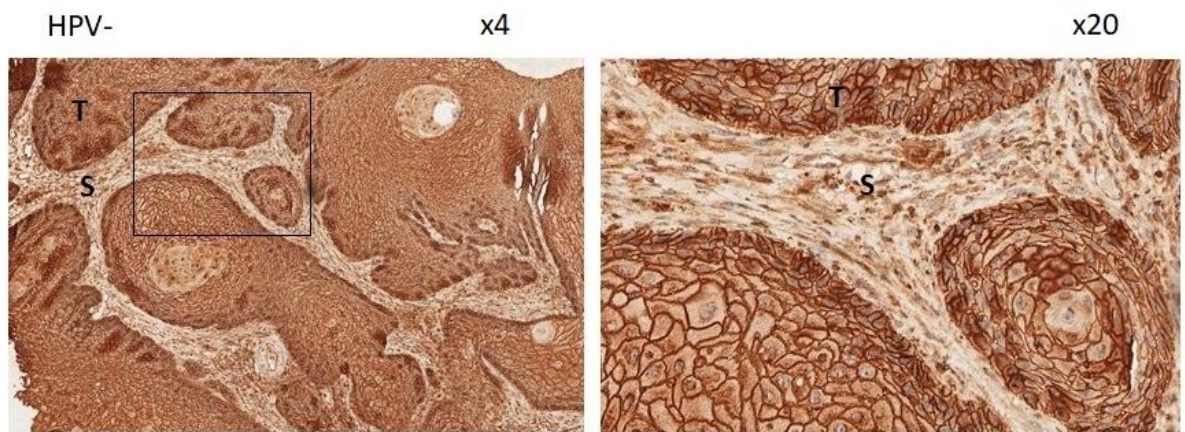


Figure 6.6. A typical example of GLUT1 expression in HPV- OPSCC.

The left photomicrograph shows widespread immunoreactivity. The rectangled area in the left is magnified in the right showing membranous expression of GLUT1 in cancer cells and cytoplasmic in CAFs. Tumour (T); stroma (S). Objective magnification as shown.

Expression of VEGF

Moderate to strong cytoplasmic VEGF staining was seen in all OPSCCs, (10/10). It was present in both cancer cells and CAFs (Fig. 6.7).

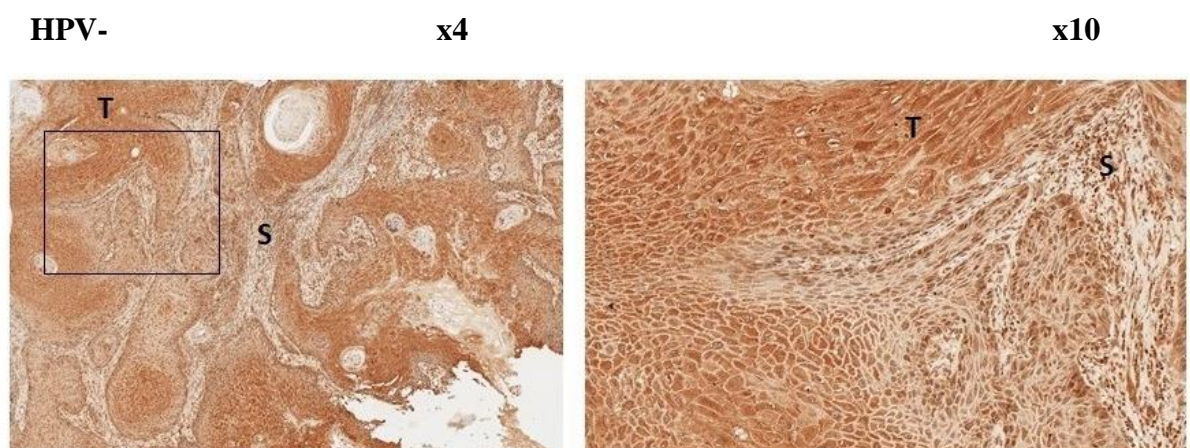


Figure 6.7. A typical example of expression VEGF in HPV- OPSCC.

The left photomicrograph shows widespread immunoreactivity. The rectangled area in the left is magnified in the right showing cytoplasmic expression of VEGF in both cancer cells and CAFs. Tumour (T); stroma (S). Objective magnification as shown.

Expression of VEGFR2

Both cancer cells and CAFs in the HPV- tumours were largely unstained (Fig. 6.8).

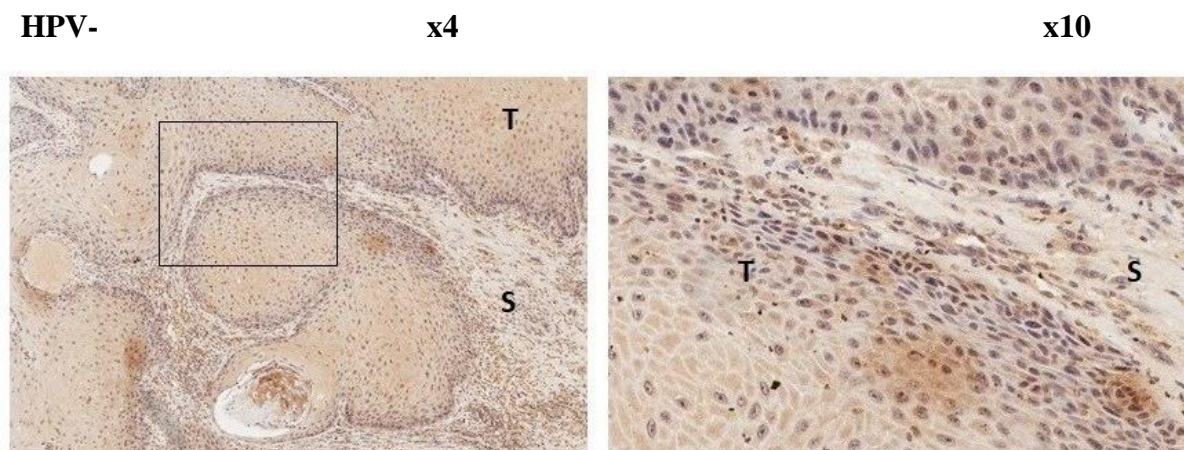


Figure 6.8. A typical example of VEGFR2 expression in HPV- OPSCC.

The left photomicrograph shows lack of staining is easily seen. The rectangled area in the left column are magnified in the right. Tumour (T); stroma (S). Objective magnification as shown.

Summary table

Marker	HPV+ OPSCC	HPV- OPSCC
HIF-1 α	Widespread/nuclear	Widespread/nuclear
GLUT-1	Widespread/cytoplasmic	Widespread/membranous
VEGF	Widespread/cytoplasmic	Widespread/cytoplasmic
VEGFR2	Widespread/cytoplasmic	Largely unstained

Table 6.2. Summary table for expression of HIF-1 α , GLUT1, VEGFR and VEGFR2 in HPV+/HPV- OPSCC.

VEGFR2 is expressed in the majority HPV+ OPSCC but is largely absent in HPV- tumours suggesting additional differences of interest between HPV+ and HPV- OPSCC.

6.3.3 Co-expression evaluation

6.3.3.1 HPV positive samples

MCT4 vs HIF-1 α

In HPV+ OPSCC co-expression was seen in 4/10 tumours. When co-expression occurred, it appeared more common at the centre of the cancer cell aggregates (Fig. 6.9). It has been described that the MCT4 facilitates lactate outflow from glycolytic cells that are relying on glycolysis in order to be used for their energy production. Also, it has been demonstrated that MCT4 expression is upregulated by HIF-1 α as a response to a decrease in oxygen concentration in the cells (hypoxia). This regarded as an adaptive response adopted by the cells and permit a rapid excretion of the accumulated lactate produced under hypoxic conditions [278].

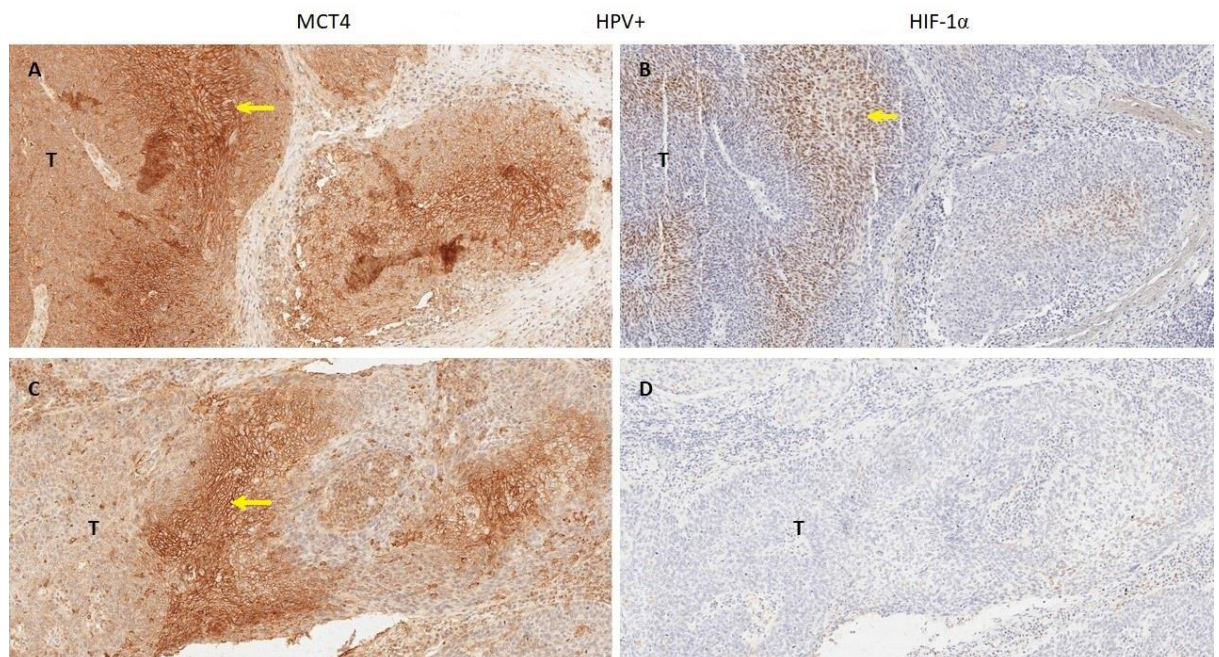


Figure 6.9. A typical example of co-expression of MCT4 and HIF-1 α in HPV+ OPSCCs.

Step sections show focal only (A, B, arrows) or absence (C, D) of MCT4 and HIF-1 α co-expression in two HPV+ OPSCCs. Note presence of MCT4 expression in (C, arrow) is not mirrored in (D) where there is absence of HIF-1 α . Tumour (T). Objective magnification, x 20.

GLUT1 vs HIF-1 α

All tumours of OPSCC showed diffuse expression of GLUT1 in the cancer cells.

Four HPV+ OPSCCs (40%) stained strongly or moderately for HIF-1 α .

Since the localisation of HIF-1 α immunoreactivity in HPV+ OPSCCs was not uniform and varied between centre and periphery of tumour cell aggregates, it did not mirror that of GLUT1 (Fig. 6.10 A and C vs B and D). Co-expression of the two immunoreactivities only occurred when there was a diffuse expression of HIF-1 α in tumour cell aggregates (Fig. 6.10 E vs F).

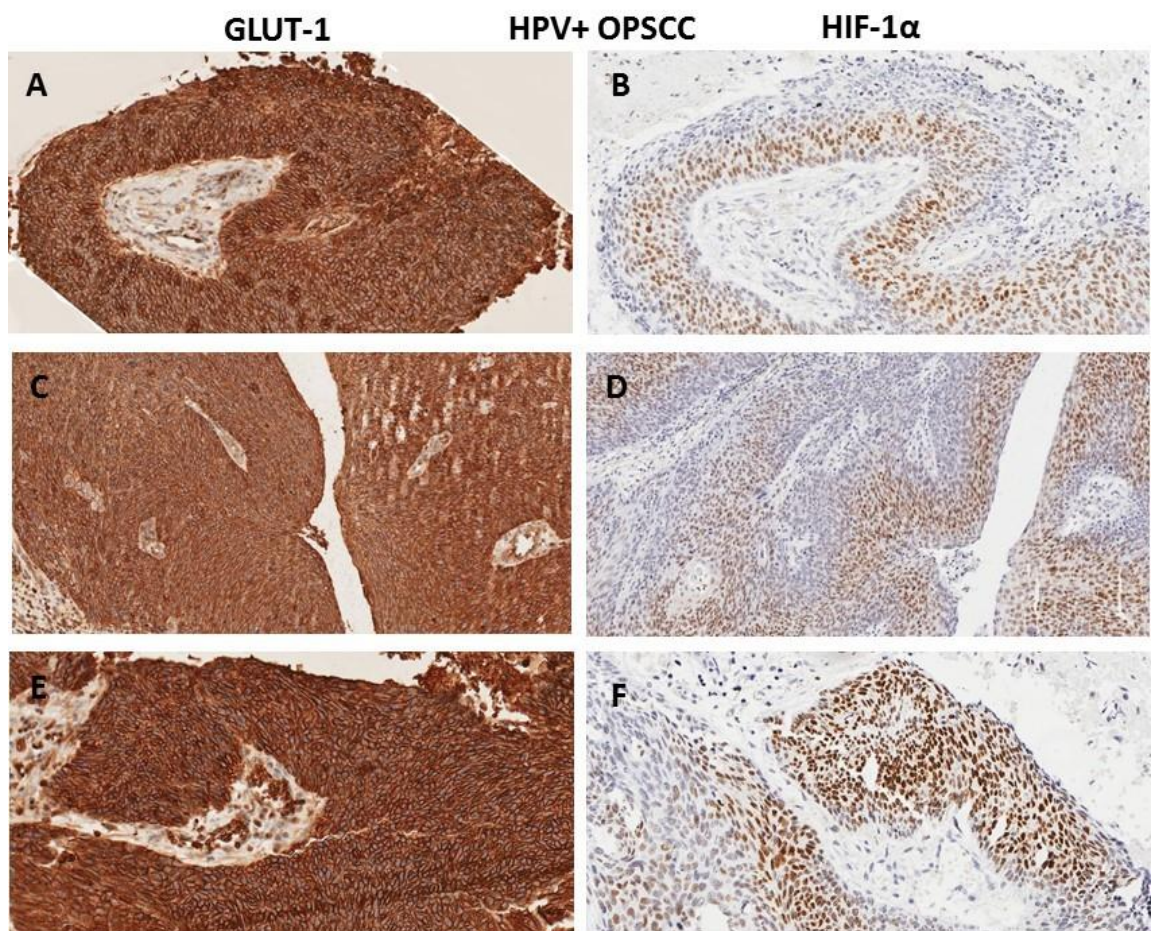


Figure 6.10. A typical example of co-expression of GLUT1 and HIF-1 α in HPV+ OPSCCs.

Step sections from a HPV+ OPSCCs tumour show differences in localisation of GLUT1 and HIF-1 α immunoreactivities. Note the localisation of HIF-1 α immunoreactivity is not uniform and varied between centre and periphery of tumour cell aggregates, it did not mirror that of GLUT1 (A and C vs B and D). Co-expression of the two immunoreactivities only occurred when there was a diffuse expression of HIF-1 α in tumour cell aggregates (E vs F). Tumour (T). Objective magnification, x 20.

VEGF vs HIF-1 α

Co-expressions were similar to those for GLUT1 (Fig 6.11).

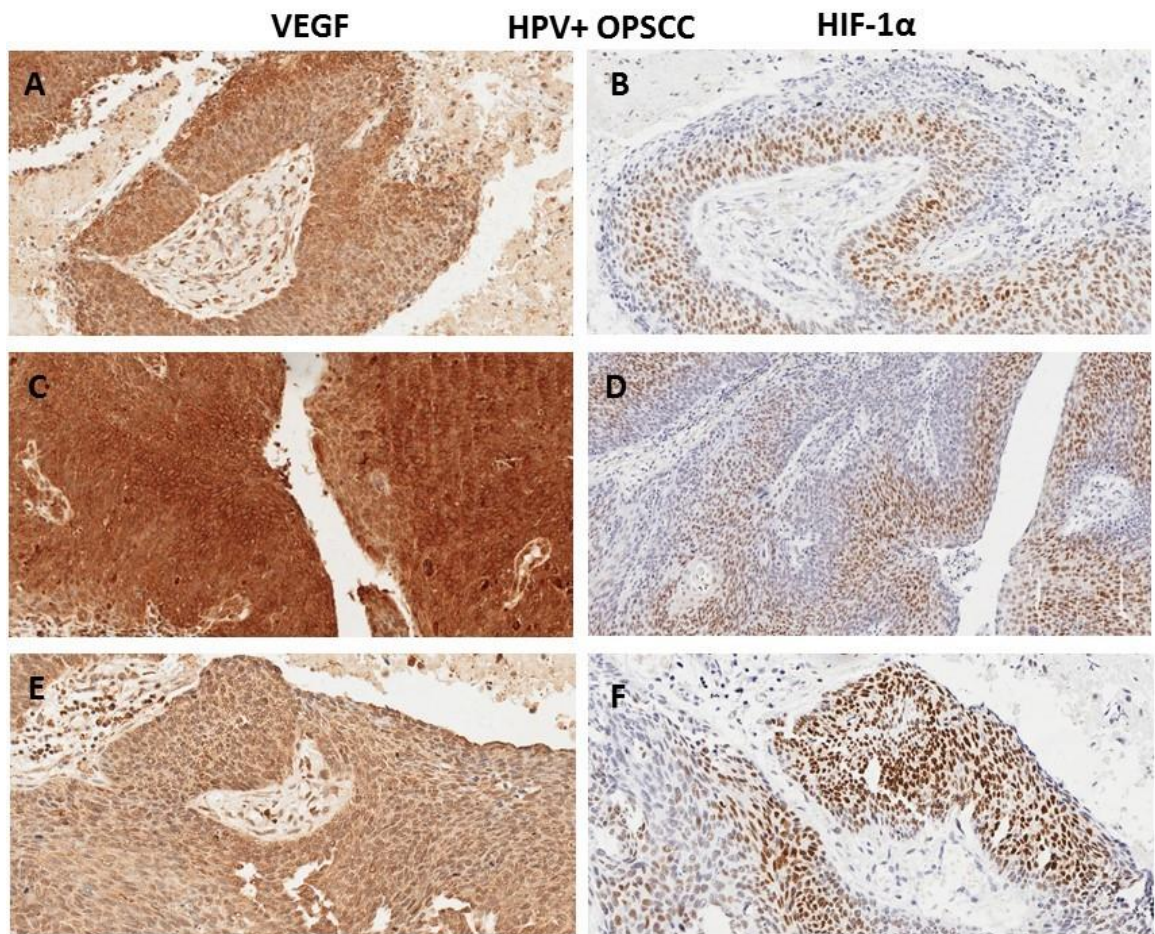


Figure 6.11. A typical example of co-expression of VEGF and HIF-1 α in HPV+ OPSCCs.

Step sections from a HPV+ OPSCCs tumour show differences in localisation of VEGF and HIF-1 α immunoreactivities. Note the localisation of HIF-1 α immunoreactivity is not uniform and varied between centre and periphery of tumour cell aggregates, it did not mirror that of VEGF (A and C vs B and D). Co-expression of the two immunoreactivities only occurred when there was a diffuse expression of HIF-1 α in tumour cell aggregates (E vs F). Tumour (T). Objective magnification, x 20.

VEGFR2 vs HIF-1 α

Co-expressions were similar to those for GLUT1 and VEGF (Fig 6.12).

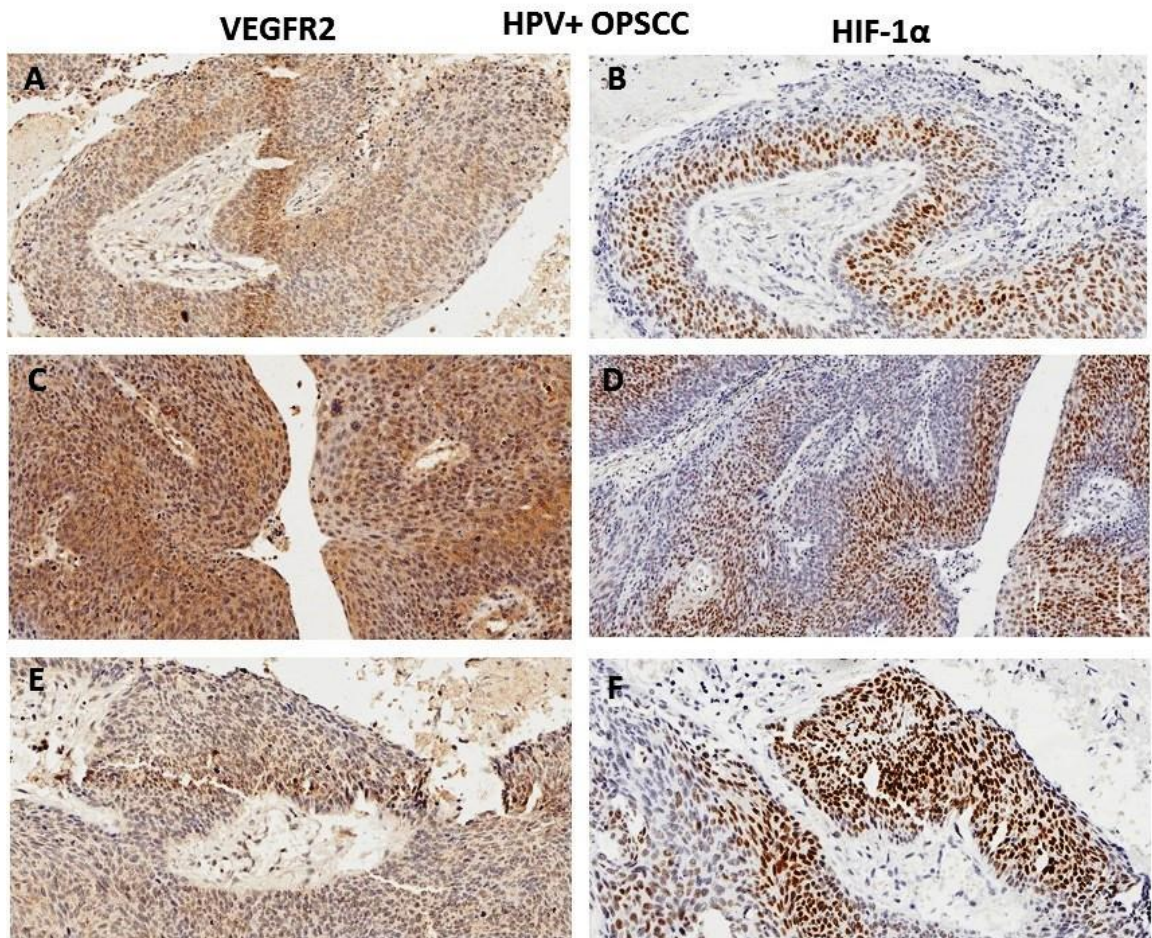


Figure 6.12. A typical example of co-expression of VEGFR2 and HIF-1 α in HPV+ OPSCCs.

Step sections from a HPV+ OPSCCs tumour show differences in localisation of VEGFR2 and HIF-1 α immunoreactivities. Note the localisation of HIF-1 α immunoreactivity is not uniform and varied between centre and periphery of tumour cell aggregates, it did not mirror that of VEGFR2 (A and C vs B and D). Co-expression of the two immunoreactivities only occurred when there was a diffuse expression of HIF-1 α in tumour cell aggregates (E vs F). Tumour (T). Objective magnification, x 20.

GLUT-1 vs TOMM20

In HPV+ OPSCC, 5/10 (50%) tumours showed co-expression of GLUT-1 and TOMM20 in the cancer cells (Fig. 6.13, A and B); one tumour (10%) showed strong expression of GLUT-1 at the centre tumour of the cancer cell aggregates, but little or no expression of TOMM20 therein (Fig. 6.13, C and D); the remainder four tumours (40%) showed weaker expression of TOMM20 compared with GLUT-1 (Fig. 6.13E and F).

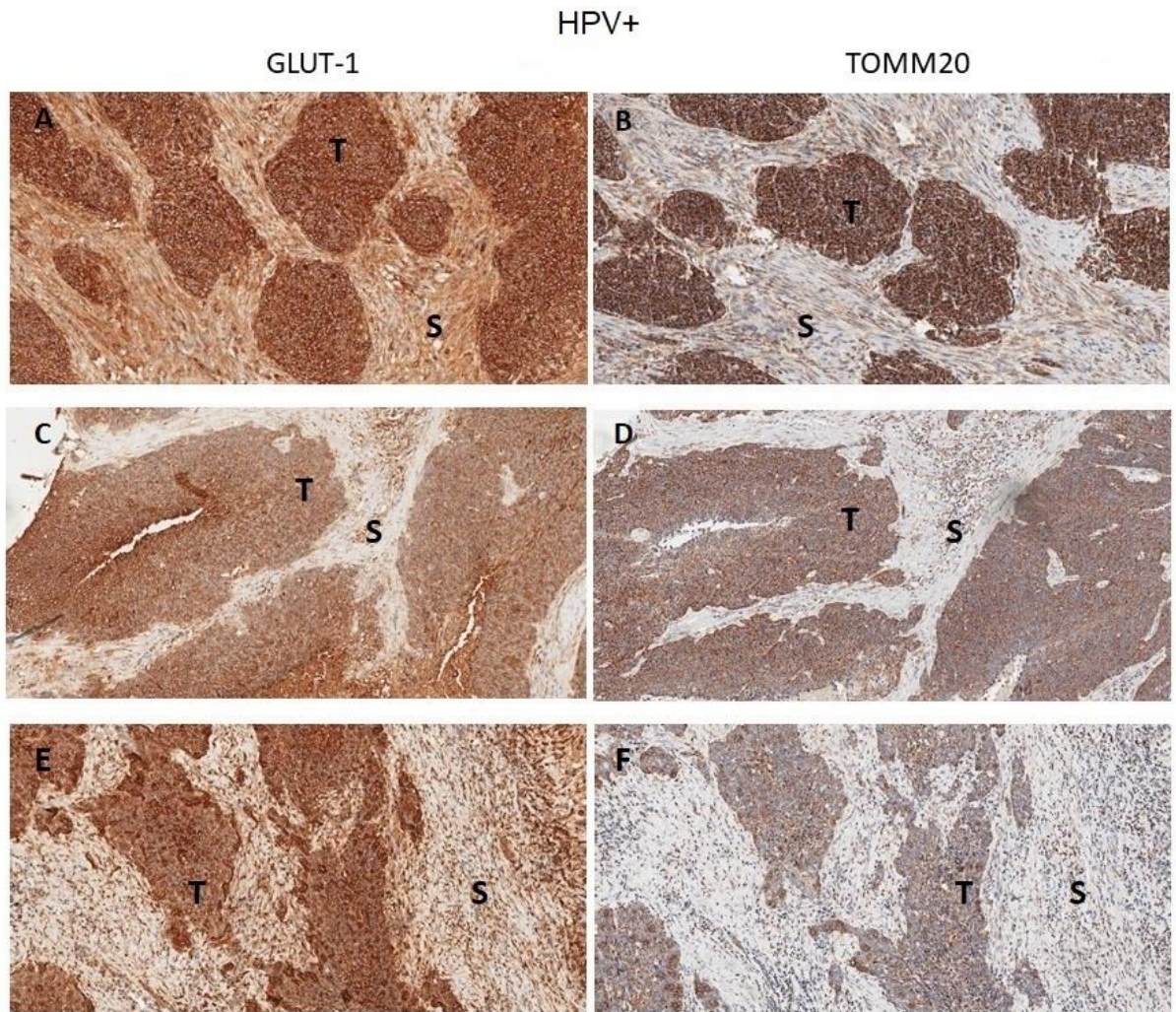


Figure 6.13. A typical example of co-expression of GLUT-1 and TOMM20 in HPV+ OPSCCs.

The microphotographs show immunoreactivities as seen in step sections of three HPV+ OPSCCs. Co-expression (A and B); differences in immunostaining at the centre of tumour cell aggregate (C and D); strong staining for GLUT-1 vs weak staining for TOMM20 (E & F). Objective magnification, x 20.

As regards CAFs, these often expressed GLUT- (Fig. 6.13 A); immunostaining for TOMM20 was less conspicuous (Fig. 6.13 B).

6.3.3.2 HPV negative samples

MCT4 vs HIF-1 α

In HPV- OPSCC co-expression was seen in 6/10 tumours. It varied between individual tumours and different parts (core vs front and centre vs periphery of cancer cell aggregates) of the same tumour. HIF-1 α expression was of similar intensity in both the core and front of the tumour; MCT4 expression was stronger in the centre of the cancer cell aggregates than their periphery (Fig. 6.14).

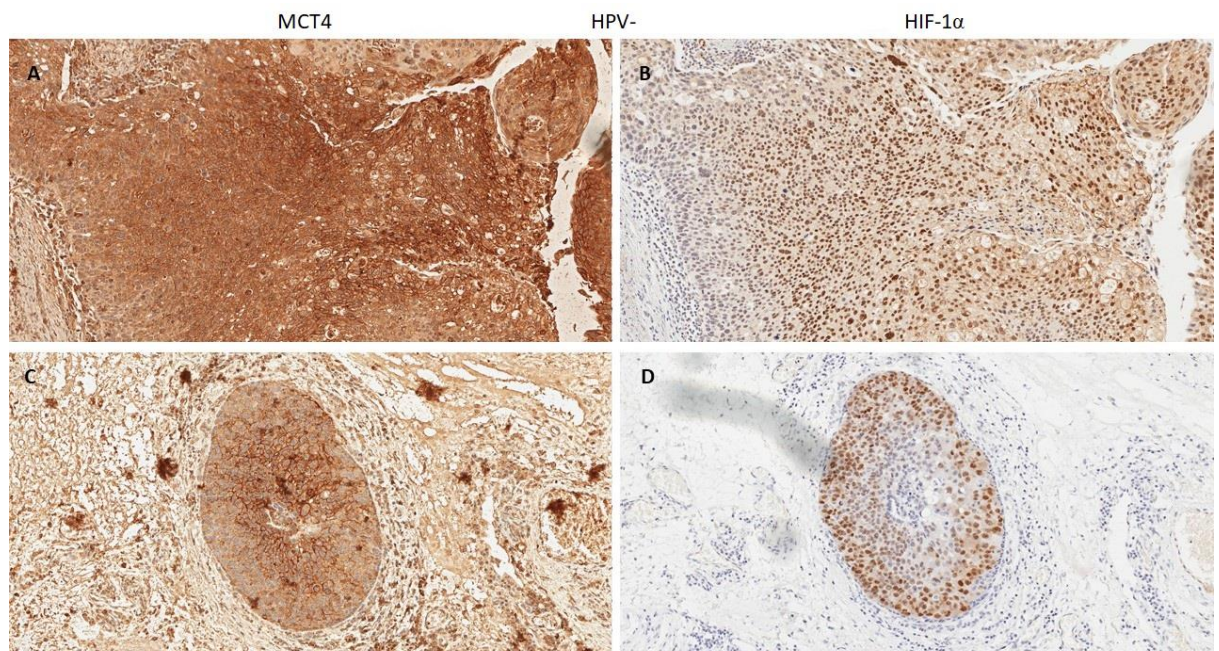


Figure 6.14. A typical example of co-expression of MCT4 and HIF-1 α in HPV-OPSCCs.

Step sections show widespread (A, B) or absence of (C, D) co-expression in two HPV-OPSCCs. Note, the preferential localisation of MCT4 and HIF-1 α at the centre and periphery of an oval tumour cell aggregate in the second tumour (2nd row). MCT4 expression was stronger in the centre of the cancer cell aggregates than their periphery (A); HIF-1 α expression was of similar intensity in both the core and front of the tumour (B). Objective magnification, x 20.

GLUT1 vs HIF-1 α

All tumours of HPV- OPSCC showed diffuse expression of GLUT1 in the cancer cells.

Seven HPV- (70%) OPSCCs stained strongly or moderately for HIF-1 α .

In HPV- OPSCC by contrast, GLUT-1 was often co-expressed with HIF-1 α . (Figure 6.15 A and C vs B and D). This was not, however, a feature when HIF-1 α was not expressed at the periphery of tumour cell aggregate (Fig. 6.15 E vs F).

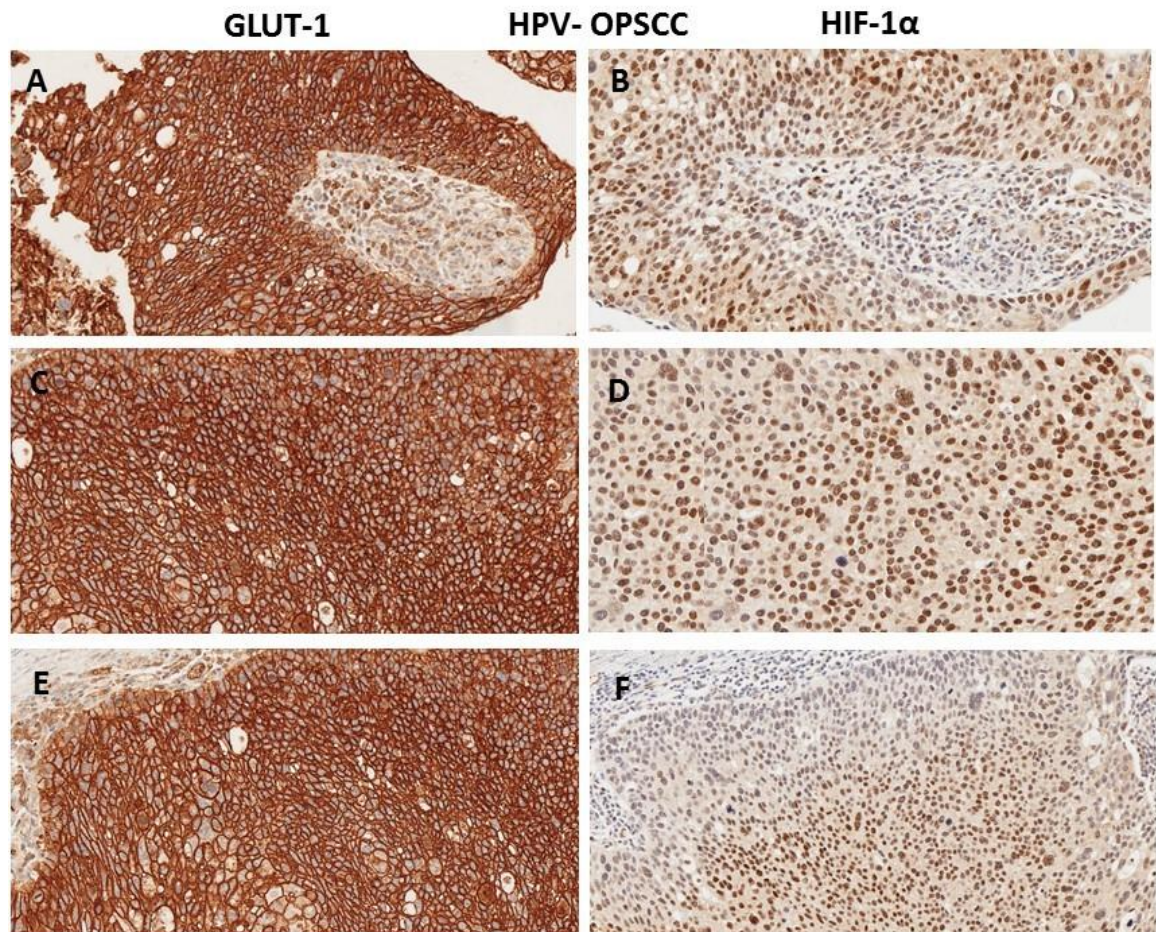


Figure 6.15. A typical example of co-expression of GLUT1 and HIF-1 α in HPV- OPSCCs.

Step sections from a HPV- OPSCCs tumour show diffuse expression of GLUT1. GLUT-1 was often co-expressed with HIF-1 α . (A and C vs B and D). This was not, however, a feature when HIF-1 α was not expressed at the periphery of tumour cell aggregate (Fig. 6.15 E vs F). Note the localisation of HIF-1 α immunoreactivity is not uniform and varied between centre and periphery of tumour cell aggregates (B and F). Tumour (T). Objective magnification, x 20.

VEGF vs HIF-1 α

Co-expressions were similar to those for GLUT1 (Fig. 6.16).

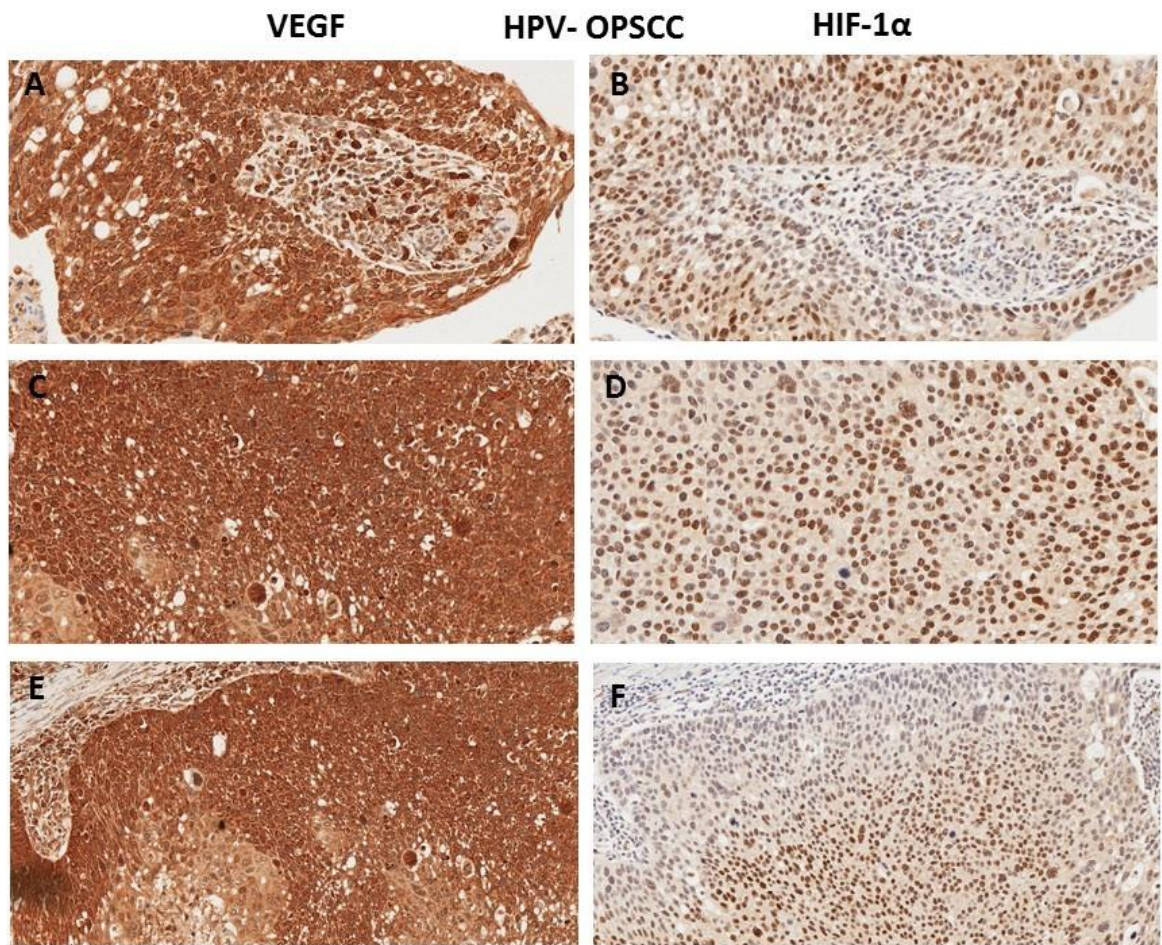


Figure 6.16. A typical example of co-expression of VEGF and HIF-1 α in HPV-OPSCCs.

Step sections from a HPV-OPSCCs tumour show diffuse expression of VEGF. VEGF was often co-expressed with HIF-1 α . (A and C vs B and D). This was not, however, a feature when HIF-1 α was not expressed at the periphery of tumour cell aggregate (E vs F). Note, the localisation of HIF-1 α immunoreactivity is not uniform and varied between centre and periphery of tumour cell aggregates (B and F). Tumour (T). Objective magnification, x 20.

VEGFR2 vs HIF-1 α

Co-expressions were similar to those for GLUT1 and VEGF (Fig. 6.17).

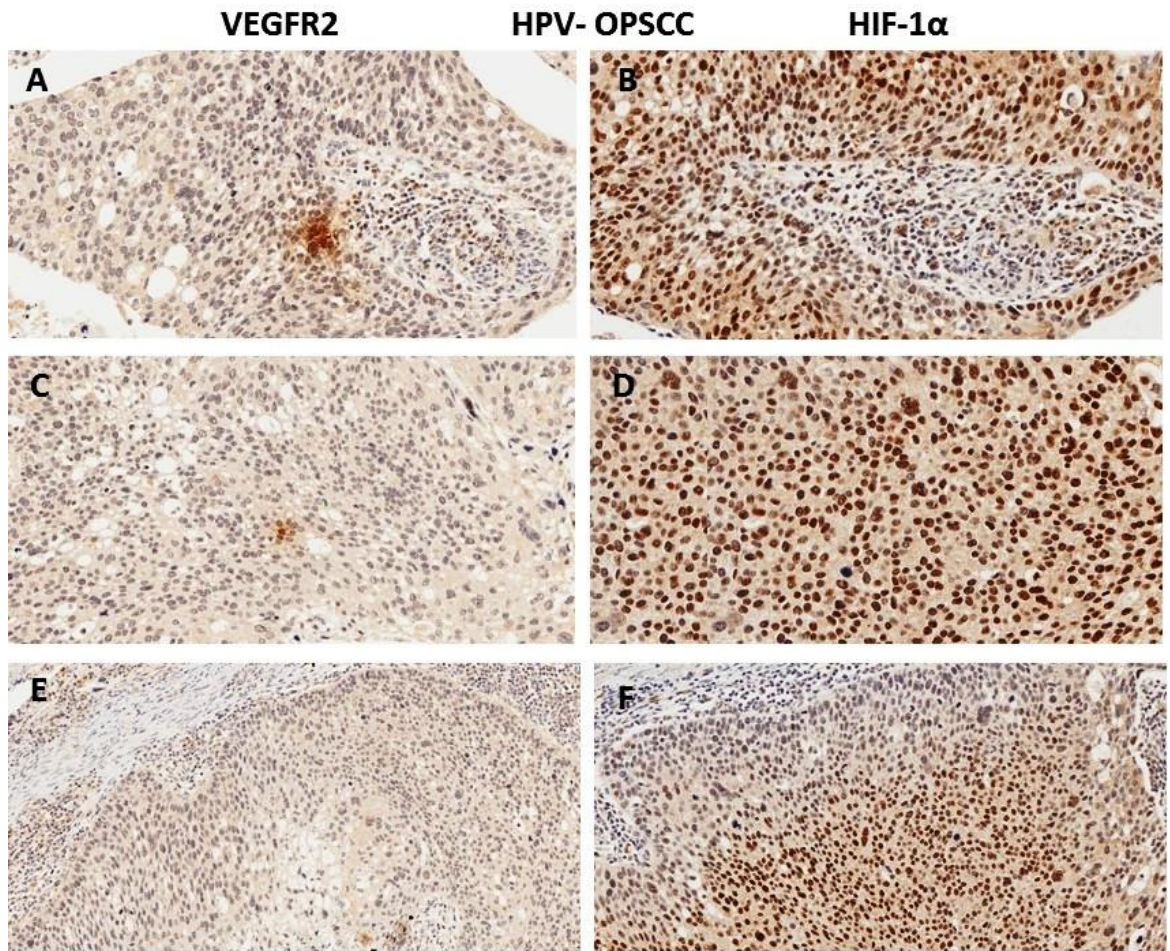


Figure 6.17. A typical example of co-expression of VEGFR2 and HIF-1 α in HPV-OPSCCs. Step sections from a HPV- OPSCCs tumour show diffuse expression of VEGFR2. VEGFR2 was often co-expressed with HIF-1 α . (A and C vs B and D). This was not, however, a feature when HIF-1 α was not expressed at the periphery of tumour cell aggregate (E vs F). Note, the localisation of HIF-1 α immunoreactivity is not uniform and varied between centre and periphery of tumour cell aggregates (B and F). Tumour (T). Objective magnification, x 20.

GLUT-1 vs TOMM20

In HPV- OPSCC, 4/10 (40%) tumours showed co-expression of GLUT-1 and TOMM20 in the cancer cells (Fig. 6.18, A and B); widespread lack of co-expression was seen in four (40%) tumours (Fig. 6.18, C and D); the remainder two (20%) tumours showed variable co-expression, particularly at the periphery of the cancer cell aggregates (Fig. 6.18E and F).

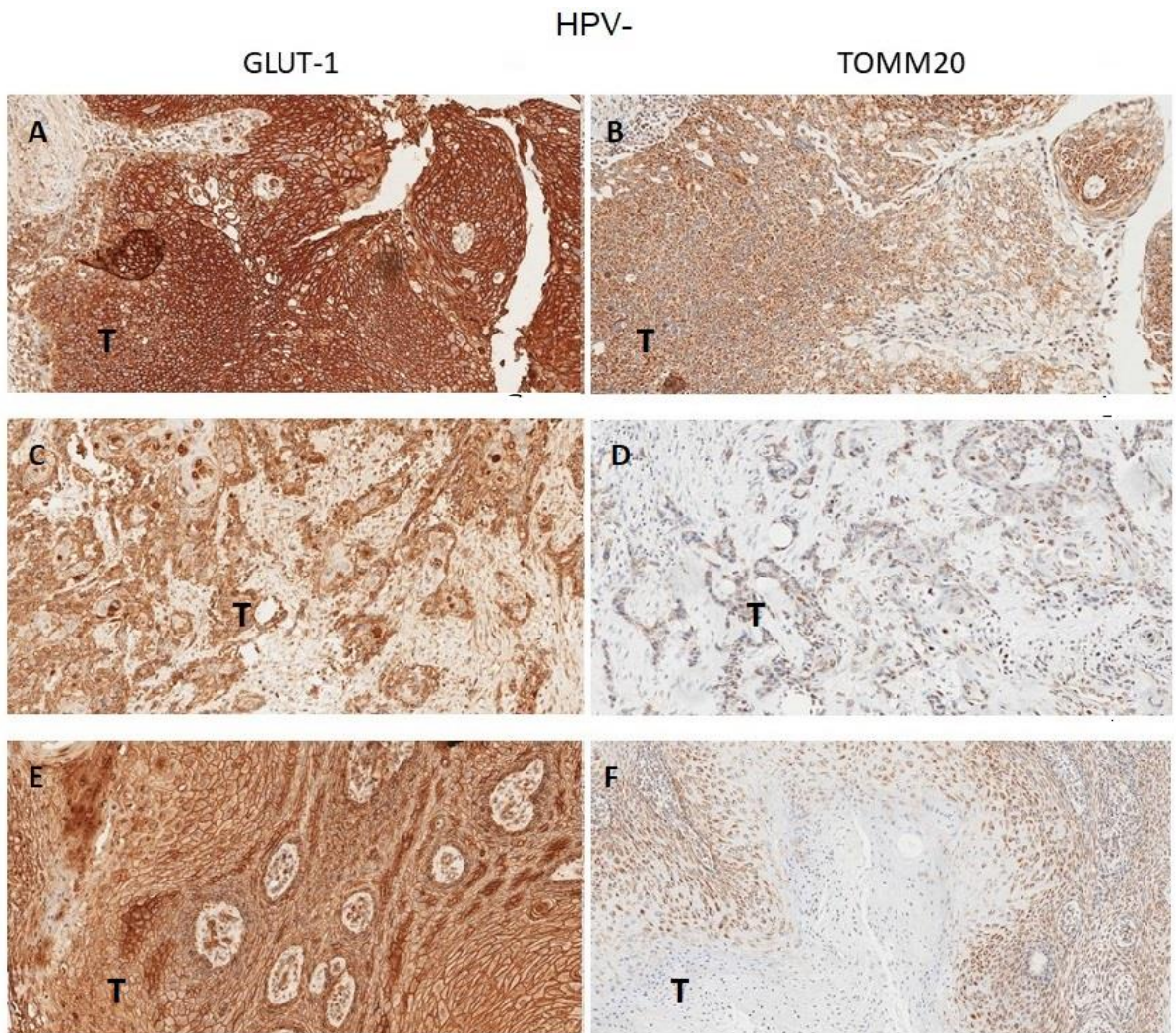


Figure 6.18. A typical example of co-expression of GLUT-1 and TOMM20 in HPV- OPSCCs.

Step sections of three of HPV- OPSCCs show Co-expression of GLUT-1 and TOMM20 in the cancer cells (A and B); widespread difference in immunostaining (C and D); co-expression at the periphery of cancer cell aggregates only i.e. absence of the co-expression in the centre (E and F). Tumour (T). Objective magnification, x 20.

As regards CAFs, these often expressed GLUT-1; immunostaining for TOMM20 was less conspicuous.

Summary table

Markers of co-expression	HPV+ OPSCC	HPV- OPSCC
MCT4 vs HIF-1 α	Different localisation of staining	Similar localisation of staining in 60% of tumours
GLUT1 vs HIF-1 α	Different localisation of staining	Similar localisation of staining
VEGF vs HIF-1 α	Different localisation of staining	Similar localisation of staining
VEGFR2 vs HIF-1 α	Different localisation of staining	Similar localisation of staining

Table 6.3. Summary table for co-expression of HIF-1 α vs MCT4, GLUT1, VEGFR and VEGFR2 in HPV+/HPV- OPSCC. Absence of correlation between HIF-1 α expression and expression of MCT4, GLUT1, VEGF and VEGFR2 in the HPV+ OPSCC whereas in HPV- OPSCC this correlation is largely present.

6.4 Discussion

Limitations

Obviously, the main limitation relates to the limited number of tumours (10 HPV+ and 10 HPV- OPSCC) studied with immunohistochemistry HIF1 α , GLUT1, VEGF and VEGFR2. This was due to availability of material. It prevented the use of advanced logistic regression analysis and thus nonparametric methods had to be used for statistical analysis. Although further study of associations discussed below is warranted, it is felt that the present investigation provides a useful starting point and best use of the available material was made. It should also be noted that all tumours examined in the present investigation were purely oropharyngeal.

General remarks

Hypoxia, a common feature of solid tumours, is believed to stimulate tumour invasiveness and metastasis [714]. HIF-1 α has received much attention as an intrinsic marker of hypoxia [715-720]. This molecule regulates responses to hypoxia in normal as well as cancer cells, and targets genes involved in metabolism, angiogenesis and metastasis, [721-724]. An association between overexpression of HIF-1 α and a good prognosis in cancer patients treated by surgery has been suggested [464, 725, 726]. In the particular setting of oropharyngeal cancer overexpression of HIF-1 α seems independently associated with improved loco-regional control, and disease-free and overall survival [464, 492]. Accordingly, a strong immunohistochemical staining for HIF-1 α may be a marker of good prognosis [464]. However, another study investigated 45 patients with HNSCC, treated by surgery alone, and reported no obvious link [727]. A borderline significant correlation ($p = 0.09$) has been reported in a cohort of 91 patients with cervical cancer who treated by radiotherapy [728]; a smaller cohort of 38 patients reported no significant correlation [729]. Tumours at different anatomical subsites show variable aetiologies, prognosis, and radio-sensitivity [730-732]; this confounds the interpretation of these investigations [464].

HIF-1 α and metabolic status

It has been suggested in Chapter 4 that HPV+ OPSCC more frequently expresses the MCT4+ phenotype, indicative of lactate release. Such release seems in keeping with anaerobic – hence, hypoxic cellular environment. This does not, however, seem consistent with the relatively infrequent HIF-1 α , a reliable hypoxia marker, expression in HPV+ OPSCC (4/10). Accordingly, caution should be exerted regarding the value MCT4 as a hypoxia marker. Alternatively, effecting a hypoxic environment may be a more complex process influenced by multiple factors and possibly poorly understood factors and explanations based on basic biochemistry may be oversimplified.

The level of MCT4 expression is found to be high in cells relying on glycolysis, and it has a significant function in lactate efflux from these cells, so it is acting typically as a lactate exporter [265]. The Reverse Warburg metabolism suggests the presence of metabolic compartmentalization in the tumour microenvironment where the less proliferative cancer cells express high levels of MCT4, whereas the highly proliferative cancer cells express less MCT4 [265]. Therefore, the described location of MCT4 expression is significant when taking into account its biological impact on a tumour and prediction of prognosis [265]. It has been demonstrated that MCT4 as a transporter of lactate has a differential expression in carcinoma cells, that is the level of MCT4 expression by cancer cells at the tumour's advancing front (leading edge) is different compared with its expression by stromal cells or by a deeper population of cancer cells (centre of the tumour as an example) [265]. The transport process, of molecules such as lactate, which takes place between the different metabolic compartments in a tumour, permits highly proliferative cancer cells to use OXPHOS, whereas CAFs and non-proliferative cancer cells provide metabolic fuels produced by glycolytic metabolism [265]. Therefore, the system of monocarboxylate transporters permits the interchange of metabolites between cells to fuel the multiple tumoral compartments. It is important to mention that stromal expression of MCT4 has been shown to be related to poor prognosis and decreased disease free survival in HNSCC [265, 733, 734].

HIF-1 α and transport of glucose

The findings suggest that the cancer cells in this sample of HPV+ and HPV- OPSCCs, are able to transport glucose to their interior and show variable mitochondrial load.

Possibly, the variable lack of TOMM20 in 6 HPV- tumours co-expression relates to the degree of keratinisation. Heavily keratinised cells as those 6.18 F are expected to show abundant tonofilaments- hence, decreased mitochondrial load. This would account for the inconspicuous TOMM20 immunoreactivity in those cells. On the one hand, the HPV+ cancer cells did not often express HIF-1 α (Fig. 6.1), which suggests that their glucose-based cytosolic metabolic pathways and mitochondria effect an oxygenated environment. On the other hand, the rather common expression of HIF-1 α in HPV- cancer cells (Fig. 6.5) suggests that cytosol and mitochondria therein are unable to effect an oxygenated environment. Possibly, the mitochondria in HPV- cells are somewhat dysfunctional.

The findings related to the HPV+ OPSCC accord with the absence of correlation between HIF-1 α and GLUT1 expression previously reported in laryngeal carcinomas treated with radiotherapy [724, 735]. The findings related to HPV- OPSCC appear to accord with the correlation between HIF-1 α and GLUT-1 expression reported by Wincewicz *et al* in CRC [723]. However, other authors failed to demonstrate this correlation in CRC [736]; and the immunolocalisation of HIF-1 α obtained by Wincewicz *et al* was cytoplasmic rather than nuclear [723]. Nevertheless, Wincewicz *et al* considered that the factor is still able to effect transcriptional activity in the nucleus [723]. They also noted that a HIF-1 α dependent induction of GLUT-1 is difficult to establish [723]; histopathological type, immunohistochemical technique, tumour stage, sampling and various transcriptional regulators are able to influence GLUT-1 expression [724, 737].

Based on our findings in HPV+ OPSCCs samples, we can conclude that the cancer cells are able to transport glucose to their interior and they did not often express HIF-1 α , which suggests that their glucose-based cytosolic metabolic pathways and mitochondria effect an oxygenated environment. The findings related to the HPV+ OPSCC accord with the absence of correlation between HIF-1 α and GLUT1 expression previously reported in the literature [724, 735]. A HIF-1 α dependent induction of GLUT-1 is not easy to establish [723]; and this is because of the multiple factors affecting the relation between the two variables [724, 737].

Given the effect of hypoxia on response to treatment, and association between expression of HIF-1 α and GLUT-1, it has been suggested that GLUT-1 is a potential

therapeutic target in strategies designed to inhibit the progression of laryngeal cancer [722, 724]. The present findings indicating co-expression of HIF-1 α and GLUT-1 in HPV- OPSCC, suggest that similar strategies for this clinically significant type of tumour are worthy of further exploration.

HIF-1 α and angiogenesis

HPV infection is associated with an improved prognosis in a subset of patients with HNSCC [505]; angiogenesis is a requisite for sustained cancer growth and metastasis [685]; and VEGF and VEGFRs are significant proangiogenic factors involved in most tumour types, including head and neck cancer [685, 686]. It is thus tempting to speculate that increased expression of VEGF and/or VEGFR2 in a tumour is an adverse prognosticator. This an oversimplification contradicted by the increased production of VEGF in HPV+ HNSCC cancer cells [703]. In addition, two previous immunohistochemical investigations showed no difference in VEGF expression between HPV+ and HPV- HNSCC [688, 704]. The findings of the present investigation support this and it may be inferred that expression of VEGF is not a useful prognosticator in HPV+ OPSCC.

In contrast, the findings of the present investigation suggest that VEGFR2 is expressed in the majority HPV+ OPSCC but is largely absent in HPV- tumours. Previous investigations reported the presence of VEGFR isoforms in HNSCC (40 to almost 90%) [695, 697, 698, 738-741], but they do not seem to agree with the present findings that HPV- OPSCCs are largely lacking VEGFR2 expression. The previous investigations were not limited to strictly OPSCC, being combined cohorts of HNSCC from different anatomical subsites; and VEGFR expression is higher in OSCC compared with HNSCC of other origin [697, 698]. There are very limited data about expression of VEGFR in OPSCC [699].

The co-expression of VEGF and VEGFR2 in the same cell likely reflects an autocrine function of the former [695, 701, 742]. Accordingly, the findings of the present investigation suggest that this function is compromised in HPV- OPSCC.

There are promising results from VEGFR inhibition in various neoplasms [743], and such inhibitors have been added to chemotherapy regimens in HNSCC with some success [695, 744]. For example, Bevacizumab, a monoclonal antibody against VEGFR, is in clinical practice in metastatic colorectal and breast cancer, NSCLC,

glioblastoma and renal cell carcinoma [745-747]; and phase II studies in HNSCC used it in combination with pemetrexed, erlotinib or cetuximab to produce response rates of 15–30% [748-750].

Summary of the findings

- 1- Absence of correlation between HIF-1 α and GLUT1 expression in the HPV+ OPSCC whereas the findings related to HPV- OPSCC showed presence of this correlation.
- 2- VEGFR2 is expressed in the majority HPV+ OPSCC but is largely absent in HPV- tumours.

Conclusions

Despite limitations, the present investigation suggests additional differences of interest between HPV+ and HPV- OPSCC. Lactate release more common in HPV+ tumours, has been discussed in Chapter 4. Here, attention is drawn to features in HPV- tumours, which possibly include increased expression of hypoxia inducible factors, cytosol and dysfunctional mitochondria effecting a hypoxic environment and compromised autocrine function. These features seem in keeping with the more complex genetics and worse prognosis of HPV- OPSCC, and worthy of further pursuit. The value of MCT4 as a hypoxia marker should be reviewed with caution.

Chapter 7

Discussion

7.1 Introduction

The experiments described in this thesis were designed primarily to investigate the possible roles of desmoplasia and metabolic proteins in the pathogenesis of OPSCC. Particular interest has been channelled at the HPV infection. Expression of desmoplasia and metabolic proteins was investigated in two cohorts of OPSCC tissues using histological, histochemical and immunohistochemical investigations (on TMAs as well as full sections), followed by correlation with clinicopathological features including recurrence and survival. The results obtained led to in vitro cell line work in which epithelial cancer cells were co-cultured with fibroblasts, to determine possible changes in functional characteristics such as metabolic activities as a result of interaction between the two cell lines. Western blotting and immunofluorescence techniques were used to investigate these functional studies.

This chapter will summarise the observations made, and discuss, limitations, challenges and future experiments aimed at better understanding of the role of stroma and metabolism in oropharyngeal cancer.

7.2 Summary of findings

- a) Histologically, more invasion has been seen in HPV+ OPSCC, when was more desmoplasia present, suggesting that the HPV infection could affect the relation between desmoplasia and depth of invasion.
- b) Presence of GAGs more often at the tumour front HPV+ OPSCCs suggests that the invasion process is probably driven more by GAGs rather than myofibroblasts.
- c) In contrast to published data from OSCC [169], presence of CAFs was observed at the tumour core as well as the front of OPSCCs.
- d) Presence of desmoplasia is not a suitable marker for survival in HPV+ OPSCC.

- e) Markers involved in the reverse Warburg metabolism (MCT1 and MCT4) are expressed in both HPV+ and HPV- OPSCC but does not coincide with the presence of myofibroblasts.
- f) 15% of HPV+ tumours demonstrating additional metabolic compartments. 85% of co-express MCT1 and MCT4.
- g) 50% of HPV- OPSCCs demonstrated co-expression of MCT1 and MCT4.(50% of tumours demonstrating additional metabolic compartments).
- h) These results suggest that three compartment tumour metabolism model is HPV dependant rather than site dependent based on OPSCC.
- i) Presence of desmoplasia and MCT4 expression are not suitable markers for survival in HPV+ OPSCC.
- j) The three compartment model is more compatible with data from HPV- OPSCC.
- k) Based on tissue data and preliminary functional data, there may be some differences in metabolism in HPV+ and HPV- tumours.

7.3 MCT4 expression in head in neck SCC

MCT4 is a marker of multiple events e.g. glycolysis, lactate and ketone body production and oxidative stress [1]. Recently, a ‘three compartment tumour metabolism’ model has been proposed in head and neck cancer[1, 625] comprising a highly proliferative cancer cell population expressing MCT1 at the tumour front, a deeper population of MCT4+ cancer cells and MCT4+ CAFs. These latter two populations serve as a source of metabolic fuels via a lactate shuttle which drives cancer cell proliferation and invasion.

Data from IHC staining of a TMAs containing cores for 109 HPV+ and HPV- OPSCC demonstrates variation in levels of MCT4 expression across the two tissue types, with some specimens from HPV- not expressing in their stroma at the tumour core as well as advancing front and others showing strong protein expression in the same locations. Markers associated with the reverse Warburg metabolism are expressed in both HPV+ and HPV- OPSCC. The three compartment model is more compatible with data from HPV- OPSCC. Differences in the stromal compartment are also observed between HPV+ and HPV- tumours.

To investigate these observations, I undertook my functional experiment in which the epithelial cancer cells with different HPV status co-cultured with fibroblasts.

Neither of the two fibroblasts cell lines were induced to express MCT4 by either of the two cancer cells. Based on tissue data (tissue data much stronger because it is much bigger cohort) and preliminary functional data, there may be some differences in metabolism in HPV+ and HPV- tumours.

7.4 Increased expression of MCT4 and its effect

HNSCCs frequently have well differentiated epithelial and stromal cell compartments that have high MCT4 staining with low OXPHOS, high glycolysis and lactate release out of cells and levels of oxidative stress.

In one study of HNSCC tumours, and typically, it was shown that a large glycolytic carcinoma cell compartment as measured by MCT4 expression and are associated with a statistically significantly decrease in DFS. It may be that these tumours are more aggressive, because they generate oxidative stress, lactate and ketone bodies to fuel mitochondrial metabolism (OXPHOS) in adjacent proliferating epithelial cancer cells a large glycolytic carcinoma compartment with MCT4 expression is associated with shorter disease-free survival in OSCC and is functionally associated with high 18FDG-PET SUV.

I was able to demonstrate increased MCT4 expressions in oropharyngeal cancer, using archival tissues, though the increased expression of MCT4 did not necessarily correspond with poor outcome. Most of cases included in our study are still alive and are being followed up, mean high MCT4 expression does not correlate with poor prognosis and death. However, Strong statistical difference has been found between the survival data of HPV+ and HPV- OPSCC ($P = 0.001$). Percentage of people who are still alive is higher in HPV+ 65% (24/37) than HPV- 43% (16/37) as shown in Table 3.8.

7.5 Clinical implications

Presence of GAGs more often at the tumour front of HPV+ OPSCCs could function as a universal marker for aggressive tumours.

Our findings can be a centre of attention from a therapeutic point of view and could result in MCT1 becoming the object of investigation for metabolic anticancer therapies. Using inhibitors that can inhibit lactate uptake and decrease the amount of mitochondrial fuel to proliferative cancer cells, the OXPHOS and ATP production required for cell division and tumour growth could be diminished. Alternatively, achieving a stage of energy uncoupling between the anabolic carcinoma cells with high proliferation rate and the catabolic epithelial cancer and stromal cells with less proliferation rate, could stop mitochondrial fuel feeding to the highly proliferative cancer cells, rendering them dependant on glycolysis as their main source of ATP production [467, 629]

The anticancer α -cyano-4-hydroxycinnamate, is a powerful MCT1 inhibitor that has an antineoplastic effects in vitro, as well as in vivo, with marginal toxicity [262, 630]. In vivo investigations in mice displayed that α -cyano-4-hydroxycinnamate considerably diminished tumour load [262]. A recent study undertaken by Amorim and his group demonstrated the various effects of inhibiting lactate transport system on cell lines from human CRC by means of different reagents known to have the ability of inhibiting lactate transport, such as α -cyano-4-hydroxycinnamate, DIDS (a stilbene derivative), and quercetin, a bioflavonoid. This study also revealed that in a dose-dependent manner, the inhibition of mono-carboxylate transport activity has the capability of preventing CRC cells biomass, reducing proliferation and augmenting their death. Furthermore, their results showed that pre-treatment of CRC cells with the mono-carboxylate transport inhibitors heighten the cytotoxicity of 5-fluorouracil [265, 631]. Nevertheless, MCT inhibitors are potent compounds, characterised by a lack of specificity and their use as inhibitors for lactate transport through plasma membrane extend to inhibit other functional activities inside the cell.

The 7-aminocarboxycoumarin (7ACC) was able to inhibit the influx of lactate, but not its efflux in cells with MCT1 and MCT4 expression with reduction in xenograft tumour growth. AR-C155858 is another anticancer drug that has been reported to be an efficient inhibitor in cancer of the prostate, by means of inhibiting MCTs (MCT1 and MCT2). Also, AR-C155858 has the ability to significantly decrease proliferation of cancer cells, increasing their apoptosis within tumour tissues from mice without substantial cytotoxicity on non-malignant tissues [265, 633]. At present, a new oral inhibitor for MCT1 and MCT2 (a second generation) called AZD-3965, is going

through first phase clinical trials and could show a therapeutic effect against solid tumours in their advanced stage, in particular PCa, gastric cancer, and diffuse large B cell lymphoma, and could be used as anticancer drug in HNSCC [265, 634].

Metformin is one of the biguanides, and is known to act as an inhibitor for mitochondrial OXPHOS. Its action is attributed to its numerous cross reactivity with the system of lactate transport as OXPHOS inhibitors. It is efficient at prevention as well as therapy of HNSCC in both *vitro* and *vivo* [262]. Due to their synergistic effect against cancer, in cases of combined treatment with MCT1, MCT4, or CD147 inhibitors, these biguanides recently became the focal point in anticancer therapy [265, 635-637]. Now, there are numerous clinical trials assessing the influence of metformin against cancer development, particularly its ability to interfere with the metabolic coupling that takes place between stromal and epithelial cancer cells in HNSCC [265].

In advanced solid tumours, including head and neck cancers, hypoxia is regarded as a key feature associated with an adverse influence on prognosis [321, 638, 639].

7.6 Limitations

Obviously, the main limitation relates to the limited number of tumours (10 HPV+ and 10 HPV- OPSCC) studied with immunohistochemistry HIF1 α , GLUT1, VEGF and VEGFR2. This was due to availability of material. It prevented the use of advanced logistic regression analysis and thus non-parametric methods had to be used for statistical analysis. Another important point is the limited number of cell lines and also the limited ability of the two dimensional plastic model used in our functional studies. Although further studies concerning these proteins and their association with each other and also with clinico-pathological variables in the two categories of OPSCC are warranted, it is felt that the present investigation provides a useful starting point and best use of the available material was made. It should also be noted that all tumours examined in the present investigation were purely oropharyngeal.

7.7 Future experiments

Our current data has shown that MCT1 is upregulated in HPV- epithelial cancer cells when co-cultured with fibroblasts originating from HPV- tumours. Moving forward, it is important to carry out several repeats of some of the experiments in this functional study by way of validating the results obtained. There is the need to enlarge the cohort

of cell lines used in the study involving both HPV- and HPV+ epithelial cancer cells, as well as fibroblasts from different HPV status for possible positive results for MCT1 and more specific results for MCT4. More assays, particularly 3D assays, and co-culture with fibroblasts are required for migration and proliferation work to make them more objective. The full sections and TMA part needs further close studies for more specific results about the intracellular distribution of MCT1 and MCT4, to aid understanding of intracellular localisation of both proteins.

7.7.1 Tissue experiments

Further optimisation of tissue experiments by means of IHC is required. Emphasis will be towards being able to correctly detect MCT1 and MCT4 proteins. Very key will be the use of highly specific primary antibodies. Antibodies specific enough to select between the two forms proteins (mature and immature) when used for IHC on the TMA cores as well as full sections. As earlier highlighted, it is expected that the mature form of MCT1 and MCT4 will be localised to the cell membrane, while the immature pool remains cytoplasm localised. But again, this may not always be distinctly the case, as the mature form which obtains its maturation in the Golgi apparatus and get trafficked to the cell membrane may also be spotted in some amount in the cytoplasm before it makes its way to the cell membrane. Two sets of identical TMAs or/and full sections, separately stained with highly selective MCT1 and MCT4 antibodies for the two forms should show different staining patterns to differentiate the two scenarios. Success will greatly depend on the quality of the antibody utilised, specific enough for the correct isoform, and able to detect the rather relatively minutely expression. Also, to make analysis as objective as possible, all samples may be collected from tissues within a very short interval, assembled and analysed for IHC the same day with similar conditions.

A large enough sample size means that there might be the possibility of assessing expression in tissues from a particular tumour site and have data that will be statistically relevant. For instance, if the entire samples size is in the range of 300, there might be about 100 base of tongue tumour samples, in which case expression among base of tongue tissues may be effectively compared. And this will ensure correlation with clinicopathological data is more direct as comparison will be made against expression protein from tissues taken from the same sub-site. This is important, giving that evidence has already shown that tissues express MCT1 and MCT4 proteins

in varying amounts, and that some tissues may not express the protein. For instance, tissues from tonsil may show different levels of MCT1 and MCT4 expression. This is because, role of MCT1 and MCT4 may vary from cell to cell, as well as, the pathogenesis or molecular basis of the same SCC may vary from site to site in head and neck region. If therefore tissues from the same site, such as soft palate are analysed together and compared against clinicopathological data, there is that sense that the baseline expression of the protein in soft palate tissues are similar ab initio and prior to carcinogenesis. This may be verified to a large extent by the use of the expressing levels in the accompanying paired normal tissues

7.7.2 Western blot experiments

Further optimisation of the Western blot experiments is required. Emphasis will be towards being able to precisely detect MCT1 and MCT4. Firstly, it will be important to employ cell lines obtained from tumours similar to those ones used for IHC. This way, a close correlation between both should be expected and serve as a means of validation of results on both sides (western blot and use of TMA). Also, very key will be the use of highly specific primary antibodies. Antibodies specific enough to select between the two forms of MCT1 and MCT4 (mature and immature) when used for the Western blot.

7.7.3 Expanding experiment with cell lines.

Our results, based on two cancer cell lines and two fibroblasts with different HPV status produced results that need to be further verified as the case, in two or three additional cell lines. Recruiting in similar fashion, one with a significant level of baseline expression of MCT1 and MCT4, one with a moderate expression level, and a non-cancer cell line with any level of MCT1 and MCT4 expression. Probing for more partners will also open a window into understanding mechanism by which MCT1 and MCT4 are involved with tumorigenesis. The use of a powerful anti-oxidants such as N-acetyl-cysteine to show effect of oxidative stress (pseudo-hypoxia), induced by the cancer cells, on upregulation of MCT4 expression in adjacent CAFs.

7.7.4 Migration and proliferation assays, and other functional studies.

Given that some interesting and notable findings have come out of the migration assay of our experiment, it will be important to expand the scope by conducting additional functional assays such as adhesion assay and migration through a membrane or barrier. Examples include transmembrane assays[751] and migration through 3D matrigel [752] to depict invasion through basement membranes by OPSCC cells. The migration assay may also be improved upon by enlisting a 3D version. This way, cell migration is multidirectional as the case is *in vivo*, therefore a more representative approach. Co-culture of the various cell strains with fibroblast will also come as an additional method to evaluate cell growth and migration.

A proposed cell proliferation assay will involve, seeding of cells to achieve discrete colonies of about the same number of cells with each cell variant. That way, a regular count will define a precise rate of growth of cells.

References

1. Curry, J.M., et al., *Cancer metabolism, stemness and tumor recurrence: MCT1 and MCT4 are functional biomarkers of metabolic symbiosis in head and neck cancer*. *Cell Cycle*, 2013. **12**(9): p. 1371-84.
2. Foulds, L., *The experimental study of tumor progression: a review*. *Cancer Res*, 1954. **14**(5): p. 327-39.
3. Hanahan, D. and R.A. Weinberg, *Hallmarks of cancer: the next generation*. *Cell*, 2011. **144**(5): p. 646-74.
4. Muinao, T., H.P. Deka Boruah, and M. Pal, *Diagnostic and Prognostic Biomarkers in ovarian cancer and the potential roles of cancer stem cells - An updated review*. *Exp Cell Res*, 2018. **362**(1): p. 1-10.
5. Kliewer, A., R.K. Reinscheid, and S. Schulz, *Emerging Paradigms of G Protein-Coupled Receptor Dephosphorylation*. *Trends Pharmacol Sci*, 2017. **38**(7): p. 621-636.
6. Roggiani, F., et al., *Guidance of Signaling Activations by Cadherins and Integrins in Epithelial Ovarian Cancer Cells*. *Int J Mol Sci*, 2016. **17**(9).
7. Multhaupt, H.A., et al., *Extracellular matrix component signaling in cancer*. *Adv Drug Deliv Rev*, 2016. **97**: p. 28-40.
8. Zhang, Q., et al., *Soluble production and function of vascular endothelial growth factor/basic fibroblast growth factor complex peptide*. *Biotechnol Prog*, 2015. **31**(1): p. 194-203.
9. Fouad, Y.A. and C. Aanei, *Revisiting the hallmarks of cancer*. *Am J Cancer Res*, 2017. **7**(5): p. 1016-1036.
10. Gradilla, A.C., et al., *From top to bottom: Cell polarity in Hedgehog and Wnt trafficking*. *BMC Biol*, 2018. **16**(1): p. 37.
11. Martinelli, E., et al., *Cancer resistance to therapies against the EGFR-RAS-RAF pathway: The role of MEK*. *Cancer Treat Rev*, 2017. **53**: p. 61-69.
12. Thomas, R. and M.H. Kim, *A HIF-1alpha-dependent autocrine feedback loop promotes survival of serum-deprived prostate cancer cells*. *Prostate*, 2009. **69**(3): p. 263-75.
13. Dreesen, O. and A.H. Brivanlou, *Signaling pathways in cancer and embryonic stem cells*. *Stem Cell Rev*, 2007. **3**(1): p. 7-17.
14. Vereb, G., et al., *Biphasic calcium response of platelet-derived growth factor stimulated glioblastoma cells is a function of cell confluence*. *Cytometry A*, 2005. **67**(2): p. 172-9.
15. Nickerson, N.K., et al., *Decreased autocrine EGFR signaling in metastatic breast cancer cells inhibits tumor growth in bone and mammary fat pad*. *PLoS One*, 2012. **7**(1): p. e30255.
16. Sjostrom, S., et al., *Genetic variations in EGF and EGFR and glioblastoma outcome*. *Neuro Oncol*, 2010. **12**(8): p. 815-21.
17. Slamon, D.J., et al., *Human breast cancer: correlation of relapse and survival with amplification of the HER-2/neu oncogene*. *Science*, 1987. **235**(4785): p. 177-82.
18. Nicholson, R.I., J.M. Gee, and M.E. Harper, *EGFR and cancer prognosis*. *Eur J Cancer*, 2001. **37 Suppl 4**: p. S9-15.
19. Forbes, S.A., et al., *COSMIC: mining complete cancer genomes in the Catalogue of Somatic Mutations in Cancer*. *Nucleic Acids Res*, 2011. **39**(Database issue): p. D945-50.

20. Evan, G.I. and K.H. Vousden, *Proliferation, cell cycle and apoptosis in cancer*. Nature, 2001. **411**(6835): p. 342-8.
21. Amin, A., et al., *Evasion of anti-growth signaling: A key step in tumorigenesis and potential target for treatment and prophylaxis by natural compounds*. Semin Cancer Biol, 2015. **35 Suppl**: p. S55-s77.
22. Kastan, M.B. and J. Bartek, *Cell-cycle checkpoints and cancer*. Nature, 2004. **432**(7015): p. 316-23.
23. Weinberg, R.A., *The retinoblastoma protein and cell cycle control*. Cell, 1995. **81**(3): p. 323-30.
24. Cobrinik, D., *Pocket proteins and cell cycle control*. Oncogene, 2005. **24**(17): p. 2796-809.
25. Wrzesinski, S.H., Y.Y. Wan, and R.A. Flavell, *Transforming growth factor-beta and the immune response: implications for anticancer therapy*. Clin Cancer Res, 2007. **13**(18 Pt 1): p. 5262-70.
26. Govinden, R. and K.D. Bhoola, *Genealogy, expression, and cellular function of transforming growth factor-beta*. Pharmacol Ther, 2003. **98**(2): p. 257-65.
27. Wong, R.S., *Apoptosis in cancer: from pathogenesis to treatment*. J Exp Clin Cancer Res, 2011. **30**: p. 87.
28. Novaleski, C.K., et al., *Apoptosis and Vocal Fold Disease: Clinically Relevant Implications of Epithelial Cell Death*. J Speech Lang Hear Res, 2017. **60**(5): p. 1264-1272.
29. Wu, H.J., et al., *The molecular mechanisms between autophagy and apoptosis: potential role in central nervous system disorders*. Cell Mol Neurobiol, 2015. **35**(1): p. 85-99.
30. Elmore, S., *Apoptosis: a review of programmed cell death*. Toxicol Pathol, 2007. **35**(4): p. 495-516.
31. McIlwain, D.R., T. Berger, and T.W. Mak, *Caspase functions in cell death and disease*. Cold Spring Harb Perspect Biol, 2015. **7**(4).
32. Laurence Cole, P.R.K., *Apoptosis*. 2016.
33. Ishizaki, Y., et al., *Programmed cell death by default in embryonic cells, fibroblasts, and cancer cells*. Mol Biol Cell, 1995. **6**(11): p. 1443-58.
34. Giancotti, F.G. and E. Ruoslahti, *Integrin signaling*. Science, 1999. **285**(5430): p. 1028-32.
35. Wang, H., et al., *Elevated circulating PAI-1 levels are related to lung function decline, systemic inflammation, and small airway obstruction in chronic obstructive pulmonary disease*. Int J Chron Obstruct Pulmon Dis, 2016. **11**: p. 2369-2376.
36. Scorrano, L. and S.J. Korsmeyer, *Mechanisms of cytochrome c release by proapoptotic BCL-2 family members*. Biochem Biophys Res Commun, 2003. **304**(3): p. 437-44.
37. Lopez, J. and S.W. Tait, *Mitochondrial apoptosis: killing cancer using the enemy within*. Br J Cancer, 2015. **112**(6): p. 957-62.
38. Green, D.R. and G.I. Evan, *A matter of life and death*. Cancer Cell, 2002. **1**(1): p. 19-30.
39. Powell, E., D. Piwnica-Worms, and H. Piwnica-Worms, *Contribution of p53 to metastasis*. Cancer Discov, 2014. **4**(4): p. 405-14.
40. Stockley, T.L., et al., *Molecular profiling of advanced solid tumors and patient outcomes with genotype-matched clinical trials: the Princess Margaret IMPACT/COMPACT trial*. Genome Med, 2016. **8**(1): p. 109.
41. Gottwein, E. and B.R. Cullen, *A human herpesvirus microRNA inhibits p21 expression and attenuates p21-mediated cell cycle arrest*. J Virol, 2010. **84**(10): p. 5229-37.

42. Tornesello, M.L., et al., *MDM2 and CDKN1A gene polymorphisms and risk of Kaposi's sarcoma in African and Caucasian patients*. *Biomarkers*, 2011. **16**(1): p. 42-50.
43. Azer, S.A., *MDM2-p53 Interactions in Human Hepatocellular Carcinoma: What Is the Role of Nutlins and New Therapeutic Options?* *J Clin Med*, 2018. **7**(4).
44. Fernald, K. and M. Kurokawa, *Evading apoptosis in cancer*. *Trends Cell Biol*, 2013. **23**(12): p. 620-33.
45. Pitti, R.M., et al., *Genomic amplification of a decoy receptor for Fas ligand in lung and colon cancer*. *Nature*, 1998. **396**(6712): p. 699-703.
46. Li, Y., et al., *Fas-mediated apoptosis is dependent on wild-type p53 status in human cancer cells expressing a temperature-sensitive p53 mutant alanine-143*. *Cancer Res*, 2003. **63**(7): p. 1527-33.
47. Owen-Schaub, L.B., et al., *Wild-type human p53 and a temperature-sensitive mutant induce Fas/APO-1 expression*. *Mol Cell Biol*, 1995. **15**(6): p. 3032-40.
48. Mishra, A.P., et al., *Programmed Cell Death, from a Cancer Perspective: An Overview*. *Mol Diagn Ther*, 2018. **22**(3): p. 281-295.
49. Effros, R.B., *Impact of the Hayflick Limit on T cell responses to infection: lessons from aging and HIV disease*. *Mech Ageing Dev*, 2004. **125**(2): p. 103-6.
50. Campisi, J. and L. Robert, *Cell senescence: role in aging and age-related diseases*. *Interdiscip Top Gerontol*, 2014. **39**: p. 45-61.
51. Blagoev, K.B., *Cell proliferation in the presence of telomerase*. *PLoS One*, 2009. **4**(2): p. e4622.
52. Wynford-Thomas, D., *Cellular senescence and cancer*. *J Pathol*, 1999. **187**(1): p. 100-11.
53. Hayflick, L., *Mortality and immortality at the cellular level. A review*. *Biochemistry (Mosc)*, 1997. **62**(11): p. 1180-90.
54. Wegwitz, F., et al., *Tumorigenic WAP-T mouse mammary carcinoma cells: a model for a self-reproducing homeostatic cancer cell system*. *PLoS One*, 2010. **5**(8): p. e12103.
55. Counter, C.M., et al., *Telomere shortening associated with chromosome instability is arrested in immortal cells which express telomerase activity*. *Embo j*, 1992. **11**(5): p. 1921-9.
56. Klement, K. and A.A. Goodarzi, *DNA double strand break responses and chromatin alterations within the aging cell*. *Exp Cell Res*, 2014. **329**(1): p. 42-52.
57. Jafri, M.A., et al., *Roles of telomeres and telomerase in cancer, and advances in telomerase-targeted therapies*. *Genome Med*, 2016. **8**(1): p. 69.
58. Wang, Z., et al., *Broad targeting of angiogenesis for cancer prevention and therapy*. *Semin Cancer Biol*, 2015. **35 Suppl**: p. S224-s243.
59. Cao, Y., et al., *Forty-year journey of angiogenesis translational research*. *Sci Transl Med*, 2011. **3**(114): p. 114rv3.
60. Guo, H.F. and C.W. Vander Kooi, *Neuropilin Functions as an Essential Cell Surface Receptor*. *J Biol Chem*, 2015. **290**(49): p. 29120-6.
61. Hanahan, D. and J. Folkman, *Patterns and emerging mechanisms of the angiogenic switch during tumorigenesis*. *Cell*, 1996. **86**(3): p. 353-64.
62. Risau, W., *Mechanisms of angiogenesis*. *Nature*, 1997. **386**(6626): p. 671-4.
63. Ferrara, N., *VEGF and the quest for tumour angiogenesis factors*. *Nat Rev Cancer*, 2002. **2**(10): p. 795-803.
64. Bull, H.A., P.M. Brickell, and P.M. Dowd, *Src-related protein tyrosine kinases are physically associated with the surface antigen CD36 in human dermal microvascular endothelial cells*. *FEBS Lett*, 1994. **351**(1): p. 41-4.

65. Wu M, W.L., Chou C., *The anticancer potential of thrombospondin-1 by inhibiting angiogenesis and stroma reaction during cervical carcinogenesis*. Gynecology and Minimally Invasive Therapy., 2016. **2016;5(2)**: p. 48-53.
66. Zhang, X. and J. Lawler, *Thrombospondin-based antiangiogenic therapy*. Microvasc Res, 2007. **74(2-3)**: p. 90-9.
67. Santagiuliana, R.F., M.; Schrefler, B. A. , *Simulation of angiogenesis in a multiphase tumor growth model*. Computer Methods in Applied Mechanics and Engineering, 2016. **Vol. 304, 01.06.2016**, : p. 197-216.
68. Ribatti, D. and E. Crivellato, *Mast cells, angiogenesis, and tumour growth*. Biochim Biophys Acta, 2012. **1822(1)**: p. 2-8.
69. Coghlin, C. and G.I. Murray, *Current and emerging concepts in tumour metastasis*. J Pathol, 2010. **222(1)**: p. 1-15.
70. Podsypanina, K., et al., *Seeding and propagation of untransformed mouse mammary cells in the lung*. Science, 2008. **321(5897)**: p. 1841-4.
71. Stefanatos, R.K. and M. Vidal, *Tumor invasion and metastasis in Drosophila: a bold past, a bright future*. J Genet Genomics, 2011. **38(10)**: p. 431-8.
72. Das, S. and S.K. Batra, *Pancreatic cancer metastasis: are we being pre-EMT'ed?* Curr Pharm Des, 2015. **21(10)**: p. 1249-55.
73. Clark, A.G. and D.M. Vignjevic, *Modes of cancer cell invasion and the role of the microenvironment*. Curr Opin Cell Biol, 2015. **36**: p. 13-22.
74. Fidler, I.J. and G. Poste, *The "seed and soil" hypothesis revisited*. Lancet Oncol, 2008. **9(8)**: p. 808.
75. Wells, A., et al., *Targeting tumor cell motility as a strategy against invasion and metastasis*. Trends Pharmacol Sci, 2013. **34(5)**: p. 283-9.
76. van Zijl, F., G. Krupitza, and W. Mikulits, *Initial steps of metastasis: cell invasion and endothelial transmigration*. Mutat Res, 2011. **728(1-2)**: p. 23-34.
77. Kotwall, C., et al., *Metastatic patterns in squamous cell cancer of the head and neck*. Am J Surg, 1987. **154(4)**: p. 439-42.
78. Jimenez, L., et al., *Mechanisms of Invasion in Head and Neck Cancer*. Arch Pathol Lab Med, 2015. **139(11)**: p. 1334-48.
79. Takes, R.P., et al., *Distant metastases from head and neck squamous cell carcinoma. Part I. Basic aspects*. Oral Oncol, 2012. **48(9)**: p. 775-9.
80. de Bree, R., et al., *Intracranial metastases in patients with squamous cell carcinoma of the head and neck*. Otolaryngol Head Neck Surg, 2001. **124(2)**: p. 217-21.
81. Chen, L., et al., *Grading of MRI-detected skull-base invasion in nasopharyngeal carcinoma and its prognostic value*. Head Neck, 2011. **33(9)**: p. 1309-14.
82. Gouliamos, A.D., et al., *MRI of nasopharyngeal carcinoma metastatic to the cerebellopontine angle*. Neuroradiology, 1996. **38(4)**: p. 375-7.
83. Boerman, R.H., et al., *Trigeminal neuropathy secondary to perineural invasion of head and neck carcinomas*. Neurology, 1999. **53(1)**: p. 213-6.
84. Djalilian, H.R., et al., *Metastatic head and neck squamous cell carcinoma to the brain*. Auris Nasus Larynx, 2002. **29(1)**: p. 47-54.
85. Majoie, C.B., et al., *Trigeminal neuropathy: evaluation with MR imaging*. Radiographics, 1995. **15(4)**: p. 795-811.
86. Nguyen, D.X. and J. Massague, *Genetic determinants of cancer metastasis*. Nat Rev Genet, 2007. **8(5)**: p. 341-52.
87. Langley, R.R. and I.J. Fidler, *The seed and soil hypothesis revisited--the role of tumor-stroma interactions in metastasis to different organs*. Int J Cancer, 2011. **128(11)**: p. 2527-35.

88. Aplin, A.E., et al., *Signal transduction and signal modulation by cell adhesion receptors: the role of integrins, cadherins, immunoglobulin-cell adhesion molecules, and selectins*. *Pharmacol Rev*, 1998. **50**(2): p. 197-263.
89. Kim, Y.N., et al., *Anoikis resistance: an essential prerequisite for tumor metastasis*. *Int J Cell Biol*, 2012. **2012**: p. 306879.
90. Zhong, X. and F.J. Rescorla, *Cell surface adhesion molecules and adhesion-initiated signaling: understanding of anoikis resistance mechanisms and therapeutic opportunities*. *Cell Signal*, 2012. **24**(2): p. 393-401.
91. Sun, Y. and L. Ma, *The emerging molecular machinery and therapeutic targets of metastasis*. *Trends in pharmacological sciences*, 2015. **36**(6): p. 349-359.
92. Gill, K.S., et al., *Glycolysis inhibition as a cancer treatment and its role in an anti-tumour immune response*. *Biochim Biophys Acta*, 2016. **1866**(1): p. 87-105.
93. Zheng, J., *Energy metabolism of cancer: Glycolysis versus oxidative phosphorylation (Review)*. *Oncol Lett*, 2012. **4**(6): p. 1151-1157.
94. Adeva-Andany, M., et al., *Comprehensive review on lactate metabolism in human health*. *Mitochondrion*, 2014. **17**: p. 76-100.
95. Milosevic, M., et al., *The human tumor microenvironment: invasive (needle) measurement of oxygen and interstitial fluid pressure*. *Semin Radiat Oncol*, 2004. **14**(3): p. 249-58.
96. BoJiang, *Aerobic glycolysis and high level of lactate in cancer metabolism and microenvironment*. *Genes & Diseases*, 2017. **4**(1): p. 25-27.
97. Otto Warburg, K.W.I.f.B., Berlin-Dahlem, *The metabolism of tumours: Investigations from the kaiser wilhelm institute for biology, berlin-dahlem*. *BJS*, 1931. **Volume19**(73): p. Pages 168.
98. Jones, R.G. and C.B. Thompson, *Tumor suppressors and cell metabolism: a recipe for cancer growth*. *Genes Dev*, 2009. **23**(5): p. 537-48.
99. DeBerardinis, R.J., et al., *The biology of cancer: metabolic reprogramming fuels cell growth and proliferation*. *Cell Metab*, 2008. **7**(1): p. 11-20.
100. Wilkie, M.D., et al., *Metabolic signature of squamous cell carcinoma of the head and neck: Consequences of TP53 mutation and therapeutic perspectives*. *Oral Oncol*, 2018. **83**: p. 1-10.
101. Kondoh, H., et al., *Glycolytic enzymes can modulate cellular life span*. *Cancer Res*, 2005. **65**(1): p. 177-85.
102. Semenza, G.L., *HIF-1: upstream and downstream of cancer metabolism*. *Curr Opin Genet Dev*, 2010. **20**(1): p. 51-6.
103. Vander Heiden, M.G., L.C. Cantley, and C.B. Thompson, *Understanding the Warburg effect: the metabolic requirements of cell proliferation*. *Science*, 2009. **324**(5930): p. 1029-33.
104. Kennedy, K.M. and M.W. Dewhirst, *Tumor metabolism of lactate: the influence and therapeutic potential for MCT and CD147 regulation*. *Future Oncol*, 2010. **6**(1): p. 127-48.
105. Vajdic, C.M. and M.T. van Leeuwen, *Cancer incidence and risk factors after solid organ transplantation*. *Int J Cancer*, 2009. **125**(8): p. 1747-54.
106. Teng, M.W., et al., *Immune-mediated dormancy: an equilibrium with cancer*. *J Leukoc Biol*, 2008. **84**(4): p. 988-93.
107. Smyth, M.J., G.P. Dunn, and R.D. Schreiber, *Cancer immunosurveillance and immunoediting: the roles of immunity in suppressing tumor development and shaping tumor immunogenicity*. *Adv Immunol*, 2006. **90**: p. 1-50.
108. Strauss, D.C. and J.M. Thomas, *Transmission of donor melanoma by organ transplantation*. *Lancet Oncol*, 2010. **11**(8): p. 790-6.

109. Fridman, W.H., et al., *Immune infiltration in human cancer: prognostic significance and disease control*. Curr Top Microbiol Immunol, 2011. **344**: p. 1-24.
110. DeNardo, D.G., P. Andreu, and L.M. Coussens, *Interactions between lymphocytes and myeloid cells regulate pro- versus anti-tumor immunity*. Cancer Metastasis Rev, 2010. **29**(2): p. 309-16.
111. Qian, B.Z. and J.W. Pollard, *Macrophage diversity enhances tumor progression and metastasis*. Cell, 2010. **141**(1): p. 39-51.
112. Grivennikov, S.I., F.R. Greten, and M. Karin, *Immunity, inflammation, and cancer*. Cell, 2010. **140**(6): p. 883-99.
113. Tiemessen, M.M., et al., *CD4+CD25+Foxp3+ regulatory T cells induce alternative activation of human monocytes/macrophages*. Proc Natl Acad Sci U S A, 2007. **104**(49): p. 19446-51.
114. Fridlender, Z.G., et al., *Polarization of tumor-associated neutrophil phenotype by TGF-beta: "N1" versus "N2" TAN*. Cancer Cell, 2009. **16**(3): p. 183-94.
115. Liu, S.Y. and Y.L. Wu, *Ongoing clinical trials of PD-1 and PD-L1 inhibitors for lung cancer in China*. J Hematol Oncol, 2017. **10**(1): p. 136.
116. Mendoza-Rodriguez, C.A. and M.A. Cerbon, *[Tumor suppressor gene p53: mechanisms of action in cell proliferation and death]*. Rev Invest Clin, 2001. **53**(3): p. 266-73.
117. Shaw, P.H., *The role of p53 in cell cycle regulation*. Pathol Res Pract, 1996. **192**(7): p. 669-75.
118. Loeb, L.A., K.R. Loeb, and J.P. Anderson, *Multiple mutations and cancer*. Proc Natl Acad Sci U S A, 2003. **100**(3): p. 776-81.
119. *Review: Histone methylation and the DNA damage response*. . Mutation Research/Reviews in Mutation Research. , 2017.
120. Kuhmann, C., et al., *Altered regulation of DNA ligase IV activity by aberrant promoter DNA methylation and gene amplification in colorectal cancer*. Hum Mol Genet, 2014. **23**(8): p. 2043-54.
121. Kheirlesei, E.A., et al., *Mismatch repair protein expression in colorectal cancer*. J Gastrointest Oncol, 2013. **4**(4): p. 397-408.
122. Levine, A.J., *p53, the cellular gatekeeper for growth and division*. Cell, 1997. **88**(3): p. 323-31.
123. Deben, C., et al., *TP53 and MDM2 genetic alterations in non-small cell lung cancer: Evaluating their prognostic and predictive value*. Crit Rev Oncol Hematol, 2016. **99**: p. 63-73.
124. Dumitrescu, R.G. and I. Cotarla, *Understanding breast cancer risk -- where do we stand in 2005?* J Cell Mol Med, 2005. **9**(1): p. 208-21.
125. Narod, S.A. and W.D. Foulkes, *BRCA1 and BRCA2: 1994 and beyond*. Nat Rev Cancer, 2004. **4**(9): p. 665-76.
126. Narod, S.A. and L. Salmena, *BRCA1 and BRCA2 mutations and breast cancer*. Discov Med, 2011. **12**(66): p. 445-53.
127. Xu, B., S. Kim, and M.B. Kastan, *Involvement of Brca1 in S-phase and G(2)-phase checkpoints after ionizing irradiation*. Mol Cell Biol, 2001. **21**(10): p. 3445-50.
128. Weaver, B.A. and D.W. Cleveland, *Does aneuploidy cause cancer?* Curr Opin Cell Biol, 2006. **18**(6): p. 658-67.
129. Tanaka, K. and T. Hirota, *Chromosomal instability: A common feature and a therapeutic target of cancer*. Biochim Biophys Acta, 2016. **1866**(1): p. 64-75.
130. Torres, E.M., B.R. Williams, and A. Amon, *Aneuploidy: cells losing their balance*. Genetics, 2008. **179**(2): p. 737-46.
131. Sheltzer, J.M. and A. Amon, *The aneuploidy paradox: costs and benefits of an incorrect karyotype*. Trends Genet, 2011. **27**(11): p. 446-53.

132. Torres, E.M., et al., *Effects of aneuploidy on cellular physiology and cell division in haploid yeast*. *Science*, 2007. **317**(5840): p. 916-24.
133. Williams, B.R., et al., *Aneuploidy affects proliferation and spontaneous immortalization in mammalian cells*. *Science*, 2008. **322**(5902): p. 703-9.
134. Oromendia, A.B., S.E. Dodgson, and A. Amon, *Aneuploidy causes proteotoxic stress in yeast*. *Genes Dev*, 2012. **26**(24): p. 2696-708.
135. Santaguida, S. and A. Amon, *Short- and long-term effects of chromosome mis-segregation and aneuploidy*. *Nat Rev Mol Cell Biol*, 2015. **16**(8): p. 473-85.
136. Zhu, J., et al., *Karyotypic determinants of chromosome instability in aneuploid budding yeast*. *PLoS Genet*, 2012. **8**(5): p. e1002719.
137. Ohashi, A., et al., *Aneuploidy generates proteotoxic stress and DNA damage concurrently with p53-mediated post-mitotic apoptosis in SAC-impaired cells*. *Nat Commun*, 2015. **6**: p. 7668.
138. Satge, D., et al., *A tumor profile in Down syndrome*. *Am J Med Genet*, 1998. **78**(3): p. 207-16.
139. Baek, K.H., et al., *Down's syndrome suppression of tumour growth and the role of the calcineurin inhibitor DSCR1*. *Nature*, 2009. **459**(7250): p. 1126-30.
140. Ried, T., et al., *The consequences of chromosomal aneuploidy on the transcriptome of cancer cells*. *Biochim Biophys Acta*, 2012. **1819**(7): p. 784-93.
141. Yurov, Y.B., et al., *X chromosome aneuploidy in the Alzheimer's disease brain*. *Mol Cytogenet*, 2014. **7**(1): p. 20.
142. Iourov, I.Y., et al., *Aneuploidy in the normal, Alzheimer's disease and ataxia-telangiectasia brain: differential expression and pathological meaning*. *Neurobiol Dis*, 2009. **34**(2): p. 212-20.
143. Thomas, P. and M. Fenech, *Chromosome 17 and 21 aneuploidy in buccal cells is increased with ageing and in Alzheimer's disease*. *Mutagenesis*, 2008. **23**(1): p. 57-65.
144. Zigman, W.B., *Atypical aging in Down syndrome*. *Dev Disabil Res Rev*, 2013. **18**(1): p. 51-67.
145. Korkola, J. and J.W. Gray, *Breast cancer genomes--form and function*. *Curr Opin Genet Dev*, 2010. **20**(1): p. 4-14.
146. Leemans, C.R., B.J. Braakhuis, and R.H. Brakenhoff, *The molecular biology of head and neck cancer*. *Nat Rev Cancer*, 2011. **11**(1): p. 9-22.
147. Hermsen, M., et al., *New chromosomal regions with high-level amplifications in squamous cell carcinomas of the larynx and pharynx, identified by comparative genomic hybridization*. *J Pathol*, 2001. **194**(2): p. 177-82.
148. Jin, C., et al., *Cytogenetic abnormalities in 106 oral squamous cell carcinomas*. *Cancer Genet Cytogenet*, 2006. **164**(1): p. 44-53.
149. Smeets, S.J., et al., *Genetic classification of oral and oropharyngeal carcinomas identifies subgroups with a different prognosis*. *Cell Oncol*, 2009. **31**(4): p. 291-300.
150. Thompson, S.L., S.F. Bakhoun, and D.A. Compton, *Mechanisms of chromosomal instability*. *Curr Biol*, 2010. **20**(6): p. R285-95.
151. Califano, J., et al., *Genetic progression model for head and neck cancer: implications for field cancerization*. *Cancer Res*, 1996. **56**(11): p. 2488-92.
152. Tabor, M.P., et al., *Comparative molecular and histological grading of epithelial dysplasia of the oral cavity and the oropharynx*. *J Pathol*, 2003. **199**(3): p. 354-60.
153. Partridge, M., et al., *A case-control study confirms that microsatellite assay can identify patients at risk of developing oral squamous cell carcinoma within a field of cancerization*. *Cancer Res*, 2000. **60**(14): p. 3893-8.

154. Tabor, M.P., et al., *Persistence of genetically altered fields in head and neck cancer patients: biological and clinical implications*. Clin Cancer Res, 2001. **7**(6): p. 1523-32.
155. Braakhuis, B.J., et al., *A genetic explanation of Slaughter's concept of field cancerization: evidence and clinical implications*. Cancer Res, 2003. **63**(8): p. 1727-30.
156. Rosin, M.P., et al., *Use of allelic loss to predict malignant risk for low-grade oral epithelial dysplasia*. Clin Cancer Res, 2000. **6**(2): p. 357-62.
157. Kresty, L.A., et al., *Alterations of p16(INK4a) and p14(ARF) in patients with severe oral epithelial dysplasia*. Cancer Res, 2002. **62**(18): p. 5295-300.
158. Shintani, S., et al., *Inactivation of the p14(ARF), p15(INK4B) and p16(INK4A) genes is a frequent event in human oral squamous cell carcinomas*. Oral Oncol, 2001. **37**(6): p. 498-504.
159. Kasamatsu, A., *Loss of heterozygosity in oral cancer*. Oral Science International, 2011. **8**: p. 37-43.
160. Weinberg, R.A., *Tumor suppressor genes*. Science, 1991. **254**(5035): p. 1138-46.
161. Maestro, R., et al., *Three discrete regions of deletion at 3p in head and neck cancers*. Cancer Res, 1993. **53**(23): p. 5775-9.
162. Virgilio, L., et al., *FHIT gene alterations in head and neck squamous cell carcinomas*. Proc Natl Acad Sci U S A, 1996. **93**(18): p. 9770-5.
163. Gonzalez, M.V., et al., *Chromosome 3p loss of heterozygosity and mutation analysis of the FHIT and beta-cat genes in squamous cell carcinoma of the head and neck*. J Clin Pathol, 1998. **51**(7): p. 520-4.
164. Uzawa, N., et al., *Functional evidence for involvement of multiple putative tumor suppressor genes on the short arm of chromosome 3 in human oral squamous cell carcinogenesis*. Cancer Genet Cytogenet, 1998. **107**(2): p. 125-31.
165. Ohlund, D., E. Elyada, and D. Tuveson, *Fibroblast heterogeneity in the cancer wound*. J Exp Med, 2014. **211**(8): p. 1503-23.
166. Martinez-Outschoorn, U.E., et al., *Cancer cells metabolically "fertilize" the tumor microenvironment with hydrogen peroxide, driving the Warburg effect: implications for PET imaging of human tumors*. Cell Cycle, 2011. **10**(15): p. 2504-20.
167. Martinez-Outschoorn, U.E., F. Sotgia, and M.P. Lisanti, *Metabolic asymmetry in cancer: a "balancing act" that promotes tumor growth*. Cancer Cell, 2014. **26**(1): p. 5-7.
168. Orimo, A. and R.A. Weinberg, *Heterogeneity of stromal fibroblasts in tumors*. Cancer Biol Ther, 2007. **6**(4): p. 618-9.
169. Marsh, D., et al., *Stromal features are predictive of disease mortality in oral cancer patients*. J Pathol, 2011. **223**(4): p. 470-81.
170. Radisky, D.C., P.A. Kenny, and M.J. Bissell, *Fibrosis and cancer: do myofibroblasts come also from epithelial cells via EMT?* J Cell Biochem, 2007. **101**(4): p. 830-9.
171. Cirri, P. and P. Chiarugi, *Cancer associated fibroblasts: the dark side of the coin*. Am J Cancer Res, 2011. **1**(4): p. 482-97.
172. Xing, F., J. Saidou, and K. Watabe, *Cancer associated fibroblasts (CAFs) in tumor microenvironment*. Front Biosci (Landmark Ed), 2010. **15**: p. 166-79.
173. Vicent, S., et al., *Cross-species functional analysis of cancer-associated fibroblasts identifies a critical role for CLCF1 and IL-6 in non-small cell lung cancer in vivo*. Cancer Res, 2012. **72**(22): p. 5744-56.
174. Kordes, C., I. Sawitza, and D. Haussinger, *Hepatic and pancreatic stellate cells in focus*. Biol Chem, 2009. **390**(10): p. 1003-12.

175. Kidd, S., et al., *Origins of the tumor microenvironment: quantitative assessment of adipose-derived and bone marrow-derived stroma*. PLoS One, 2012. **7**(2): p. e30563.
176. Zeisberg, E.M., et al., *Discovery of endothelial to mesenchymal transition as a source for carcinoma-associated fibroblasts*. Cancer Res, 2007. **67**(21): p. 10123-8.
177. Iwano, M., et al., *Evidence that fibroblasts derive from epithelium during tissue fibrosis*. J Clin Invest, 2002. **110**(3): p. 341-50.
178. Prime, S.S., et al., *Fibroblast activation and senescence in oral cancer*. J Oral Pathol Med, 2017. **46**(2): p. 82-88.
179. Kawashiri, S., et al., *Significance of stromal desmoplasia and myofibroblast appearance at the invasive front in squamous cell carcinoma of the oral cavity*. Head Neck, 2009. **31**(10): p. 1346-53.
180. Vered, M., et al., *Cancer-associated fibroblasts and epithelial-mesenchymal transition in metastatic oral tongue squamous cell carcinoma*. Int J Cancer, 2010. **127**(6): p. 1356-62.
181. Pitiyage, G.N., et al., *Senescent mesenchymal cells accumulate in human fibrosis by a telomere-independent mechanism and ameliorate fibrosis through matrix metalloproteinases*. J Pathol, 2011. **223**(5): p. 604-17.
182. Hayflick, L., *THE LIMITED IN VITRO LIFETIME OF HUMAN DIPLOID CELL STRAINS*. Exp Cell Res, 1965. **37**: p. 614-36.
183. Di Micco, R., et al., *Oncogene-induced senescence is a DNA damage response triggered by DNA hyper-replication*. Nature, 2006. **444**(7119): p. 638-42.
184. Parkinson, E.K., *Senescence as a modulator of oral squamous cell carcinoma development*. Oral Oncol, 2010. **46**(12): p. 840-53.
185. Bavik C, C.I., Dean JP, Knudsen B, Plymate S, Nelson and PS., *The gene expression profile of prostate fibroblast senescence modulates neoplastic epithelial cell proliferation through paracrine mechanisms*. . Cancer Res, 2006(66): p. 794–802.
186. Kuilman, T. and D.S. Peeper, *Senescence-messaging secretome: SMS-ing cellular stress*. Nat Rev Cancer, 2009. **9**(2): p. 81-94.
187. Coppe, J.P., et al., *The senescence-associated secretory phenotype: the dark side of tumor suppression*. Annu Rev Pathol, 2010. **5**: p. 99-118.
188. Coppe, J.P., et al., *Senescence-associated secretory phenotypes reveal cell-nonautonomous functions of oncogenic RAS and the p53 tumor suppressor*. PLoS Biol, 2008. **6**(12): p. 2853-68.
189. Hassona, Y., et al., *Progression of genotype-specific oral cancer leads to senescence of cancer-associated fibroblasts and is mediated by oxidative stress and TGF-beta*. Carcinogenesis, 2013. **34**(6): p. 1286-95.
190. Hassona, Y., et al., *Senescent cancer-associated fibroblasts secrete active MMP-2 that promotes keratinocyte dis-cohesion and invasion*. Br J Cancer, 2014. **111**(6): p. 1230-7.
191. Calon, A., D.V. Tauriello, and E. Batlle, *TGF-beta in CAF-mediated tumor growth and metastasis*. Semin Cancer Biol, 2014. **25**: p. 15-22.
192. Zheng, X., et al., *Epithelial-to-mesenchymal transition is dispensable for metastasis but induces chemoresistance in pancreatic cancer*. Nature, 2015. **527**(7579): p. 525-530.
193. Kalluri, R., *The biology and function of fibroblasts in cancer*. Nat Rev Cancer, 2016. **16**(9): p. 582-98.
194. Tarin, D. and C.B. Croft, *Ultrastructural features of wound healing in mouse skin*. J Anat, 1969. **105**(Pt 1): p. 189-90.

195. Strutz, F., et al., *Identification and characterization of a fibroblast marker: FSP1*. J Cell Biol, 1995. **130**(2): p. 393-405.
196. Chang, H.Y., et al., *Diversity, topographic differentiation, and positional memory in human fibroblasts*. Proc Natl Acad Sci U S A, 2002. **99**(20): p. 12877-82.
197. Ryan, G.B., et al., *Myofibroblasts in an avascular fibrous tissue*. Lab Invest, 1973. **29**(2): p. 197-206.
198. Tsukada, T., et al., *HHF35, a muscle actin-specific monoclonal antibody. II. Reactivity in normal, reactive, and neoplastic human tissues*. Am J Pathol, 1987. **127**(2): p. 389-402.
199. Schor, S.L., et al., *Foetal and cancer patient fibroblasts produce an autocrine migration-stimulating factor not made by normal adult cells*. J Cell Sci, 1988. **90 (Pt 3)**: p. 391-9.
200. Durning, P., S.L. Schor, and R.A. Sellwood, *Fibroblasts from patients with breast cancer show abnormal migratory behaviour in vitro*. Lancet, 1984. **2**(8408): p. 890-2.
201. Elenbaas, B. and R.A. Weinberg, *Heterotypic signaling between epithelial tumor cells and fibroblasts in carcinoma formation*. Exp Cell Res, 2001. **264**(1): p. 169-84.
202. Lohr, M., et al., *Transforming growth factor-beta1 induces desmoplasia in an experimental model of human pancreatic carcinoma*. Cancer Res, 2001. **61**(2): p. 550-5.
203. Aoyagi, Y., et al., *Overexpression of TGF-beta by infiltrated granulocytes correlates with the expression of collagen mRNA in pancreatic cancer*. Br J Cancer, 2004. **91**(7): p. 1316-26.
204. Bronzert, D.A., et al., *Synthesis and secretion of platelet-derived growth factor by human breast cancer cell lines*. Proc Natl Acad Sci U S A, 1987. **84**(16): p. 5763-7.
205. Guido, C., et al., *Metabolic reprogramming of cancer-associated fibroblasts by TGF-beta drives tumor growth: connecting TGF-beta signaling with "Warburg-like" cancer metabolism and L-lactate production*. Cell Cycle, 2012. **11**(16): p. 3019-35.
206. Simpkins, S.A., et al., *Clinical and functional significance of loss of caveolin-1 expression in breast cancer-associated fibroblasts*. J Pathol, 2012. **227**(4): p. 490-8.
207. Goetz, J.G., et al., *Biomechanical remodeling of the microenvironment by stromal caveolin-1 favors tumor invasion and metastasis*. Cell, 2011. **146**(1): p. 148-63.
208. Orimo, A., et al., *Stromal fibroblasts present in invasive human breast carcinomas promote tumor growth and angiogenesis through elevated SDF-1/CXCL12 secretion*. Cell, 2005. **121**(3): p. 335-48.
209. Olumi, A.F., et al., *Carcinoma-associated fibroblasts direct tumor progression of initiated human prostatic epithelium*. Cancer Res, 1999. **59**(19): p. 5002-11.
210. Scherz-Shouval, R., et al., *The reprogramming of tumor stroma by HSF1 is a potent enabler of malignancy*. Cell, 2014. **158**(3): p. 564-78.
211. Calvo, F., et al., *Mechanotransduction and YAP-dependent matrix remodelling is required for the generation and maintenance of cancer-associated fibroblasts*. Nat Cell Biol, 2013. **15**(6): p. 637-46.
212. Procopio, M.G., et al., *Combined CSL and p53 downregulation promotes cancer-associated fibroblast activation*. Nat Cell Biol, 2015. **17**(9): p. 1193-204.
213. Boire, A., et al., *PAR1 is a matrix metalloprotease-1 receptor that promotes invasion and tumorigenesis of breast cancer cells*. Cell, 2005. **120**(3): p. 303-13.
214. Stetler-Stevenson, W.G., S. Aznavoorian, and L.A. Liotta, *Tumor cell interactions with the extracellular matrix during invasion and metastasis*. Annu Rev Cell Biol, 1993. **9**: p. 541-73.
215. Sternlicht, M.D., et al., *The stromal proteinase MMP3/stromelysin-1 promotes mammary carcinogenesis*. Cell, 1999. **98**(2): p. 137-46.

216. Lochter, A., et al., *Matrix metalloproteinase stromelysin-1 triggers a cascade of molecular alterations that leads to stable epithelial-to-mesenchymal conversion and a premalignant phenotype in mammary epithelial cells*. J Cell Biol, 1997. **139**(7): p. 1861-72.
217. Kahlert, C. and R. Kalluri, *Exosomes in tumor microenvironment influence cancer progression and metastasis*. J Mol Med (Berl), 2013. **91**(4): p. 431-7.
218. Luga, V. and J.L. Wrana, *Tumor-stroma interaction: Revealing fibroblast-secreted exosomes as potent regulators of Wnt-planar cell polarity signaling in cancer metastasis*. Cancer Res, 2013. **73**(23): p. 6843-7.
219. Hu, Y., et al., *Fibroblast-Derived Exosomes Contribute to Chemoresistance through Priming Cancer Stem Cells in Colorectal Cancer*. PLoS One, 2015. **10**(5): p. e0125625.
220. Elkabets, M., et al., *Human tumors instigate granulysin-expressing hematopoietic cells that promote malignancy by activating stromal fibroblasts in mice*. J Clin Invest, 2011. **121**(2): p. 784-99.
221. Bruzzese, F., et al., *Local and systemic protumorigenic effects of cancer-associated fibroblast-derived GDF15*. Cancer Res, 2014. **74**(13): p. 3408-17.
222. Calon, A., et al., *Dependency of colorectal cancer on a TGF-beta-driven program in stromal cells for metastasis initiation*. Cancer Cell, 2012. **22**(5): p. 571-84.
223. Pena, C., et al., *STC1 expression by cancer-associated fibroblasts drives metastasis of colorectal cancer*. Cancer Res, 2013. **73**(4): p. 1287-97.
224. O'Connell, J.T., et al., *VEGF-A and Tenascin-C produced by S100A4+ stromal cells are important for metastatic colonization*. Proc Natl Acad Sci U S A, 2011. **108**(38): p. 16002-7.
225. Olaso, E., et al., *Tumor-dependent activation of rodent hepatic stellate cells during experimental melanoma metastasis*. Hepatology, 1997. **26**(3): p. 634-42.
226. Kataoka, H., et al., *Tumor cell-derived collagenase-stimulatory factor increases expression of interstitial collagenase, stromelysin, and 72-kDa gelatinase*. Cancer Res, 1993. **53**(13): p. 3154-8.
227. Nakamura, T., et al., *Induction of hepatocyte growth factor in fibroblasts by tumor-derived factors affects invasive growth of tumor cells: in vitro analysis of tumor-stromal interactions*. Cancer Res, 1997. **57**(15): p. 3305-13.
228. Wu, X., et al., *Stromal cell heterogeneity in fibroblast growth factor-mediated stromal-epithelial cell cross-talk in premalignant prostate tumors*. Cancer Res, 2003. **63**(16): p. 4936-44.
229. De Wever, O. and M. Mareel, *Role of tissue stroma in cancer cell invasion*. J Pathol, 2003. **200**(4): p. 429-47.
230. Desmouliere, A., C. Guyot, and G. Gabbiani, *The stroma reaction myofibroblast: a key player in the control of tumor cell behavior*. Int J Dev Biol, 2004. **48**(5-6): p. 509-17.
231. Dvorak, H.F., *Tumors: wounds that do not heal. Similarities between tumor stroma generation and wound healing*. N Engl J Med, 1986. **315**(26): p. 1650-9.
232. Gabbiani, G. and G. Majno, *Dupuytren's contracture: fibroblast contraction? An ultrastructural study*. Am J Pathol, 1972. **66**(1): p. 131-46.
233. Tomasek, J.J., et al., *Myofibroblasts and mechano-regulation of connective tissue remodelling*. Nat Rev Mol Cell Biol, 2002. **3**(5): p. 349-63.
234. Chen, Y., et al., *Critical role of type IV collagens in the growth of bile duct carcinoma. In vivo and in vitro studies*. Pathol Res Pract, 2001. **197**(9): p. 585-96.
235. Woolgar, J.A. and A. Triantafyllou, *Pitfalls and procedures in the histopathological diagnosis of oral and oropharyngeal squamous cell carcinoma and a review of the role of pathology in prognosis*. Oral Oncol, 2009. **45**(4-5): p. 361-85.

236. P., M., *Genesis of the stroma*. In: Masson P, editor. *Human tumors: histology, diagnosis and technique*. . 1970: p. 146–56.
237. Parrott, J.A., et al., *Stromal-epithelial interactions in the progression of ovarian cancer: influence and source of tumor stromal cells*. *Mol Cell Endocrinol*, 2001. **175**(1-2): p. 29-39.
238. Hewitt, R.E., et al., *Desmoplasia and its relevance to colorectal tumour invasion*. *Int J Cancer*, 1993. **53**(1): p. 62-9.
239. Sis, B., et al., *Desmoplasia measured by computer assisted image analysis: an independent prognostic marker in colorectal carcinoma*. *J Clin Pathol*, 2005. **58**(1): p. 32-8.
240. Liotta, L.A. and E.C. Kohn, *The microenvironment of the tumour-host interface*. *Nature*, 2001. **411**(6835): p. 375-9.
241. Tuxhorn, J.A., et al., *Stromal cells promote angiogenesis and growth of human prostate tumors in a differential reactive stroma (DRS) xenograft model*. *Cancer Res*, 2002. **62**(11): p. 3298-307.
242. Dingemans, K.P., et al., *Transplantation of colon carcinoma into granulation tissue induces an invasive morphotype*. *Int J Cancer*, 1993. **54**(6): p. 1010-6.
243. Maeshima, A.M., et al., *Modified scar grade: a prognostic indicator in small peripheral lung adenocarcinoma*. *Cancer*, 2002. **95**(12): p. 2546-54.
244. Ronnov-Jessen, L., O.W. Petersen, and M.J. Bissell, *Cellular changes involved in conversion of normal to malignant breast: importance of the stromal reaction*. *Physiol Rev*, 1996. **76**(1): p. 69-125.
245. Breuninger, H., et al., *Desmoplastic squamous cell carcinoma of skin and vermilion surface: a highly malignant subtype of skin cancer*. *Cancer*, 1997. **79**(5): p. 915-9.
246. Hammond, M.E., et al., *College of American Pathologists Conference XXXV: solid tumor prognostic factors-which, how and so what? Summary document and recommendations for implementation*. *Cancer Committee and Conference Participants*. *Arch Pathol Lab Med*, 2000. **124**(7): p. 958-65.
247. Halvorsen, T.B. and E. Seim, *Association between invasiveness, inflammatory reaction, desmoplasia and survival in colorectal cancer*. *J Clin Pathol*, 1989. **42**(2): p. 162-6.
248. Dhand, J., et al., *SERPINE1 and SMA expression at the invasive front predict extracapsular spread and survival in oral squamous cell carcinoma*. *Br J Cancer*, 2014. **111**(11): p. 2114-21.
249. Baker, E.A., et al., *Plasminogen activator system in oral squamous cell carcinoma*. *Br J Oral Maxillofac Surg*, 2007. **45**(8): p. 623-7.
250. Hayashido, Y., et al., *Plasminogen activator/plasmin system suppresses cell-cell adhesion of oral squamous cell carcinoma cells via proteolysis of E-cadherin*. *Int J Oncol*, 2005. **27**(3): p. 693-8.
251. Duffy, M.J., *The urokinase plasminogen activator system: role in malignancy*. *Curr Pharm Des*, 2004. **10**(1): p. 39-49.
252. Dano, K., et al., *Plasminogen activation and cancer*. *Thromb Haemost*, 2005. **93**(4): p. 676-81.
253. Gandolfo, G.M., L. Conti, and M. Vercillo, *Fibrinolysis components as prognostic markers in breast cancer and colorectal carcinoma*. *Anticancer Res*, 1996. **16**(4b): p. 2155-9.
254. Ashton, T.M., et al., *Oxidative Phosphorylation as an Emerging Target in Cancer Therapy*. *Clin Cancer Res*, 2018. **24**(11): p. 2482-2490.
255. DeBerardinis, R.J. and N.S. Chandel, *Fundamentals of cancer metabolism*. *Sci Adv*, 2016. **2**(5): p. e1600200.

256. Warburg, O., *On respiratory impairment in cancer cells*. Science, 1956. **124**(3215): p. 269-70.
257. Racker, E., *History of the Pasteur effect and its pathobiology*. Mol Cell Biochem, 1974. **5**(1-2): p. 17-23.
258. Newsholme, E.A., B. Crabtree, and M.S. Ardawi, *The role of high rates of glycolysis and glutamine utilization in rapidly dividing cells*. Biosci Rep, 1985. **5**(5): p. 393-400.
259. Mankoff, D.A., et al., *Tumor-specific positron emission tomography imaging in patients: [18F] fluorodeoxyglucose and beyond*. Clin Cancer Res, 2007. **13**(12): p. 3460-9.
260. Rajendran, J.G., et al., *Hypoxia and glucose metabolism in malignant tumors: evaluation by [18F]fluoromisonidazole and [18F]fluorodeoxyglucose positron emission tomography imaging*. Clin Cancer Res, 2004. **10**(7): p. 2245-52.
261. Clavo, A.C., R.S. Brown, and R.L. Wahl, *Fluorodeoxyglucose uptake in human cancer cell lines is increased by hypoxia*. J Nucl Med, 1995. **36**(9): p. 1625-32.
262. Sonveaux, P., et al., *Targeting lactate-fueled respiration selectively kills hypoxic tumor cells in mice*. J Clin Invest, 2008. **118**(12): p. 3930-42.
263. Pavlides, S., et al., *The reverse Warburg effect: aerobic glycolysis in cancer associated fibroblasts and the tumor stroma*. Cell Cycle, 2009. **8**(23): p. 3984-4001.
264. Martinez-Outschoorn, U.E., F. Sotgia, and M.P. Lisanti, *Power surge: supporting cells "fuel" cancer cell mitochondria*. Cell Metab, 2012. **15**(1): p. 4-5.
265. Bovenzi, C.D., et al., *Prognostic Indications of Elevated MCT4 and CD147 across Cancer Types: A Meta-Analysis*. Biomed Res Int, 2015. **2015**: p. 242437.
266. Fiaschi, T., et al., *Reciprocal metabolic reprogramming through lactate shuttle coordinately influences tumor-stroma interplay*. Cancer Res, 2012. **72**(19): p. 5130-40.
267. Zhao, Z., et al., *Stromal-epithelial metabolic coupling in gastric cancer: stromal MCT4 and mitochondrial TOMM20 as poor prognostic factors*. Eur J Surg Oncol, 2014. **40**(10): p. 1361-8.
268. Zhao, Z., et al., *Downregulation of MCT1 inhibits tumor growth, metastasis and enhances chemotherapeutic efficacy in osteosarcoma through regulation of the NF-kappaB pathway*. Cancer Lett, 2014. **342**(1): p. 150-8.
269. Martinez-Outschoorn, U., F. Sotgia, and M.P. Lisanti, *Tumor microenvironment and metabolic synergy in breast cancers: critical importance of mitochondrial fuels and function*. Semin Oncol, 2014. **41**(2): p. 195-216.
270. Whitaker-Menezes, D., et al., *Evidence for a stromal-epithelial "lactate shuttle" in human tumors: MCT4 is a marker of oxidative stress in cancer-associated fibroblasts*. Cell Cycle, 2011. **10**(11): p. 1772-83.
271. Lunt, S.Y. and M.G. Vander Heiden, *Aerobic glycolysis: meeting the metabolic requirements of cell proliferation*. Annu Rev Cell Dev Biol, 2011. **27**: p. 441-64.
272. Pfeiffer, T., S. Schuster, and S. Bonhoeffer, *Cooperation and competition in the evolution of ATP-producing pathways*. Science, 2001. **292**(5516): p. 504-7.
273. Feron, O., *Pyruvate into lactate and back: from the Warburg effect to symbiotic energy fuel exchange in cancer cells*. Radiother Oncol, 2009. **92**(3): p. 329-33.
274. Bergersen, L.H., *Is lactate food for neurons? Comparison of monocarboxylate transporter subtypes in brain and muscle*. Neuroscience, 2007. **145**(1): p. 11-9.
275. Pierre, K. and L. Pellerin, *Monocarboxylate transporters in the central nervous system: distribution, regulation and function*. J Neurochem, 2005. **94**(1): p. 1-14.
276. Dimmer, K.S., et al., *The low-affinity monocarboxylate transporter MCT4 is adapted to the export of lactate in highly glycolytic cells*. Biochem J, 2000. **350 Pt 1**: p. 219-27.

277. Martinez-Outschoorn, U.E., et al., *Oncogenes and inflammation rewire host energy metabolism in the tumor microenvironment: RAS and NFkappaB target stromal MCT4*. *Cell Cycle*, 2013. **12**(16): p. 2580-97.
278. Ullah, M.S., A.J. Davies, and A.P. Halestrap, *The plasma membrane lactate transporter MCT4, but not MCT1, is up-regulated by hypoxia through a HIF-1alpha-dependent mechanism*. *J Biol Chem*, 2006. **281**(14): p. 9030-7.
279. Gladden, L.B., *A lactatic perspective on metabolism*. *Med Sci Sports Exerc*, 2008. **40**(3): p. 477-85.
280. Brooks, G.A., *Lactate: link between glycolytic and oxidative metabolism*. *Sports Med*, 2007. **37**(4-5): p. 341-3.
281. Brooks, G.A., *Current concepts in lactate exchange*. *Med Sci Sports Exerc*, 1991. **23**(8): p. 895-906.
282. Magistretti, P.J., *Neuron-glia metabolic coupling and plasticity*. *J Exp Biol*, 2006. **209**(Pt 12): p. 2304-11.
283. Magistretti, P.J., *Role of glutamate in neuron-glia metabolic coupling*. *Am J Clin Nutr*, 2009. **90**(3): p. 875s-880s.
284. Magistretti, P.J. and L. Pellerin, *The contribution of astrocytes to the 18F-2-deoxyglucose signal in PET activation studies*. *Mol Psychiatry*, 1996. **1**(6): p. 445-52.
285. Hashimoto, T., et al., *Immunohistochemical analysis of MCT1, MCT2 and MCT4 expression in rat plantaris muscle*. *J Physiol*, 2005. **567**(Pt 1): p. 121-9.
286. Mesker, W.E., et al., *The carcinoma-stromal ratio of colon carcinoma is an independent factor for survival compared to lymph node status and tumor stage*. *Cell Oncol*, 2007. **29**(5): p. 387-98.
287. Dewhirst, M.W., Y. Cao, and B. Moeller, *Cycling hypoxia and free radicals regulate angiogenesis and radiotherapy response*. *Nat Rev Cancer*, 2008. **8**(6): p. 425-37.
288. Cardenas-Navia, L.I., et al., *The pervasive presence of fluctuating oxygenation in tumors*. *Cancer Res*, 2008. **68**(14): p. 5812-9.
289. Semenza, G.L., et al., *Structural and functional analysis of hypoxia-inducible factor 1*. *Kidney Int*, 1997. **51**(2): p. 553-5.
290. Papp-Szabo, E., P.D. Josephy, and B.L. Coomber, *Microenvironmental influences on mutagenesis in mammary epithelial cells*. *Int J Cancer*, 2005. **116**(5): p. 679-85.
291. Flier, J.S., et al., *Elevated levels of glucose transport and transporter messenger RNA are induced by ras or src oncogenes*. *Science*, 1987. **235**(4795): p. 1492-5.
292. Shim, H., et al., *c-Myc transactivation of LDH-A: implications for tumor metabolism and growth*. *Proc Natl Acad Sci U S A*, 1997. **94**(13): p. 6658-63.
293. Elstrom, R.L., et al., *Akt stimulates aerobic glycolysis in cancer cells*. *Cancer Res*, 2004. **64**(11): p. 3892-9.
294. Bensaad, K., et al., *TIGAR, a p53-inducible regulator of glycolysis and apoptosis*. *Cell*, 2006. **126**(1): p. 107-20.
295. Liu, G. and X. Chen, *The ferredoxin reductase gene is regulated by the p53 family and sensitizes cells to oxidative stress-induced apoptosis*. *Oncogene*, 2002. **21**(47): p. 7195-204.
296. Fischer, M., *Census and evaluation of p53 target genes*. *Oncogene*, 2017. **36**(28): p. 3943-3956.
297. Cairns, R.A., I.S. Harris, and T.W. Mak, *Regulation of cancer cell metabolism*. *Nat Rev Cancer*, 2011. **11**(2): p. 85-95.
298. Chi, J.T., et al., *Gene expression programs in response to hypoxia: cell type specificity and prognostic significance in human cancers*. *PLoS Med*, 2006. **3**(3): p. e47.

299. Lum, J.J., et al., *The transcription factor HIF-1alpha plays a critical role in the growth factor-dependent regulation of both aerobic and anaerobic glycolysis*. Genes Dev, 2007. **21**(9): p. 1037-49.
300. Chen, C., et al., *Regulation of glut1 mRNA by hypoxia-inducible factor-1. Interaction between H-ras and hypoxia*. J Biol Chem, 2001. **276**(12): p. 9519-25.
301. Iyer, N.V., et al., *Cellular and developmental control of O2 homeostasis by hypoxia-inducible factor 1 alpha*. Genes Dev, 1998. **12**(2): p. 149-62.
302. Wang, G.L., et al., *Hypoxia-inducible factor 1 is a basic-helix-loop-helix-PAS heterodimer regulated by cellular O2 tension*. Proc Natl Acad Sci U S A, 1995. **92**(12): p. 5510-4.
303. Semenza, G.L., *Targeting HIF-1 for cancer therapy*. Nat Rev Cancer, 2003. **3**(10): p. 721-32.
304. Liu, C., Q. Lin, and Z. Yun, *Cellular and molecular mechanisms underlying oxygen-dependent radiosensitivity*. Radiat Res, 2015. **183**(5): p. 487-96.
305. Gray, L.H., *Oxygenation in radiotherapy. I. Radiobiological considerations*. Br J Radiol, 1957. **30**(356): p. 403-6.
306. Gray, L.H., *Radiobiologic basis of oxygen as a modifying factor in radiation therapy*. Am J Roentgenol Radium Ther Nucl Med, 1961. **85**: p. 803-15.
307. Gray, L.H., et al., *The concentration of oxygen dissolved in tissues at the time of irradiation as a factor in radiotherapy*. Br J Radiol, 1953. **26**(312): p. 638-48.
308. Thomlinson, R.H. and L.H. Gray, *The histological structure of some human lung cancers and the possible implications for radiotherapy*. Br J Cancer, 1955. **9**(4): p. 539-49.
309. Griffiths, E.A., et al., *Is the hypoxia-inducible factor pathway important in gastric cancer?* Eur J Cancer, 2005. **41**(18): p. 2792-805.
310. Rockwell, S., et al., *Hypoxia and radiation therapy: past history, ongoing research, and future promise*. Curr Mol Med, 2009. **9**(4): p. 442-58.
311. Kirkpatrick, J.P., L.I. Cardenas-Navia, and M.W. Dewhirst, *Predicting the effect of temporal variations in PO2 on tumor radiosensitivity*. Int J Radiat Oncol Biol Phys, 2004. **59**(3): p. 822-33.
312. Alexander, P. and A. Charlesby, *Energy transfer in macromolecules exposed to ionizing radiations*. Nature, 1954. **173**(4404): p. 578-9.
313. Johansen, I. and P. Howard-Flanders, *MACROMOLECULAR REPAIR AND FREE RADICAL SCAVENGING IN THE PROTECTION OF BACTERIA AGAINST X-RAYS*. Radiat Res, 1965. **24**: p. 184-200.
314. Vaupel, P., *Tumor microenvironmental physiology and its implications for radiation oncology*. Semin Radiat Oncol, 2004. **14**(3): p. 198-206.
315. Bertout, J.A., S.A. Patel, and M.C. Simon, *The impact of O2 availability on human cancer*. Nat Rev Cancer, 2008. **8**(12): p. 967-75.
316. Shannon, A.M., et al., *Tumour hypoxia, chemotherapeutic resistance and hypoxia-related therapies*. Cancer Treat Rev, 2003. **29**(4): p. 297-307.
317. Minchinton, A.I. and I.F. Tannock, *Drug penetration in solid tumours*. Nat Rev Cancer, 2006. **6**(8): p. 583-92.
318. Erler, J.T., et al., *Lysyl oxidase is essential for hypoxia-induced metastasis*. Nature, 2006. **440**(7088): p. 1222-6.
319. Chan, D.A. and A.J. Giaccia, *Hypoxia, gene expression, and metastasis*. Cancer Metastasis Rev, 2007. **26**(2): p. 333-9.
320. Horsman, M.R. and J. Overgaard, *The impact of hypoxia and its modification of the outcome of radiotherapy*. J Radiat Res, 2016. **57 Suppl 1**: p. i90-i98.

321. Nordsmark, M., et al., *Prognostic value of tumor oxygenation in 397 head and neck tumors after primary radiation therapy. An international multi-center study.* Radiother Oncol, 2005. **77**(1): p. 18-24.
322. Fitzmaurice, C., et al., *Global, Regional, and National Cancer Incidence, Mortality, Years of Life Lost, Years Lived With Disability, and Disability-Adjusted Life-years for 32 Cancer Groups, 1990 to 2015: A Systematic Analysis for the Global Burden of Disease Study.* JAMA Oncol, 2017. **3**(4): p. 524-548.
323. Faraji, F., et al., *Molecular mechanisms of human papillomavirus-related carcinogenesis in head and neck cancer.* Microbes Infect, 2017. **19**(9-10): p. 464-475.
324. Carvalho, A.L., et al., *Trends in incidence and prognosis for head and neck cancer in the United States: a site-specific analysis of the SEER database.* Int J Cancer, 2005. **114**(5): p. 806-16.
325. Chaturvedi, A.K., et al., *Human papillomavirus and rising oropharyngeal cancer incidence in the United States.* J Clin Oncol, 2011. **29**(32): p. 4294-301.
326. Schache, A.G., et al., *HPV-Related Oropharynx Cancer in the United Kingdom: An Evolution in the Understanding of Disease Etiology.* Cancer Res, 2016. **76**(22): p. 6598-6606.
327. Tiwana, M.S., et al., *25 year survival outcomes for squamous cell carcinomas of the head and neck: population-based outcomes from a Canadian province.* Oral Oncol, 2014. **50**(7): p. 651-6.
328. Chaturvedi, A.K., et al., *Worldwide trends in incidence rates for oral cavity and oropharyngeal cancers.* J Clin Oncol, 2013. **31**(36): p. 4550-9.
329. D'Souza, G., et al., *Oral sexual behaviors associated with prevalent oral human papillomavirus infection.* J Infect Dis, 2009. **199**(9): p. 1263-9.
330. Panwar, A., et al., *Human papilloma virus positive oropharyngeal squamous cell carcinoma: a growing epidemic.* Cancer Treat Rev, 2014. **40**(2): p. 215-9.
331. Herrero, R., et al., *Reduced prevalence of oral human papillomavirus (HPV) 4 years after bivalent HPV vaccination in a randomized clinical trial in Costa Rica.* PLoS One, 2013. **8**(7): p. e68329.
332. Ferlito, A., et al., *Which is the single most important factor in deciding the management and determining the prognosis of head and neck cancer?* Eur Arch Otorhinolaryngol, 2010. **267**(3): p. 325-6.
333. Woolgar, J.A., et al., *Cervical lymph node metastasis in oral cancer: the importance of even microscopic extracapsular spread.* Oral Oncol, 2003. **39**(2): p. 130-7.
334. Jose, J., et al., *Cervical node metastases in squamous cell carcinoma of the upper aerodigestive tract: the significance of extracapsular spread and soft tissue deposits.* Head Neck, 2003. **25**(6): p. 451-6.
335. Woolgar, J.e.a., *Neck dissections: A practical guide for the reporting histopathologist.* Diagnostic Histopathology, 2007, . **13**(6): p. 499 - 511
336. Woolgar, J.A., *Histopathological prognosticators in oral and oropharyngeal squamous cell carcinoma.* Oral Oncol, 2006. **42**(3): p. 229-39.
337. Woolgar, J.A., et al., *Survival and patterns of recurrence in 200 oral cancer patients treated by radical surgery and neck dissection.* Oral Oncol, 1999. **35**(3): p. 257-65.
338. Ambrosch, P., et al., *Micrometastases in carcinoma of the upper aerodigestive tract: detection, risk of metastasizing, and prognostic value of depth of invasion.* Head Neck, 1995. **17**(6): p. 473-9.
339. Woolgar, J.A. and A. Triantafyllou, *A histopathological appraisal of surgical margins in oral and oropharyngeal cancer resection specimens.* Oral Oncol, 2005. **41**(10): p. 1034-43.

340. Akhter, M., et al., *A study on histological grading of oral squamous cell carcinoma and its co-relationship with regional metastasis*. J Oral Maxillofac Pathol, 2011. **15**(2): p. 168-76.
341. Anneroth, G., L.S. Hansen, and S. Silverman, Jr., *Malignancy grading in oral squamous cell carcinoma. I. Squamous cell carcinoma of the tongue and floor of mouth: histologic grading in the clinical evaluation*. J Oral Pathol, 1986. **15**(3): p. 162-8.
342. Tsujino, T., et al., *Stromal myofibroblasts predict disease recurrence for colorectal cancer*. Clin Cancer Res, 2007. **13**(7): p. 2082-90.
343. Kellermann, M.G., et al., *Myofibroblasts in the stroma of oral squamous cell carcinoma are associated with poor prognosis*. Histopathology, 2007. **51**(6): p. 849-53.
344. Surowiak, P., et al., *Occurrence of stromal myofibroblasts in the invasive ductal breast cancer tissue is an unfavourable prognostic factor*. Anticancer Res, 2007. **27**(4c): p. 2917-24.
345. SNELL, R.S., *Clinical anatomy for medical students*. 4th ed. ed. 1992, Boston: Little, Brown.
346. JUNQUEIRA, L.C., R.O. KELLEY, and J. CARNEIRO, *Basic histology*. 8th ed. Lange medical books. 1995: Appleton & Lange, Norwalk (Conn.).
347. Williams, P.L. and L.H. Bannister, *Gray's anatomy : the anatomical basis of medicine and surgery*. 38th ed ed. 1995, New York Churchill Livingstone.
348. Perry, M.E., *The specialised structure of crypt epithelium in the human palatine tonsil and its functional significance*. J Anat, 1994. **185 (Pt 1)**: p. 111-27.
349. Rautava, J. and S. Syrjanen, *Biology of human papillomavirus infections in head and neck carcinogenesis*. Head Neck Pathol, 2012. **6 Suppl 1**: p. S3-15.
350. Alpan, O., G. Rudomen, and P. Matzinger, *The role of dendritic cells, B cells, and M cells in gut-oriented immune responses*. J Immunol, 2001. **166**(8): p. 4843-52.
351. Tommasino, M., *The human papillomavirus family and its role in carcinogenesis*. Semin Cancer Biol, 2014. **26**: p. 13-21.
352. Bernard, H.U., et al., *Classification of papillomaviruses (PVs) based on 189 PV types and proposal of taxonomic amendments*. Virology, 2010. **401**(1): p. 70-9.
353. zur Hausen, H., *Papillomaviruses and cancer: from basic studies to clinical application*. Nat Rev Cancer, 2002. **2**(5): p. 342-50.
354. Bouvard, V., et al., *A review of human carcinogens--Part B: biological agents*. Lancet Oncol, 2009. **10**(4): p. 321-2.
355. Pinidis, P., et al., *Human Papilloma Virus' Life Cycle and Carcinogenesis*. Maedica (Buchar), 2016. **11**(1): p. 48-54.
356. DiMaio, D. and L.M. Petti, *The E5 proteins*. Virology, 2013. **445**(1-2): p. 99-114.
357. Chen, J.J., *Genomic Instability Induced By Human Papillomavirus Oncogenes*. N Am J Med Sci (Boston), 2010. **3**(2): p. 43-47.
358. Stanley, M.A., *Epithelial cell responses to infection with human papillomavirus*. Clin Microbiol Rev, 2012. **25**(2): p. 215-22.
359. Korzeniewski, N., et al., *Genomic instability and cancer: lessons learned from human papillomaviruses*. Cancer Lett, 2011. **305**(2): p. 113-22.
360. Doorbar, J., et al., *The biology and life-cycle of human papillomaviruses*. Vaccine, 2012. **30 Suppl 5**: p. F55-70.
361. Buck, C.B., et al., *Arrangement of L2 within the papillomavirus capsid*. J Virol, 2008. **82**(11): p. 5190-7.
362. Finnen, R.L., et al., *Interactions between papillomavirus L1 and L2 capsid proteins*. J Virol, 2003. **77**(8): p. 4818-26.

363. Johnson, K.M., et al., *Role of heparan sulfate in attachment to and infection of the murine female genital tract by human papillomavirus*. J Virol, 2009. **83**(5): p. 2067-74.
364. Combita, A.L., et al., *Gene transfer using human papillomavirus pseudovirions varies according to virus genotype and requires cell surface heparan sulfate*. FEMS Microbiol Lett, 2001. **204**(1): p. 183-8.
365. Giroglou, T., et al., *Human papillomavirus infection requires cell surface heparan sulfate*. J Virol, 2001. **75**(3): p. 1565-70.
366. Culp, T.D., et al., *Keratinocyte-secreted laminin 5 can function as a transient receptor for human papillomaviruses by binding virions and transferring them to adjacent cells*. J Virol, 2006. **80**(18): p. 8940-50.
367. Kines, R.C., et al., *The initial steps leading to papillomavirus infection occur on the basement membrane prior to cell surface binding*. Proc Natl Acad Sci U S A, 2009. **106**(48): p. 20458-63.
368. Richards, R.M., et al., *Cleavage of the papillomavirus minor capsid protein, L2, at a furin consensus site is necessary for infection*. Proc Natl Acad Sci U S A, 2006. **103**(5): p. 1522-7.
369. Doorbar, J., *The papillomavirus life cycle*. J Clin Virol, 2005. **32 Suppl 1**: p. S7-15.
370. Bergant Marusic, M., et al., *Human papillomavirus L2 facilitates viral escape from late endosomes via sorting nexin 17*. Traffic, 2012. **13**(3): p. 455-67.
371. Schelhaas, M., et al., *Entry of human papillomavirus type 16 by actin-dependent, clathrin- and lipid raft-independent endocytosis*. PLoS Pathog, 2012. **8**(4): p. e1002657.
372. Pyeon, D., et al., *Establishment of human papillomavirus infection requires cell cycle progression*. PLoS Pathog, 2009. **5**(2): p. e1000318.
373. Parish, J.L., et al., *ChlR1 is required for loading papillomavirus E2 onto mitotic chromosomes and viral genome maintenance*. Mol Cell, 2006. **24**(6): p. 867-76.
374. McBride, A.A., *Replication and partitioning of papillomavirus genomes*. Adv Virus Res, 2008. **72**: p. 155-205.
375. Holmgren, S.C., et al., *The minor capsid protein L2 contributes to two steps in the human papillomavirus type 31 life cycle*. J Virol, 2005. **79**(7): p. 3938-48.
376. Day, P.M., et al., *The papillomavirus minor capsid protein, L2, induces localization of the major capsid protein, L1, and the viral transcription/replication protein, E2, to PML oncogenic domains*. J Virol, 1998. **72**(1): p. 142-50.
377. Buck, C.B., et al., *Maturation of papillomavirus capsids*. J Virol, 2005. **79**(5): p. 2839-46.
378. Thorland, E.C., et al., *Common fragile sites are preferential targets for HPV16 integrations in cervical tumors*. Oncogene, 2003. **22**(8): p. 1225-37.
379. Wentzensen, N., et al., *Characterization of viral-cellular fusion transcripts in a large series of HPV16 and 18 positive anogenital lesions*. Oncogene, 2002. **21**(3): p. 419-26.
380. Jeon, S., B.L. Allen-Hoffmann, and P.F. Lambert, *Integration of human papillomavirus type 16 into the human genome correlates with a selective growth advantage of cells*. J Virol, 1995. **69**(5): p. 2989-97.
381. Pett, M.R., et al., *Acquisition of high-level chromosomal instability is associated with integration of human papillomavirus type 16 in cervical keratinocytes*. Cancer Res, 2004. **64**(4): p. 1359-68.
382. Melsheimer, P., et al., *DNA aneuploidy and integration of human papillomavirus type 16 e6/e7 oncogenes in intraepithelial neoplasia and invasive squamous cell carcinoma of the cervix uteri*. Clin Cancer Res, 2004. **10**(9): p. 3059-63.

383. Schmitz, M., et al., *Non-random integration of the HPV genome in cervical cancer*. PLoS One, 2012. **7**(6): p. e39632.
384. Gravitt, P.E., *The known unknowns of HPV natural history*. J Clin Invest, 2011. **121**(12): p. 4593-9.
385. Zhang, P., et al., *Induction of E6/E7 expression in cottontail rabbit papillomavirus latency following UV activation*. Virology, 1999. **263**(2): p. 388-94.
386. Maglennon, G.A., P. McIntosh, and J. Doorbar, *Persistence of viral DNA in the epithelial basal layer suggests a model for papillomavirus latency following immune regression*. Virology, 2011. **414**(2): p. 153-63.
387. Welters, M.J., et al., *Frequent display of human papillomavirus type 16 E6-specific memory t-Helper cells in the healthy population as witness of previous viral encounter*. Cancer Res, 2003. **63**(3): p. 636-41.
388. de Jong, A., et al., *Human papillomavirus type 16-positive cervical cancer is associated with impaired CD4+ T-cell immunity against early antigens E2 and E6*. Cancer Res, 2004. **64**(15): p. 5449-55.
389. Vinokurova, S., et al., *Type-dependent integration frequency of human papillomavirus genomes in cervical lesions*. Cancer Res, 2008. **68**(1): p. 307-13.
390. Wentzensen, N., S. Vinokurova, and M. von Knebel Doeberitz, *Systematic review of genomic integration sites of human papillomavirus genomes in epithelial dysplasia and invasive cancer of the female lower genital tract*. Cancer Res, 2004. **64**(11): p. 3878-84.
391. Olthof, N.C., et al., *Viral load, gene expression and mapping of viral integration sites in HPV16-associated HNSCC cell lines*. Int J Cancer, 2015. **136**(5): p. E207-18.
392. Olthof, N.C., et al., *Comprehensive analysis of HPV16 integration in OSCC reveals no significant impact of physical status on viral oncogene and virally disrupted human gene expression*. PLoS One, 2014. **9**(2): p. e88718.
393. *Comprehensive genomic characterization of squamous cell lung cancers*. Nature, 2012. **489**(7417): p. 519-25.
394. Pim, D. and L. Banks, *Interaction of viral oncoproteins with cellular target molecules: infection with high-risk vs low-risk human papillomaviruses*. Apmis, 2010. **118**(6-7): p. 471-93.
395. Marur, S., et al., *HPV-associated head and neck cancer: a virus-related cancer epidemic*. Lancet Oncol, 2010. **11**(8): p. 781-9.
396. McLaughlin-Drubin, M.E. and K. Munger, *The human papillomavirus E7 oncoprotein*. Virology, 2009. **384**(2): p. 335-44.
397. Duensing, S. and K. Munger, *The human papillomavirus type 16 E6 and E7 oncoproteins independently induce numerical and structural chromosome instability*. Cancer Res, 2002. **62**(23): p. 7075-82.
398. Duensing, S. and K. Munger, *Human papillomavirus type 16 E7 oncoprotein can induce abnormal centrosome duplication through a mechanism independent of inactivation of retinoblastoma protein family members*. J Virol, 2003. **77**(22): p. 12331-5.
399. Duensing, S. and K. Munger, *Mechanisms of genomic instability in human cancer: insights from studies with human papillomavirus oncoproteins*. Int J Cancer, 2004. **109**(2): p. 157-62.
400. Duensing, A., et al., *Centrosome overduplication, chromosomal instability, and human papillomavirus oncoproteins*. Environ Mol Mutagen, 2009. **50**(8): p. 741-7.
401. Javier, R.T., *Cell polarity proteins: common targets for tumorigenic human viruses*. Oncogene, 2008. **27**(55): p. 7031-46.
402. Culp, T.D., et al., *Papillomavirus particles assembled in 293TT cells are infectious in vivo*. J Virol, 2006. **80**(22): p. 11381-4.

403. Galloway, D.A., et al., *Regulation of telomerase by human papillomaviruses*. Cold Spring Harb Symp Quant Biol, 2005. **70**: p. 209-15.
404. Gewin, L. and D.A. Galloway, *E box-dependent activation of telomerase by human papillomavirus type 16 E6 does not require induction of c-myc*. J Virol, 2001. **75**(15): p. 7198-201.
405. Klingelhutz, A.J., S.A. Foster, and J.K. McDougall, *Telomerase activation by the E6 gene product of human papillomavirus type 16*. Nature, 1996. **380**(6569): p. 79-82.
406. Fu, L., et al., *Degradation of p53 by human Alphapapillomavirus E6 proteins shows a stronger correlation with phylogeny than oncogenicity*. PLoS One, 2010. **5**(9).
407. Zanier, K., et al., *Solution structure analysis of the HPV16 E6 oncoprotein reveals a self-association mechanism required for E6-mediated degradation of p53*. Structure, 2012. **20**(4): p. 604-17.
408. Kuhne, C., et al., *Differential regulation of human papillomavirus E6 by protein kinase A: conditional degradation of human discs large protein by oncogenic E6*. Oncogene, 2000. **19**(51): p. 5884-91.
409. Hong, A.M., et al., *Squamous cell carcinoma of the oropharynx in Australian males induced by human papillomavirus vaccine targets*. Vaccine, 2010. **28**(19): p. 3269-72.
410. Wierzbicka, M., et al., *The rationale for HPV-related oropharyngeal cancer de-escalation treatment strategies*. Contemp Oncol (Pozn), 2015. **19**(4): p. 313-22.
411. Aldalwg, M.A.H. and B. Brestovac, *Human Papillomavirus Associated Cancers of the Head and Neck: An Australian Perspective*. Head Neck Pathol, 2017. **11**(3): p. 377-384.
412. de Martel, C., et al., *Global burden of cancers attributable to infections in 2008: a review and synthetic analysis*. Lancet Oncol, 2012. **13**(6): p. 607-15.
413. Blomberg, M., et al., *Trends in head and neck cancer incidence in Denmark, 1978-2007: focus on human papillomavirus associated sites*. Int J Cancer, 2011. **129**(3): p. 733-41.
414. Upile, N.S., et al., *Squamous cell carcinoma of the head and neck outside the oropharynx is rarely human papillomavirus related*. Laryngoscope, 2014. **124**(12): p. 2739-44.
415. Westra, W.H., *The morphologic profile of HPV-related head and neck squamous carcinoma: implications for diagnosis, prognosis, and clinical management*. Head Neck Pathol, 2012. **6 Suppl 1**: p. S48-54.
416. Begum, S., et al., *Tissue distribution of human papillomavirus 16 DNA integration in patients with tonsillar carcinoma*. Clin Cancer Res, 2005. **11**(16): p. 5694-9.
417. Fakhry, C., et al., *Improved survival of patients with human papillomavirus-positive head and neck squamous cell carcinoma in a prospective clinical trial*. J Natl Cancer Inst, 2008. **100**(4): p. 261-9.
418. Gillison, M.L., et al., *Distinct risk factor profiles for human papillomavirus type 16-positive and human papillomavirus type 16-negative head and neck cancers*. J Natl Cancer Inst, 2008. **100**(6): p. 407-20.
419. Heck, J.E., et al., *Sexual behaviours and the risk of head and neck cancers: a pooled analysis in the International Head and Neck Cancer Epidemiology (INHANCE) consortium*. Int J Epidemiol, 2010. **39**(1): p. 166-81.
420. Dahlstrom, K.R., et al., *Differences in history of sexual behavior between patients with oropharyngeal squamous cell carcinoma and patients with squamous cell carcinoma at other head and neck sites*. Head Neck, 2011. **33**(6): p. 847-55.
421. Herrero, R., et al., *Human papillomavirus and oral cancer: the International Agency for Research on Cancer multicenter study*. J Natl Cancer Inst, 2003. **95**(23): p. 1772-83.

422. D'Souza, G., et al., *Case-control study of human papillomavirus and oropharyngeal cancer*. N Engl J Med, 2007. **356**(19): p. 1944-56.
423. Smith, E.M., et al., *Age, sexual behavior and human papillomavirus infection in oral cavity and oropharyngeal cancers*. Int J Cancer, 2004. **108**(5): p. 766-72.
424. Satterwhite, C.L., et al., *Sexually transmitted infections among US women and men: prevalence and incidence estimates, 2008*. Sex Transm Dis, 2013. **40**(3): p. 187-93.
425. Plummer, M., et al., *Global burden of cancers attributable to infections in 2012: a synthetic analysis*. Lancet Glob Health, 2016. **4**(9): p. e609-16.
426. Giuliano, A.R., et al., *Age-specific prevalence, incidence, and duration of human papillomavirus infections in a cohort of 290 US men*. J Infect Dis, 2008. **198**(6): p. 827-35.
427. O'Sullivan, B., et al., *Outcomes of HPV-related oropharyngeal cancer patients treated by radiotherapy alone using altered fractionation*. Radiother Oncol, 2012. **103**(1): p. 49-56.
428. Marur, S. and A.A. Forastiere, *Head and neck cancer: changing epidemiology, diagnosis, and treatment*. Mayo Clin Proc, 2008. **83**(4): p. 489-501.
429. Li, W., et al., *Human papillomavirus positivity predicts favourable outcome for squamous carcinoma of the tonsil*. Int J Cancer, 2003. **106**(4): p. 553-8.
430. Ang, K.K. and E.M. Sturgis, *Human papillomavirus as a marker of the natural history and response to therapy of head and neck squamous cell carcinoma*. Semin Radiat Oncol, 2012. **22**(2): p. 128-42.
431. Muller, S., et al., *HPV positive squamous cell carcinoma of the oropharynx. Are we observing an unusual pattern of metastases?* Head Neck Pathol, 2012. **6**(3): p. 336-44.
432. Huang, S.H., et al., *Natural course of distant metastases following radiotherapy or chemoradiotherapy in HPV-related oropharyngeal cancer*. Oral Oncol, 2013. **49**(1): p. 79-85.
433. Huang, S.H., et al., *Atypical clinical behavior of p16-confirmed HPV-related oropharyngeal squamous cell carcinoma treated with radical radiotherapy*. Int J Radiat Oncol Biol Phys, 2012. **82**(1): p. 276-83.
434. Jain, K.S., et al., *Synchronous cancers in patients with head and neck cancer: risks in the era of human papillomavirus-associated oropharyngeal cancer*. Cancer, 2013. **119**(10): p. 1832-7.
435. Peck, B.W., et al., *Low risk of second primary malignancies among never smokers with human papillomavirus-associated index oropharyngeal cancers*. Head Neck, 2013. **35**(6): p. 794-9.
436. Strati, K. and P.F. Lambert, *HUMAN PAPILLOMAVIRUS ASSOCIATION WITH HEAD AND NECK CANCERS: UNDERSTANDING VIRUS BIOLOGY AND USING IT IN THE DEVELOPMENT OF CANCER DIAGNOSTICS*. Expert Opin Med Diagn, 2008. **2**(1): p. 11-20.
437. Jung, Y.S., et al., *HPV-associated differential regulation of tumor metabolism in oropharyngeal head and neck cancer*. Oncotarget, 2017. **8**(31): p. 51530-51541.
438. Jemal, A., et al., *Annual Report to the Nation on the Status of Cancer, 1975-2009, featuring the burden and trends in human papillomavirus(HPV)-associated cancers and HPV vaccination coverage levels*. J Natl Cancer Inst, 2013. **105**(3): p. 175-201.
439. Channir, H.I., et al., *Comparison of clinical, radiological and morphological features including the distribution of HPV E6/E7 oncogenes in resection specimens of oropharyngeal squamous cell carcinoma*. Oral Oncol, 2018. **78**: p. 163-170.
440. Rietbergen, M.M., et al., *No evidence for active human papillomavirus (HPV) in fields surrounding HPV-positive oropharyngeal tumors*. J Oral Pathol Med, 2014. **43**(2): p. 137-42.

441. Kim, S.H., et al., *HPV integration begins in the tonsillar crypt and leads to the alteration of p16, EGFR and c-myc during tumor formation*. *Int J Cancer*, 2007. **120**(7): p. 1418-25.
442. Gillespie, M.B., et al., *Human papillomavirus and oropharyngeal cancer: what you need to know in 2009*. *Curr Treat Options Oncol*, 2009. **10**(5-6): p. 296-307.
443. Lydiatt, W.M., et al., *Head and Neck cancers-major changes in the American Joint Committee on cancer eighth edition cancer staging manual*. *CA Cancer J Clin*, 2017. **67**(2): p. 122-137.
444. Kelly, J.R., Z.A. Husain, and B. Burtness, *Treatment de-intensification strategies for head and neck cancer*. *Eur J Cancer*, 2016. **68**: p. 125-133.
445. Kreimer, A.R., et al., *Human papillomavirus types in head and neck squamous cell carcinomas worldwide: a systematic review*. *Cancer Epidemiol Biomarkers Prev*, 2005. **14**(2): p. 467-75.
446. Klussmann, J.P., et al., *Human papillomavirus-positive tonsillar carcinomas: a different tumor entity?* *Med Microbiol Immunol*, 2003. **192**(3): p. 129-32.
447. Chernock, R.D., et al., *HPV-related nonkeratinizing squamous cell carcinoma of the oropharynx: utility of microscopic features in predicting patient outcome*. *Head Neck Pathol*, 2009. **3**(3): p. 186-94.
448. Bishop, J.A. and W.H. Westra, *Human papillomavirus-related small cell carcinoma of the oropharynx*. *Am J Surg Pathol*, 2011. **35**(11): p. 1679-84.
449. Joo, Y.H., et al., *High-risk human papillomavirus and cervical lymph node metastasis in patients with oropharyngeal cancer*. *Head Neck*, 2012. **34**(1): p. 10-4.
450. Kim, S.H., et al., *Correlations of oral tongue cancer invasion with matrix metalloproteinases (MMPs) and vascular endothelial growth factor (VEGF) expression*. *J Surg Oncol*, 2006. **93**(4): p. 330-7.
451. Joo, Y.H., et al., *Relationship between vascular endothelial growth factor and Notch1 expression and lymphatic metastasis in tongue cancer*. *Otolaryngol Head Neck Surg*, 2009. **140**(4): p. 512-8.
452. Im, S.S., et al., *Early stage cervical cancers containing human papillomavirus type 18 DNA have more nodal metastasis and deeper stromal invasion*. *Clin Cancer Res*, 2003. **9**(11): p. 4145-50.
453. Mirghani, H. and P. Blanchard, *Treatment de-escalation for HPV-driven oropharyngeal cancer: Where do we stand?* *Clin Transl Radiat Oncol*, 2018. **8**: p. 4-11.
454. Ang, K.K., et al., *Human papillomavirus and survival of patients with oropharyngeal cancer*. *N Engl J Med*, 2010. **363**(1): p. 24-35.
455. O'Sullivan, B., et al., *Development and validation of a staging system for HPV-related oropharyngeal cancer by the International Collaboration on Oropharyngeal cancer Network for Staging (ICON-S): a multicentre cohort study*. *Lancet Oncol*, 2016. **17**(4): p. 440-451.
456. Jung, Y.S., et al., *HPV-associated differential regulation of tumor metabolism in oropharyngeal head and neck cancer*. *Oncotarget*, 2017.
457. Garber, K., *Energy deregulation: licensing tumors to grow*. *Science*, 2006. **312**(5777): p. 1158-9.
458. Yeung, S.J., J. Pan, and M.H. Lee, *Roles of p53, MYC and HIF-1 in regulating glycolysis - the seventh hallmark of cancer*. *Cell Mol Life Sci*, 2008. **65**(24): p. 3981-99.
459. Quennet, V., et al., *Tumor lactate content predicts for response to fractionated irradiation of human squamous cell carcinomas in nude mice*. *Radiother Oncol*, 2006. **81**(2): p. 130-5.

460. Meijer, T.W., et al., *Targeting hypoxia, HIF-1, and tumor glucose metabolism to improve radiotherapy efficacy*. Clin Cancer Res, 2012. **18**(20): p. 5585-94.
461. Sandulache, V.C., et al., *Glucose, not glutamine, is the dominant energy source required for proliferation and survival of head and neck squamous carcinoma cells*. Cancer, 2011. **117**(13): p. 2926-38.
462. Dwarkanath, B.S., et al., *Heterogeneity in 2-deoxy-D-glucose-induced modifications in energetics and radiation responses of human tumor cell lines*. Int J Radiat Oncol Biol Phys, 2001. **50**(4): p. 1051-61.
463. Varshney, R., B. Dwarakanath, and V. Jain, *Radiosensitization by 6-aminonicotinamide and 2-deoxy-D-glucose in human cancer cells*. Int J Radiat Biol, 2005. **81**(5): p. 397-408.
464. Silva, P., et al., *Prognostic significance of tumor hypoxia inducible factor-1alpha expression for outcome after radiotherapy in oropharyngeal cancer*. Int J Radiat Oncol Biol Phys, 2008. **72**(5): p. 1551-9.
465. Schache, A.G., et al., *Evaluation of human papilloma virus diagnostic testing in oropharyngeal squamous cell carcinoma: sensitivity, specificity, and prognostic discrimination*. Clin Cancer Res, 2011. **17**(19): p. 6262-71.
466. Halestrap, A.P. and N.T. Price, *The proton-linked monocarboxylate transporter (MCT) family: structure, function and regulation*. Biochem J, 1999. **343 Pt 2**: p. 281-99.
467. Sonveaux, P., et al., *Targeting the lactate transporter MCT1 in endothelial cells inhibits lactate-induced HIF-1 activation and tumor angiogenesis*. PLoS One, 2012. **7**(3): p. e33418.
468. Bonen, A., *The expression of lactate transporters (MCT1 and MCT4) in heart and muscle*. Eur J Appl Physiol, 2001. **86**(1): p. 6-11.
469. Ganapathy, V., M. Thangaraju, and P.D. Prasad, *Nutrient transporters in cancer: relevance to Warburg hypothesis and beyond*. Pharmacol Ther, 2009. **121**(1): p. 29-40.
470. Brooks, G.A., *Cell-cell and intracellular lactate shuttles*. J Physiol, 2009. **587**(Pt 23): p. 5591-600.
471. Yano, M., K. Terada, and M. Mori, *Mitochondrial import receptors Tom20 and Tom22 have chaperone-like activity*. J Biol Chem, 2004. **279**(11): p. 10808-13.
472. Yano, M., et al., *Functional analysis of human mitochondrial receptor Tom20 for protein import into mitochondria*. J Biol Chem, 1998. **273**(41): p. 26844-51.
473. Wurm, C.A., et al., *Nanoscale distribution of mitochondrial import receptor Tom20 is adjusted to cellular conditions and exhibits an inner-cellular gradient*. Proc Natl Acad Sci U S A, 2011. **108**(33): p. 13546-51.
474. Gerdes, J., et al., *Immunobiochemical and molecular biologic characterization of the cell proliferation-associated nuclear antigen that is defined by monoclonal antibody Ki-67*. Am J Pathol, 1991. **138**(4): p. 867-73.
475. Brown, D.C. and K.C. Gatter, *Ki67 protein: the immaculate deception?* Histopathology, 2002. **40**(1): p. 2-11.
476. van Diest, P.J., E. van der Wall, and J.P. Baak, *Prognostic value of proliferation in invasive breast cancer: a review*. J Clin Pathol, 2004. **57**(7): p. 675-81.
477. Pich, A., et al., *Argyrophilic nucleolar organizer region counts and proliferating cell nuclear antigen scores are two reliable indicators of survival in pharyngeal carcinoma*. J Cancer Res Clin Oncol, 1992. **119**(2): p. 106-10.
478. Sasaki, K., et al., *The cell cycle associated change of the Ki-67 reactive nuclear antigen expression*. J Cell Physiol, 1987. **133**(3): p. 579-84.

479. Gerdes, J., et al., *Cell cycle analysis of a cell proliferation-associated human nuclear antigen defined by the monoclonal antibody Ki-67*. J Immunol, 1984. **133**(4): p. 1710-5.
480. Andreasen, P.A., et al., *The urokinase-type plasminogen activator system in cancer metastasis: a review*. Int J Cancer, 1997. **72**(1): p. 1-22.
481. Wilkins-Port, C.E., et al., *TGF-beta1 + EGF-initiated invasive potential in transformed human keratinocytes is coupled to a plasmin/MMP-10/MMP-1-dependent collagen remodeling axis: role for PAI-1*. Cancer Res, 2009. **69**(9): p. 4081-91.
482. Freytag, J., et al., *PAI-1 Regulates the Invasive Phenotype in Human Cutaneous Squamous Cell Carcinoma*. J Oncol, 2009. **2009**: p. 963209.
483. Hundsdorfer, B., et al., *[The prognostic importance of urokinase type plasminogen activators (uPA) and plasminogen activator inhibitors (PAI-1) in the primary resection of oral squamous cell carcinoma]*. Mund Kiefer Gesichtschir, 2004. **8**(3): p. 173-9.
484. Annecke, K., et al., *uPA and PAI-1 in breast cancer: review of their clinical utility and current validation in the prospective NNBC-3 trial*. Adv Clin Chem, 2008. **45**: p. 31-45.
485. Vairaktaris, E., et al., *Plasminogen activator inhibitor-1 polymorphism is associated with increased risk for oral cancer*. Oral Oncol, 2006. **42**(9): p. 888-92.
486. Illemann, M., et al., *Leading-edge myofibroblasts in human colon cancer express plasminogen activator inhibitor-1*. Am J Clin Pathol, 2004. **122**(2): p. 256-65.
487. Offersen, B.V., et al., *The myofibroblast is the predominant plasminogen activator inhibitor-1-expressing cell type in human breast carcinomas*. Am J Pathol, 2003. **163**(5): p. 1887-99.
488. Maquerlot, F., et al., *Dual role for plasminogen activator inhibitor type 1 as soluble and as extracellular regulator of epithelial alveolar cell wound healing*. Am J Pathol, 2006. **169**(5): p. 1624-32.
489. Kunz-Schughart, L.A. and R. Knuechel, *Tumor-associated fibroblasts (part I): Active stromal participants in tumor development and progression?* Histol Histopathol, 2002. **17**(2): p. 599-621.
490. Seemayer, T.A., et al., *Myofibroblasts in the stroma of invasive and metastatic carcinoma: a possible host response to neoplasia*. Am J Surg Pathol, 1979. **3**(6): p. 525-33.
491. Seemayer, T.A., et al., *The myofibroblast: biologic, pathologic, and theoretical considerations*. Pathol Annu, 1980. **15**(Pt 1): p. 443-70.
492. Aebbersold, D.M., et al., *Expression of hypoxia-inducible factor-1alpha: a novel predictive and prognostic parameter in the radiotherapy of oropharyngeal cancer*. Cancer Res, 2001. **61**(7): p. 2911-6.
493. Hui, E.P., et al., *Coexpression of hypoxia-inducible factors 1alpha and 2alpha, carbonic anhydrase IX, and vascular endothelial growth factor in nasopharyngeal carcinoma and relationship to survival*. Clin Cancer Res, 2002. **8**(8): p. 2595-604.
494. Koukourakis, M.I., et al., *Endogenous markers of two separate hypoxia response pathways (hypoxia inducible factor 2 alpha and carbonic anhydrase 9) are associated with radiotherapy failure in head and neck cancer patients recruited in the CHART randomized trial*. J Clin Oncol, 2006. **24**(5): p. 727-35.
495. Koukourakis, M.I., et al., *Hypoxia inducible factor 1 alpha and 2 alpha expression is independent of anemia in patients with stage I endometrial cancer*. Anticancer Res, 2002. **22**(6c): p. 4137-40.
496. Karamysheva, A.F., *Mechanisms of angiogenesis*. Biochemistry (Mosc), 2008. **73**(7): p. 751-62.

497. Ferrara, N., H.P. Gerber, and J. LeCouter, *The biology of VEGF and its receptors*. Nat Med, 2003. **9**(6): p. 669-76.
498. Goel, H.L. and A.M. Mercurio, *VEGF targets the tumour cell*. Nat Rev Cancer, 2013. **13**(12): p. 871-82.
499. Koch, S., et al., *Signal transduction by vascular endothelial growth factor receptors*. Biochem J, 2011. **437**(2): p. 169-83.
500. Meadows, K.N., P. Bryant, and K. Pumiglia, *Vascular endothelial growth factor induction of the angiogenic phenotype requires Ras activation*. J Biol Chem, 2001. **276**(52): p. 49289-98.
501. Zachary, I., *Signaling mechanisms mediating vascular protective actions of vascular endothelial growth factor*. Am J Physiol Cell Physiol, 2001. **280**(6): p. C1375-86.
502. Gerber, H.P., et al., *Vascular endothelial growth factor regulates endothelial cell survival through the phosphatidylinositol 3'-kinase/Akt signal transduction pathway. Requirement for Flk-1/KDR activation*. J Biol Chem, 1998. **273**(46): p. 30336-43.
503. Ritta, M., et al., *Cell cycle and viral and immunologic profiles of head and neck squamous cell carcinoma as predictable variables of tumor progression*. Head Neck, 2009. **31**(3): p. 318-27.
504. Dalianis, T., *Human papillomavirus and oropharyngeal cancer, the epidemics, and significance of additional clinical biomarkers for prediction of response to therapy (Review)*. Int J Oncol, 2014. **44**(6): p. 1799-805.
505. Chakravarthy, A., et al., *Human Papillomavirus Drives Tumor Development Throughout the Head and Neck: Improved Prognosis Is Associated With an Immune Response Largely Restricted to the Oropharynx*. J Clin Oncol, 2016. **34**(34): p. 4132-4141.
506. Alvi, A. and J.T. Johnson, *Extracapsular spread in the clinically negative neck (N0): implications and outcome*. Otolaryngol Head Neck Surg, 1996. **114**(1): p. 65-70.
507. Myers, J.N., et al., *Extracapsular spread. A significant predictor of treatment failure in patients with squamous cell carcinoma of the tongue*. Cancer, 2001. **92**(12): p. 3030-6.
508. Greenberg, J.S., et al., *Extent of extracapsular spread: a critical prognosticator in oral tongue cancer*. Cancer, 2003. **97**(6): p. 1464-70.
509. Shaw, R.J., et al., *Extracapsular spread in oral squamous cell carcinoma*. Head Neck, 2010. **32**(6): p. 714-22.
510. De Wever, O., et al., *Stromal myofibroblasts are drivers of invasive cancer growth*. Int J Cancer, 2008. **123**(10): p. 2229-38.
511. Yang, N., et al., *Syndecan-1 in breast cancer stroma fibroblasts regulates extracellular matrix fiber organization and carcinoma cell motility*. Am J Pathol, 2011. **178**(1): p. 325-35.
512. Vered, M., et al., *Tumor-host histopathologic variables, stromal myofibroblasts and risk score, are significantly associated with recurrent disease in tongue cancer*. Cancer Sci, 2010. **101**(1): p. 274-80.
513. Darshika Gandhi, D.T.a.K.H., *COMPARISON OF GLYCOPROTEIN LEVELS IN ORAL CARCINOMA BY SPECTROPHOTOMETRIC ESTIMATION USING HISTOCHEMICAL STAINS*. International Journal of Current Research, 2016. **8**(02): p. 26921-26928.
514. Triantafyllou, A., et al., *Functional Histology of Salivary Gland Pleomorphic Adenoma: An Appraisal*. Head Neck Pathol, 2015. **9**(3): p. 387-404.
515. Spicer, S.S. and D.B. Meyer, *Histochemical differentiation of acid mucopolysaccharides by means of combined aldehyde fuchsin-alcian blue staining*. Tech Bull Regist Med Technol, 1960. **30**: p. 53-60.

516. Lewis, M.P., et al., *Tumour-derived TGF-beta1 modulates myofibroblast differentiation and promotes HGF/SF-dependent invasion of squamous carcinoma cells*. Br J Cancer, 2004. **90**(4): p. 822-32.
517. Marsh, D., et al., *alpha vbeta 6 Integrin promotes the invasion of morphoeic basal cell carcinoma through stromal modulation*. Cancer Res, 2008. **68**(9): p. 3295-303.
518. Jesinghaus, M., et al., *A Novel Grading System Based on Tumor Budding and Cell Nest Size Is a Strong Predictor of Patient Outcome in Esophageal Squamous Cell Carcinoma*. Am J Surg Pathol, 2017. **41**(8): p. 1112-1120.
519. Huang, S.H. and B. O'Sullivan, *Overview of the 8th Edition TNM Classification for Head and Neck Cancer*. Curr Treat Options Oncol, 2017. **18**(7): p. 40.
520. *Treatment options for oral cavity and oropharyngeal cancer by stage*. . 2017.
521. Rivera, C.A., et al., *Chronic restraint stress in oral squamous cell carcinoma*. J Dent Res, 2011. **90**(6): p. 799-803.
522. Rivera, C. and B. Venegas, *Histological and molecular aspects of oral squamous cell carcinoma (Review)*. Oncol Lett, 2014. **8**(1): p. 7-11.
523. Oliveira, L.R., et al., *Prognostic factors and survival analysis in a sample of oral squamous cell carcinoma patients*. Oral Surg Oral Med Oral Pathol Oral Radiol Endod, 2008. **106**(5): p. 685-95.
524. Amin, M.B., et al., *The Eighth Edition AJCC Cancer Staging Manual: Continuing to build a bridge from a population-based to a more "personalized" approach to cancer staging*. CA Cancer J Clin, 2017. **67**(2): p. 93-99.
525. Larsen, S.R., et al., *The prognostic significance of histological features in oral squamous cell carcinoma*. J Oral Pathol Med, 2009. **38**(8): p. 657-62.
526. Elrefaey, S., et al., *HPV in oropharyngeal cancer: the basics to know in clinical practice*. Acta Otorhinolaryngol Ital, 2014. **34**(5): p. 299-309.
527. Schache, A.G., et al., *Validation of a novel diagnostic standard in HPV-positive oropharyngeal squamous cell carcinoma*. Br J Cancer, 2013. **108**(6): p. 1332-9.
528. El-Mofty, S.K., M.Q. Zhang, and R.M. Davila, *Histologic identification of human papillomavirus (HPV)-related squamous cell carcinoma in cervical lymph nodes: a reliable predictor of the site of an occult head and neck primary carcinoma*. Head Neck Pathol, 2008. **2**(3): p. 163-8.
529. Ringstrom, E., et al., *Human papillomavirus type 16 and squamous cell carcinoma of the head and neck*. Clin Cancer Res, 2002. **8**(10): p. 3187-92.
530. Gillison, M.L., *Human papillomavirus-related diseases: oropharynx cancers and potential implications for adolescent HPV vaccination*. J Adolesc Health, 2008. **43**(4 Suppl): p. S52-60.
531. Husain, N. and A. Neyaz, *Human papillomavirus associated head and neck squamous cell carcinoma: Controversies and new concepts*. J Oral Biol Craniofac Res, 2017. **7**(3): p. 198-205.
532. Goldenberg, D., et al., *Cystic lymph node metastasis in patients with head and neck cancer: An HPV-associated phenomenon*. Head Neck, 2008. **30**(7): p. 898-903.
533. Gillison, M.L., *Human papillomavirus-associated head and neck cancer is a distinct epidemiologic, clinical, and molecular entity*. Semin Oncol, 2004. **31**(6): p. 744-54.
534. Rampias, T., et al., *E6 and e7 gene silencing and transformed phenotype of human papillomavirus 16-positive oropharyngeal cancer cells*. J Natl Cancer Inst, 2009. **101**(6): p. 412-23.
535. Chaturvedi, A.K., *Epidemiology and clinical aspects of HPV in head and neck cancers*. Head Neck Pathol, 2012. **6 Suppl 1**: p. S16-24.
536. Spector, M.E., et al., *Patterns of nodal metastasis and prognosis in human papillomavirus-positive oropharyngeal squamous cell carcinoma*. Head Neck, 2014. **36**(9): p. 1233-40.

537. Keane, F.K., et al., *Changing prognostic significance of tumor stage and nodal stage in patients with squamous cell carcinoma of the oropharynx in the human papillomavirus era*. *Cancer*, 2015. **121**(15): p. 2594-602.
538. Cai, C., et al., *Keratinizing-type squamous cell carcinoma of the oropharynx: p16 overexpression is associated with positive high-risk HPV status and improved survival*. *Am J Surg Pathol*, 2014. **38**(6): p. 809-15.
539. Chernock, R.D., *Morphologic features of conventional squamous cell carcinoma of the oropharynx: 'keratinizing' and 'nonkeratinizing' histologic types as the basis for a consistent classification system*. *Head Neck Pathol*, 2012. **6 Suppl 1**: p. S41-7.
540. Fukano, H., et al., *Depth of invasion as a predictive factor for cervical lymph node metastasis in tongue carcinoma*. *Head Neck*, 1997. **19**(3): p. 205-10.
541. P, O.c., et al., *Tumour thickness predicts cervical nodal metastases and survival in early oral tongue cancer*. *Oral Oncol*, 2003. **39**(4): p. 386-90.
542. Mohit-Tabatabai, M.A., et al., *Relation of thickness of floor of mouth stage I and II cancers to regional metastasis*. *Am J Surg*, 1986. **152**(4): p. 351-3.
543. Moore, C., J.G. Kuhns, and R.A. Greenberg, *Thickness as prognostic aid in upper aerodigestive tract cancer*. *Arch Surg*, 1986. **121**(12): p. 1410-4.
544. Spiro, R.H., et al., *Predictive value of tumor thickness in squamous carcinoma confined to the tongue and floor of the mouth*. *Am J Surg*, 1986. **152**(4): p. 345-50.
545. Shingaki, S., et al., *Evaluation of histopathologic parameters in predicting cervical lymph node metastasis of oral and oropharyngeal carcinomas*. *Oral Surg Oral Med Oral Pathol*, 1988. **66**(6): p. 683-8.
546. Rasgon, B.M., et al., *Relation of lymph-node metastasis to histopathologic appearance in oral cavity and oropharyngeal carcinoma: a case series and literature review*. *Laryngoscope*, 1989. **99**(11): p. 1103-10.
547. Morton, R.P., et al., *Tumor thickness in early tongue cancer*. *Arch Otolaryngol Head Neck Surg*, 1994. **120**(7): p. 717-20.
548. Martinez-Gimeno, C., et al., *Squamous cell carcinoma of the oral cavity: a clinicopathologic scoring system for evaluating risk of cervical lymph node metastasis*. *Laryngoscope*, 1995. **105**(7 Pt 1): p. 728-33.
549. Yuen, A.P., et al., *A comparison of the prognostic significance of tumor diameter, length, width, thickness, area, volume, and clinicopathological features of oral tongue carcinoma*. *Am J Surg*, 2000. **180**(2): p. 139-43.
550. Asakage, T., et al., *Tumor thickness predicts cervical metastasis in patients with stage I/II carcinoma of the tongue*. *Cancer*, 1998. **82**(8): p. 1443-8.
551. Frierson, H.F., Jr. and P.H. Cooper, *Prognostic factors in squamous cell carcinoma of the lower lip*. *Hum Pathol*, 1986. **17**(4): p. 346-54.
552. Thompson, S.H., *Cervical lymph node metastases of oral carcinoma related to the depth of invasion of the primary lesion*. *J Surg Oncol*, 1986. **31**(2): p. 120-2.
553. Brown, B., et al., *Prognostic factors in mobile tongue and floor of mouth carcinoma*. *Cancer*, 1989. **64**(6): p. 1195-202.
554. Gonzalez-Moles, M.A., et al., *Importance of tumour thickness measurement in prognosis of tongue cancer*. *Oral Oncol*, 2002. **38**(4): p. 394-7.
555. Matsuura, K., et al., *Treatment results of stage I and II oral tongue cancer with interstitial brachytherapy: maximum tumor thickness is prognostic of nodal metastasis*. *Int J Radiat Oncol Biol Phys*, 1998. **40**(3): p. 535-9.
556. Al-Rajhi, N., et al., *Early stage carcinoma of oral tongue: prognostic factors for local control and survival*. *Oral Oncol*, 2000. **36**(6): p. 508-14.
557. Po Wing Yuen, A., et al., *Prognostic factors of clinically stage I and II oral tongue carcinoma-A comparative study of stage, thickness, shape, growth pattern, invasive*

- front malignancy grading, Martinez-Gimeno score, and pathologic features.* Head Neck, 2002. **24**(6): p. 513-20.
558. Yamazaki, H., et al., *Tongue cancer treated with brachytherapy: is thickness of tongue cancer a prognostic factor for regional control?* Anticancer Res, 1998. **18**(2b): p. 1261-5.
559. Ohno, K., et al., *Diagnosis of desmoplastic reaction by immunohistochemical analysis, in biopsy specimens of early colorectal carcinomas, is efficacious in estimating the depth of invasion.* Int J Mol Sci, 2013. **14**(7): p. 13129-36.
560. Martin, M., P. Pujuguet, and F. Martin, *Role of stromal myofibroblasts infiltrating colon cancer in tumor invasion.* Pathol Res Pract, 1996. **192**(7): p. 712-7.
561. Wallwork, B.D., S.R. Anderson, and W.B. Coman, *Squamous cell carcinoma of the floor of the mouth: tumour thickness and the rate of cervical metastasis.* ANZ J Surg, 2007. **77**(9): p. 761-4.
562. Lee, D.J., et al., *Histopathologic predictors of lymph node metastasis and prognosis in tonsillar squamous cell carcinoma.* Korean J Pathol, 2013. **47**(3): p. 203-10.
563. Baredes, S., et al., *Significance of tumor thickness in soft palate carcinoma.* Laryngoscope, 1993. **103**(4 Pt 1): p. 389-93.
564. Quaranta, V. and G. Giannelli, *Cancer invasion: watch your neighbourhood!* Tumori, 2003. **89**(4): p. 343-8.
565. Lieubeau, B., et al., *Immunomodulatory effects of tumor-associated fibroblasts in colorectal-tumor development.* Int J Cancer, 1999. **81**(4): p. 629-36.
566. Netti, P.A., et al., *Role of extracellular matrix assembly in interstitial transport in solid tumors.* Cancer Res, 2000. **60**(9): p. 2497-503.
567. Kouniavsky, G., et al., *Stromal extracellular matrix reduces chemotherapy-induced apoptosis in colon cancer cell lines.* Clin Exp Metastasis, 2002. **19**(1): p. 55-60.
568. Severino, P., et al., *Global gene expression profiling of oral cavity cancers suggests molecular heterogeneity within anatomic subsites.* BMC Res Notes, 2008. **1**: p. 113.
569. Franceschi, D., et al., *Improved survival in the treatment of squamous carcinoma of the oral tongue.* Am J Surg, 1993. **166**(4): p. 360-5.
570. Dobrossy, L., *Epidemiology of head and neck cancer: magnitude of the problem.* Cancer Metastasis Rev, 2005. **24**(1): p. 9-17.
571. Timar, J., et al., *Progression of head and neck squamous cell cancer.* Cancer Metastasis Rev, 2005. **24**(1): p. 107-27.
572. Yu, Y.H., H.K. Kuo, and K.W. Chang, *The evolving transcriptome of head and neck squamous cell carcinoma: a systematic review.* PLoS One, 2008. **3**(9): p. e3215.
573. Ragin, C.C., et al., *11q13 amplification status and human papillomavirus in relation to p16 expression defines two distinct etiologies of head and neck tumours.* Br J Cancer, 2006. **95**(10): p. 1432-8.
574. Slebos, R.J., et al., *Gene expression differences associated with human papillomavirus status in head and neck squamous cell carcinoma.* Clin Cancer Res, 2006. **12**(3 Pt 1): p. 701-9.
575. Schlecht, N.F., et al., *Gene expression profiles in HPV-infected head and neck cancer.* J Pathol, 2007. **213**(3): p. 283-93.
576. Shaw, R.J., et al., *Molecular staging of surgical margins in oral squamous cell carcinoma using promoter methylation of p16(INK4A), cytoglobin, E-cadherin, and TMEFF2.* Ann Surg Oncol, 2013. **20**(8): p. 2796-802.
577. van Hooff, S.R., et al., *Validation of a gene expression signature for assessment of lymph node metastasis in oral squamous cell carcinoma.* J Clin Oncol, 2012. **30**(33): p. 4104-10.

578. Blatt, S., et al., *Biomarkers in diagnosis and therapy of oral squamous cell carcinoma: A review of the literature*. J Craniomaxillofac Surg, 2017. **45**(5): p. 722-730.
579. Wittekindt, C. and J.P. Klussmann, *Tumor Staging and HPV-Related Oropharyngeal Cancer*. Recent Results Cancer Res, 2017. **206**: p. 123-133.
580. Malm, I.J., et al., *Evaluation of proposed staging systems for human papillomavirus-related oropharyngeal squamous cell carcinoma*. Cancer, 2017. **123**(10): p. 1768-1777.
581. Wurdemann, N., et al., *Prognostic Impact of AJCC/UICC 8th Edition New Staging Rules in Oropharyngeal Squamous Cell Carcinoma*. Front Oncol, 2017. **7**: p. 129.
582. Haughey, B.H., et al., *Pathology-based staging for HPV-positive squamous carcinoma of the oropharynx*. Oral Oncol, 2016. **62**: p. 11-19.
583. Saadi, A., et al., *Stromal genes discriminate preinvasive from invasive disease, predict outcome, and highlight inflammatory pathways in digestive cancers*. Proc Natl Acad Sci U S A, 2010. **107**(5): p. 2177-82.
584. Hofmeister, V., D. Schrama, and J.C. Becker, *Anti-cancer therapies targeting the tumor stroma*. Cancer Immunol Immunother, 2008. **57**(1): p. 1-17.
585. Sharma, M., et al., *Molecular changes in invasive front of oral cancer*. J Oral Maxillofac Pathol, 2013. **17**(2): p. 240-7.
586. Hoos, A. and C. Cordon-Cardo, *Tissue microarray profiling of cancer specimens and cell lines: opportunities and limitations*. Lab Invest, 2001. **81**(10): p. 1331-8.
587. Gulmann, C., et al., *Biopsy of a biopsy: validation of immunoprofiling in gastric cancer biopsy tissue microarrays*. Histopathology, 2003. **42**(1): p. 70-6.
588. Sridhara, S.U., et al., *Stromal myofibroblasts in nonmetastatic and metastatic oral squamous cell carcinoma: An immunohistochemical study*. J Oral Maxillofac Pathol, 2013. **17**(2): p. 190-4.
589. Rao, S.J., J.B.M. Rao, and P.J. Rao, *Immunohistochemical analysis of stromal fibrocytes and myofibroblasts to envision the invasion and lymph node metastasis in oral squamous cell carcinoma*. J Oral Maxillofac Pathol, 2017. **21**(2): p. 218-223.
590. Prasad, B.V., et al., *Expression of Myofibroblasts in Oral Squamous Cell Carcinoma: An Immunohistochemical Study*. J Contemp Dent Pract, 2016. **17**(10): p. 857-860.
591. Jayaraj, G., et al., *Stromal myofibroblasts in oral squamous cell carcinoma and potentially malignant disorders*. Indian J Cancer, 2015. **52**(1): p. 87-92.
592. Ha, S.Y., et al., *The prognostic significance of cancer-associated fibroblasts in esophageal squamous cell carcinoma*. PLoS One, 2014. **9**(6): p. e99955.
593. Nielsen, M.F., M.B. Mortensen, and S. Detlefsen, *Key players in pancreatic cancer-stroma interaction: Cancer-associated fibroblasts, endothelial and inflammatory cells*. World J Gastroenterol, 2016. **22**(9): p. 2678-700.
594. Jones, J.H. and J.I. Coyle, *Squamous carcinoma of the lip: a study of the interface between neoplastic epithelium and the underlying mesenchyma*. J Dent Res, 1969. **48**(5): p. 702-8.
595. Woolgar, J.A. and A. Triantafyllou, *Squamous cell carcinoma and precursor lesions: clinical pathology*. Periodontol 2000, 2011. **57**(1): p. 51-72.
596. Woolgar, J.e.a., *Neck dissections: A practical guide for the reporting histopathologist*. Current Diagnostic Pathology **13**(6): p. 499 - 511
597. Selman, M. and A. Pardo, *Idiopathic pulmonary fibrosis: an epithelial/fibroblastic cross-talk disorder*. Respir Res, 2002. **3**: p. 3.
598. Kalluri, R. and R.A. Weinberg, *The basics of epithelial-mesenchymal transition*. J Clin Invest, 2009. **119**(6): p. 1420-8.

599. Scheel, C. and R.A. Weinberg, *Cancer stem cells and epithelial-mesenchymal transition: concepts and molecular links*. *Semin Cancer Biol*, 2012. **22**(5-6): p. 396-403.
600. Jolly, M.K., et al., *Towards elucidating the connection between epithelial-mesenchymal transitions and stemness*. *J R Soc Interface*, 2014. **11**(101): p. 20140962.
601. Bhowmick, N.A., et al., *TGF-beta signaling in fibroblasts modulates the oncogenic potential of adjacent epithelia*. *Science*, 2004. **303**(5659): p. 848-51.
602. Borges, F.T., et al., *TGF-beta1-containing exosomes from injured epithelial cells activate fibroblasts to initiate tissue regenerative responses and fibrosis*. *J Am Soc Nephrol*, 2013. **24**(3): p. 385-92.
603. Shimoda, M., et al., *Loss of the Timp gene family is sufficient for the acquisition of the CAF-like cell state*. *Nat Cell Biol*, 2014. **16**(9): p. 889-901.
604. Klein, R.M., et al., *SERPINE1 expression discriminates site-specific metastasis in human melanoma*. *Exp Dermatol*, 2012. **21**(7): p. 551-4.
605. Czekay, R.P., et al., *PAI-1: An Integrator of Cell Signaling and Migration*. *Int J Cell Biol*, 2011. **2011**: p. 562481.
606. Brooks, T.D., et al., *Antibodies to PAI-1 alter the invasive and migratory properties of human tumour cells in vitro*. *Clin Exp Metastasis*, 2000. **18**(6): p. 445-53.
607. van Muijen, G.N., et al., *Properties of metastasizing and nonmetastasizing human melanoma cells*. *Recent Results Cancer Res*, 1995. **139**: p. 105-22.
608. Bryne, M., et al., *Malignancy grading of the deep invasive margins of oral squamous cell carcinomas has high prognostic value*. *J Pathol*, 1992. **166**(4): p. 375-81.
609. Piffko, J., et al., *Molecular assessment of p53 abnormalities at the invasive front of oral squamous cell carcinomas*. *Head Neck*, 1998. **20**(1): p. 8-15.
610. Kato, K., et al., *Expression form of p53 and PCNA at the invasive front in oral squamous cell carcinoma: correlation with clinicopathological features and prognosis*. *J Oral Pathol Med*, 2011. **40**(9): p. 693-8.
611. Levine, A.J. and A.M. Puzio-Kuter, *The control of the metabolic switch in cancers by oncogenes and tumor suppressor genes*. *Science*, 2010. **330**(6009): p. 1340-4.
612. Vaughn, A.E. and M. Deshmukh, *Glucose metabolism inhibits apoptosis in neurons and cancer cells by redox inactivation of cytochrome c*. *Nat Cell Biol*, 2008. **10**(12): p. 1477-83.
613. Schafer, Z.T., et al., *Antioxidant and oncogene rescue of metabolic defects caused by loss of matrix attachment*. *Nature*, 2009. **461**(7260): p. 109-13.
614. Walenta, S., et al., *Correlation of high lactate levels in head and neck tumors with incidence of metastasis*. *Am J Pathol*, 1997. **150**(2): p. 409-15.
615. Brizel, D.M., et al., *Elevated tumor lactate concentrations predict for an increased risk of metastases in head-and-neck cancer*. *Int J Radiat Oncol Biol Phys*, 2001. **51**(2): p. 349-53.
616. Fantin, V.R., J. St-Pierre, and P. Leder, *Attenuation of LDH-A expression uncovers a link between glycolysis, mitochondrial physiology, and tumor maintenance*. *Cancer Cell*, 2006. **9**(6): p. 425-34.
617. Witkiewicz, A.K., et al., *Using the "reverse Warburg effect" to identify high-risk breast cancer patients: stromal MCT4 predicts poor clinical outcome in triple-negative breast cancers*. *Cell Cycle*, 2012. **11**(6): p. 1108-17.
618. Liu, M., et al., *Predictive value of the fraction of cancer cells immunolabeled for proliferating cell nuclear antigen or Ki67 in biopsies of head and neck carcinomas to identify lymph node metastasis: comparison with clinical and radiologic examinations*. *Head Neck*, 2003. **25**(4): p. 280-8.

619. Pich, A., L. Chiusa, and R. Navone, *Prognostic relevance of cell proliferation in head and neck tumors*. *Ann Oncol*, 2004. **15**(9): p. 1319-29.
620. Gillison, M.L., et al., *Evidence for a causal association between human papillomavirus and a subset of head and neck cancers*. *J Natl Cancer Inst*, 2000. **92**(9): p. 709-20.
621. Fouret, P., et al., *Human papillomavirus in head and neck squamous cell carcinomas in nonsmokers*. *Arch Otolaryngol Head Neck Surg*, 1997. **123**(5): p. 513-6.
622. Haraf, D.J., et al., *Human papilloma virus and p53 in head and neck cancer: clinical correlates and survival*. *Clin Cancer Res*, 1996. **2**(4): p. 755-62.
623. De Petrini, M., et al., *Head and neck squamous cell carcinoma: role of the human papillomavirus in tumour progression*. *New Microbiol*, 2006. **29**(1): p. 25-33.
624. Tripathi, P., et al., *Delineating metabolic signatures of head and neck squamous cell carcinoma: phospholipase A2, a potential therapeutic target*. *Int J Biochem Cell Biol*, 2012. **44**(11): p. 1852-61.
625. Jensen, D.H., M.H. Therkildsen, and E. Dabelsteen, *A reverse Warburg metabolism in oral squamous cell carcinoma is not dependent upon myofibroblasts*. *J Oral Pathol Med*, 2015. **44**(9): p. 714-21.
626. Button, K.S., et al., *Power failure: why small sample size undermines the reliability of neuroscience*. *Nat Rev Neurosci*, 2013. **14**(5): p. 365-76.
627. Curry, J., et al., *Tumor Metabolism in the Microenvironment of Nodal Metastasis in Oral Squamous Cell Carcinoma*. *Otolaryngol Head Neck Surg*, 2017: p. 194599817709224.
628. Liu, J., et al., *Ki67 Expression has Prognostic Significance in Relation to Human Papillomavirus Status in Oropharyngeal Squamous Cell Carcinoma*. *Ann Surg Oncol*, 2015. **22**(6): p. 1893-900.
629. Semenza, G.L., *Tumor metabolism: cancer cells give and take lactate*. *J Clin Invest*, 2008. **118**(12): p. 3835-7.
630. Fang, J., et al., *The H⁺-linked monocarboxylate transporter (MCT1/SLC16A1): a potential therapeutic target for high-risk neuroblastoma*. *Mol Pharmacol*, 2006. **70**(6): p. 2108-15.
631. Amorim, R., et al., *Monocarboxylate transport inhibition potentiates the cytotoxic effect of 5-fluorouracil in colorectal cancer cells*. *Cancer Lett*, 2015. **365**(1): p. 68-78.
632. Draoui, N., et al., *Antitumor activity of 7-aminocarboxycoumarin derivatives, a new class of potent inhibitors of lactate influx but not efflux*. *Mol Cancer Ther*, 2014. **13**(6): p. 1410-8.
633. Pertega-Gomes, N., et al., *A glycolytic phenotype is associated with prostate cancer progression and aggressiveness: a role for monocarboxylate transporters as metabolic targets for therapy*. *J Pathol*, 2015. **236**(4): p. 517-30.
634. Jones, N.P. and A. Schulze, *Targeting cancer metabolism--aiming at a tumour's sweet-spot*. *Drug Discov Today*, 2012. **17**(5-6): p. 232-41.
635. Marchiq, I., et al., *Genetic disruption of lactate/H⁺ symporters (MCTs) and their subunit CD147/BASIGIN sensitizes glycolytic tumor cells to phenformin*. *Cancer Res*, 2015. **75**(1): p. 171-80.
636. Granja, S., et al., *Disruption of BASIGIN decreases lactic acid export and sensitizes non-small cell lung cancer to biguanides independently of the LKB1 status*. *Oncotarget*, 2015. **6**(9): p. 6708-21.
637. Pollak, M., *Potential applications for biguanides in oncology*. *J Clin Invest*, 2013. **123**(9): p. 3693-700.
638. Kaanders, J.H., et al., *Pimonidazole binding and tumor vascularity predict for treatment outcome in head and neck cancer*. *Cancer Res*, 2002. **62**(23): p. 7066-74.

639. Doyen, J., et al., *Expression of the hypoxia-inducible monocarboxylate transporter MCT4 is increased in triple negative breast cancer and correlates independently with clinical outcome*. *Biochem Biophys Res Commun*, 2014. **451**(1): p. 54-61.
640. Weinberg, F., et al., *Mitochondrial metabolism and ROS generation are essential for Kras-mediated tumorigenicity*. *Proc Natl Acad Sci U S A*, 2010. **107**(19): p. 8788-93.
641. Pike, L.S., et al., *Inhibition of fatty acid oxidation by etomoxir impairs NADPH production and increases reactive oxygen species resulting in ATP depletion and cell death in human glioblastoma cells*. *Biochim Biophys Acta*, 2011. **1807**(6): p. 726-34.
642. Walenta, S., et al., *Tissue gradients of energy metabolites mirror oxygen tension gradients in a rat mammary carcinoma model*. *Int J Radiat Oncol Biol Phys*, 2001. **51**(3): p. 840-8.
643. Hirayama, A., et al., *Quantitative metabolome profiling of colon and stomach cancer microenvironment by capillary electrophoresis time-of-flight mass spectrometry*. *Cancer Res*, 2009. **69**(11): p. 4918-25.
644. De Saedeleer, C.J., et al., *Glucose deprivation increases monocarboxylate transporter 1 (MCT1) expression and MCT1-dependent tumor cell migration*. *Oncogene*, 2014. **33**(31): p. 4060-8.
645. Dhup, S., et al., *Multiple biological activities of lactic acid in cancer: influences on tumor growth, angiogenesis and metastasis*. *Curr Pharm Des*, 2012. **18**(10): p. 1319-30.
646. Kirk, P., et al., *CD147 is tightly associated with lactate transporters MCT1 and MCT4 and facilitates their cell surface expression*. *Embo j*, 2000. **19**(15): p. 3896-904.
647. Le Floch, R., et al., *CD147 subunit of lactate/H⁺ symporters MCT1 and hypoxia-inducible MCT4 is critical for energetics and growth of glycolytic tumors*. *Proc Natl Acad Sci U S A*, 2011. **108**(40): p. 16663-8.
648. Carpenter, L. and A.P. Halestrap, *The kinetics, substrate and inhibitor specificity of the lactate transporter of Ehrlich-Lette tumour cells studied with the intracellular pH indicator BCECF*. *Biochem J*, 1994. **304 (Pt 3)**: p. 751-60.
649. https://web.expasy.org/cellosaurus/CVCL_7779, UMSCC 74A
650. Brenner, J.C., et al., *Genotyping of 73 UM-SCC head and neck squamous cell carcinoma cell lines*. *Head Neck*, 2010. **32**(4): p. 417-26.
651. https://www.lgcstandards-atcc.org/Products/Cells_and_Microorganisms/By_Tissue/Other_Tissues/Tongue/CRL-3241.aspx?geo_country=gb, UPCI:SCC154
652. https://web.expasy.org/cellosaurus/CVCL_2230, UPCI-SCC-154
653. Diers, A.R., et al., *Pyruvate fuels mitochondrial respiration and proliferation of breast cancer cells: effect of monocarboxylate transporter inhibition*. *Biochem J*, 2012. **444**(3): p. 561-71.
654. Sliwka, L., et al., *The Comparison of MTT and CVS Assays for the Assessment of Anticancer Agent Interactions*. *PLoS One*, 2016. **11**(5): p. e0155772.
655. Chiba, K., K. Kawakami, and K. Tohyama, *Simultaneous evaluation of cell viability by neutral red, MTT and crystal violet staining assays of the same cells*. *Toxicol In Vitro*, 1998. **12**(3): p. 251-8.
656. Saotome, K., H. Morita, and M. Umeda, *Cytotoxicity test with simplified crystal violet staining method using microtitre plates and its application to injection drugs*. *Toxicol In Vitro*, 1989. **3**(4): p. 317-21.
657. Vistica, D.T., et al., *Tetrazolium-based assays for cellular viability: a critical examination of selected parameters affecting formazan production*. *Cancer Res*, 1991. **51**(10): p. 2515-20.
658. Shoemaker, M., I. Cohen, and M. Campbell, *Reduction of MTT by aqueous herbal extracts in the absence of cells*. *J Ethnopharmacol*, 2004. **93**(2-3): p. 381-4.

659. Wang, P., S.M. Henning, and D. Heber, *Limitations of MTT and MTS-based assays for measurement of antiproliferative activity of green tea polyphenols*. PLoS One, 2010. **5**(4): p. e10202.
660. Bruggisser, R., et al., *Interference of plant extracts, phytoestrogens and antioxidants with the MTT tetrazolium assay*. Planta Med, 2002. **68**(5): p. 445-8.
661. Berridge, M.V., P.M. Herst, and A.S. Tan, *Tetrazolium dyes as tools in cell biology: new insights into their cellular reduction*. Biotechnol Annu Rev, 2005. **11**: p. 127-52.
662. Porporato, P.E., et al., *Anticancer targets in the glycolytic metabolism of tumors: a comprehensive review*. Front Pharmacol, 2011. **2**: p. 49.
663. Halestrap, A.P. and M.C. Wilson, *The monocarboxylate transporter family--role and regulation*. IUBMB Life, 2012. **64**(2): p. 109-19.
664. Asada, K., et al., *Reduced expression of GNA11 and silencing of MCT1 in human breast cancers*. Oncology, 2003. **64**(4): p. 380-8.
665. Wallace, D.C., *Mitochondria and cancer*. Nat Rev Cancer, 2012. **12**(10): p. 685-98.
666. Lee, G.H., et al., *Lysyl oxidase-like-1 enhances lung metastasis when lactate accumulation and monocarboxylate transporter expression are involved*. Oncol Lett, 2011. **2**(5): p. 831-838.
667. Ferretti, A.C., M.C. Larocca, and C. Favre, *Nutritional stress in eukaryotic cells: oxidative species and regulation of survival in time of scarceness*. Mol Genet Metab, 2012. **105**(2): p. 186-92.
668. Iacono, K.T., et al., *CD147 immunoglobulin superfamily receptor function and role in pathology*. Exp Mol Pathol, 2007. **83**(3): p. 283-95.
669. Boidot, R., et al., *Regulation of monocarboxylate transporter MCT1 expression by p53 mediates inward and outward lactate fluxes in tumors*. Cancer Res, 2012. **72**(4): p. 939-48.
670. Ke, X., et al., *Hypoxia upregulates CD147 through a combined effect of HIF-1alpha and Sp1 to promote glycolysis and tumor progression in epithelial solid tumors*. Carcinogenesis, 2012. **33**(8): p. 1598-607.
671. Merezhinskaya, N. and W.N. Fishbein, *Monocarboxylate transporters: past, present, and future*. Histol Histopathol, 2009. **24**(2): p. 243-64.
672. Rademakers, S.E., et al., *Metabolic markers in relation to hypoxia; staining patterns and colocalization of pimonidazole, HIF-1alpha, CAIX, LDH-5, GLUT-1, MCT1 and MCT4*. BMC Cancer, 2011. **11**: p. 167.
673. Cheng, C., et al., *Alterations of monocarboxylate transporter densities during hypoxia in brain and breast tumour cells*. Cell Oncol (Dordr), 2012. **35**(3): p. 217-27.
674. Dang, C.V., *MYC, microRNAs and glutamine addiction in cancers*. Cell Cycle, 2009. **8**(20): p. 3243-5.
675. Dang, C.V., et al., *Therapeutic targeting of cancer cell metabolism*. J Mol Med (Berl), 2011. **89**(3): p. 205-12.
676. Warburg, O., *On the origin of cancer cells*. Science, 1956. **123**(3191): p. 309-14.
677. Hussien, R. and G.A. Brooks, *Mitochondrial and plasma membrane lactate transporter and lactate dehydrogenase isoform expression in breast cancer cell lines*. Physiol Genomics, 2011. **43**(5): p. 255-64.
678. Pagliarini, D.J., et al., *A mitochondrial protein compendium elucidates complex I disease biology*. Cell, 2008. **134**(1): p. 112-23.
679. Li, J.Z., et al., *Hypoxia in head and neck squamous cell carcinoma*. ISRN Otolaryngol, 2012. **2012**: p. 708974.
680. McKeown, S.R., *Defining normoxia, physoxia and hypoxia in tumours-implications for treatment response*. Br J Radiol, 2014. **87**(1035): p. 20130676.

681. Kennedy, A.S., et al., *Proliferation and hypoxia in human squamous cell carcinoma of the cervix: first report of combined immunohistochemical assays*. Int J Radiat Oncol Biol Phys, 1997. **37**(4): p. 897-905.
682. Nordsmark, M., et al., *Measurements of hypoxia using pimonidazole and polarographic oxygen-sensitive electrodes in human cervix carcinomas*. Radiother Oncol, 2003. **67**(1): p. 35-44.
683. Harriss, W., et al., *Measurement of reoxygenation during fractionated radiotherapy in head and neck squamous cell carcinoma xenografts*. Australas Phys Eng Sci Med, 2010. **33**(3): p. 251-63.
684. Hockel, M. and P. Vaupel, *Tumor hypoxia: definitions and current clinical, biologic, and molecular aspects*. J Natl Cancer Inst, 2001. **93**(4): p. 266-76.
685. Jo, S., et al., *Human papillomavirus infection as a prognostic factor in oropharyngeal squamous cell carcinomas treated in a prospective phase II clinical trial*. Anticancer Res, 2009. **29**(5): p. 1467-74.
686. Sauter, E.R., et al., *Vascular endothelial growth factor is a marker of tumor invasion and metastasis in squamous cell carcinomas of the head and neck*. Clin Cancer Res, 1999. **5**(4): p. 775-82.
687. Hicklin, D.J. and L.M. Ellis, *Role of the vascular endothelial growth factor pathway in tumor growth and angiogenesis*. J Clin Oncol, 2005. **23**(5): p. 1011-27.
688. Troy, J.D., et al., *Expression of EGFR, VEGF, and NOTCH1 suggest differences in tumor angiogenesis in HPV-positive and HPV-negative head and neck squamous cell carcinoma*. Head Neck Pathol, 2013. **7**(4): p. 344-55.
689. Kyzas, P.A., I.W. Cunha, and J.P. Ioannidis, *Prognostic significance of vascular endothelial growth factor immunohistochemical expression in head and neck squamous cell carcinoma: a meta-analysis*. Clin Cancer Res, 2005. **11**(4): p. 1434-40.
690. Dunst, J., et al., *Tumor hypoxia and systemic levels of vascular endothelial growth factor (VEGF) in head and neck cancers*. Strahlenther Onkol, 2001. **177**(9): p. 469-73.
691. Mohamed, K.M., et al., *Correlation between VEGF and HIF-1alpha expression in human oral squamous cell carcinoma*. Exp Mol Pathol, 2004. **76**(2): p. 143-52.
692. Kyzas, P.A., et al., *Hypoxia-induced tumor angiogenic pathway in head and neck cancer: an in vivo study*. Cancer Lett, 2005. **225**(2): p. 297-304.
693. Martins, S.F., et al., *Clinicopathological correlation and prognostic significance of VEGF-A, VEGF-C, VEGFR-2 and VEGFR-3 expression in colorectal cancer*. Cancer Genomics Proteomics, 2013. **10**(2): p. 55-67.
694. Pradeep, C.R., E.S. Sunila, and G. Kuttan, *Expression of vascular endothelial growth factor (VEGF) and VEGF receptors in tumor angiogenesis and malignancies*. Integr Cancer Ther, 2005. **4**(4): p. 315-21.
695. Pianka, A., et al., *Vascular endothelial growth factor receptor isoforms: are they present in oral squamous cell carcinoma?* J Oral Maxillofac Surg, 2015. **73**(5): p. 897-904.
696. Aggarwal, S., et al., *Expression of vascular endothelial growth factor (VEGF) in patients with oral squamous cell carcinoma and its clinical significance*. Clin Chim Acta, 2014. **436**: p. 35-40.
697. Kyzas, P.A., et al., *Potential autocrine function of vascular endothelial growth factor in head and neck cancer via vascular endothelial growth factor receptor-2*. Mod Pathol, 2005. **18**(4): p. 485-94.
698. Lalla, R.V., et al., *Expression of vascular endothelial growth factor receptors on tumor cells in head and neck squamous cell carcinoma*. Arch Otolaryngol Head Neck Surg, 2003. **129**(8): p. 882-8.

699. Ciurea, R., et al., *VEGF and his R1 and R2 receptors expression in mast cells of oral squamous cells carcinomas and their involvement in tumoral angiogenesis*. Rom J Morphol Embryol, 2011. **52**(4): p. 1227-32.
700. Masood, R., et al., *Vascular endothelial growth factor (VEGF) is an autocrine growth factor for VEGF receptor-positive human tumors*. Blood, 2001. **98**(6): p. 1904-13.
701. Ahluwalia, A., et al., *Aberrant, ectopic expression of VEGF and VEGF receptors 1 and 2 in malignant colonic epithelial cells. Implications for these cells growth via an autocrine mechanism*. Biochem Biophys Res Commun, 2013. **437**(4): p. 515-20.
702. Li, C., et al., *Expression of angiopoietin-2 and vascular endothelial growth factor receptor-3 correlates with lymphangiogenesis and angiogenesis and affects survival of oral squamous cell carcinoma*. PLoS One, 2013. **8**(9): p. e75388.
703. Weinberger, P.M., et al., *Defining molecular phenotypes of human papillomavirus-associated oropharyngeal squamous cell carcinoma: validation of three-class hypothesis*. Otolaryngol Head Neck Surg, 2009. **141**(3): p. 382-9.
704. Fei, J., et al., *Prognostic significance of vascular endothelial growth factor in squamous cell carcinomas of the tonsil in relation to human papillomavirus status and epidermal growth factor receptor*. Ann Surg Oncol, 2009. **16**(10): p. 2908-17.
705. Grimminger, C.M. and P.V. Danenberg, *Update of prognostic and predictive biomarkers in oropharyngeal squamous cell carcinoma: a review*. Eur Arch Otorhinolaryngol, 2011. **268**(1): p. 5-16.
706. Mandriota, S.J., et al., *Vascular endothelial growth factor-C-mediated lymphangiogenesis promotes tumour metastasis*. Embo j, 2001. **20**(4): p. 672-82.
707. Su, J.L., et al., *The VEGF-C/Flt-4 axis promotes invasion and metastasis of cancer cells*. Cancer Cell, 2006. **9**(3): p. 209-23.
708. Smith, B.D., et al., *Prognostic significance of vascular endothelial growth factor protein levels in oral and oropharyngeal squamous cell carcinoma*. J Clin Oncol, 2000. **18**(10): p. 2046-52.
709. Lopez-Ocejo, O., et al., *Oncogenes and tumor angiogenesis: the HPV-16 E6 oncoprotein activates the vascular endothelial growth factor (VEGF) gene promoter in a p53 independent manner*. Oncogene, 2000. **19**(40): p. 4611-20.
710. Kim, S.H., et al., *Human papillomavirus 16 E5 up-regulates the expression of vascular endothelial growth factor through the activation of epidermal growth factor receptor, MEK/ ERK1,2 and PI3K/Akt*. Cell Mol Life Sci, 2006. **63**(7-8): p. 930-8.
711. Tang, X., et al., *Overexpression of human papillomavirus type 16 oncoproteins enhances hypoxia-inducible factor 1 alpha protein accumulation and vascular endothelial growth factor expression in human cervical carcinoma cells*. Clin Cancer Res, 2007. **13**(9): p. 2568-76.
712. Alkharsah, K.R., *VEGF Upregulation in Viral Infections and Its Possible Therapeutic Implications*. Int J Mol Sci, 2018. **19**(6).
713. Li, F. and J. Cui, *Human telomerase reverse transcriptase regulates vascular endothelial growth factor expression via human papillomavirus oncogene E7 in HPV-18-positive cervical cancer cells*. Med Oncol, 2015. **32**(7): p. 199.
714. Weljie, A.M. and F.R. Jirik, *Hypoxia-induced metabolic shifts in cancer cells: moving beyond the Warburg effect*. Int J Biochem Cell Biol, 2011. **43**(7): p. 981-9.
715. Eckert, A.W., et al., *Coexpression of hypoxia-inducible factor-1alpha and glucose transporter-1 is associated with poor prognosis in oral squamous cell carcinoma patients*. Histopathology, 2011. **58**(7): p. 1136-47.
716. Ogane, N., et al., *Clinicopathological implications of expressions of hypoxia-related molecules in esophageal superficial squamous cell carcinoma*. Ann Diagn Pathol, 2010. **14**(1): p. 23-9.

717. Sulkowska, M., et al., *Relations of TGF-beta1 with HIF-1 alpha, GLUT-1 and longer survival of colorectal cancer patients*. Pathology, 2009. **41**(3): p. 254-60.
718. Iida, T., et al., *Hypoxic status in ovarian serous and mucinous tumors: relationship between histological characteristics and HIF-1alpha/GLUT-1 expression*. Arch Gynecol Obstet, 2008. **277**(6): p. 539-46.
719. Lidgren, A., et al., *Glucose transporter-1 expression in renal cell carcinoma and its correlation with hypoxia inducible factor-1 alpha*. BJU Int, 2008. **101**(4): p. 480-4.
720. Palit, V., et al., *Expression of HIF-1alpha and Glut-1 in human bladder cancer*. Oncol Rep, 2005. **14**(4): p. 909-13.
721. Pez, F., et al., *The HIF-1-inducible lysyl oxidase activates HIF-1 via the Akt pathway in a positive regulation loop and synergizes with HIF-1 in promoting tumor cell growth*. Cancer Res, 2011. **71**(5): p. 1647-57.
722. Zhou, S.H., et al., *Inhibition of cell proliferation and glucose uptake in human laryngeal carcinoma cells by antisense oligonucleotides against glucose transporter-1*. Head Neck, 2009. **31**(12): p. 1624-33.
723. Wincewicz, A., et al., *Clinicopathological significance and linkage of the distribution of HIF-1alpha and GLUT-1 in human primary colorectal cancer*. Pathol Oncol Res, 2007. **13**(1): p. 15-20.
724. Wu, X.H., et al., *Expression and significance of hypoxia-inducible factor-1alpha and glucose transporter-1 in laryngeal carcinoma*. Oncol Lett, 2013. **5**(1): p. 261-266.
725. Beasley, N.J., et al., *Hypoxia-inducible factors HIF-1alpha and HIF-2alpha in head and neck cancer: relationship to tumor biology and treatment outcome in surgically resected patients*. Cancer Res, 2002. **62**(9): p. 2493-7.
726. Fillies, T., et al., *HIF1-alpha overexpression indicates a good prognosis in early stage squamous cell carcinomas of the oral floor*. BMC Cancer, 2005. **5**: p. 84.
727. Koukourakis, M.I., et al., *Hypoxia-activated tumor pathways of angiogenesis and pH regulation independent of anemia in head-and-neck cancer*. Int J Radiat Oncol Biol Phys, 2004. **59**(1): p. 67-71.
728. Burri, P., et al., *Significant correlation of hypoxia-inducible factor-1alpha with treatment outcome in cervical cancer treated with radical radiotherapy*. Int J Radiat Oncol Biol Phys, 2003. **56**(2): p. 494-501.
729. Ishikawa, H., et al., *Expression of hypoxic-inducible factor 1alpha predicts metastasis-free survival after radiation therapy alone in stage IIIB cervical squamous cell carcinoma*. Int J Radiat Oncol Biol Phys, 2004. **60**(2): p. 513-21.
730. Overgaard, J., et al., *Five compared with six fractions per week of conventional radiotherapy of squamous-cell carcinoma of head and neck: DAHANCA 6 and 7 randomised controlled trial*. Lancet, 2003. **362**(9388): p. 933-40.
731. Amdur, R.J., et al., *Postoperative irradiation for squamous cell carcinoma of the head and neck: an analysis of treatment results and complications*. Int J Radiat Oncol Biol Phys, 1989. **16**(1): p. 25-36.
732. Hunter, K.D., E.K. Parkinson, and P.R. Harrison, *Profiling early head and neck cancer*. Nat Rev Cancer, 2005. **5**(2): p. 127-35.
733. Pertega-Gomes, N., et al., *A lactate shuttle system between tumour and stromal cells is associated with poor prognosis in prostate cancer*. BMC Cancer, 2014. **14**: p. 352.
734. Andersen, S., et al., *Organized metabolic crime in prostate cancer: The coexpression of MCT1 in tumor and MCT4 in stroma is an independent prognosticator for biochemical failure*. Urol Oncol, 2015. **33**(8): p. 338.e9-17.
735. Schrijvers, M.L., et al., *Overexpression of intrinsic hypoxia markers HIF1alpha and CA-IX predict for local recurrence in stage T1-T2 glottic laryngeal carcinoma treated with radiotherapy*. Int J Radiat Oncol Biol Phys, 2008. **72**(1): p. 161-9.

736. Koukourakis, M.I., et al., *Comparison of metabolic pathways between cancer cells and stromal cells in colorectal carcinomas: a metabolic survival role for tumor-associated stroma*. *Cancer Res*, 2006. **66**(2): p. 632-7.
737. Yasuda, M., et al., *Expression of hypoxia inducible factor-1alpha (HIF-1alpha) and glucose transporter-1 (GLUT-1) in ovarian adenocarcinomas: difference in hypoxic status depending on histological character*. *Oncol Rep*, 2008. **19**(1): p. 111-6.
738. Neuchrist, C., et al., *Vascular endothelial growth factor receptor 2 (VEGFR2) expression in squamous cell carcinomas of the head and neck*. *Laryngoscope*, 2001. **111**(10): p. 1834-41.
739. Neuchrist, C., et al., *Vascular endothelial growth factor C and vascular endothelial growth factor receptor 3 expression in squamous cell carcinomas of the head and neck*. *Head Neck*, 2003. **25**(6): p. 464-74.
740. Herold-Mende, C., et al., *[Functional expression of vascular endothelial growth factor receptor Flt-1 on squamous cell carcinoma of the head and neck]*. *Hno*, 1999. **47**(8): p. 706-11.
741. Denhart, B.C., et al., *Vascular permeability factor/vascular endothelial growth factor and its receptors in oral and laryngeal squamous cell carcinoma and dysplasia*. *Lab Invest*, 1997. **77**(6): p. 659-64.
742. Matsuura, M., et al., *Autocrine loop between vascular endothelial growth factor (VEGF)-C and VEGF receptor-3 positively regulates tumor-associated lymphangiogenesis in oral squamoid cancer cells*. *Am J Pathol*, 2009. **175**(4): p. 1709-21.
743. Peng, H.S., et al., *Synergistic inhibitory effect of hyperbaric oxygen combined with sorafenib on hepatoma cells*. *PLoS One*, 2014. **9**(6): p. e100814.
744. Fury, M.G., et al., *A phase 2 study of bevacizumab with cisplatin plus intensity-modulated radiation therapy for stage III/IVB head and neck squamous cell cancer*. *Cancer*, 2012. **118**(20): p. 5008-14.
745. Marin-Pozo, J.F., J.M. Duarte-Perez, and P. Sanchez-Rovira, *Safety, Effectiveness, and Costs of Bevacizumab-Based Therapy in Southern Spain: A Real World Experience*. *Medicine (Baltimore)*, 2016. **95**(19): p. e3623.
746. Tebbutt, N.C., et al., *Capecitabine, bevacizumab, and mitomycin in first-line treatment of metastatic colorectal cancer: results of the Australasian Gastrointestinal Trials Group Randomized Phase III MAX Study*. *J Clin Oncol*, 2010. **28**(19): p. 3191-8.
747. Herbst, R.S., et al., *Phase II study of efficacy and safety of bevacizumab in combination with chemotherapy or erlotinib compared with chemotherapy alone for treatment of recurrent or refractory non small-cell lung cancer*. *J Clin Oncol*, 2007. **25**(30): p. 4743-50.
748. Argiris, A., et al., *Cetuximab and bevacizumab: preclinical data and phase II trial in recurrent or metastatic squamous cell carcinoma of the head and neck*. *Ann Oncol*, 2013. **24**(1): p. 220-5.
749. Argiris, A., et al., *Phase II trial of pemetrexed and bevacizumab in patients with recurrent or metastatic head and neck cancer*. *J Clin Oncol*, 2011. **29**(9): p. 1140-5.
750. Cohen, E.E., et al., *Erlotinib and bevacizumab in patients with recurrent or metastatic squamous-cell carcinoma of the head and neck: a phase I/II study*. *Lancet Oncol*, 2009. **10**(3): p. 247-57.
751. Hulkower, K.I. and R.L. Herber, *Cell migration and invasion assays as tools for drug discovery*. *Pharmaceutics*, 2011. **3**(1): p. 107-24.
752. Chandrasekaran, S., H. Deng, and Y. Fang, *PTEN deletion potentiates invasion of colorectal cancer spheroidal cells through 3D Matrigel*. *Integr Biol (Camb)*, 2015. **7**(3): p. 324-34.

APPENDICIES

Appendix 1. Clinical and pathological characteristics of the HPV+ OPSCC study cohort.

	pN0	pN+ECS-	pN+ECS+
Age (years)			
Range	28-67	40-70	34-70
Mean	55	55	55
Gender			
Male	7	8	20
Female	1	6	1
Tumour site			
Soft Palate	1	0	1
Base of tongue	1	3	5
Tonsil	3	6	12
Oropharynx	3	5	4
Pathological T-stage			
pT1	1	0	1
pT2	5	7	10
pT3	2	6	8
pT4	0	1	1
Pathological N-stage			
N0	8	0	0
N1	0	3	3

N2	0	11	19
----	---	----	----

Appendix 2. Clinical and pathological characteristics of the HPV- OPSCC study cohort.

	pN0	pN+ECS-	pN+ECS+
Age (years)			
Range	40-80	40-80	40-80
Mean	60	60	60
Gender			
No data available			
Tumour site			
Soft Palate	2	1	3
Base of tongue	1	0	3
Tonsil	3	5	10
Oropharynx	1	0	0
Pathological T-stage			
T1	1	0	0
T2	3	1	8
T3	1	3	5
pT4	2	2	3
Pathological N-stage			
N0	7	0	0
N1	0	2	4
N2	1	4	12

Appendix 3. Contingency table for the correlation between serpin E1 expression and desmoplasia and its two components at tumour core and advancing front.

	Tumour core											
	Alcian Blue			eSMA			Desmoplasia					
	Low	High	Total	Low	High	Total	Low	High	Total	Low	High	Total
HPV-	Low			12	17	29						
	High			4	20	24						
	Total			16	37	53						
HPV-	Low						25	1	26			P=0.003
	High						5	4	9			
	Total						30	5	35			
HPV-	Low						18	1	19			P=0.038
	High						8	4	12			
	Total						26	5	31			
	Tumour front											
HPV-	Low						25	1	26			P=0.017
	High						6	3	9			
	Total						31	4	35			
HPV-	Low			9	11	20						
	High			1	11	12						P=0.030
	Total			10	22	32						
HPV-	Low			9	11	20						
	High			0	8	8						P=0.021
	Total			9	19	28						
HPV-	Low						18	8				
	High											P=0.040
	Total						8	7				
HPV+	Low			11	15	26						
	High			0	16	16						P=0.019
	Total			6	31	37						

Appendix 4. Correlation of α SMA, Alcian Blue and serpin E1 expression with clinicopathological variables at tumour core in HPV+ and HPV- OPSCC.

		Tumour core								
		Alcian Blue		α SMA		Serpine E1 tumour		Serpine E1 stroma		
		Low	High	Low	High	Low	High	Low	High	
HPV-	Age	30-40	2	0	0	2	1	1	2	0
		40-50	1	6	2	4	5	3	4	4
		50-60	3	11	4	10	8	7	7	8
		60-70	6	11	4	10	7	9	11	6
		70-80	2	12	5	9	6	8	8	6
		80-90	1	0	0	1	0	1	0	1
HPV+	Age	90-100	1	0	1	0	1	0	1	0
		20-30			1	0	0	1	1	0
		30-40	0	1	0	2	1	1	0	1
		40-50	1	3	1	3	0	4	2	2
		50-60	8	7	0	15	0	15	8	7
		60-70	6	2	3	6	0	9	3	5
HPV-	Survival	Alive	8	7	5	7	10	5	11	4
		Died of disease	1	12	3	10	10	4	10	5
		Died other	0	5	2	4	5	1	4	2
HPV+	Survival	Alive	14	12	5	24	1	28	13	14
		Died of disease	1	0	0	1	0	1	0	1
HPV-	Recurrence	No	11	24	12	19	21	16	22	15
		Yes	3	13	4	12	6	9	9	7
HPV+	Recurrence	No	13	9	5	20	1	24	10	13
		Yes	2	3	0	5	0	5	3	2
HPV-	Histological Sub-type	Non-Keratinising	1			1	0	1	1	0
		Keratinising	3			3	1	2	2	1
HPV+	Histological Sub-type	Non- Keratinising	12	11	4	22	1	25	12	12
		Keratinising	1	0	1	0	0	1	0	1
		Mixed	2	2	0	4	0	4	2	2
HPV-	Site	Base of tongue	1	9	8	4	3	9	7	5
		Soft palate	4	8	2	8	4	6	4	6
		Tonsil	8	18	5	17	18	9	17	11
		Oropharynx	3	6	1	8	3	6	5	4
HPV+	Site	Base of tongue	4	1	0	2	0	2	1	1
		Soft palate	2	0	1	4	0	5	1	4
		Tonsil	4	6	2	8	0	10	6	3
		(Tonsil + soft palate) or (Tonsil + base of tongue)	1	0	0	2	1	1	0	1
		Oropharynx	4	3	2	6	0	8	2	6
		Pharyngeal wall	0	1	0	2	0	2	2	0
HPV-	pT-stage	pT1	1	0	1	0	1	0	1	0
		pT2	3	8	4	6	7	3	6	4
		pT3	2	5	0	6	6	2	7	2
		pT4	0	6	2	3	6	1	3	4
		pTX	1	0	0	1	1	0	1	0
HPV+	pT-stage	pT2	11	4	2	15	1	16	7	9
		pT3	3	6	3	7	0	10	5	4
		pT4	1	1	0	2	0	2	0	2
HPV-	pN-stage	N0	2	4	3	2	6	0	4	2
		N1	1	5	1	3	5	1	3	3
		N2	4	11	4	11	11	5	12	5
HPV+	pN-stage	N0	5	1	2	5	0	7	5	2
		N1	1	2	0	3	0	3	0	3
		N2	9	8	3	16	1	18	7	10
HPV-	ECS	No	3	12	5	8	12	3	12	4
		Yes	5	11	4	11	12	6	11	7
HPV+	ECS	No	10	5	5	12	0	17	8	8
		Yes	4	6	0	11	1	10	4	6
HPV-	LNM	Yes	3			3	1	2	2	1
HPV+	LNM	No	5	1	2	5	0	7	5	2
		Yes	10	11	3	20	1	22	8	13

Appendix 5. Correlation of α SMA, Alcian Blue and serpin E1 expression with clinico pathological variables at tumour front in HPV+ and HPV- OPSCC.

		Tumour front								
			Alcian Blue		α SMA		Serpine E1 tumour		Serpine E1 stroma	
			Low	High	Low	High	Low	High	Low	High
HPV-	Age	30-40	0	1	2	5	0	1	1	0
		40-50	0	7	3	6	4	3	4	3
		50-60	2	4	3	5	7	2	5	2
		60-70	6	3	2	5	6	3	7	2
		70-80	4	4	0	1	4	3	6	1
HPV+	Age	20-30			0	1	0	1	0	1
		30-40	1	1	0	2	0	2	1	1
		40-50	0	4	1	3	1	3	2	1
		50-60	4	10	3	12	4	11	8	4
		60-70	4	2	1	8	0	9	5	4
HPV-	Survival	Alive	7	6	8	5	9	5	11	1
		Died of disease	4	8	1	11	7	5	8	4
		Died other	0	4	0	5	3	2	2	3
HPV+	Survival	Alive	9	15	5	24	5	24	16	9
		Died of disease	0	1	0	1	0	1	0	1
HPV-	Recurrence	No	7	14	8	14	15	7	15	7
		Yes	5	3	2	7	6	3	7	1
HPV+	Recurrence	No	9	12	5	20	4	21	13	9
		Yes	0	4	0	5	1	4	3	1
HPV-	Histological Sub-type	Non- Keratinising	0	1	1	0	1	0	1	
		Keratinising	1	2	0	2	0	3	1	
HPV+	Histological Sub-type	Non- Keratinising	7	15	5	21	4	22	1	0
		Keratinising	1	0	0	1	0	1	2	1
		Mixed	1	2	0	4	1	3	16	11
HPV-	Site	Base of tongue	2	4	1	5	1	5	3	2
		Soft Palate	0	5	0	6	3	3	1	4
		Tonsil	8	8	8	9	14	3	16	1
		Oropharynx	2	2	1	2	3	1	3	1
HPV+	Site	Base of tongue	0	1	0	2	0	2	1	1
		Soft Palate	2	2	1	4	1	4	4	1
		Tonsil	3	7	2	8	3	7	3	4
		(Tonsil + Soft Palate) or (Tonsil + Base of tongue)	2	0	1	1	0	2	2	0
		Oropharynx	1	4	1	7	1	7	3	4
		Pharyngeal wall	1	1	0	2	0	2	2	0
HPV-	pT-stage	pT1	0	1	0	1	0	1	0	1
		pT2	2	7	2	7	6	3	5	3
		pT3	5	2	4	3	5	2	6	0
		pT4	2	2	1	5	4	2	6	1
		pTX	0	1	7	16	0	1	1	0
HPV+	pT-stage	pT2	7	7	3	7	2	15	10	6
		pT3	2	6	0	2	3	7	5	2
		pT4	0	2	5	24	0	2	0	2
HPV-	pN-stage	N0	1	4	2	4	4	2	4	2
		N1	2	1	2	2	2	2	5	0
		N2	6	9	3	11	9	6	9	4
HPV+	pN-stage	N0	2	3	1	6	0	7	5	2
		N1	0	2	0	3	0	3	0	3
		N2	7	10	4	15	5	14	10	5
HPV-	Recurrence	No	4	8	5	8	7	6	10	3
		Yes	7	8	5	10	12	4	12	3
HPV+	Recurrence	No	6	7	3	14	1	16	10	6
		Yes	3	7	2	9	4	7	4	4
HPV-	Lymph node metastasis	Yes	1	2	1	1	1	2	1	
HPV+	Lymph node metastasis	No	2	3	1	6	0	7	5	2
		Yes	7	13	4	19	5	18	10	9

Appendix 6. Components of resolving (sufficient for two gels) -10% SDS.

Component	Volume / Mass	Remark
Water	35 ml	Double Distilled
0.5 M Tris (8.8)	20 ml	Stored in fridge (Fisher Scientific)
30% Acrylamide	23 ml	Stored in fridge (Fisher Scientific)
10% SDS	900 μ l	Storage – room temperature (Fisher Scientific)
10% APS	500 μ l	Prepared fresh from powder (Sigma)
TEMED	120 μ l	Stored in fridge (Sigma)

Appendix 7. Components of stacking (sufficient for two gels) -10% SDS.

Component	Volume / Mass	Remark
Water	15 ml	Double Distilled
1.5 M Tris (6.8)	6.6 ml	Stored in fridge (Fisher Scientific)
30% Acrylamide	3.3 ml	Stored in fridge (Fisher Scientific)
10% SDS	250 μ l	Storage – room temperature (Fisher Scientific)
10% APS	150 μ l	Prepared fresh from powder (Sigma)
TEMED	60 μ l	Stored in fridge (Sigma)

Appendix 8. Electrophoresis running buffer.

Component	Volume / Mass (per volume of buffer)	Remarks
Tris Base	3g	Room temperature storage (Fisher Scientific)
Glycine	14.4g	Room temperature storage (Fisher Scientific)
10% SDS	10ml	Room temperature storage (Fisher Scientific)

Appendix 9. Western blotting transfer buffer.

Component	Volume / Mass (per volume of buffer)	Remarks
Tris Base	3g	Room temperature storage (Fisher Scientific)
Glycine	14.4g	Room temperature storage (Fisher Scientific)
Methanol	200ml	Room temperature storage (Fisher Scientific)

Appendix 10. Clinical and pathological characteristics of the cohort subset used for Chapter 6.

	HPV+ OPSCC	HPV- OPSCC
Age (years)		
Range	50-70	40-80
Mean	60	60
Gender		
Male	8	No data available
Female	2	No data available
Tumour site		
Soft Palate	1	3
Base of tongue	1	1
Tonsil	6	4
Oropharynx	2	2
Pathological T-stage		
pT1	1	1
pT2	5	2
pT3	2	
pT4	1	3
Pathological N-stage		
N0	2	2
N1	3	
N2	4	4
ECS	3	2